The effects of high dose ionizing radiation on transcriptional regulation and paracrine signaling in human peripheral blood mononuclear cells

Doctoral thesis at the Medical University of Vienna
for obtaining the academic degree

Doctor of Philosophy

Submitted by

Dr. med. univ. Lucian Beer

Supervisor:
Assoc. Prof. Univ. Doz.
Dr. med. univ. Hendrik Jan Ankersmit, MBA
Department of Thoracic Surgery
Christian Doppler Laboratory for Cardiac and
Thoracic Diagnosis and Regeneration
Medical University of Vienna
Währinger Gürtel 18-20
1090 Vienna, Austria

Vienna, 28.07.2015

1 Declaration

This work was done at the Department of Surgery (Medical University of Vienna) in cooperation with the Department of Dermatology (Medical University of Vienna), the Department of Pediatrics (Medical University of Vienna), the Department of Cell Biology and Ultrastructure Research (Medical University of Vienna), the Institute of Physiology (Medical University of Vienna), the Center for Medical Statistics, Informatics and Intelligent Systems (Medical University of Vienna) and the Department of Cardiology (Medical University of Vienna). The *in vitro* experiments, FACS analysis and immunoblots were performed in cooperation with Michael Mildner (Department of Dermatology). Bioinformatics analysis was performed in cooperation with Robin Ristl (Center for Medical Statistics, Informatics and Intelligent Systems) and Rudolf Seeman (University Hospital of Craniomaxillofacial and Oral Surgery). Lipid analysis was performed in cooperation with Florian Gruber (Department of Dermatology). Electron microscopy images were done by Adolf Ellinger (Department of Cell Biology and Ultrastructure Research). DIGE analysis was performed in cooperation with Maria Zellner (Institute of Physiology). Large animal model experiments were performed in Kaposvar by Mariann Pavone-Gyöngyösi (Department of Cardiology). Production of viral cleared PBMC secretome for large animal model experiments was produced at the Red Cross Blutbankzentrale under supervision of Prim. Christian Gabriel. Data evaluation and interpretation of results as well as preparation of original papers was performed by Lucian Beer (Department of Surgery, Medical University of Vienna) under the supervision of Hendrik Jan Ankersmit (Department of Surgery, Medical University of Vienna) with support of the mentors Barbara Bohle (Institute of Pathophysiology and Allergy Research, Medical University of Vienna) and Maria Zellner (Institute of Physiology, Medical University of Vienna).

2 Table of contents

3   List of figures

4 List of tables

5 Zusammenfassung

Parakrine Signalwege treten zunehmend in Focus des wissenschaftlichen Interesses im Feld der regenerativen Medizin. Während ursprünglich angenommen wurde, dass direkte Zell-Zell Interaktion und die Integration von injizierten Stammzellen ausschlaggebend für die Induktion von regenerativen Prozessen sind, zeigen neue Daten, dass es die von diesen Zellen freigesetzten parakrine Faktoren sind, welche zytoprotektiv und regeneratorisch wirken.

Die Zellen werden heutzutage als Bioreaktoren gesehen, welche lösliche Faktoren freisetzen die als Therapeutikum eingesetzt werden können. Um die parakrine Kapazität dieser Zellen zu verstärken, sind so genannte Konditionierungsstrategien beschrieben. Unsere Arbeitsgruppe konnte in mehreren Publikationen zeigen, dass periphere mononukleäre Blutzellen eine Vielzahl an parakrinen Faktoren freisetzen, welche die Wundheilung beschleunigen, den Herzmuskel im Zuge eines akuten Infarktes schützen, die Verlegung der Mikrovaskulatur verhindern, das neurologische Outcome nach einem ischämischen Schlaganfall und traumatischer Rückenmarksverletzung verbessern und die Entwicklung einer autoimmun meditierten Myokarditis in der Maus verhindern. Obwohl diese Studien die gesehenen Effekte detailliert beschrieben haben, wissen wir derzeit nicht, welche biologischen Prozesse in den weißen Blutkörperchen im Zuge der ionisierenden Bestrahlung aktiviert oder supprimiert werden. Weiters ist unbekannt, welche parakrine Faktoren von den weißen Blutkörperchen freigesetzt werden.

Im Zuge dieser Doktorarbeit untersuchten wir die induzierten oder supprimierten zellulären Vorgänge in bestrahlen (60 Gray) weißen Blutkörperchen ($25 \times 10^{\wedge 6}$ Zellen/ml) als auch deren Sekretome. Durch Zuhilfenahme von bioinformatischen Auswertealgorithmen konnten wir komplexe mRNA und microRNA Interaktionsnetzwerke generieren, welche im Zuge der Bestrahlung vermehrt aktiviert werden. Es zeigte sich, dass der Transkriptionsfaktor hepatic leukemia factor (HLF) eine Schlüsselfunktion in der Regulation der mRNA und microRNA Netzwerke in irradiierten Zellen einnimmt. Weiters konnten wir feststellen, dass Bestrahlung zu einer vermehrten Freisetzung von Proteinen führt, welche die Zellmigration und Wundheilung induzieren. Bestrahlte weiße Blutkörperchen setzten oxidierte Phosphatidylcholine frei, welche bekannte entzündungsmodulierende und proangio-genetische Eigenschaften aufweisen. Weiters führte eine Bestrahlung der Zellen zu einer gesteigerten Ausschüttung von Mikropartikeln und Exosomen.

In vitro Versuche identifizierten Proteine und Exosomen als die zwei Hauptkomponenten, welche zu einer gesteigerten Zellmigration und Zellaktivierung von Fibroblasten und Keratinozyten führten. In vivo Versuchen im Großtiermodel des akuten Herzinfarkts konnten wir erstmals zeigen, dass das Sekretome von weißen Blutkörperchen seine biologische

Aktivität nicht verliert wenn es nach den Richtlinien des *good manufacturing process* hergestellt wird. Die herzmuskelschützende Wirkung war vergleichbar mit dem Zellsekretome, welches auf konventionelle Art hergestellt worden war. Aus diesen Daten lässt sich schließen, dass die biologisch wirksamen Komponenten stabil gegenüber einer externen Herstellung und den Lagerungsbedingungen sind.

In dieser Arbeit konnten wir zeigen, dass ionisierende Bestrahlung weißer Blutkörperchen zu einer Änderung der Genexpression, als auch der Freisetzung einer Vielzahl unterschiedlicher molekularer parakrine Faktoren führt. Diese Daten sollen die Grundlage für zukünftige Studien darstellen, welche die Rolle von Exosomen und Proteinen als Therapeutikum im Felde der regenerativen Medizin evaluieren.

6 Abstract

While it has long been accepted that direct cell-cell interactions and the replacement of injured tissues with injected cells exerts therapeutic effects, it is currently believed that, in addition, paracrine factors released from different cell types activate cytoprotective and regenerative processes. Cells are now seen as bioreactors that produce and release soluble factors which might be used as therapeutics. We have previously shown that peripheral blood mononuclear cells (PBMCs) release a plethora of paracrine factors that enhance wound healing, attenuate myocardial damage following acute myocardial infarction, abolish microvascular obstruction, improve neurological outcome after acute ischemic stroke and spinal cord injury and protect mice from experimental autoimmune myocarditis. These PBMC derived paracrine factors may exert their effects via the induction of cytoprotective pathways, augmentation of angiogenesis, induction of NO-depended vasodilation and inhibition of VASP dependent platelet aggregation, as well as driving auto-reactive CD4+ cells into apoptosis. To enhance the cellular secretory capacity, treatments which induce stress responses, such as hypoxic preconditioning or ionizing irradiation (IR), have been developed. Although these effects have been evaluated in several disease states there is little data available on the cellular effects of ionizing irradiation on human PBMCs and their secretome. In this study, we have thus undertaken to investigate the effects of IR on human PBMCs in terms of the induction of transcriptional changes and release of pleiotropic paracrine factors.

There are three primary aims of this doctoral thesis: 1. To investigate cellular processes activated or repressed in human PBMCs following high dose ionizing radiation (60Gy) and high density cell cultivation ($25*10^6$ cells/ml) for up to 24 hours. 2. To identify paracrine factors released from these cells using a multi-methodical biochemical/bioinformatics approach. 3. To evaluate whether the viral cleared secretome, produced according to the good manufacturing practice (GMP) guidelines, retains its ability to attenuate acute myocardial infarction in a large animal model. Using this counterintuitive approach, a sophisticated mRNA and microRNA expression analysis coupled with bioinformatics revealed a complex interaction network activated in response to IR. Irradiated PBMCs released proteins involved in the regulation of cell migration and wound healing, produced oxidized phosphatidylcholines with known inflammation-modulating and angiogenic properties, and released higher amounts of microparticles and exosomes. In particular, we were able to identify the transcription factor, hepatic leukemia factor (HLF), as a central node in these mRNA-microRNA-transcription factor regulatory networks, and showed it to be significantly repressed in irradiated PBMCs.

By using *in vitro* functional assays we were able to show for the first time that the protein fractions and exosomes were the main biologically active components that enhance cell migration and activation of fibroblasts and keratinocytes. A pathogen cleared, good manufacturing process produced PBMC secretome in a porcine closed chest model of acute myocardial infarction attenuated the myocardial damage as effectively as the control, indicating a high stability of the biologically active components. Our data may provide a basis for further studies to investigate the role of exosomes and proteins as a novel therapeutic approach in the field of regenerative medicine.

7 Publications arising from this thesis

1. High dose ionizing radiation regulates micro RNA and gene expression changes in human peripheral blood mononuclear cells

2. Analysis of the Secretome of Apoptotic Peripheral Blood Mononuclear Cells: Impact of Released Proteins and Exosomes for Tissue Regeneration

8 Abbreviations

PBMC   peripheral blood mononuclear cell

KC: keratinocyte

FB: fibroblast

qRT-PCR   quantitative reverse transcriptase polymerase chain reaction

EV   extracellular vesicle

MP   microparticle

MSC   mesenchymal stem cell

CM   conditioned media

miRNA   micro RNA

mRNA   messenger RNA

HPLC   high pressure liquid chromatography

DDR   DNA damage response

ROS   reactive oxygen species

SSB   single strand brakes

DSB   double strand breaks

9 Acknowledgments

I would like to thank Hendrik Jan Ankersmit for providing me the opportunity to carry out this PhD thesis and all my colleagues in the Christian Doppler Laboratory for Cardiac and Thoracic Diagnosis and Regeneration for their technical support and fruitful discussions. For their names and contributions, I would like to refer you to the individual publications.

I especially thank Michael Mildner for sharing his scientific knowledge with me, and for providing me with the opportunity to perform important parts of my experiments at the Department of Dermatology.

This thesis was only possible in the research surroundings offered by the Christian Doppler Laboratory for Cardiac and Thoracic Diagnosis and Regeneration.

Finally, I am grateful to my parents, grandparents and my sister for their lifelong support.

The results of this thesis were presented at several international and national congresses including: 37th Seminar der Österreichischen Gesellschaft für Chirurgische Forschung, Gosau (2013), 2nd Vascular Biology Meeting, Vienna (2014), 55th Österreichischer Chirurgenkongress, Graz (2014), EACTS Meeting on Cardiac and Pulmonary Regeneration and Stem Cell Technology, Bern (2014), 4th EACTS Meeting on Cardiac and Pulmonary Regeneration (2015); Bern and 59th Kongress der Kardiologischen Gesellschaft, Salzburg (2015).

The publications arising from this thesis are given in the results section.

10 Introduction

10.1 Regenerative medicine and tissue regeneration

The concept of regenerative medicine was established in the last decade of the 20th century, and pursues the aim of replacing or engineering tissues to re-establish normal biological function. The number of articles published on the subject of regenerative techniques is rapidly increasing [1]: as shown in **Figure 1**. A Pubmed search performed in 2015 revealed that more than 18,000 articles with the term "regenerative medicine" have appeared, with approximately 4,200 articles published in 2014 alone, compared to a mere 248 publications a decade ago.

Because of its global distribution, ischemic heart disease has become the disease most investigated in the field of regenerative medicine. This disease is responsible for about 7.25 million deaths each year worldwide and research has focused on acute myocardial infarction (AMI), since it represents the most common cause of heart failure and overall mortality [2].
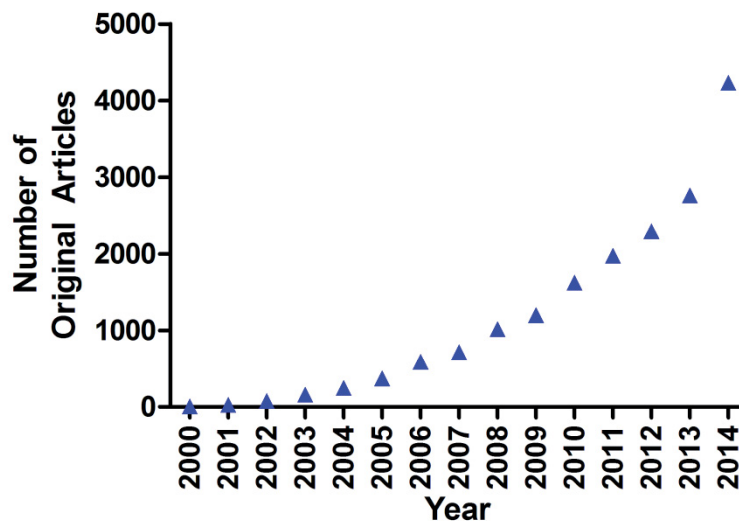
Figure 1 Number of articles published between 2000 to 2014 tagged with the term „regenerative medicine" obtained via pubmed.org.

10.2 Efficacy of Stem cells in regenerative medicine

It has long been believed that an injured tissue cannot be repaired, however, this view has changed in light of studies showing increased cell proliferation in hearts of patients suffering from congestive heart failure [3]. These proliferating cells have been proposed to be of extra cardiac origin, migrating towards the damaged tissue and replacing the damaged cells [4]. Regeneration of an injured organ necessitates considerable cell replacement, likely in the order of a billion cells in the case of myocardial injury. Furthermore, these cells must interact with resident cells in order to form a unit and restore organ function [5]. Stem cells were

considered an attractive therapeutic option in regenerative medicine as their number could be increased almost indefinitely and they are able to differentiate into the resident cell type.

The first large randomized controlled clinical trials (RCT) using transferred cells were conducted in patients suffering from acute myocardial infarction. In 2002 the TOPCARE-AMI clinical trial showed improvements of left ventricular function after intracoronary application of autologous progenitor cells [6]. During the following years several other clinical trials have been published demonstrating favorable effects of stem cell therapy in terms of left ventricular ejection fraction and clinical outcome. [7, 8]. However, while these individual clinical trials have documented that MSC application is safe [9], the long-term clinical outcome remains unclear and is still under debate.

Meta-analyses of cohort studies and data from randomized controlled trials (RCT) can be used to extract data and provide the basis for satisfactory analysis of different clinical aspects that could not be answered within individual studies. In 2012 the largest meta-analysis that investigated the therapeutic effects of bone marrow cell (BMC) transplantation in patients with AMI was published [10]. The authors included data of 50 studies that enrolled 2,625 patients. BMC therapy showed improved LV-EF and reduced infarct size in comparison to controls. In contrast, the meta-analysis of de Jong et al published in 2014 was not able to support these data as neither LV-EF nor clinical parameters were improved in their analysis, including 30 RCT covering 2037 patients [11].

A drawback of these meta-analyses is the heterogeneity of the trials analysed. The trials used different follow-up times, clinical measurements and patient populations. Furthermore, publication-based meta-analyses might include trials that exhibit statistical errors, misrepresented survival graphs and publish median values of skewed data [12]. To overcome these problems individual participant data (IPD) meta-analyses can be used. IPD meta-analyses contain original data from each patient of each trial. They are seen as the golden standard for systematic reviews as they display both clinical and statistical advantages [13]. In 2015 Gyöngyösi et al. published an IPD meta-analysis consisting of 12 RCT with 1252 patients. They investigated the effects of intracoronary cell transplantation after AMI. The authors were able to show that neither clinical events nor left ventricular functions were significantly affected by intracoronary cell therapy [14]. These data indicate the lack of clinical efficacy in stem cell transplantation for myocardial regeneration and can be seen as a damper on the resource-intensive research of stem cell therapy. However, large RCT such as the BAMI trial (ClinicalTrials.gov Identifier: NCT01569178) with a planned enrolment of 3000 patients are currently ongoing and will further verify or otherwise the efficacy of stem cell therapy in cardiac regeneration.

Besides therapy in AMI, stem cells have been evaluated in patients with chronic ischemic cardiomyopathy [15], neurological diseases [16], kidney ischemia-reperfusion injury [17] and liver failure [17], highlighting the broad spectrum of putative therapeutic application possibilities.

10.3 Mesenchymal stem cell derived paracrine factors in myocardial regeneration

Although these recently published studies indicate that stem cell therapy has only minor effects on clinical outcomes following AMI, there is a body of evidence derived from preclinical studies that demonstrate that stem cells are capable of inducing regenerative processes and enhancing myocardial function. However, the mechanism by which stem cells possiblly promote tissue regeneration and repair is still under debate. Gnecchi [21] proposed either direct cell-cell interaction, leading to cardiomyocyte regeneration and/or vasculogenesis, or indirect effects via the secretion of paracrine factors (see **Figure 2)**. Trans-differentiation of injected stem cells had initially been seen as the principle mechanism underlying the beneficial therapeutic effects [18]. However, animal studies revealed that only ~2% of administered mesenchymal stem cells (MSC) engraft in the injured organ and exhibit limited potential to transdifferentiate into resident cells [19]. The direct replacement of damaged resident cells by stem cells therefore seems unlikely to be the underlying therapeutic mechanism. In addition, the intracoronary injection of stem cells has been shown to reduce myocardial blood flow resulting, on the one hand, in a reduced invasion of stem cells into the injured area, and on the other hand, to a possible deterioration of the injured myocardium due to this reduced blood flow [20]. Reduction in microvasculature blood flow due to MSC obstruction can therefore in some cases exacerbate the myocardial damage following AMI.

Regardless of whether stems cells transdifferentiate into resident cells or not, it has been shown in several studies that the clinical improvements achieved by stem cells cannot be explained by the relatively low number of newly generated resident cells [21]. It has therefore been proposed that paracrine factors released by stem cells are more important than the cells themselves in promoting tissue regeneration and cytoprotection [21-23].
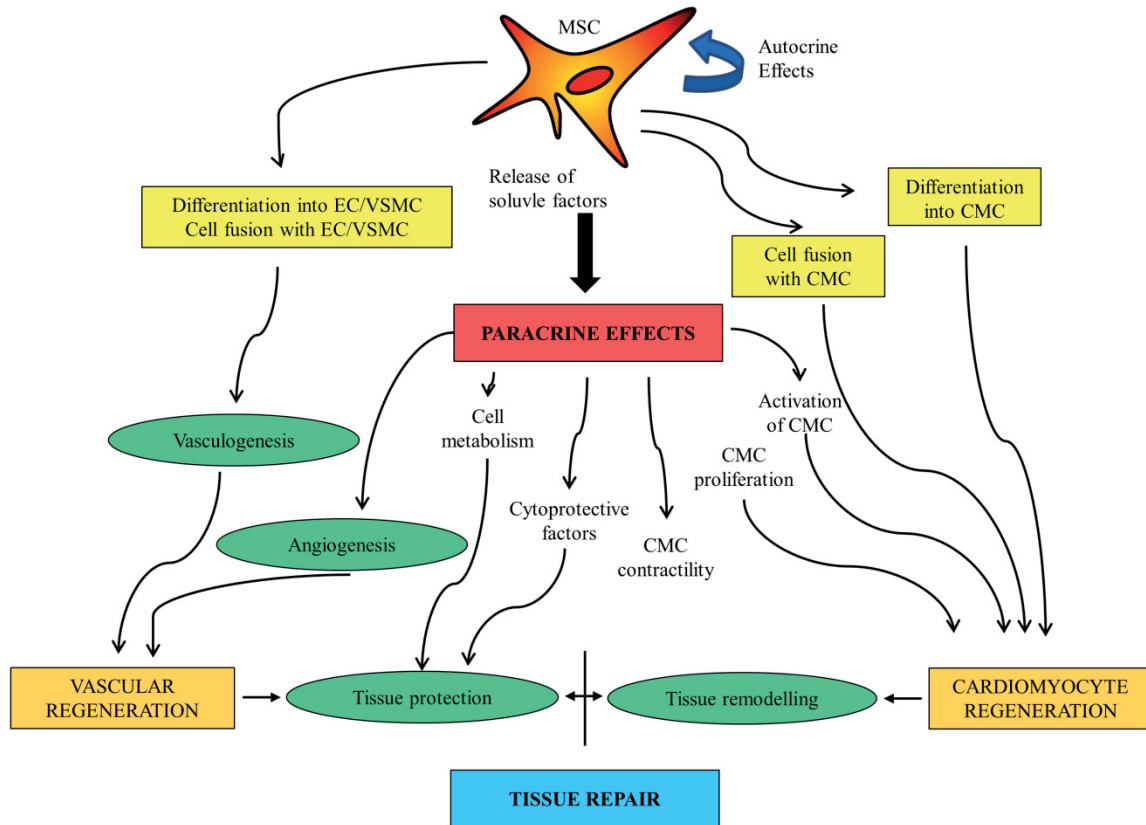
Figure 2: Mesenchymal stem cells (MSC) in myocardial regeneration. MSC can directly regenerate cardiomyocyte und vascular cell damage. In addition MCS release soluble factors which exert beneficial clinical effects, resulting in cardiac regeneration. (CMC=cardiomyocytes) (adopted from Gnecchi et al. 2008)

Inspired by the idea of using paracrine factors instead of stem cells, several preclinical trials have been conducted in order to evaluate possible areas of application. Uemura and colleagues were able to show that bone marrow derived stem cells release paracrine factors that attenuate left ventricular remodeling following murine coronary artery ligation [24]. In 2008 Chen et al. published data highlighting that MSCs secrete paracrine factors that enhance endothelial cell migration and promote wound healing [25]. Similar results have been published with paracrine factors as therapeutics in kidney ischemia-reperfusion injury [26]. These data indicate that the paracrine factors rather than the cell itself display the beneficial biological effects.

With this in mind, researchers have focused in detail on the investigation of factors involved in intercellular communication, in order to improve tissue engineering strategies and regenerative therapies.

10.4 The dying stem cell hypothesis and PBMCs

In 2005 Thum and colleagues put forward the hypothesis that the injection of apoptotic stem cells down-regulates innate and adaptive immunity, thereby attenuating cardiomyocyte

4

apoptosis , scar formation and improving myocardial function [27]. They drew attention to the fact that up to 25% of injected stem cells undergo programmed cell death [8, 28, 29], and proposed that these apoptotic cells inhibit inflammation via up-regulation of anti-inflammatory cytokines (e.g. IL-10, TGF-beta) by macrophages. Anti-inflammatory mediators released by macrophages ingesting apoptotic cells might counterbalance pro-inflammatory cytokines released by the infarcted heart [27]. In addition, apoptotic cells are recognized by antigen presenting cells that might further lead to enhanced cell-type specific expression of immune suppressive mediators and attenuation of inflammatory cytokines. Fadok et al were able to show that apoptotic neutrophils stimulate the production TGF-beta, prostaglandin E2 (PGE2) and platelet activating factor in phagocytes, whereas the pro-inflammatory cytokines IL-1beta, IL-8 and TNF-alpha were reduced [30]. The former proteins are able to attenuate LPS mediated macrophage activation, indicating that apoptotic cells simultaneously enhance anti-inflammatory processes and suppress inflammatory pathways. Interestingly, PGE2 is known to induce angiogenesis in vivo [31], thus highlighting the important role of apoptotic cells, not only in regulation of inflammation, but also in the regulation of angiogenesis.

These local immune reactions induced by apoptotic stem cells are deemed to be the major therapeutic mechanism responsible for the beneficial effects observed. These workers further hypothesized that instead of stem cells any other cell type (e.g. blood mononuclear cells) that is undergoing ex vivo triggered apoptosis could improve myocardial regeneration [27]. PBMCs instead of stem cells as bioreactors was proposed to show several advantages: I) The raw material is easily obtainable, II) PBMC cell number is almost unlimited in comparison to stem cells, III) cell cultivation requirements are less stringent as the cells will undergo apoptosis and are not pluripotent [32].

This hypothesis was investigated by Ankersmit et al. in a pilot study [32] which sought to evaluate whether a suspension of apoptotic PBMCs and conditioned media are able to induce immune suppression and display cardioprotective potential *in vitro* and *in vivo*. Indeed, these authors could show that irradiated PBMCs attenuated the LPS induced secretion of IL-1beta and IL-6 in co-cultured monocytes and PBMCs. Furthermore, irradiated PBMCs decreased the T cell proliferation in a mixed lymphocyte reaction assay [32].

The *in vivo* effects of the application of irradiated PBMCs together with their cell culture supernatant were subsequently, tested in a rodent model of AMI induced by ligation of the left anterior descending artery (LAD). Histological analysis of hearts explanted 6 weeks after myocardial ischemia evidenced significantly reduced infarct sizes in animals treated with irradiated PBMC suspensions in comparison to animals treated with viable PBMCs or medium alone. In line with these findings, the intravenous injection of suspensions of irradiated PBMCs improved functional parameters; ejection fraction, end-systolic and end

diastolic diameters as well as end-systolic and end-diastolic volumes were almost completely preserved in animals treated with intravenous injections of apoptotic PBMCs [32]. Moreover the authors observed quantitative and qualitative changes in myocardial cell infiltrates 72 hours after AMI in irradiated PBMC treated rats. Whereas animals treated with cell culture media or viable PBMCs evidenced a mixed cellular infiltrate in the border zone (e.g. neutrophils, macrophages/monocytes, lymphomononuclear cell, fibroblasts, endothelial cells and dystrophic cardiomyocytes), animals receiving irradiated PBMC suspensions predominantly displayed a CD68+ mononuclear cell infiltrate (monocytes/macrophages). Further analysis of these cells revealed that they were found mostly within the ischemic myocard of animals treated with apoptotic PBMC suspensions and were positive for c-kit (CD 117) and vascular endothelial growth factor receptor 2 (VEGF-R2). c-kit positive cells are multipotent cardiac progenitor cells [33] that have been shown to be involved in cardiac regeneration and their application can improve myocardial function following AMI [34].

This was the first study that showed that suspensions of apoptotic PBMCs display anti-inflammatory activity and can attenuate myocardial damage following AMI. The cardioprotecitve effects observed were comparable to those reported in initial preclinical stem cell publications [21]. However, since none of these early studies used PBMCs as a control for the stem cell group, it was unclear whether PBMCs also exert their protective functions via the production of paracrine factors, or whether the apoptotic cells themselves .were the active principle. Thus although Ankersmit et al. were able to confirm Thum´s data [32] the underlying mechanism(s) still remained to be elucidated.

10.5 The paracrine paradigm

Intercellular communication can either take place via direct cell-cell contact and transduction of information through cell junction or adhesion molecules, or via endocrine or paracrine mechanisms [21]. While processes involving direct cell-cell contacts and endocrine mechanisms via hormones traveling through blood have been investigated in detail in the last century, the idea that paracrine mediators are remarkable contributors to the intercellular communication system has arisen only lately [21]. In general, paracrine factors are regarded to be cell-derived soluble molecules that induce biochemical changes in neighboring cells. They consist of proteins, lipids, regulatory RNAs and extracellular vesicles [35].

Pioneering work in this research area was published in 2005 by Gnecchi et al. who reported that "conditioned" cell cultures of hypoxic stem cells over-expressing the survival gene Akt1 inhibit apoptosis of rat cardiomyocytes [36]. These findings were corroborated by subsequent studies showing that paracrine factors released from different cell types, attenuate cell injury and modulate immune activation in response to cell damage [35, 37-45]. More recently it has

been shown that the paracrine effects are of particular importance in the field of regenerative medicine, where they induce a higher regenerative capacity in comparison to the administered cells themselves [21, 46].

10.5.1 Preconditioning strategies to enhance the paracrine activity

Several preconditioning strategies have been investigated in order to promote paracrine capacity. In vitro preconditioning with small molecules, hypoxia or radiation can influence cell proliferation, cell survival and paracrine activity [47].

Cell starvation and hypoxic Preconditioning

Although these encouraging results tempt one to use hypoxia to stimulate paracrine activity, several unresolved issues remain. Firstly, it is unclear how long hypoxic conditions must be maintained in order to augment paracrine activity most effectively. There was a considerable variation between studies in terms of hypoxic cell cultivation and magnitude of 0_2 tension. In addition, it has not been evaluated whether hypoxia can increase the formation of ROS, which might display negative biological activity. Beside direct cultivation under hypoxic conditions, serum deprivation has been shown to act as an in vitro model for ischemia. Serum deprivation of rat bone marrow derived MSC induces comparable cellular pathways, to hypoxia leading to secretion of IL-10 and attenuation of cardiac fibroblast proliferation and collagen expression, thereby suppressing cardiac fibrosis [48]. These data are in line with those of Oskowitz et al. who show that serum starved bone marrow derived MSCs up-regulated expression of pro-angiogenic and cytoprotective factors (e.g. VEGF-A, HGF, IGF-1). Paracrine factors from these cells evidenced enhanced angiogenic potential in chick chorioallantoic membrane assays as compared to MSCs [49]. In 2013 Przybyt et al reported that adipose derived stromal cells cultured under hypoxic (2% O2) conditions promote rat cardiomyocyte proliferation via JAK/STAT and MAPK dependent signaling pathways [50]. In addition Kinnaird and colleagues showed that human MSCs cultured under hypoxia for 72 hours secreted multiple arteriogenic cytokines in comparison to normoxic conditions [51]. Conditioned media (CM) of MCS was able to stimulate endothelial cell proliferation and migration in a dose dependent manner *in vitro.* Furthermore, it enhanced smooth muscle cell proliferation and attenuated tissue injury in a murine hindlimb ischemia model [52].

Genetic modification

Manipulation of the genome and the introduction of transgenes for additional gene expression aim to augment MSC secretomes. Gnecchi et a observed that Akt-overexpressing rat MSCs attenuated ventricular remodeling and improved myocardial function, evaluated 2 weeks after AMI. Infarct size at 72 hours after injection of an MSC

suspension was analyzed with triphenyltetrazolium chloride (TTC) staining and showed a significant improvement in MCS treated animals in comparison to controls. Furthermore Gnecchi et al. reported that the CM of Akt overexpressing cells contained higher concentrations of pro-angiogenic factors (VEGF, HGF and IGF-1) than controls. In addition, Akt-MSC CM inhibited hypoxia-induced cardiomyocyte apoptosis and improved cardiomyocyte contraction in vitro [53]. These data are in line with those of Mirotsou et al. who reported enhanced cardiomyocyte survival and attenuated myocardial damage following the injection of murine Akt overexpressing MSC [54]. Other workers directly overexpressed factors such as IGF-1 [55] or VEGF [56] and SDF-1 [57], hypothesizing that the concentration of one single protein could augment the biological activity. However the use of genetically modified cells as bioreactors poses regulatory hurdles (e.g. viral approaches, risk of developing malignancies). In addition, several biologically active candidate factors in cell secretomes have not yet been identified and their underlying pathways are not known.

Preconditioning using proteins

TNF-alpha, INF-beta or LPS have been used for MSC stimulation. CM of MSC stimulated with TNF-alpha showed a dose dependent enhancement in monocyte migration and upregulation of CXCL8 and CCL2 chemokine concentrations [58]. Yao and colleagues reported that LPS stimulated MSC upregulate myocardial VEGF expression and enhanced MSC survival of engrafted MSCs [59].

Physical preconditioning

Physical preconditioning strategies involve the application of shear stress, cell cultivation on hydrogels or irradiation [47]. Irradiation in particular has been shown to promote the angiogenic capacity of different cell types. Irradiation induces apoptosis, the process of programmed cell death, which has been shown to be involved in regenerative capacities as it mediates mitogenic signals that promote stem cell proliferation [60].

Irradiated mouse embryonic fibroblasts induced wound healing and tissue regeneration via caspases-3 dependent pathways. Li and colleagues reported that caspse-3 activates inducible phospholipase 2 (iPLA2) that enhances the secretion of PGE2. PGE2 stimulated stem cell proliferation, contributing to enhanced tissue regeneration [61]. These data are in line with those of Huang et al who showed that radiotherapy enhances tumor cell proliferation *in vitro* and *in vivo* via caspase-3 mediated PGE2 secretion. Loss of caspase-3 enhanced radiosensitivity and reduced proliferative capacity in response to irradiation [62].

Therefore, radiation is a promising preconditioning method. It can be easily utilized, it does not introduce any substances into the CM and it can be performed without the necessity of different cell cultivation steps [60].

8

10.6 Components of the cell secretome

The supernatant of cells contains not only proteins, but also lipids and extracellular vesicles. In the following paragraphs these different paracrine factors will be discussed in sequence, with special focus on factors released by apoptotic cells. To our knowledge there is no literature available that has investigated these components simultaneously in the conditioned media of cultured cells. So far each study has focused only on a selected class, without taking a comprehensive interaction of the different molecular classes into account. In contrast, in our study we have made a global evaluation of paracrine factors, and have therefore included proteins, lipids and extracellular vesicles in our final analysis.

10.6.1 Cytokines, chemokines, growth factors

Several cytoprotective, pro-angiogenic and immune-modulating secreted proteins have been identified in the supernatant of cells [41, 45, 63]. Pre-conditioning of cells with either hypoxia [36, 64, 65] or ionizing radiation [41, 44, 66] was shown to induce the secretion of these factors and to enhance the *in vitro* and *in vivo* potency of the conditioned media [44, 64-66].

Table 1 shows an overview of protein concentrations in conditioned media from irradiated and-non irradiated PBMCs. The table illustrates that IR is a strong stimulus for the secretion of several pro-angiogenic chemokines.

Table 1: Comparison of protein concentrations in the CM of non-irradiated and irradiated PBMCs

Soluble factors (ng/ml)	non-irradiated PBMC			irradiated PBMC			Sig.
	1×10^6	2.5×10^6	25×10^6	1×10^6	2.5×10^6	25×10^6	
CXCL8	1.74 ± 0.40	1.93 ± 0.09	10.49 ± 3.53	1.22 ± 0.29	2.30 ± 0.13	18.01 ± 2.87	nsns[¥]
CXCL1	0.17 ± 0.09	0.36 ± 0.09	2.06 ± 1.58	0.07 ± 0.02	0.48 ± 0.09	3.95 ± 0.93	nsnsns
CXCL5	3.41 ± 1.34	29.93 ± 3.41	34.89 ± 16.33	3.93 ± 1.43	37.86 ± 12.73	108.86 ± 27.88	nsns[¥]
CCL2	1.66 ± 0.65	0.47 ± 0.21	0.27 ± 0.00	0.76 ± 0.19	0.74 ± 0.17	0.27 ± 0.00	nsnsns
CCL5	8.32 ± 0.18	18.62 ± 3.21	37.63 ± 2.72	4.01 ± 0.05	22.25 ± 3.64	51.58 ± 4.44	nsnsns
HMGB1	0.63 ± 0.39	3.44 ± 2.11	33.57 ± 6.45	2.74 ± 0.27	6.46 ± 1.12	20.51 ± 3.62	ns ns[†]
MMP9	4.14 ± 0.91	14.59 ± 2.75	29.46 ± 8.29	0.99 ± 0.16	3.61 ± 0.59	19.35 ± 5.34	ns[†,‡]
sICAM-1	0.14 ± 0.04	1.43 ± 0.25	7.43 ± 0.85	0.42 ± 0.25	2.09 ± 0.42	9.40 ± 1.29	nsns[¥]
$VEGF_{165}$	0.13 ± 0.01	0.42 ± 0.04	0.82 ± 0.34	0.15 ± 0.02	0.64 ± 0.04	4.39 ± 1.22	nsns[¥]
CXCL9	4.84 ± 0.09	17.79 ± 0.95	13.24 ± 0.85	5.85 ± 0.22	20.15 ± 1.14	58.99 ± 1.17	nsns[¥]
PAI-1	1.25 ± 0.35	1.93 ± 0.29	49.60 ± 9.04	0.00 ± 0.00	5.06 ± 3.25	45.86 ± 1.43	nsnsns
IL-16	0.0 ± 0.0	0.11 ± 0.02	0.84 ± 0.31	0.00 ± 0.00	1.25 ± 0.07	5.25 ± 0.52	ns[‡,¥]
IL-1ra	0.35 ± 0.09	0.52 ± 0.17	2.16 ± 0.96	0.13 ± 0.04	0.41 ± 0.17	6.43 ± 1.33	nsns[¥]
IL-10	0.01 ± 0.00	0.00 ± 0.0	0.05 ± 0.01	0.02 ± 0.01	0.02 ± 0.01	0.06 ± 0.01	nsnsns
IGF-I	0.00 ± 0.00	0.01 ± 0.0	0.03 ± 0.02	0.00 ± 0.00	0.01 ± 0.01	0.03 ± 0.03	nsns ns
HGF	0.33 ± 0.08	0.16 ± 0.01	0.69 ± 0.19	0.11 ± 0.03	0.07 ± 0.02	0.79 ± 0.19	nsns ns
FGF-2	0.56 ± 0.02	0.53 ± 0.00	0.59 ± 0.01	0.48 ± 0.01	0.53 ± 0.02	0.55 ± 0.02	nsns ns
TGF-β	0.08 ± 0.01	0.10 ± 0.01	0.21 ± 0.07	0.06 ± 0.01	0.09 ± 0.02	0.39 ± 0.09	nsns ns
SDF-1	0.17 ± 0.0	0.19 ± 0.0	0.22 ± 0.03	0.16 ± 0.01	0.15 ± 0.07	0.12 ± 0.04	nsns ns
G-CSF	0.00 ± 0.00	0.00 ± 0.00	0.00 ± 0.00	0.00 ± 0.00	0.00 ± 0.00	0.00 ± 0.00	nsns ns
GM-CSF	0.00 ± 0.00	0.00 ± 0.00	0.07 ± 0.02	0.00 ± 0.00	0.00 ± 0.00	0.08 ± 0.02	nsnsns

PMBC were cultured in three different cell concentrations for 24 hours. Conditioned media were evaluated for selected proteins (n = 5)
ns $p > 0.05$ non-irradiated PBMC versus irradiated PBMC (of corresponding cell density)
[†] $p < 0.05$ 1×10^6 non-irradiated PBMC versus 1×10^6 irradiated PBMC
[‡] $p < 0.05$ 2.5×10^6 non-irradiated PBMC versus 2.5×10^6 irradiated PBMC
[¥] $p < 0.05$ 25×10^6 non-irradiated PBMC versus 25×10^6 irradiated PBMC

adopted from Lichtenauer et al. 2011 [42].

10.6.1.1 Proteome profiling and the albumin dilemma

The human genome codes for more than 45,000 genes, of which 21,574 are described as protein-coding [67], and approximately 10% of these transcripts code for secretory proteins [68]. It is thus clear that the analysis of cultured cell supernatants is very challenging.

Several different methods are available that can be used to detect the different biological components in the cell secretome. **Table 2** summarizes the most commonly used techniques.

Table 2: Techniques for protein analysis in conditioned media

Technique	Pros	Cons
Antibody & bead arrays	Specific and sensitive Reproducible	High costs per sample Non-specific reactions Availability of specific Ab Rapid digestion of proteins

Mass spectrometry
  2D
  DIGE
  ICAT
  iTRAO
  SELDI-TOF
	High numbers of proteins detectable
	Good sequence coverage
		Low concentrated proteins not detectable with 2-DE and DIGE
		Restricted reproducibility with 2-DE and DIGE
		Restricted dyamic range interfere with albumin

DNA microarray	High-throughput, quantitative method	Availability of nucleotide sequence Rare transcripts missed only expressed transcripts are detected atypical secreted proteins are not detected

This table summarizes different techniques for protein analysis in conditioned media.
2D 2 dimensional; DIGE difference gel electrophoresis; ICAT isotope coded affinity tag; iTRAO isobaric tag for relative and absolute quantification; SELDI-TOF surface-enhanced lacer desorption/ionization (adopted from Mukherjee et al. 2013 [69]).

As shown in **Figure 3** microarray analysis, RNA-sequencing in combination with bioinformatics are applicable for secreted proteins with known sequences, whereas antibody based arrays and mass spectrometry can detect proteins with unknown primary sequences.

Techniques used for known sequenzes	←	Secretory Proteins	→	Techniques used for unknown sequenzes
RNA seq	←	**-SP**	→	Mass Spectometry
Bioinformatics	←			
DNA microarry	←	**+SP**	→	Antibody / Bead Array
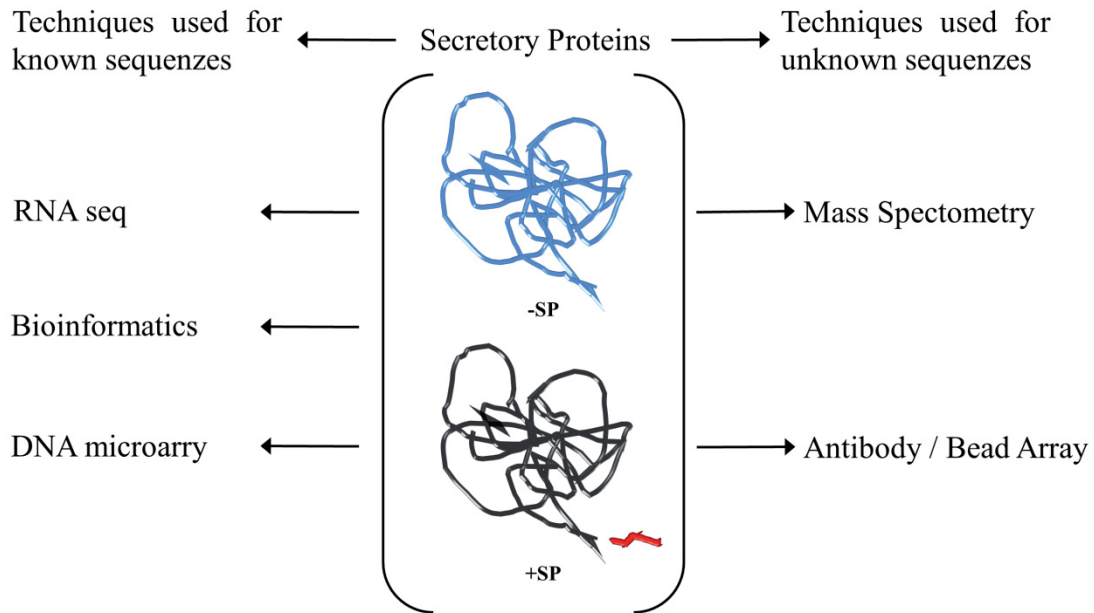
Figure 3: Methods used for secretome profiling. RNA sequencing, bioinformatics and DNA microarrays can be used if the amino acid sequence of the secreted proteins are known, or mass spectrometry if the sequences are unknown. (adopted from Mukherjee et al. 2013 [69])

Probably the most commonly used method is to detect proteins directly using either antibody based arrays or mass spectrometry techniques. Antibody based arrays generate reliable results and can detect proteins present at low concentrations in CM. However, the number of simultaneously detectable molecules is small, a specific antibody is needed and high costs per sample arise [69], thus making this technique unsuitable for the detection of high numbers of proteins.

Techniques based on mass spectrometry are powerful tools for detecting a high number of proteins in a single sample in one analytic run. The major disadvantage of these methods is the low sensitivity for the detection of proteins present at low concentrations, especially when working with cells cultured in serum containing media. Typically, cell culture media contains serum (e.g. fetal bovine serum) ranging from 5%-20%. The most abundant protein in serum is albumin, with an average concentration of 35-50 mg/l (= 35-$50*10^9$pg/ml). Albumen can thus mask the presence of low-abundance proteins (e.g. cytokines, chemokines). Furthermore small proteins, including many cytokines and chemokines are often not detectable using this approach.

To avoid the problem arising from serum proteins, several groups have used serum free media for cells cultured up to 72 hours prior to CM analysis, enabling mass spectrometry based analysis [70]. However, cell cultivation in serum free media might affect the secretion of paracrine factors and modulate the biological properties of the CM. For instance, serum starvation is a strong activator of multiple signaling pathways in primary human myotubes, human embryonic kidney cells and rat myotubes [75].

12

Moreover, 'serum free' media are distributed either with or without the ingredient albumin. Albumin may affect biological processes in cultured cells in a beneficial way, so that it cannot be excluded that the secretome of cells, cultivated with or without an albumin supplement has different regenerative effects. Although albumin can be removed by using immune-affinity depletion- [71, 72], or different chromatographic methods [73] a concomitant depletion of other proteins, especially those bound to albumin cannot be excluded [74].

Moreover, it has been shown by that albumin is a bio-active molecule that can interact with lipids, proteins and cell receptors, thereby regulating diverse cellular processes [76]. Researchers should keep in mind that 60% (~50g/l) of total serum protein consists of albumin and that more than half of total body albumin is located in the extravascular space, indicating its important role in maintaining homeostasis [77]. In cell culture systems albumin can serve as an antioxidant and protects against reactive oxygen species (ROS) mediated lipid peroxidation. Free ions such as Cu^{1+} or Fe^{2+} give rise of ROS in response to contact with dissolved oxygen. When bound to albumin these ions are less prone to activate ROS formation with resulting cell death [76, 78].

Furthermore, *in vitro* albumin-lipid complexes can maintain pluripotency of human embryonic stem cells. Removing lipids from albumin resulted in a loss of this cell self-renewal potency which was also detected to a smaller extent when albumin was digested using trypsin [79]. In human endothelial cells albumin inhibits apoptosis via activation of PI3K and Akt [80] and in cultured retinal precursors cells albumin augments cell proliferation in combination with EGF treatment [81].

In order to further evaluate whether albumin effects the secretory capacity of human PBMCs we have investigated the effects of variable albumin concentrations the CXCL1 and CXCL8 concentrations in the cell culture supernatant. As shown in **Figure 4** cell cultivation without albumin supplement reduces the paracrine capacity of cultured PBMCs.
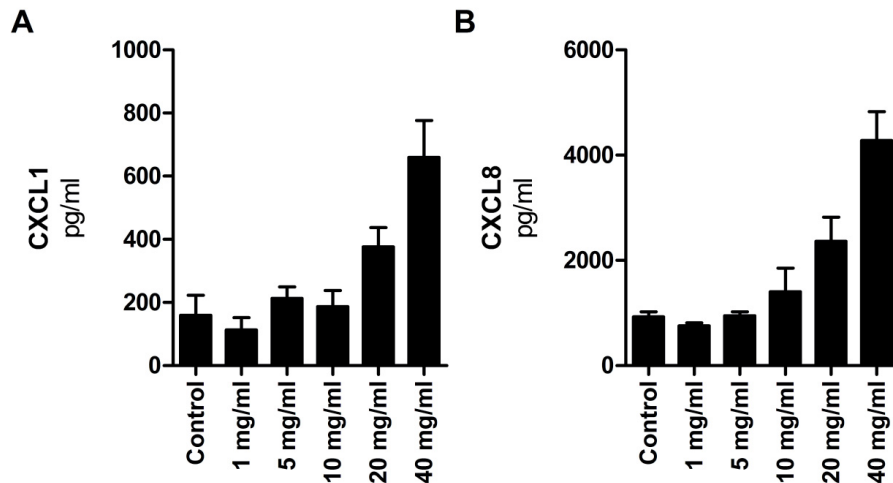
Figure 4: Albumin induces secretion of CXLC1 and CXCL8 in human PBMCs. 1Mio/ml PBMCs were cultured for 24 hours with increasing concentrations of albumin. Albumin induces the secretion of both CXCL1 and CXCL8 in human PBMCs in a dose dependent manner. (unpublished data)

In summary, cell cultivation in serum free or albumin free media can severely influence cellular processes and might have an impact on secreted paracrine factors, and should therefore be avoided whenever possible. This must be considered especially when comparing studies using different cultivation protocols and when changing an established preexisting protocol to fulfill regulatory requirements. On the other hand, serum, or albumin supplementation in particular, interferers with mass spectrometry methods, thereby lowering the detection rate of proteins present at low concentrations. Because of these procedural and technical problems the protein analysis in cell culture supernatants can be a challenging issue with diverse putative pitfalls.

DNA microarrays and next generation sequencing (ref-Seq) techniques in combination with bioinformatics as tools have been proposed to be suitable techniques that permit the analysis of the protein content of albumin containing cell culture supernatants [63, 69, 82]. A DNA microarray is a small glass, nylon or silicon chip onto which DNA from several different transcripts is printed, spotted or synthesized [83]. In general two different microarray technologies exist: cDNA and oligonucleotide based platforms. The former are spotted with cDNA from PCR-amplified segments on glass slides. These cDNA microarrays are less expensive, however only a limited number of probes can be detected with one chip. Furthermore, as on each chip RNA samples of 2 entities (e.g. treatment vs. control) are plotted and labeled with different dyes, only a direct comparison of these two samples is possible, whereas a direct comparison with other samples is not feasible. The second type of DNA microarrays are oligonucleotide microarrays which are commercially available from manufactures such as Agilent, Illumina or Affymetrix. Single oligonucleotides are spotted on these chips, which increases the total number of detectable transcripts per chip.RNA samples are hybridized to each oligonucleotide. Therefore two microarrays are needed for

14

comparison of two samples [83]. Approximately 200,000 probes are spotted on Affymetrix microarrays, enabling the detection of the whole human genome simultaneously. In addition to each human gene, at least 11 oligonucleotide sequences are spotted on the chip, therefore minimizing hybridization errors and improving the reliability of the results [83].

Hence microarray analysis is a commonly available, reproducible technique, providing an overview of all genes expressed in a sample at a given time point. The disadvantages of this method are: 1) The lack of detecting passively released proteins (e.g. during cell necrosis); 2) Genes expressed at low levels will not be detected. 3) The amino acid sequence of the protein must be known. 4) Gene expression does not necessarily correlate with protein expression. Once a given gene list is constructed, a subsequent bioinformatics workup is needed to screen for genes coding for secretory proteins. This *in silico* secretome profiling is based on the fact that secreted proteins have a signal peptide sequence that shows a highly conserved structural composition: a positively charged hydrophilic N-terminus followed by a hydrophobic core and a hydrophilic C-terminus at the -3 and -1 position relative to the cleavage site [82]. Several bioinformatics programs can identify this classical SP in a sequence list of given proteins

A class of atypically secreted proteins does not share a SP and thus cannot be predicted by programs such as SignalP [82]. Typically, membrane shed proteins, exosome proteins and other secretory vesicles belong to this class of secreted proteins. Therefore, bioinformatics tools such as SecretomeP have been developed based on the assumption that extracellular proteins display specific characteristics regardless of the pathway by which they are released [85, 86].

The above mentioned tools positively select proteins and assign them as secreted proteins. To remove the number of false positives, a further bioinformatics analysis should be coupled with the tools described above. The membrane protein prediction program TMHMM (trans-membrane hidden Markov model) is a free web based program that identifies transmembrane helices of proteins. Proteins possessing transmembrane helices are rather membrane anchored proteins than secreted proteins [87]. Therefore, TMHMM displays a filter function to reduce false positive results generated by SignalP and SecretomeP programs. **Figure 5** presents a schematic summary of a transcriptomics based secretome analysis.
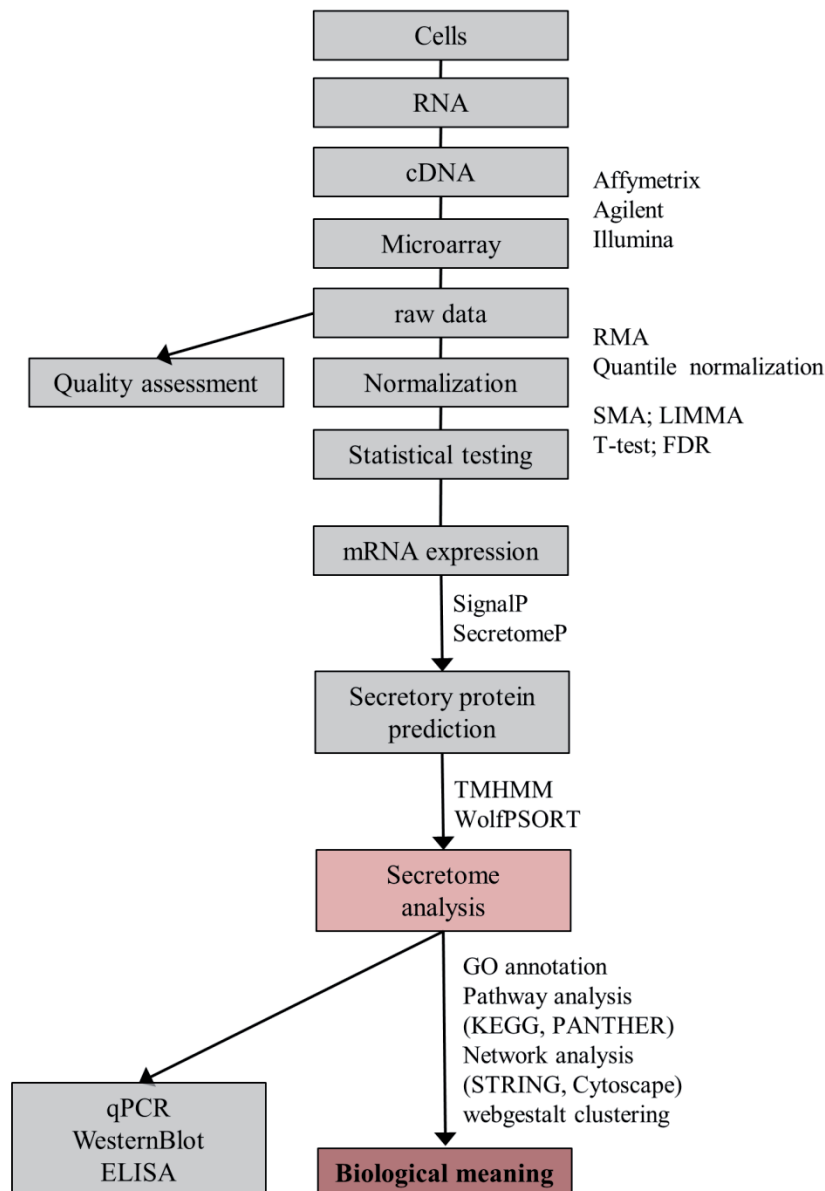
Figure 5: Experimental workflow of a transcriptomics based secretome analysis. Starting from cellular RNA the mRNA expression can be identified by performing microarray analysis. The bioinformatics tools SignalP and SecretomeP are able to identify secretory proteins, whereas the two programs TMHMM and WolfPSORT identify proteins with transmembrane helices, thus indicating that these proteins are less likely to be secreted. Ultimately, the biological relevance of the identified transcripts can be assessed using GO-term analysis and canonical pathway analysis.

Several studies have been published in the last decade which have used bioinformatics based secretome analysis to uncover secreted proteins. Szalowska et al. performed microarray analysis in combination with isotope-labeled amino acid incorporation rates to detect secretory proteins in the supernatant of human liver and adipose tissue. They were able to show that the microarray data correlated highly significantly with proteomic data [88]. Mutch et al. investigated the secretome of differentiating human preadipocytes, using microarray based secretome prediction in combination with proteomics. They identified 18 novel secretory proteins upregulated in differentiated adipocytes [89]. A combination of these three different computational tools can be successfully used to discover newly secreted

proteins, especially in experimental settings in which mass spectrometry does not provide satisfying results [69, 82]. Korf-Klingebiel *et al.* have investigated the ability of paracrine factors released by bone marrow cells to promote myocardial repair following acute myocardial infarction. [63]. They used the above mentioned bioinformatics programs to identify secreted proteins. Subsequent *in vitro* and *in vivo* experiments revealed that a protein named myeloid-derived growth factor (C19orf10) is a crucial mediator in cardiac regenerative pathways and promotes tissue repair. This study summarizes the experimental workflow beginning with the identification of secreted paracrine factors, then the *in vitro* testing to uncover the biologically active components, and eventually the evaluation of these factors in *in vivo* experiments.

In conclusion, each of the methods mentioned has its advantages and disadvantages. Both transcriptomic and proteomics based approaches have been identified as powerful tools in the analysis of secreted proteins when performed correctly. It is the researcher's responsibility to select the most suitable method based on the experimental conditions.

10.6.2 Lipids

Apoptosis is an active rather than a passive process of cell death, and aims to avoid injury of surrounding cells by preventing the release of inflammatory or intracellular components [90]. A growing number of publications have revealed that apoptotic cells release lipids which exert paracrine activity [91]. In 2003 Lauber and colleagues showed that apoptotic cells stimulate cell migration and phagocytosis via the release of soluble lysophosphadylcholine (LPC) in a caspase-3 dependent manner [92]. Caspase-3 is an activator of the calcium-independent phoshpolipase A_2 ($iPLA_2$) which is the primary enzyme generating LPC. Subsequent work showed that the so called "find me" signals released from apoptotic cells are either soluble or membrane bound lipids which act as chemoattractants [93, 94]. LCP, ATP, UTP or CX3CL1 are known chemoattractants for monocytes, neutrophils and macrophages [94]. Additionally, apoptotic cells need a further signal called "eat-me" in order to be cleared. Especially oxidatively modified phosphatidylserine is a strong "eat me" signal for phagocytes and therefore enhances clearance of apoptotic cell fragments [95, 96]. The importance of lipid peroxidation in terms of their ability to induce phagocytosis is highlighted by the fact that non-oxidized phosphatidylserine is constantly detectable on the outer cell membrane in different cell types under physiological conditions. Non-oxidized phosphatidylserine does not induce clearance of these cells whereas oxidized phosphatidylserine is a strong chemoattractant [97]. Moreover, necrotic cells present phosphatidylserine in variable amounts on their cell surface [98] without the activation of the

phagocyte system [94]. These data highlight that oxidized lipids can activate the immune system and clearance of damaged cells.

In addition, arachidonic acid (AA) and its derivative prostaglandin E2 (PGE$_2$) are lipids known to be released from apoptotic cells. The formation of AA is caspase-3 dependent. iPLA$_2$ activates AA by cleaving a phospholipid molecule that gives rise to PGE$_2$. PGE$_2$ has been shown to promote angiogenesis *in vivo* and *in vitro* via activation of the Wnt/β-catenin pathway [62, 99]. This IR induced pro-angiogenic and wound healing pathway has been described by Li et al. as the 'Phoenix Rising Pathway' [61]. The role of caspase-3 as a key player in this regulative network has recently been highlighted by a sophisticated bioinformatics analysis which calculates the individual impact of 17 molecules described in the 'Phoenix Rising Pathway'. While knockdown of caspase-7 showed only minor effects, the knockdown of caspase-3 significantly reduced PGE$_2$ production [100].

Similar results were obtained by a study investigating the effects of paracrine factors, released from apoptotic pancreatic β-cells, on the regenerative capacity of neighboring cells. The supernatant of β- cells but not the cells themselves undergoing caspase mediated apoptosis have been shown to induce regenerative gene expression in surrounding cells. This effect was mediated via shedding of annexin-V positive microvesicles from apoptotic cells [101].

In **Figure 6** the current knowledge on paracrine pathways activated by caspase-3 are summarized.
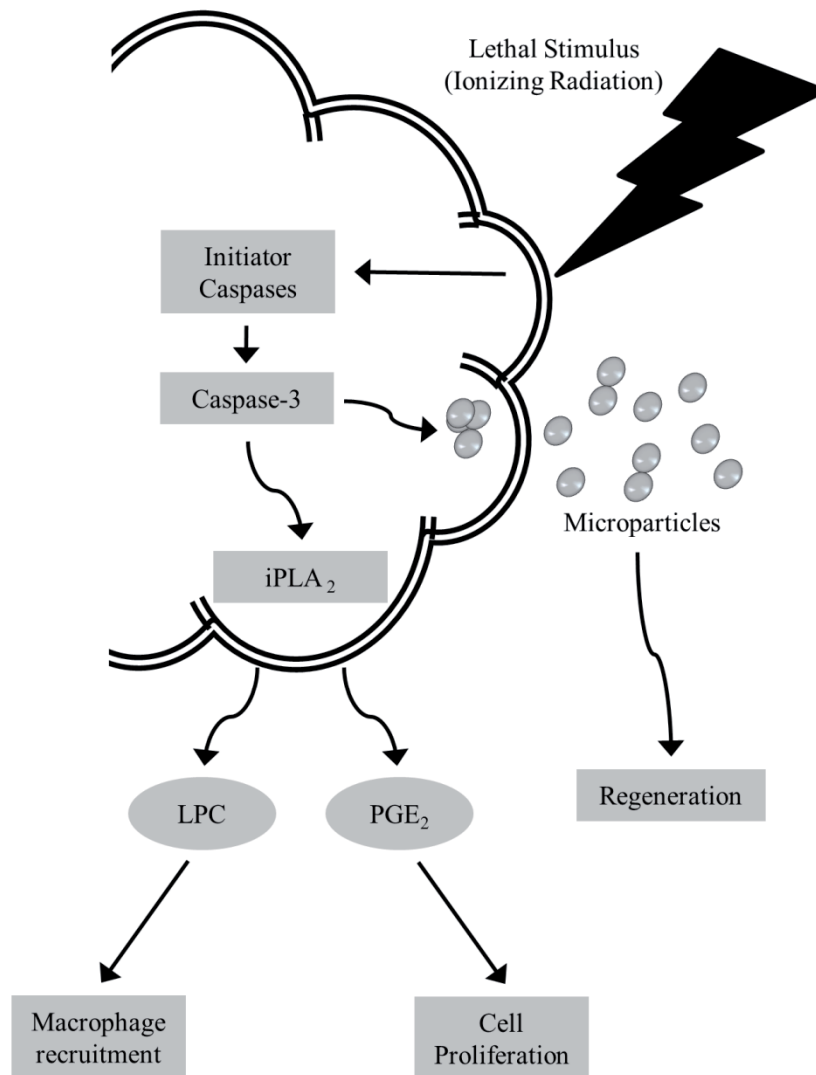
Figure 6: Paracrine factors released from apoptotic cells: Different stimuli are able to induce activation of the caspase-cascade eventually resulting in the cleavage/activation of the effector caspase-3. Caspase-3 activates $iPLA_2$ which itself stimulates extracellular release of LCP. LCP is a known chemoattractant for macrophages. Furthermore, $iPLA_2$ activates production of AA and PGE_2 that exert pro-angiogenic and proliferative effects. Shed microparticles from apoptotic cells may promote regenerative effects. (adopted from Boland et al. 2013; Jager et al 2012; Sebbagh et al. 2001 [91, 102, 103])

10.6.3 Extracellular vesicles

Although observed more than 40 years ago [104,] small membrane coated extracellular vesicles (EVs) have gained growing scientific interest in the last years [105]. These vesicles are currently deemed to play an important role in intercellular communication.

Several attempts have been carried out in order to establish a commonly accepted classification of EVs [106]. The currently most utilized classification defines three distinct classes of EVs, namely apoptotic bodies, microparticles (MPs) and exosomes [107]. In **Table 3** the main characteristics, isolation methods and molecular markers of these three different

classes of EVs are presented. In the following paragraphs a short description of each EV class will be given focusing on the effects of apoptosis associate EV release.

Table 3: Extracellular vesicles: Comparison of morphological and physiochemical characteristics between exosomes, microparticles and apoptotic bodies.

Feature	Exosomes	Microparticles	Apoptotic Bodies
Size	50-100 nm	100-1,000 nm	500-5,000 nm
Density in sucrose	1.13-1.19 g/ml	ND	1.16-1.28 g/ml
Shape by ELMI	Cup shape	Irregular shape and electron-dense	Heterogeneous
Sedimentation	100,000 g	10,000 – 20,000 g	1,000 – 2,000 g
Markers	Tetraspins (CD9, CD63, CD81), Alix, LAMP1, Tsg101	Tissue factor, CD40 Ligand, PS	PS, histones, genomic DNA
Biogenesis	Exocytosis from MVB	Cell surface ectocytosis and membrane shedding	Apoptotic blebbing and fragmentation
Contents	miRNA, RNA, Proteins, Lipids	miRNA, RNA, Proteins, Lipids	Cell organells, Proteins, DNA, RNA, miRNA
Cell membrane characteristics	Membrane impermeable (PI negative)	Membrane impermeable (PI negative)	Membrane permeable (PI positive)

MVB multi vesicular bodies; PS phosphatidylserine; PI propidium iodide, ND not defined; adopted from Kowal et al. 2014; Ling et al. 2011; Thery et al. 2009 [105, 107, 108]

10.6.3.1 Apoptotic Bodies

Apoptotic Bodies are the largest class of EVs with a diameter above 1,000 nm. Whereas exosomes and MPs are released from viable cells, the release of apoptotic bodies is a coherent process associated with the execution of programmed cell death [109]. Furthermore, apoptotic bodies contain intracellular organelles as well as genomic DNA. Propidium iodide can therefore be used to identify apoptotic bodies, as propidium iodide binds to DNA which can then be detected by FACS analysis [110]. Whereas it has been assumed that apoptotic cells in general and apoptotic bodies in particular are characterized by the maintenance of an intact plasma membrane and retention of intracellular/intravesicular components, new data reveal that the membrane of apoptotic bodies is leaky and therefore limited membrane permeation occurs even in early stages of apoptosis [111].

The formation of apoptotic bodies is mediated via the contraction of actomysin. Actomyosin is under control of the ROCK1 kinase [103, 112] which is activated via caspase-3 cleavage [103, 112]. The efficient clearance of apoptotic bodies enables cells to prevent the release of intracellular organelles. Apoptotic bodies are detected by phagocytes via the presence of plasma membrane modification of lipids, proteins and carbohydrates, enabling a selective clearance of apoptotic cell fragments. These markers should be selectively expressed on apoptotic bodies. Oxidized phosphatidyl serine has been shown to act as a scavenger receptor which acts as the driving force in promoting phagocytosis [95]. Apoptotic cells display an enrichment of oxidized phospholipids that are further enriched in the cell membrane of apoptotic bodies [113].

10.6.3.2 Microparticles

Microparticles (MPs), also referred to as microvesicles are smaller than apoptotic bodies (100-1,000 nm) and are released differently. MPs are formed via the outward budding and division of the plasma membrane. The ADP-ribosylation factor 6 (ARF6) is crucial for MP shedding as it activates a signaling pathway involving phoshpolipase D (PLD), extracellular signal-regulated kinase (ERK) and myosin light-chain kinase (MLCK), which triggers release of microparticles [110]. Like exosomes, the composition of different molecular classes is significantly different in microparticles of different donor cells. The outer side of the plasma membrane is highly enriched in phosphatidyl serine, which can be used to detect microparticles in FACS analysis, based on their ability to bind annexin-V. MPs contain selected species of miRNA, proteins and lipids and mediate intercellular transfer of these factors [114, 115]. Apoptotic cells have been shown to release higher amounts of microparticles in comparison to non-apoptotic cells [116] suggesting that apoptotic pathways are involved in the biogenesis of this class of EV.

10.6.3.3 Exosomes

Exosomes are the smallest class of EV. They are formed via intraluminal budding of the endosomal lumen. These newly formed intraluminal vesicles (ILV) fuse and aggregate to give rise of the multivesicular bodies (MVB). Exosomes are stored in MVB, and upon stimulation, the MVB fuse with the cell membrane and release exosomes in an exocytic manner [105].

Because of their intracellular origin exosomes are highly enriched in lysosomal and endosomal proteins, whereas mitochondrial or cytoplasmatic proteins are nearly absent. Furthermore, exosomes contain high amounts of functional miRNA and mRNA. Exosomes can transfer miRNA and mRNA from donor to recipient cells, thereby modulating biological processes [117]. Using next generation sequencing other small non-coding RNA species can

21

also be detected in exosomes [118]. Because of the enrichment of small RNAs in exosomes in comparison to the cytosol it is hypothesized that small RNAs are selectively recruited and sorted into exosomes [105, 119]. However, the exact mechanism has not yet been described.

A further molecular species investigated in exosomes and associated with their function are lipids. According to the literature exosomes are enriched in sphingomyelin, phosphatidyl serine, ceramide and in part cholesterol, whereas PC is present in lower amounts compared to the donor cells [120]. However, recent studies have revealed that although overall PC components are relatively low in exosomes, selective PC subgroups such as lyso-PC are significantly enriched in the exosome compartment [121].

In order to collect proteomic, lipidomic and transcriptomic data from exosomes the database Vesiclepedia [122] and EVpedia [123] were founded in 2012 and 2013 respectively.

Only a few studies have so far investigated the effect of apoptosis activation on the biogenesis of exosomes. Yu et. al were able to show that IR (5 Gy) stimulates exosome release in a p53 mediated manner. It has been suggested that these vesicles were released by a non-classical secretion pathway via the endosomal compartment [124]. This work was further corroborated by Sioris et al. who identified a caspase-3 dependent exosome secretion pathway in apoptotic endothelial cells. These exosomes contained the translationally controlled tumor protein (TCTP) which was responsible for the anti-apototic exosome effects on smooth muscle cells [125]. In addition, IR has been shown to increase the absolute number of released exosomes in astrocytes and glioblastoma cells and modulate the miRNA and protein content in exosomes [66]. Interestingly, these effects were observed in tumor cell lines lacking p53, previously shown to be a crucial factor for IR enhanced exosome release [124, 126].

10.6.4 Paracrine factors as therapeutics in regenerative medicine

Cell free strategies using soluble or vesicle bound factors display several promising advantages in comparison to cell based therapies in the field of regenerative medicine. While the latter are governed by strict legal requirements the former can be easily utilized for clinical trials. Paracrine factors can be quantified more easily and are less complex in their composition compared to cellular therapies. In addition, soluble proteins or extracellular vesicles can be produced generically and serve as either stand alone therapies or can be used as drug carriers (e.g. exosomes as carriers for endogenous small RNAs or proteins).

10.6.4.1 Unprocessed paracrine factors for therapeutic delivery

Probably the most obvious utilization of paracrine factors as therapeutics is to use the factors directly upon harvest, without any further processing steps. Microparticles and exosomes are currently the most commonly investigated components in the field of regenerative medicine and tissue engineering [22]. EVs are purified from cell culture supernatants by a serial centrifugation protocol, immunoprecipitation, or chromatographic methods [127, 128]. Although considerable improvements have been achieved in the isolation protocols for EVs, several published investigations did not distinguish between exosomes and microvesicles, thereby making it difficult to determine whether, and if so, to what extent exosomes or MPs exert the beneficial effects. However, other studies have shown that EVs alone can be used for therapeutic interventions [129]. In order to enhance the cellular capacity to release EVs, Lim and co-workers have developed a method whereby oncogenic immortalized human embryonic stem cell-derived MSCs release EVs that are biologically active. An advantage of these methods is that exosomes can be produced in infinite amounts, thus reducing the production costs[130]. While genetic manipulation of donor cells in the field of cell based regenerative medicine is inadmissible, these types of interventions can be applied when genetically modified cells are exclusively used for the production of paracrine factors without the possibility of any direct *in vivo* contact with the donor.

10.6.4.2 Engineered paracrine factors as alternatives for cell therapies

Although straightforward utilization and administration of paracrine factors is of value the potential of these factors can be further improved by biomedical engineering. EVs can be loaded with small regulatory RNAs, proteins or drugs that exert additional therapeutic effects. A landmark paper was published in 2011 by Alvarez-Erviti and colleagues. They were able to generate a tissue specific delivery of short interfering (si)RNA to the brain in mice. EVs obtained from murine dendritic cells were transfected with Lamp2b, an exosome membrane protein, with a central NS-specific targeting peptide sequence. These EVs were selectively delivered to oligodendrocytes, microglia and neurons in the brain, leading to a tissue specific knockdown of BACE1 mRNA and protein levels [131], BACE1 being a protease involved in neurodegenerative diseases in wild type mice.

Others have shown that EVs can be loaded with drugs (e.g. doxorubicin [132]) that can be used for targeted cancer therapy, thus avoiding unspecific organ toxicity. Interestingly, beside mammalian cells, EVs can also be isolated from plants, and can be used to deliver therapeutic drugs, proteins, and short RNA and DNA expression vectors to target cells [133, 134].

10.6.5 Regulatory requirements for cell free therapies – implementations for clinical trials

While the effects of paracrine factors can be investigated in preclinical studies without special regulatory requirements, their application in human trials harbors several pitfalls. In the following paragraph the most important regulatory restrictions will be discussed.

Figure 7 depicts the selected issues that must be considered when investigating the effects of paracrine factors in clinical trials.
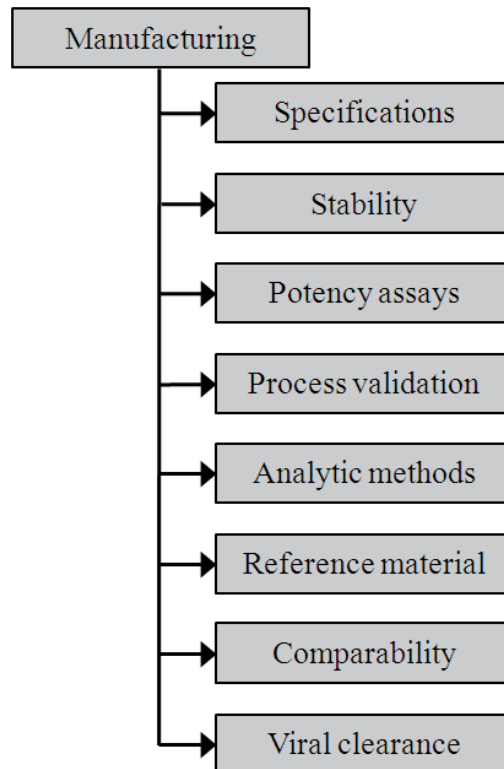
Figure 7: Schematic workflow for issues that must be considered before conducting a clinical trial using paracrine factors.

Firstly, researchers must describe the conditioned media in terms of its appearance, its content, and its purity and impurities. The term 'impuritities' summarizes product-related impurities, process-related impurities and contaminants. Whereas product-related and process-related impurities cannot be avoided, the presence of contaminants (e.g. bacteria, adventitious agents) can be prevented. Once the content of a material has been described its stability must be investigated. Commonly, the concentration stability of proteins present in the conditioned media is used for this purpose. Furthermore, the biological activity using potency assays over a given time period can be used to assess the stability of paracrine factors. Testing the biological activity requires the knowledge of suitable test systems that provide reliable test results. Potency is especially important as it can be used to compare the biological activity of different product batches [135].

Furthermore, all experimental setups and materials used for cell cultivation must be validated by the authorities and approved for use in clinical trials. It is prohibited to use cell culture medium that contains indicator dyes (e.g. phenol red) or serum components. In order to compare different product batches a valid reference material must be defined. The comparability of different product batches in terms of their content and biological function is a further important issue if different batches are used in clinical trials. To prove comparability of different product batches either the concentrations of lead product ingredients (e.g. growth factors, cytokines) or their biological activity can be determined.

To fulfill safety issues for clinical trials it must be shown that the conditioned medium is free from pathogens (e.g. bacteria, viruses). These pathogens can either be incorporated during the manufacturing process (e.g. contaminated cell culture material) or can originate from the cultured cells themselves (e.g. hepatitis infected donors). Therefore, regulators recommend using at least two different pathogen eliminating methods during the manufacturing process [136]. The most commonly used methods for pathogen reduction are given In **Table 4** (adopted from [136-138]).

Table 4: Pathogen reducing methods

Method	Advantages	Disadvantages	Pitfalls
Pasteurization	Inactivates both enveloped and non-enveloped viruses	Inactive against parovirus-B19 and in part hepatitis viruses	Temperature Duration Stabilizer concentrations
Chromatography	Purifies proteins Can be effective against both enveloped and non-enveloped viruses	Efficacy is highly variable depending on the selected virus . Resin must be cleaned between batches Sophisticated method	Resin contamination Protein elution profiles
Nanofiltration	Effective against enveloped viruses Preserves protein structure Enrichment of small molecular weight proteins	Ineffective elimination of small viruses Pore size determines virus removal Hazard of filter defects that may not be detected	Ratio of produce volume to filter surface area Filter integrity Pressure
Gamma-Irradiation	Effective against large viruses Easy to perform No risk of contamination	Ineffective against small viruses Might change protein structure	Irradiation dose Temperature stability
Precipitation	Effective against both enveloped and non-enveloped viruses Purifies proteins	Sophisticated method In general low virus removal	Suitable precipitation agents Precipitation agents can contaminate the supernatant Protein concentrations, pH and ionic strength
UV Methylene-blue	Effective against enveloped virus	Not effective against non-enveloped virus	Contamination of methylene blue in the final product Light intensity must be defined
Terminal dry heat	Effective against both enveloped and non-enveloped viruses	Requires at least 80°C for elimination of hepatitis viruses Lyophilization and freezing procedure might modulate ingredients	Stabilizer concentration Freeze cycle Lyohpilization cycle
Vapour heat	Effective against both enveloped and non-enveloped viruses	Complex method Lyophilization and freezing procedure might modulate ingredients	Freeze and lyophilization cycle needed
Acid pH	Powerful against enveloped viruses easy to perform	lacks efficiency against non-enveloped viruses can denature proteins	pH Temperature Duration

adopted from WHO report 2004; Gauvin et al. 2010; Nims et al. 2011

The most appropriate methods should be selected based on the type of product, the type of expected viruses and bacteria and the characteristics of the manufacturing process. A combination of two or more virus inactivation steps is recommended if a high viral load is expected and if one method alone would not cover enveloped and non-enveloped viruses appropriately. In addition, it must be proven that the selected methods do not affect the clinical potency of the final product. Regulators require a detailed description of the implemented viral clearance methods, describing how a method is incorporated into the manufacturing process [136].

The implementation of pathogen reducing steps is a challenging issue for researchers commencing with human studies However, the strict adherence to safety requirements not only protects study patients, but also the principle investigator against experiencing adverse events [136].

10.6.6 Products deserving the 'Good manufactured' label– from bench to bedside

In order to make the use PBMC supernatants possible in clinical trials. our laboratory has established a production pipeline of PBMC supernatants in accordance with GMP guidelines, and fulfilling the above mentioned regulatory requirements, Instead of using phenol red and bovine serum containing cell culture media we used phenol red free and serum free GMP approved media. The ingredients of our cell culture media used were albumin, transferrin and insulin, and met GMP standards.

We further established two different viral reduction steps (IR and methylene-blue) during the production process. In two xenograft preclinical studies we were able to show that CM from human PBMCs, produced in accordance with GMP guidelines, was able to attenuate neurological damage following ischemic stroke [139] and spinal cord injury [140]. However, the question still remained whether, and if so, to what extent the process of viral reduction influences the cell supernatant composition and the *in vivo* efficacy in comparison to non-processed conditioned media.

10.7 Apoptosis

The term 'Apoptosis' (Greek: *apo* = off, away + *ptosis* = a falling) was coined by Kerr, Wyllie and Currie in 1972, and describes a cellular death phenomenon which displays characteristic morphological changes[141]. Research during the following decades revealed that apoptotic processes are involved not only in normal development and morphogenesis, but are active during the while lifetime of an adult organism. [142]. The number of apoptotic cells in different tissues and developmental stages highlight the abundance of this form of cell death. Every day 1×10^{11} circulating neutrophils undergo apoptosis[143] and more than 3000 erythrocytes

each second enter programmed cell death [144] and are eliminated in the reticulo-endoplasmatic system in spleen and liver, or are phagocytosed by immune cells [144]. 95% of all thymocytes originating in the thymus were negatively selected and undergo apoptosis in order to remove auto-reactive cells targeting endogenous antigens [145]. Even tissues with low cellular turnover such as the mammalian brain remove up to 50% of cells during morphogenesis [146].

10.7.1 Morphological changes of apoptotic cells

Programmed cell death displays characteristic morphological features (reviewed in [147]) such as nuclear shrinkage and chromatin condensation, a process called pyknosis. Apoptotic cells are generally smaller in size compared to non-apoptotic cells, and their organelles are compactly arranged. Electron microscopy reveals that the condensed chromatin is enriched in the peripheral areas of the nucleolus. In later stages of apoptosis, plasma membrane blebs called apoptotic bodies are "budded" from cells. Apoptotic bodies are crowded with organelles and nuclear fragments. Although it was previously thought that the plasma membrane of these apoptotic bodies prevents the release of intraluminal contents [147, 148], it has recently been shown that it is in fact leaky, and several proteins are released from these vesicles [111]. Numerous membrane bound and soluble molecules from these apoptotic bodies initiate a rapid activation of phagocytes, which quickly phagocytose these vesicles and thereby inhibit development of secondary necrosis and release of intravesicular compartments [147, 148].

10.7.2 Caspase Cascade

Apoptosis can be initiated either via binding of death ligands to death receptors on the cell surface, resulting in the formation of the death-inducing signal complex, or through initiation of mitochondrial outer membrane permeabilization [149]. Caspases are cysteine proteases of the interleukin-1 beta-converting enzyme family crucially involved in controlling apoptosis and inflammation [90, 150]. They are produced as inactive monomeric zymogens known as pro-caspases. Caspases can either undergo auto-activation or are cleaved by other active caspases. Cleaved monomeric enzymes must dimerize in order to gain full activity [90]. Based on their primary structure caspases can be classified into three subfamilies. Caspase-2, Caspase-8, Caspase-9 and Caspase-10 belong to the apotosis initiator or activator caspases. Their substrates are other inactive pro-caspases, which are thereby activated. The executioner or effector caspases, caspase-3, caspase-6 and caspase-7 must be cleaved by activator caspases, and subsequently form dimers. Upon cleavage, effector caspases can auto-activate each other caspases, resulting in a positive feedback loop enhancing effector caspase activation [90, 150].

The two different currently accepted pathways that result in the activation of the caspase cascade are discussed in the following paragraphs. **Figure 8** presents an overview of the extrinsic and intrinsic signaling pathway activated during the caspase cascade mediated apoptosis.

10.7.3 Extrinsic signaling pathways

Extracellular mediators such as FasL, TNFSF10 (tumor necrosis factor ligand superfamily member 10, TRAIL), or TNF (tumor necrosis factor) have been shown to initiate the apoptotic program through transmembrane receptor mediated signal transduction[151]. These mediators bind to death receptors which transmit their signal to the intracellular adaptor molecule FADD (Fas associated via death domain), which itself activates caspase-8. The complex of the death receptor (e.g. FasL receptor) FADD and activated caspase-8 constitute the death inducing signaling complex (DISC) which transduces the extracellular signal for downstream induction of apoptosis [149]. The target of caspase-8 cleaves pro-caspase-3, thereby releasing the active enzyme which can then act as an executioner caspase [147, 149].

10.7.4 Intrinsic signaling pathways

The intrinsic signaling pathway can be activated by different stimuli such as irradiation, DNA damage, cell starvation, or growth factor deprivation. It is regulated by proteins containing BH3-only protein domains which themselves modulate the balance of pro- and anti-apoptotic BCL-2 family members. Under normal conditions the activity of pro-apoptotic BCL-2 proteins Bax and Bak is counterbalanced by members of the anti-apoptotic group Bcl-2, Bcl-w, Blc-B, AI and Mcl. Upon apoptotic triggering BH3 proteins activate Bax/Bak which are located at the mitochondrial outer membrane (MOM) resulting in MOM permeabilization and the release of several apoptosis-regulating mediators. Among these mediators cytochrome c is necessary for the induction of oligomerization and activation of the apoptotic protease activating factor-1 (Apaf-1), as well as procaspase-9, thereby initiating apoptosome formation [147]. Subsequently, the apoptosome initiates activation of caspase-3 and caspase-7 [142, 149].

10.7.5 The Execution Pathway

Both the intrinsic as well as extrinsic pathways converge in the activation of caspase-3, which is a key player for the execution of apoptosis, and which is activated by any of the initiator caspases [92]. Beside caspase-3, the two executioner caspases (caspase-6 and caspase-7) activate several proteins such as cytokeratins and cytoskeletal protein alpha. Caspase-3 mediates the blebbing of apoptotic vesicles via activation of Rho-associated coiled-coil containing protein kinase 1 (ROCK1) [103, 112]. Furthermore, caspase-3

contributes to externalization of phosphatidylserine to the outer cell membrane, which then acts as a strong chemoattractant signal for phagocytes [147].
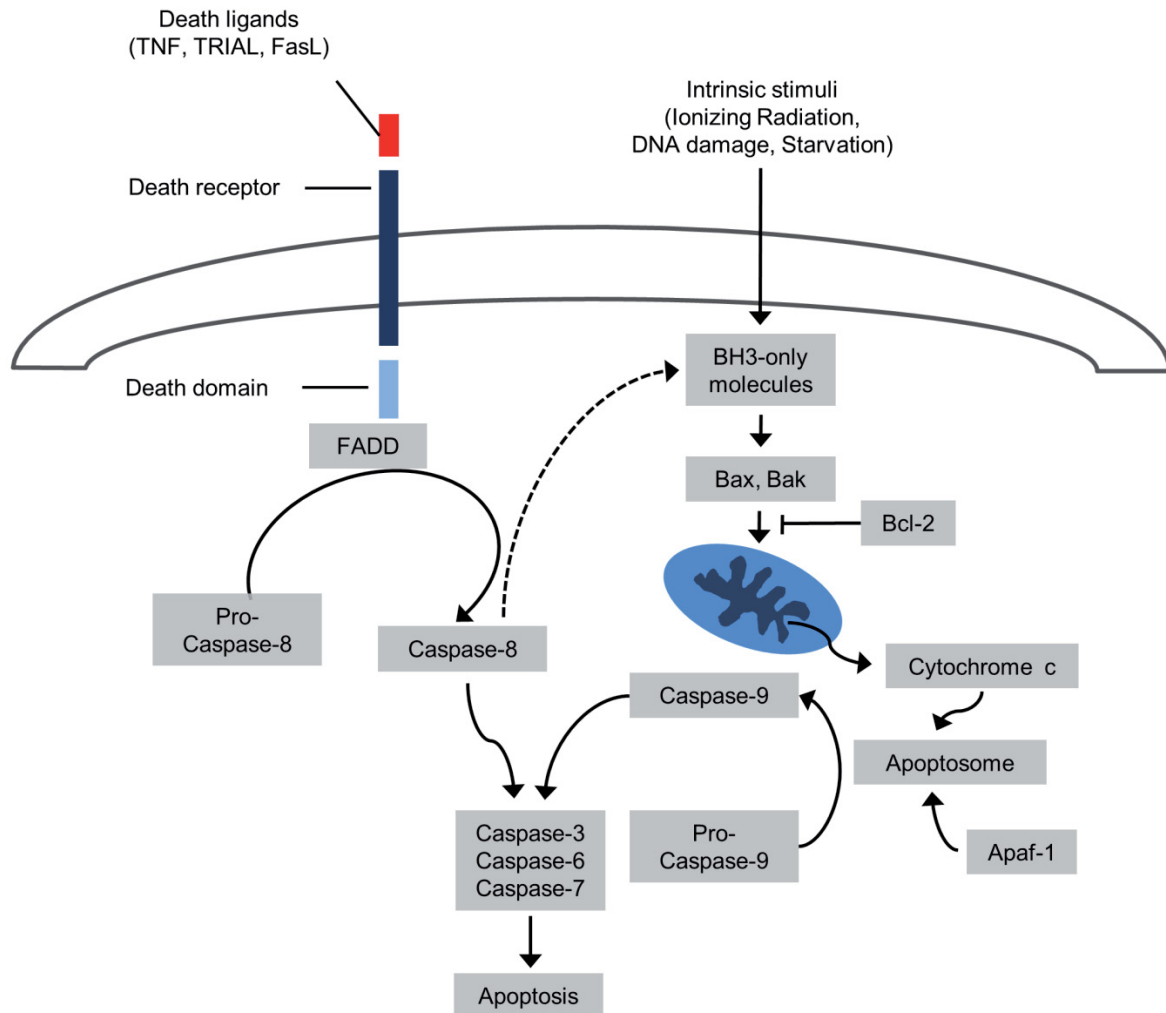
Figure 8: Caspase cascade activation induces apoptosis via extrinsic and intrinsic signaling pathways. The extrinsic pathway is activated by binding of death inducing ligands to their corresponding death receptors. After recruitment of the adapter proteins FADD, this complex associates with pro-caspase-8, activates it, and forms the death-inducing signaling complex (DISC). The DISC can then either initiate apoptosis by cleaving effector caspases (-3, -6, -7) or instead cleave BH3 only proteins which in turn activate Bax and Bak. The intrinsic pathway is initiated through several different cellular stresses, resulting in the activation of BH3 only proteins and subsequently Bax and Bak. These mediate the release of mitochondrial proteins such as cytochrome c. Cytochrome c forms a complex with apoptotic protease activating factor (Apaf-1), which is then called the apoptosome. Caspase-9 is activated via the apoptosome, and subsequently stimulates the caspase cascade by cleaving the executioner caspases [90, 91].

10.7.6 Caspase functionality beyond programmed cell death

Beside the activation of apoptotic pathways, several caspases are involved in regulating innate immune responses in inflammation. Especially Caspases-1, -4, -5, and -12 have been shown to exert immune-regulatory functions, Caspase-1 having probably the best described

inflammatory functions. Pro-caspase-1 is activated via complex formation with members of the pattern-recognition receptor (PRR) family and associated proteins. These caspase containing complexes are called inflammasomes and promote inflammatory responses through activation of the pro-inflammatory proteins IL-1beta, IL-18 and IL-33 [90]. While PRR proteins, such as members of the toll-like receptor family (TLF), promote a caspase-1 dependent pro-inflammatory stimulus, the activation of apoptosis regulated caspase-3 and caspase-7 has been associated with the release of anti-inflammatory mediators promoting immune suppression [91, 152].

These anti-inflammatory reactions initiated by apoptosis executing caspases are seen as a cellular mechanism for the attenuation of overwhelming immune activation at sites of tissue injury. This immune suppressive capacity of apoptotic cells is markedly different to necrotic cell death, which lacks this anti-inflammatory reaction. It has been proposed that the activation of caspases in apoptotic cells is of central importance in inhibiting autoimmune reactions. [91, 153]. Especially the release of paracrine factors were found to be controlled by caspsae-3 [62, 91, 92, 154].

To conclude, apoptosis is an actively enforced and highly regulated biological process, whose purpose is to protect neighboring cells.

10.8 Ionizing radiation

A major contribution towards the understanding of the relationship between paracrine factors and IR was made by Ankersmit et. al and Lichtenauer et. al, who showed that IR induced the release of paracrine factors that exert cytoprotective functions. The concept of conditioning methods to trigger the release of paracrine factors has also been described for hypoxia and cell starvation.

IR is an energy rich type of radiation displaying multiple biological effects on targeted organisms. The two major types of IR consist of high speed particles, namely alpha and beta particles, neutrons and electromagnetic radiation. The latter consists of x-rays, gamma rays and low frequency UV light, with wavelengths less than 700 nm. Whereas x-rays have energies ranging from 50 eV to 500 keV, gamma radiation has higher energy values (1 ev = 1.602×10^{-19}J) [155].

Each particle or photon penetrating a cell leaves behind a trace based on the effects elicited. Whereas charged particles directly induce a detectable ionization trace, indirectly ionizing particles such as photons do not induce these cellular disturbances. Their track is produced by the generation of secondary particles, which themselves are directly ionizing and produce a visible ionization track. However, the energy released by ionizing particles and photons in biological material is non-randomly distributed along these tracks, and in order to better

classify the effect of IR on biological systems the linear energy transfer (LET) model was introduced. The LET model attempts to characterize the different types of IR by describing the average energy transferred in a normalized unit length of the radiation track, γ-rays transfer relatively low amounts of energy per unit track as they have low mass and move with high speed. Therefore, they are considered to be low-LET radiation. Protons and neutrons have higher mass compared to photons, and are considered to be intermediate-LET radiation. Heavy ions and alpha particles possess the highest mass and are classed as high-LET radiation [155-157].

Based on this classification, IR exerts pleiotropic biological activities [158]. γ-radiation generates reactive oxygen species (ROS) and reactive nitrogen species (RNS). ROS and RNS can induce DNA strand breaks, modulate macromolecules and induce telomere dysfunction [158]. On the other hand, particle radiation primarily induces DNA single (SSB), or double (DSB) strand breaks [159]. DNA damage sensors recognize SSB or DSB and initiate the recruitment of mediators which amplify the signal and transduces it to effector molecules. Depending on the severity of the DNA damage, the injured cells repair the damage, undergo apoptosis or enter senescence or autophagy pathways [160]. These SSB and DSB activated biological process are called DNA damage responses (DDR). Importantly, IR stress refers to all effects caused by these different radiation types.

Other stressors beside IR that induce the DDR pathway are replicative stress, activation of oncogenes, reactive oxygen species (ROS), cell cultivation or exogenous agents (see **Figure 9**). The DDR contains several regulatory motives with different biological characteristics and these are classified according to their biological functions.

Given that IR induces apoptosis, we tried to investigate the effects of high dose IR in combination with high density cell cultivation on apoptosis induction. We hypothesized that high density cell cultivation (25 Mio PBMCs/ml) might display an additional effect on the induction of apoptosis.
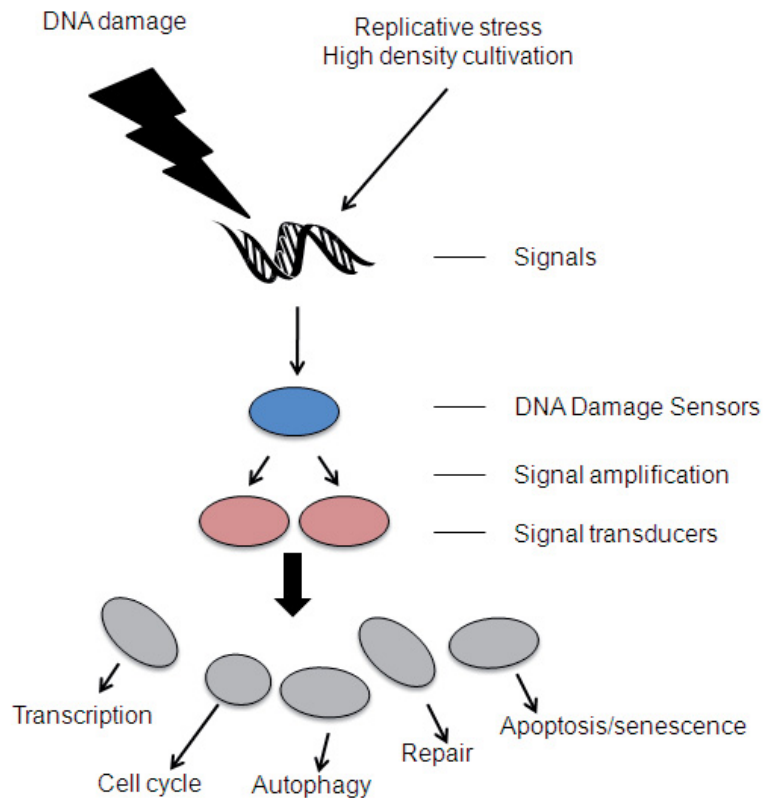
Figure 9: DNA damage and replicative stress induced cellular reactions. Both DNA damage and replicative stress can activate DNA damage sensors. In addition to p53 as a key DNA damage sensor, other genes such as BRCA1, Rad1, Rad9, and Rad17 are activated upon DNA damage. The signals from these DNA damage sensors are subsequently amplified and transferred to signal transducers. Two highly conserved signal transducers in the upstream DNA damage response are ATM and ATR which are members of the PI(3) kinase family. These kinases control the activation of several biological processes in general, aiming either to repair the damage, initiate programmed cell death or induce cellular senescence (adopted from Zhour et al. 2000; [161]).

In the last decade it has become commonly accepted that besides macromolecules, small RNA transcripts are involved in the regulation of DDR pathways

10.8.1 microRNA; small molecules large effect

microRNAs (miRNA) are a group of short (21 to 23-nucleotide long) non-coding endogenous RNA molecules that regulate gene expression at the post-transcriptional level [162]. Approximately 30% of all protein-coding genes are regulated by miRNAs via base binding with complementary sequences located at the 3' or the 5' untranslated regions (UTRs) of the mRNA[163, 164]. To date more than 1800 miRNAs have been identified in humans, with numbers still increasing [165].

miRNAs derive from precursor molecules (pri-miRNA), which exist in a double stranded RNA structure. The pri-miRNA is further processed in the nucleolus by the RNAse III type endonucleases, Drosha and Dicer, resulting in formation of pre-miRNA, which consist of ~ 70-nuleotide hairpins. The pre-miRNA is subsequently selectively exported into the

cytoplasm and passes through a further maturation process in which the second mRNA strand is degraded [166]. Finally, the remaining miRNA strand forms a protein complex referred to as RNA-induced silencing complexes (RISC). RISC mediates the posttranscriptional regulation of mRNA expression by targeting mRNA for degradation or repression of gene transcription. The miRNA inserted into the RISC specifies the target genes, which have a complementary sequence [162, 167].

Beside the function of miRNAs as repressors of gene translation discussed above, recent evidence has emerged highlighting that miRNAs and their associated protein complexes (miRNP) can induce gene expression [164, 168-170]. Translational activation is generally seen with miRNA targeting the 5'UTR of transcripts, whereas translational repression is associated with binding at the 3'UTR. In terms of transcriptional activation, Argonaute 2 (Ago2) has been identified as an important regulator of the RISC complex [169, 170], highlighting the diametric role of the RISC either as an activator or an inhibitor of translation.

10.8.2 Involvement of miRNA in IR-induced DDR

Several studies have shown that IR modulates biological processes both *in vitro* [171-173] and *in vivo* [174], by regulating miRNA expression. Interestingly these studies indicate that the modulation of miRNA expression in response to DNA damage is cell-type specific, showing huge differences in miRNA alterations between different cell-types [175]. Beside IR, other DNA damaging agents have been shown to alter miRNA expression. Pothof et al. showed that UV radiation changed miRNA expression in HeLa cells and human fibroblasts [176]. In addition hydrogen peroxide (H_2O_2) and the chemotherapeutic drugs cisplatin, etoposide [177] and 4-fluorouracil [178] induced miRNA alterations that showed a unique expression pattern depending on the DNA damaging agent.

The observed changes in miRNA expression following DNA damage are regulated on both the transcriptional and the posttranscriptional levels [175]. The kinase ATM has been identified as a key player in the regulation of miRNA expression. Knockdown of ATM abolished the induction of several DNA damage sensitive miRNAs, and approximately 25% of miRNAs were up-regulated upon DNA damage in an ATM-dependent manner [179]. Several different mechanisms by with ATM modulates miRNA expression have so far been proposed. For instance, ATM phosphorylates KSPR (KH-type splicing regulatory protein), a co-factor for both the Dicer and Drosha miRNA processing complexes. Furthermore the phosphorylated KSPR evidences an enhanced affinity to pri-miRNAs, thereby increasing miRNA processing activity [179]. Beside these KSRP dependent mechanisms, ATM modulates miRNA expression via other molecular pathways., the most prominent being via ATM mediated, Chk2-dependent, p53 activation [175]. p53 regulates several miRNAs by

interacting with RNA processing helicases, thereby inducing the transcription of selected miRNAs [180]. The miR-34 family in particular has been shown to be directly regulated by p53 in response to IR and DNA damaging agents [181]. Many of these regulated miRNAs are involved in cell cycle regulation, modulation of apoptosis and cell proliferation. IR represses miR-7a and miR-7b transcription in an ATM-p53 dependent manner [182]. The miR-34 family is a further direct target of p53 [171, 183, 184]. miR-21 is another miRNA whose transcription is under p53 control and is activated in response to IR [174, 185]. While the miR-7 and miR-34 families are targets of p53, miR-12b, miR-504 and miR-33 itself target p53 (reviewed in Hermeking et al. 2012 [186]).

Although the molecular mechanisms by which miRNAs modulate the DDR response have been investigated, their role in the DDR still remains to be elucidated. In 2013 Wang et al published a schematic model consisting of 4 possibilities of the function of miRNAs in the DDR [175] (see **Figure 10**). A) Up-regulated miRNAs enhance the DDR pathways by down-regulating DDR pathway inhibitors. B) Down-regulated miRNAs enhance the DDR pathways by de-repression of positive regulators of the DDR. C) In this model down-regulated miRNAs target DDR repressors and up-regulated miRNAs target DDR activators. This model proposes that miRNAs function as fine-tuning agents in the DDR, either turning off DNA repair in case of restoration of DNA integrity or in terms of exhausted and irreparable DNA damage. D) Wang et al hypothesize that the DNA damage modulates the interaction between miRNAs and regulators of the DNA repair (e.g. higher affinity of miRNAs to its target genes).
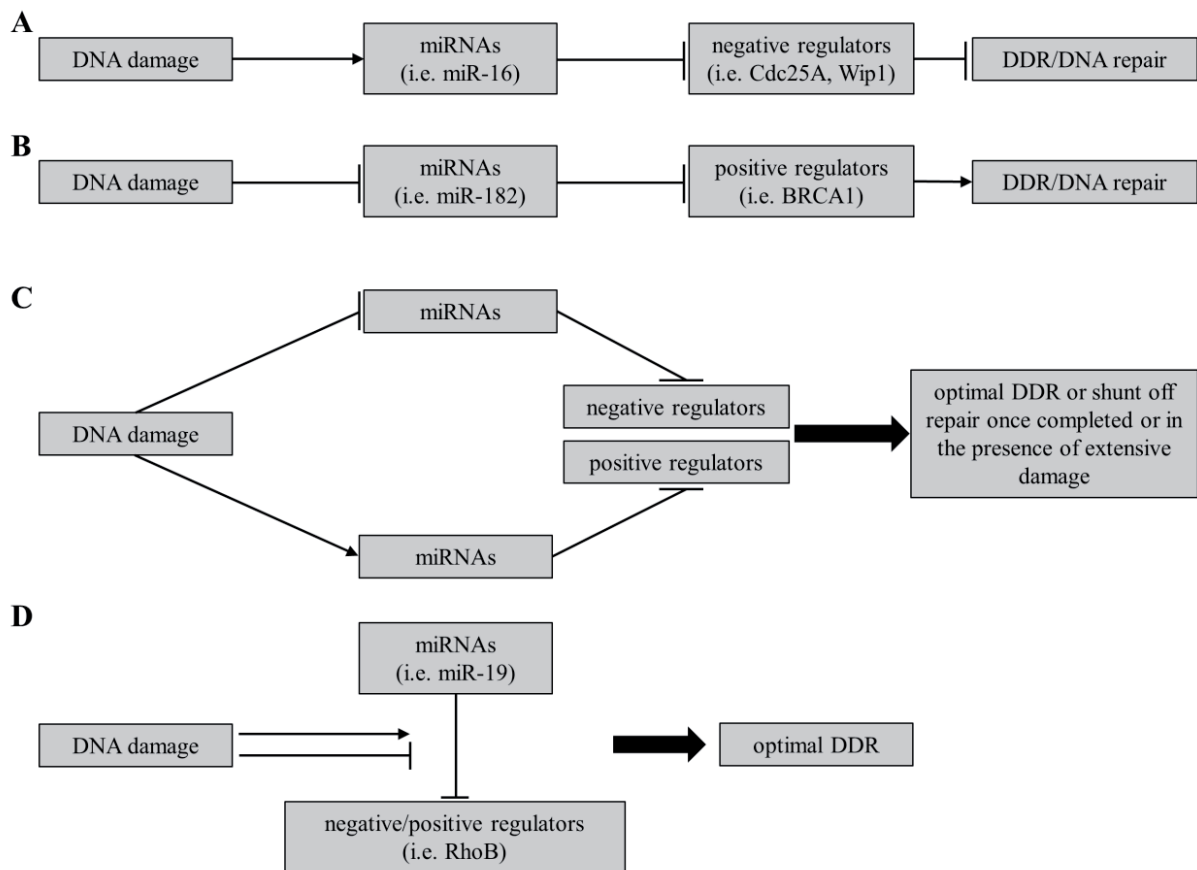
Figure 10: Proposed function of miRNAs in the DDR. (A) Up-regulated miRNAs in response to DNA damage inhibit negative regulators of the DDR thereby enhancing the DDR; (B) down-regulated miRNAs in response to DNA damage de-repress positive regulators of the DDRN thereby activating the DDR; (C) down-regulated miRNAs target DDR repressors and up-regulated miRNAs target DDR activators. In this model miRNAs are fine tuning agents that turn off DNA repair once finished, or in terms of irreparable damage. (D) DNA damage modulates the affinity of unaffected miRNAs and their positive or negative regulators of the DDR/DNA repair. Adopted from Wang et al. [175]

In summary, several DNA repair and DDR genes are controlled at the post-transcription level by miRNAs. Although the expression changes of several miRNAs are only slightly affected, we propose that these miRNA expression changes have significant effects on the cellular response to IR. Firstly, many genes can be targeted by different miRNAs. Secondly, miRNAs can target multiple DNA/DDR repair genes, thereby enhancing the effect on a common pathway (e.g. DNA repair, homologous recombination repair, cell cycle checkpoint) [175].

10.8.3 mRNA and microRNA Expression Profiling

Since the discovery of mRNA and miRNA various techniques to measure expression levels have been developed [187, 188]. Except for some technical differences mRNA and miRNA – profiling approaches follow the same principles. In the following paragraph the currently available methods for mRNA and miRNA expression profiling will be discussed.

10.8.3.1 RNA expression profiling methods

The commonly used methods for miRNA (and for mRNA) profiling are: quantitative reverse transcription PCR (qRT-PCR), microRNA microarray and RNA sequencing, using next generation sequencing platforms [188]. Each of these platforms displays strengths and limitations, making it necessary to evaluate the best method suitable for the given experiment. qRT-PCR is an accurate method which can be used for absolute quantification and validation of miRNA microarray data. However the costs per evaluated miRNA are high, and the test procedure is time consuming. miRNA microarrays are a high-throughput method with relatively low costs per evaluated miRNA. The disadvantages are the lack of absolute quantification and the lower specificity in comparison to qRT-PCR or RNA sequencing. RNA sequencing displays the advantages of qRT-PCR and is furthermore able to detect novel miRNAs. A drawback of RNA sequencing is the high computational effort necessary for data evaluation and the costs per sample [188]. **Figure 11** depicts a decision tree which aims to help choose the appropriate miRNA expression profiling method for each experiment.
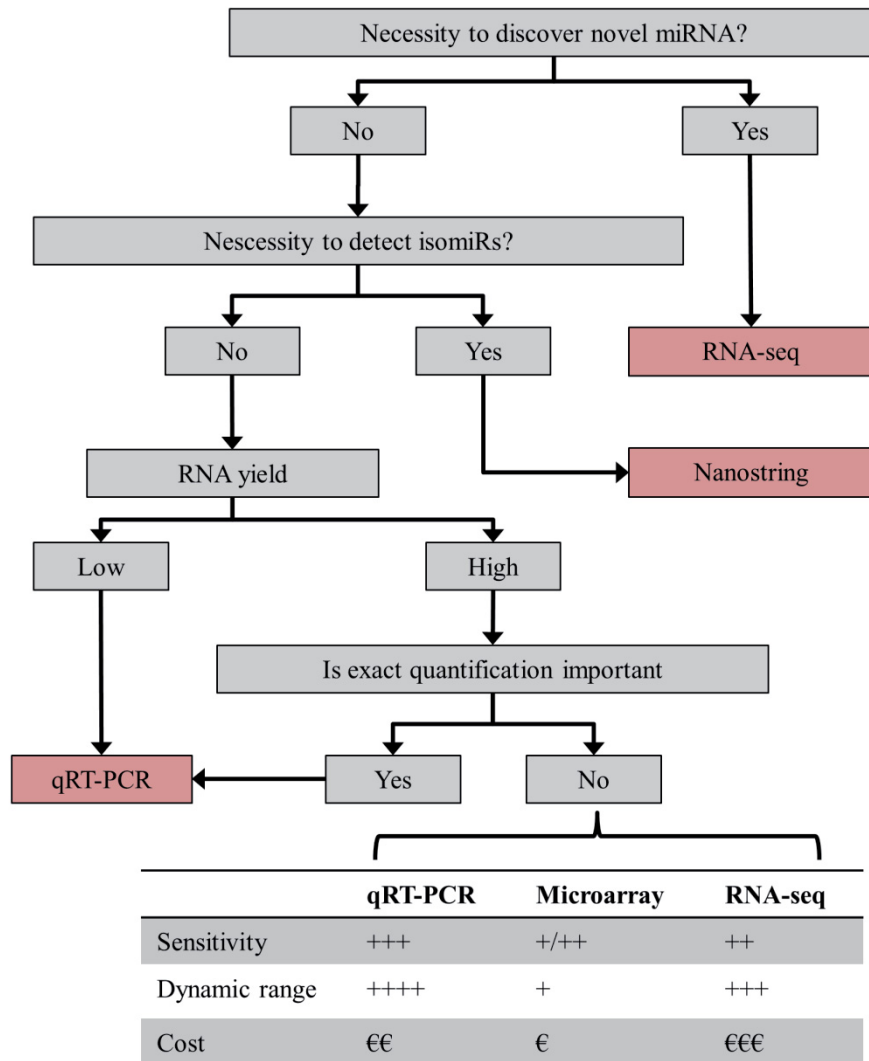
Figure 11: Decision tree for microRNA profiling techniques. Based on the specific demands of the project different methods for miRNA analysis are available. By following the decision tree, researchers can decide whether to use RNA-sequencing, which is compulsory if no miRNAs will be detected. If exact miRNA quantification is necessary or the RNA concentration of the sample is low than qRT-PCR is recommended for miRNA analysis. For projects using samples containing high miRNA concentrations without the necessity of discovering new miRNAs, qRT-PCR, microarray or RNA-sequencing are possible techniques, which differ in terms of sensitivity, dynamic range and costs per sample. (adopted from Pritchard et al. 2012; [188])

10.8.3.2 Processing RNA expression data

After performing an RNA expression profiling experiment the correct analysis of data is crucial in order to obtain reliable results. The following basic steps must be performed in sequence: data processing > data quality assessment > normalization of data > testing for differential RNA expression> testing for biological significance. In the following paragraph the different bioinformatics tools commonly used for processing RNA expression profiles will be discussed, focusing on miRNA expression data.

Depending on the method used for RNA profiling, different data processing programs are available. For microarray analysis, commercial programs and open source bioinformatics tools available are mostly written in *R* (http://www.bioconductor.org/; http://www.r-project.org/). After importing microarray raw data there is a quality assessment necessary. This can be done by either testing the expression of replicate values on the chip or by using internal controls. This is especially important for microarray analysis, as it has been shown that expression values perform differentially on the chip according to a phenomenon known as "geographic bias" [188].

Data normalization is a further important step for obtaining reliable results from RNA expression profiling. Different methods can be applied for normalizing data within a chip (e.g. geographic bias) and between chips [189]. For qRT-PCR several miRNAs, small nucleolar and small nuclear RNAs have been proposed as reference genes for miRNA expression value normalization. The most commonly used genes for qRT-PCR normalization are RNU44 and RNU6B [189]. For mRNA expression normalization commonly used housekeeping genes are beta-2 microglobulin (B2M), GAPDH, TATA box binding protein (TBP) and ribosomal proteins [188].

Statistically significant differences in expression of miRNA or mRNA levels between two groups are usually detected using t-test, ANOVA, Bayesian method or cluster analysis [188, 190]. After obtaining significantly regulated miRNA, a subsequent integrative analysis of miRNA and mRNA interaction can be performed. These bioinformatics programs rely on two distinct attributes when predicting a miRNA target- they check whether there are complementary 8-mer and 7-mer sites on the mRNA that match the seed region of a miRNA, and they evaluate whether there is perfect base pairing at the 3' end of the miRNA which could compensate the short base pairing in the seed region of the miRNA [164].

An extension of the simple miRNA-mRNA correlation target sequence analysis represents a further *in silico* tool that takes into account that transcription factors can serve as regulatory elements modulating expression of both miRNA and mRNA. Magia^2 [191]and mirConnX [192] are two algorithms which provide a platform for integrating miRNA-mRNA and transcription factor analysis. They incorporate two functional aspects in the bioinformatics analysis: Firstly they identify transcription factors that modulate both a given miRNA and its targeted mRNA, and secondly a miRNA that modulates both a given transcription factor and its targeted mRNA. Simultaneously Magia^2 and miRConnX provide a user interface for calculating the involvement of the predicted miRNA-mRNA and transcription factor network in known biological processes and canonical pathways [191, 192]. These calculations should be performed preferably by using the miRNA and mRNA data of the same biological samples in

order to strengthen the biological power of the data. A schematic workflow of miRNA target prediction analysis is given in **Figure 12**.
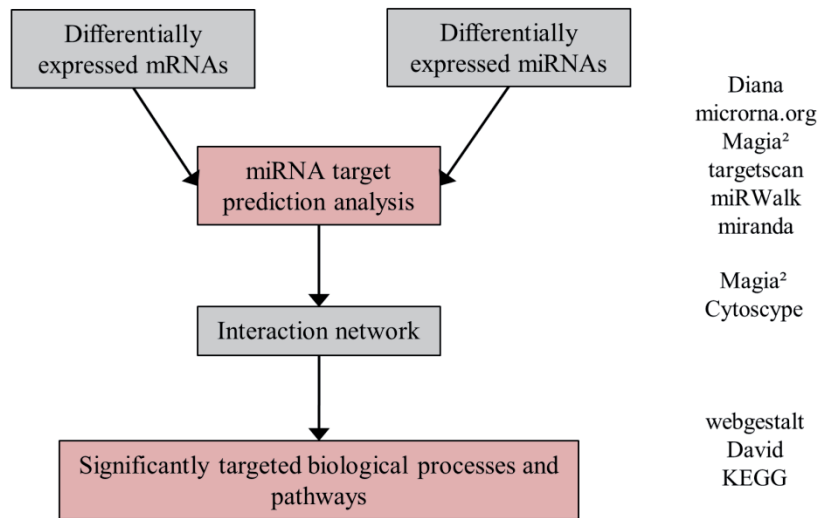
Figure 12: Schematic workflow of miRNA-mRNA target prediction analysis.

10.8.3.3 Functional Enrichment Analysis

Once significantly differently expressed miRNAs or mRNAs are detected in a gene expression profiling experiment, several tools are available for identifying their involvement in biological processes and canonical pathways. These analyses are based on the gene ontology (GO) terms which are attributed to mRNA. The GO terms consist of three different classes of vocabularies that describe a mRNA product in terms of its associated molecular function, biological process and cellular components. The GO term annotation follows uniform principles and structures in order to enable comparison of classes of genes with respect to their annotated GO terms [193]. Several bioinformatics programs use the annotated GO terms of genes to predict their involvement in biological functions and canonical pathways [194, 195].

A further class of bioinformatics tools is available that provides protein-protein interaction data, helping to summarize a high degree of complex interactions graphically. The most commonly used data bases are STRING [196], VisANT [197], GeneMANIA [198], I2D [199] and IMP [200]. These tools predict protein interactions based on different parameters termed neighborhood, fusion, occurrence, co-expression, experiments, database and text mining [196]. In prokaryotes, genomically neighboring genes often reflect the same biological functionality and are therefore predicted as functional partners based on the "neighborhood" classification. Protein fusions are predicted via bioinformatics algorithms, as well as phylogenetic co-occurrence of genes. The term co-expression defines genes that were commonly co-expressed in tissues and therefore considered to code for interacting proteins. Experimentally validated protein interactions are the strongest class of evidence of protein

interaction used by these databases. On the other hand, database and text mining are the lowest class of evidence, as they predict protein-protein interactions based on the co-occurrence of gene names in publications and databases, and therefore attribute to them a biological interaction [201].

11 Aim of the study

We have shown that the PBMC secretome promotes myocardial and neurological cytoprotection, induces vasodilation, inhibits platelets, attenuates microvascular obstruction and enhances wound healing in vitro and in vivo [38-40, 42, 139, 140].

The goal of the first part of the dissertation was to investigate transcriptomic changes in response to ionizing radiation (60 Gy) in human PBMCs cultured at high density. In the second part of the dissertation a large animal model was used to investigate the effects of IR on the release of paracrine factors from PBMCs, and the effects of viral clearance of PBMC supernatant on its ability to reduce myocardial damage following acute ischemia.

12 Results

12.1 High dose ionizing radiation regulates micro RNA and gene expression changes in human peripheral blood mononuclear cells

Prologue

High dose ionizing radiation is known to induce cell damage via direct DNA damage and the generation of free oxygen species [202, 203].In the last decade transcriptional profiling has gained increasing popularity in radiation research since it provides researchers with the opportunity to obtain an excellent overview of biological changes in response to IR. More recently miRNAs have come into focus as regulators of IR modulated cellular processes. miRNAs are small non-coding RNA transcripts that regulate 30% to 60% of all protein coding genes via RNA silencing and post-transcriptional gene expression regulation [163]. However, a combined analysis of gene and microRNA expression analysis in human PBMCs was still missing. In the paper "*High dose ionizing radiation regulates micro RNA and gene expression changes in human peripheral blood mononuclear cells*" we investigated miRNA and gene expression changes of human PBMCs of the same cells simultaneously in order to identify biological interaction networks that regulate biological processes induced or repressed by ionizing radiation. We identified several mRNA and miRNA expression networks in response to IR. Furthermore, we were able to show that miRNAs are involved in the regulation of IR induced biological processes at a posttranscriptional level [204].

RESEARCH ARTICLE

Open Access

High dose ionizing radiation regulates micro RNA and gene expression changes in human peripheral blood mononuclear cells

Lucian Beer[1,2], Rudolf Seemann[3], Robin Ristl[4], Adolf Ellinger[5], Mohammad Mahdi Kasiri[1,2], Andreas Mitterbauer[1,2], Matthias Zimmermann[1,2], Christian Gabriel[6,7], Mariann Gyöngyösi[8], Walter Klepetko[2], Michael Mildner[9*] and Hendrik Jan Ankersmit[1,2*]

Abstract

Background: High dose ionizing radiation (IR) induces potent toxic cell effects mediated by either direct DNA damage or the production of reactive oxygen species (ROS). IR-induced modulations in multiple biological processes have been proposed to be partly regulated by radiosensitive microRNA (miRNA). In order to gain new insights into the role of miRNAs in the regulation of biological processes after IR, we have investigated changes in mRNA and miRNA expression after high dose IR.

Results: IR induced changes in the mRNA and miRNA profiles of human peripheral blood mononuclear cells (PBMCs). When comparing non-irradiated and irradiated samples, we detected a time-dependent increase in differentially expressed mRNAs and miRNAs, with the highest differences detectable 20 hours after exposure. Gene ontology analysis revealed that very early events (up to 4 hours) after irradiation were specifically associated with p53 signaling and apoptotic pathways, whereas a large number of diverse cellular processes were deregulated after 20 hours. Transcription factor analysis of all up-regulated genes confirmed the importance of p53 in the early post-irradiation phase. When analyzing miRNA expression, we found 177 miRNAs that were significantly regulated in the late post-irradiation phase. Integrating miRNA and target gene expression data, we found a significant negative correlation between miRNA-mRNA and identified hepatic leukemia factor (HLF) as a transcription factor down-regulated in the response to IR. These regulated miRNAs and the HLF target genes were involved in modulating radio-responsive pathways, such as apoptosis, the MAKP signaling pathway, endocytosis, and cytokine-cytokine interactions.

Conclusion: Using a large dataset of mRNA and miRNA expression profiles, we describe the interplay of mRNAs and miRNAs in the regulation of gene expression in response to IR at a posttranscriptional level and their involvement in the modulation of radiation-induced biological pathways.

Keywords: Microarray, MicroRNAs, Messenger RNA, Apoptosis, Mononuclear leukocytes, p53, Ionizing radiation

* Correspondence:
michael.mildner@meduniwien.ac.at; hendrik.ankersmit@meduniwien.ac.at
[9]Department of Dermatology, Research Division of Biology and Pathobiology of the Skin, Medical University Vienna, Lazarettgasse 14, 1090 Vienna, Austria
[1]Department of Thoracic Surgery, Medical University of Vienna, Währinger Gürtel 18-20, 1090 Vienna, Austria
Full list of author information is available at the end of the article

Background

Exposure of living cells to ionizing radiation (IR) results in the generation of free radicals and reactive oxygen species (ROS) [1]. IR has been shown to cause severe cell damage and cell stress, mediated either directly by disturbing DNA integrity or indirectly via formation of ROS and bystander effects [2]. A wide range of different methods have been used to identify cellular responses to IR, ranging from the detection of chromosomal changes and cell viability assays to transcriptional profiling using gene expression array techniques [3-9]. The latter has acquired growing attention in the scientific community because it enables researchers to gain an excellent over-view of molecular mechanisms that are altered in response to IR.

The magnitude of the radiation dose [3,5,10] and the type of radiation influence gene expression differently [11]. High-dose radiation (>2 Gy) is associated with increased DNA lesion complexity , such as genotoxic stress responses including DNA damage sensing and altered repair mechanisms, as well as immunological alterations [3]. In contrast, the complex mechanisms underlying the altered biological processes after high dose radiation have still not been elucidated completely.

MicroRNAs (miRNAs) are short non-coding RNAs (21 to 23 nucleotides long) that regulate approximately 30-60% of all protein coding genes via imprecise binding of bases with complementary sequences, usually on the 3' end of the target mRNA [12]. More than 1800 miRNAs have been discovered [13]. miRNAs mediate translational repression by forming RNA-induced silencing complexes and targeting mRNAs by either inhibiting translation or initiating mRNA degradation [14]. A single miRNA can target a sequence of up to thousands of genes. miRNA target genes can be identified using bioinformatics algorithms. These programs mainly determine potential binding sites in 3'UTRs, called seed sequences, which consist of complementary base pairs and are recognized by miRNA base-pairing [15]. In recent years, the accuracy and reliability of computer programs predicting miRNA targets has greatly improved, and novel strategies have been developed for predicting miRNA targets that take into account that miRNAs and their target genes are co-regulated by common transcription factors [15]. Furthermore, bioinformatics databases providing functional information on miRNA-targeted genes are growing and provide deeper insight into the involvement of mRNAs and miRNAs in biological processes at the posttranscriptional level.

Thus, the most valuable information from miRNA profiling can be acquired by comparing the mRNA and miRNA expression profiles of the same biological samples. No paired miRNA-mRNA data from human PBMCs after IR have been published thus far [16-19], and a precise analysis of negatively correlated miRNA-mRNA pairs has been hindered by a lack of paired mRNA transcripts.

In order to improve the biological validity of the data, we analyzed parallel mRNA and miRNA whole genome expression profiles from the same biological samples after exposure to high dose gamma radiation. We used up-to-date bioinformatics analysis to predict IR-inducible expression of transcription factors for miRNAs and mRNAs, as well as miRNA target genes, and the interplay between miRNAs and mRNAs in the regulation of bio-logical pathways. We identified strong alterations in gene and miRNA expression in irradiated versus non-irradiated cells and show that transcription factor p53 and its downstream effector proteins play a central role in the biological response to IR.

Methods

Ethics statement

Cell separation and irradiation

Human peripheral blood mononuclear cells (PBMCs) were obtained from four healthy male volunteers by venous blood draw. Cells were separated by Ficoll-Paque (GE Healthcare Bio-Sciences AB, Sweden) density gradient centrifugation. Heparinized anticoagulated blood specimens were processed immediately after venipuncture, diluted 1:2 in Hanks balanced salt solution (HBBS, Lonza, Basel, Switzerland), and transferred carefully to 50 ml tubes containing Ficoll-Paque solution (GE Healthcare Bio-Sciences AB, Sweden). The tubes were centrifuged for 15 minutes at 800 g at room temperature without braking and buffy coats with mononuclear cells obtained. Cells were washed in HBSS and resuspended in CellGro serum-free medium (CellGenix, Freiburg, Germany; 25×10^6 cells/ml). Cell concentrations were determined on a Sysmex automated cell counter (Sysmex Inc., USA). PBMCs from the four donors were γ-irradiated with 60 Gray (Gy) of Caesium-137 irradiation. For each experiment, irradiated and non-irradiated PBMCs from the same donor were in-cubated for 2, 4, and 20 hours.

Total RNA isolation

At the end of the incubation and immediately after PBMC separation (0 h), total RNA was isolated from approximately 25×10^6 irradiated or non-irradiated PBMCs

using Trizol® Reagent (Invitrogen, Carlsbad, CA) according to the manufacturer's instructions. Total RNA was quantified using a NanoDrop-1000 spectrophotometer (Peqlab, Erlangen, Germany) and RNA quality monitored by an Agilent 2100 Bioanalyzer (Agilent, Böblingen, Germany). All RNA samples used in further steps had an RNA integrity score between 5.7 and 10. A total of 28 samples were generated from the four different donors .

mRNA and microRNA microarray hybridization

mRNA and miRNA expression profiles were obtained for the same samples using the Agilent Whole Human Genome Oligo Microarray (8 × 60K; G4851A; #028004; Agilent Technologies), which detects 27,958 target Entrez gene mRNAs and 7,419 lincRNAs. Briefly, 600 ng Cy3-labeled fragmented cRNA was hybridized overnight to an Agilent whole human genome oligo microarray, washed twice, blocked, and scanned using Agilent's microarray scanner.

Agilent Human miRNA Microarray Kit (8×60K; G4872A; #031181) based on miRBase release 16.0 and detecting 1,205 human miRNAs was used to analyze miRNA expression. Briefly, 100 ng total RNA was labeled and hybridized to an Agilent human miRNA microarray overnight at 55°C. The microarray was washed twice and fluorescence detected using Agilent's Microarray Scanner System. Agilent's Feature Extraction software was used for image analysis. Microarray gene analysis was performed by Milteny (Milteny Biotec GmBH, Germany).

Both mRNA and miRNA data were generated according to the MIAME guidelines [20] and are available on the Gene Expression Omnibus (GEO) website (http://www.ncbi.nlm.nih.gov/geo/) under accession number GEO: GSE55955.

Statistical analysis of gene expression data

Background-corrected fluorescence intensity values were imported into GeneSpring v.11, log2-transformed, and then normalized by quantile normalization. The mean values of identical replicate probes on each chip were calculated by GeneSpring. The Agilent whole human genome mRNA chip uses different probes for some transcripts. For statistical analysis these transcripts were treated as distinct transcripts, whereas functional analysis was executed with summarized values for different probes of the same gene. A filtering step was applied in order to reduce the number of multiple hypotheses. Only genes for which at least 100% of the values in one of the two conditions (irradiated vs. non-irradiated) were above the 40th percentile of the average expression of all samples were included in the final analysis. The threshold of 40% was chosen because approximately 30-60% of all human genes are expressed [21,22].

Statistical analysis of miRNA expression data

The miRNA data were processed as described above for mRNA data. "Filter on Flags" was used as a filtering step for miRNA samples. Flags were attributes that denote the quality of the entities. These values were generated based on the feature quality on the chip. Genes that were given a low significant attribute in the data file were marked as "Absent" and high significant values were marked as "Present". We used the default settings for GeneSpring in the filtering process, obtaining a total of 241 available human miRNAs. Differentially expressed mRNAs and miRNAs were identified by paired t-tests in GeneSpring. The resulting p-values were corrected for multiplicity by applying Benjamini-Hochberg adjustment to all p-values calculated for a time point with a false discovery rate (FDR) < 5% [23]. Genes with an adjusted p-value <0.05 were considered significant.

Functional analysis of radiation-responsive genes

To gain information on the significantly expressed genes, we functionally categorized them using the WEB-based Gene Stet Analysis Toolkit (WebGestalt) database [24]. This web-based analysis tool enables the detection of enrichment of gene ontology (GO) terms in a set of genes and uses the Kyoto Encyclopedia of Genes and Genomes (KEGG) annotation to assign pathways that are significantly affected. We used the whole human genome as a reference set for enrichment analysis and applied the Benjamini-Hochberg method for multiple testing with a significance level of p ≤ 0.05 and FDR < 5%.

Hierarchic clustering

GeneSpring software was used for hierarchic clustering of the miRNA and mRNA expression data. A Euclidean distance metric and complete average-linkage clustering was used for hierarchic clustering.

Visualization of protein-protein interactions

To visualize known and predicted protein-protein interactions, the web-based database STRING v9.1 (Search Tool for the Retrieval of Interacting Genes/Proteins) was used [25].

Sylamer analysis

The Sylamer program was used to predict miRNA binding site differences in the 3'UTRs of differentially expressed miRNAs in human PBMCs 20 hours after irradiation [26]. A total of 1,018 up-regulated genes and 1,285 down-regulated genes with a fold change >1.0 in irradiated samples and ordered by relative expression were used for analysis.

Identification of miRNA target genes and negative-correlation analysis of miRNA and mRNA expression data

The Magia^2 web tool was used to identify the targets of miRNAs significantly differentially expressed in irradiated PBMCs [27]. Because of the small number of samples, we used the non-parametric Spearman correlation coefficient to estimate the degree of negative correlation (e.g., up-regulated miRNA and down-regulated mRNA target). The TargetScan algorithm was used to predict the biological targets of miRNAs with a stringency of 0.7. Genes with a Spearman correlation coefficient < –0.7 were used to identify enriched biological processes and pathways using the WebGestalt tool.

Transcription factor binding site analysis

The web-based platform oPOSSUM3.0 (http://opossum.cisreg.ca/oPOSSUM3) was used for transcription factor binding site analysis [28]. oPOSSUM 3.0 detects known transcription factor binding sites in the promoter sequences of co-expressed genes in order to evaluate whether a transcription factor binding site is enriched within the gene set [29]. Upstream sequences (2000 bp) of up-regulated genes were analyzed using the default parameters in oPOSSUM 3.0 Sequence-based Single Site Analysis (SSA). We interrogated the oPOSSUM database for SSA analysis on two sets of genes corresponding to all up-regulated genes 2 or 4 hours after irradiation, and for the highest 1000 up-regulated transcripts 20 hours after radiation.

Quantitative reverse transcriptase PCR (qPCR) analysis of mRNA

To validate the data on IR-induced genes, changes in the expression of selected mRNAs were evaluated by qPCR. cDNA were transcribed using the IScriptc DNA synthesis kit (BioRad, Hercules, USA) as indicated in the instruction manual. Amplified PCR products were unstitched on a 1.5% agarose gel and stained with GelRed (Biotium, Hayward, USA). DNA Molecular Weight Marker VI (Roche Applied Science, Penzberg, Germany) was used as a reference marker. mRNA expression was quantified by qPCR with Light Cycler Fast Start DNA Master SYBR Green I (Roche Applied Science, Penzberg, Germany) according to the manufacturer's protocol. The primer pairs were designed as described previously [30] and synthesized by Microsynth AG (Vienna, Austria). The primer sequences are provided in the supplementary material (Additional file 1). The specificity of the PCR products was confirmed by sequencing. The relative expression of target genes was compared to the housekeeping gene beta-2-microglobulin using a formula described by Pfaff et al. [31]. The efficiencies of the primer pairs were determined as described previously [30].

qPCR analysis of miRNA

The miRNA expression analysis was validated using the TaqMan® MicroRNA Assay Kit (Applied Biosystems, Foster City, CA). Briefly, each RT reaction contained 10 ng of total purified RNA, 5× stem-loop RT primer, 1× RT buffer, 0.25 mM of each dNTP, 50 U Multi-Scribe™ reverse transcriptase, and 3.8 U RNase inhibitor. The reactions were incubated for 30 min at 16°C, 30 min at 42°C, 5 min at 85°C, and then held at 4°C. The resulting cDNA was amplified quantitatively using LightCycler® Probes Master Mix and Taqman microRNA assays for miR-99b*, miR-887, miR-4299, and miR-RNU44 as an endogenous control. The relative expression levels between samples were calculated as described above.

FACS analysis

The induction of apoptosis was measured by annexin V-fluorescein/propidium iodide (FITC/PI) co-staining (Becton Dickinson, Franklin Lakes, NJ, USA) using a flow cytometer as described previously [32].

Apoptosis membrane array and ELISA analysis

An apoptosis antibody membrane-array (Proteom Profiler Arrays, R&D Systems, Minneapolis USA) was used to detect the relative protein concentrations of 35 apoptosis-related proteins. Lysates of irradiated and non-irradiated PBMCs from two donors (cell count 10×10^6 cells) 20 hours after exposure were used according to the manufacturer's instructions. The dot intensities of apoptosis membrane arrays for semi-quantitative analysis were quantified by volume densitometry using BioRad Image Lab software. Supernatant levels of IL-16 secreted by irradiated and non-irradiated PBMCs at 2, 4, and 20 hours were measured by a commercially available enzyme-linked immunosorbent assay (ELISA, Duoset, R&D Systems, Minneapolis, USA).

Immunoblot analysis

For the preparation of whole cell lysates, PBMCs were lysed in SDS–PAGE loading buffer, sonicated, centrifuged, and denatured before loading. The protein content of 10^6 cells 20 hours after irradiation or 10^6 non-irradiated cells was used for Western blotting. SDS–PAGE was performed on 8–18% gradient gels (GE Amersham Pharmacia Biotech, Uppsala, Sweden). The proteins were then electro-transferred onto nitrocellulose membranes (Bio-Rad, Hercules, CA, USA) and immunodetected using primary antibodies against p53 (1 μg/ml; Abcam, Cambridge, UK), p21(1 μg/ml; Abcam), SP1 (2 μg/ml; New England Biolabs, Beverly, MA, USA), ZFX (1 μg/ml; New England Biolabs), CRTR1 (also known as TFCP2L1; 2 μg/ml; Abcam), HLF (2 μg/ml; Abcam), and KLF4 (1 μg/ml; Abcam). Glyceraldehyde-3-phosphate dehydrogenase

(GAPDH) served as the housekeeping protein (0.2 μg/ml; Biogenesis, Poole, UK). Reaction products were detected by chemiluminescence with the Chemi Glow reagent (Biozyme Laboratories Limited, South Wales, UK) according to the manufacturer's instructions.

Transmission electron microscopy (TEM)

Irradiated and non-irradiated PBMCs (20 hours after exposure) were dehydrated in a graded ethanol series (50%, 70%, 90%, 96%, and twice in 100%) and embedded in Epon (Serva, Heidelberg, Germany). Ultrathin sections (80–100 nm) were cut using an UltraCut-UCT ultramicrotome (Leica Inc., Vienna, Austria), transferred to copper grids, and viewed either unstained or stained with 1% uranyl acetate and 5% lead citrate (Merck, Darmstadt, Germany) using an EM-900 TEM (Carl Zeiss, Oberkochen, Germany) at an acceleration voltage of 50 kV. Digital images were recorded using a wide-angle dual speed CCD camera (Albert Tröndle, Dünzelbach, Moorenweis, Germany).

Statistical analysis

Statistical analysis was performed using GraphPad Prism4 software (GraphPad Software, La Jolla, CA, USA). Comparisons between the two groups at a given time point were tested by a paired t-test. Data are expressed as mean ± standard deviation (SD) or displayed as box plots. A two-sided corrected p-value <0.05 was considered significant.

Results

Ionizing radiation induces apoptosis in human PBMCs

IR is known to initiate apoptosis in different cell types, but the underlying molecular mechanisms have not been fully elucidated. To allow comparisons between our study and others, we evaluated the already established effects of irradiation on human PBMCs. Twenty hours after irradiation, the numbers of early apoptotic PBMCs (annexin V-positive cells) and advanced apoptotic PBMCs (annexin V and propidium iodide-positive cells) were significantly higher in irradiated PBMCs than non-irradiated PBMCs (Figure 1A). Approximately 30% of irradiated PBMCs were in a late apoptotic phase, compared to 2% of non-irradiated PBMCs (Figure 1B). A slight increase in the number of early and late apoptotic PBMCs was detectable as early as 2 hours after irradiation (Figure 1C, D). As shown in Figure 1E by electron microscopy, exposure to IR induced morphological abnormalities in PBMCs, such as nucleolus fragmentation and the presence of apoptotic bodies. As IR is known to induce DNA double strand breaks following activation of the tumor suppressor p53, we performed Western blot analysis to quantify p53 and its downstream target p21. As shown in Figure 1F, irradiation

of PBMCs with high dose IR (60 Gy) strongly increased the expression of both p53 and p21.

Ionizing radiation induces the expression of apoptosis-related proteins

Next, we analyzed the expression of 35 proteins associated with apoptotic signaling using an antibody membrane array. Cell lysates from irradiated or non-irradiated PBMCs 20 hours after exposure were used for this experiment. A representative picture of the membrane array is shown in Figure 2. All proteins exhibited moderate to high induction in irradiated samples compared to non-irradiated samples (Figure 2D).

We were interested in describing the post-transcriptional regulatory signaling cascades between mRNA and miRNA; therefore, we initially analyzed the regulation and activation of proteins associated with apoptosis and cell cycle in response to IR. As shown in Figure 2, anti-apoptotic proteins such as Bad, BAX, BCL-2, ciap-1, ciap-2, XIAP, and survivin were highly enriched in lysates from irradiated PBMCs. We also detected increased activation of caspase-3, as well as p53 and Rad17, in irradiated cells, which are not regulated at the transcriptional level, but activated by post-translational modifications. Some of the up-regulated proteins, such as p53, p21, p27, and XIAP, are known to induce cell cycle arrest, whereas others exert anti-oxidative functions (e.g., PON2, HO-1, HO-2). We also found heat shock proteins 27, 60, and 70 are up-regulated after irradiation, suggesting an additional impact of molecular chaperones in preserving cell integrity and function. Though the de novo production of proteins takes some time, the activation of pre-synthesized proteins via phosphorylation or cleavage can occur rapidly. Within the caspase cascade, caspase-3 plays a key role in executing apoptosis [33]. Active IL-16 serves as a surrogate marker of caspase-3 activation because pro-IL-16 is cleaved by caspase-3 in monocytes undergoing apoptosis [34]. Therefore, we evaluated the time-dependency of IL-16 concentrations in supernatants from cultures of irradiated and non-irradiated PBMCs as a surrogate marker of caspase-3 activity (Figure 3). Four and 20 hours after irradiation, IL-16 levels were higher in the supernatant from irradiated cells compared to non-irradiated cells (Figure 3), showing a strong correlation with the number of apoptotic cells and the time after irradiation (Figure 1C, D). Caspase-3 activity has been shown to be controlled by miRNA-378 [35]. In this experimental setting miRNA-378 was notably reduced in irradiated cells.

Matched gene and miRNA expression analysis in irradiated and non-irradiated human PBMCs

Based on the protein data, we obtained the miRNA and mRNA expression profiles of 28 samples obtained from four donors. This dataset includes non-irradiated PBMCs
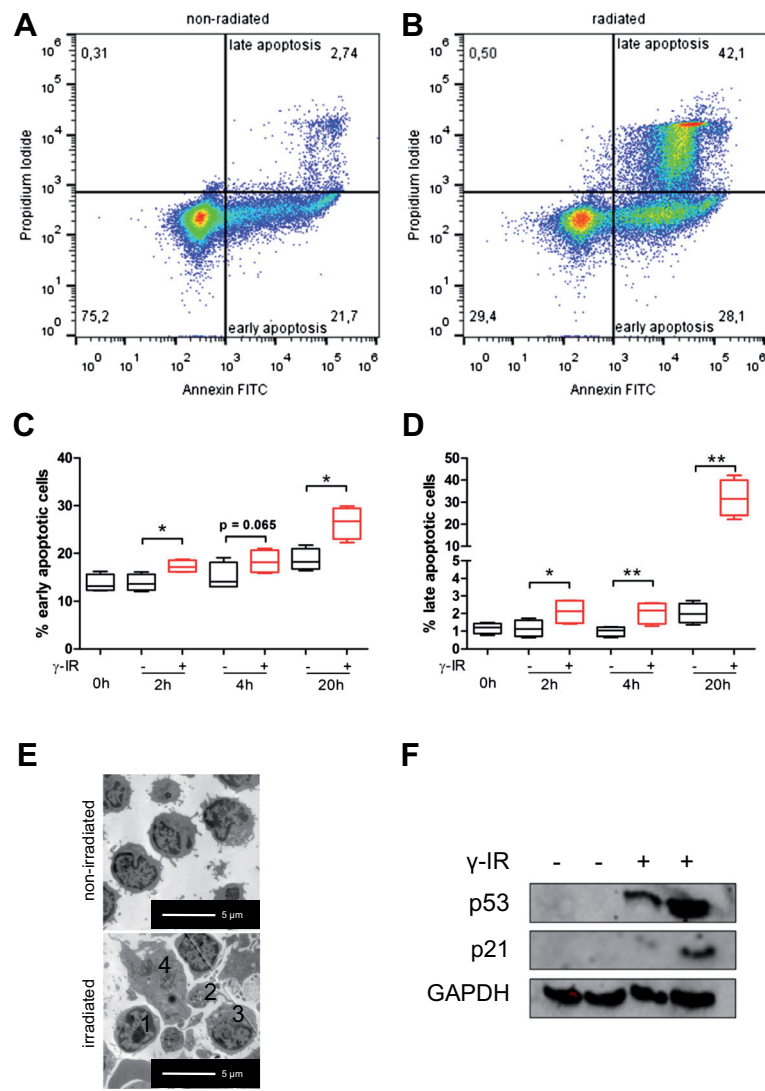
Figure 1 Ionizing radiation induces apoptosis in PBMCs. To detect the percentage of early and late phase apoptotic cells, the cells were stained with annexin V and propidium iodide 2, 4, and 20 hours after exposure to IR. FACS analyses of non-irradiated **(A)** and irradiated **(B)** PBMCs 20 hours after exposure are shown. Viable cells are annexin V and propidium iodide-negative (lower left quadrant), whereas early apoptotic cells are annexin V-positive and propidium iodide-negative (lower right quadrant) and late apoptotic cells are double-positive (upper right quadrant). **(C, D)** Quantitative analysis of the FACS data 2, 4, and 20 hours after irradiation is shown. **(E)** Representative electron microscope picture of non-irradiated (upper panel) and irradiated (lower panel) PBMCs 20 hours after exposure. Irradiated PBMCs exhibited morphological signs of late apoptosis, such as chromatin condensation in the nucleus (1), free apoptotic bodies (2), vesicle formation (3), and dissolution of the cell membrane (4). **(F)** A representative immunoblot of p53 and p21 in cell lysates from 10×10^6 PBMCs 20 hours after exposure to IR. Irradiation up-regulated the protein levels of both p53 and its downstream target p21. *$p < 0.05$, **$p < 0.01$; n = 4.

and irradiated PBMCs 2, 4, and 20 hours after exposure to IR, as well as control PBMCs without any cultivation period.

Time-dependent changes in mRNA expression after irradiation

In order to evaluate time-dependent changes in expression, we compared mRNAs from irradiated PBMCs and non-irradiated PBMCs 2, 4, and 20 hours after exposure to IR. The Agilent Whole Human Genome Microarray

$(8 \times 60K)$ includes 27,950 mRNAs and 7,419 linc-RNAs. The mRNA expression data is displayed in a principal component analysis (PCA) in Figure 4. PCA depicts expression values as points on a three-dimensional scale. Each dot in the figure represents averaged expression data of one unique sample. A total of 28 dots are visible in Figure 4, corresponding to the 28 experiments performed. Based on this analysis, samples are clustered and separated from each other according to the treatment and time after exposure. Irradiated samples form three distinct
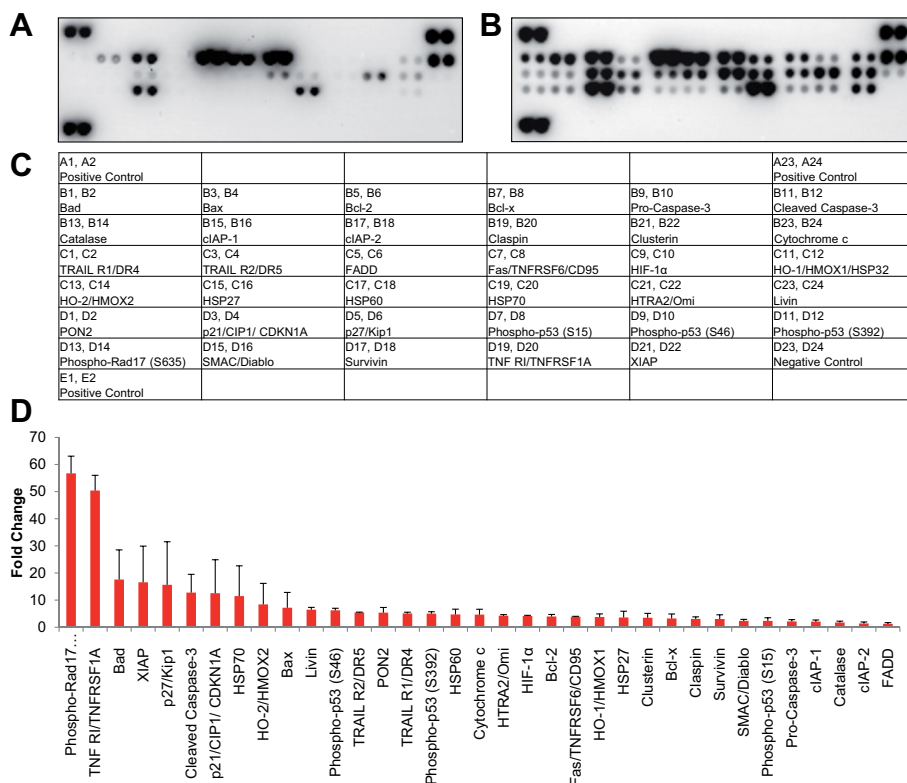
Figure 2 Proteins involved in executing apoptosis are up-regulated in response to ionizing radiation. A membrane array detecting 35 apoptosis-related proteins was incubated with cell lysates from 10^6 non-irradiated **(A)** or irradiated **(B)** human PBMCs 20 hours after exposure. **(C)** The legend for the spotted proteins. **(D)** The average pixel intensities of two independent experiments were averaged and are depicted as the fold change in up-regulation of irradiated PBMCs compared to non-irradiated PBMCs. For relative quantification in **(C)**, an exposure time of 60 seconds was used for proteins with high expression values, and an exposure time of 625 seconds was used for proteins with lower expression values. Data are presented as mean + SD; n = 2.

clusters are visible on the right side of the figure. Time-dependent irradiated samples increase on the Y-axis and decrease on the Z-axis, whereas the position on the X-axis remains constant. Non-irradiated samples and expression data from PBMCs without any cultivation build a separate cluster on the left side of the figure. Compared to irradiated PBMCs, the non-irradiated PBMCs had higher X-axis values, but the Y-axis and Z-axis values were comparable between matched time points for irradiation and non-irradiated PBMCs. The figure also shows that cultivation of human PBMCs per se alters gene expression, as the 0 h cells can be separated from non-irradiated PBMCs at 2, 4, and 20 hours after cultivation.

We performed statistical analyses on gene expression data in order to quantify differentially expressed transcripts in irradiated versus non-irradiated PBMCs. Only genes for which at least 100% of the expression values in one of the two conditions were above the 40th percentile were used for statistical analysis. We detected a time-dependent increment of differentially expressed mRNA. Two hours after irradiation, 16,660 transcripts were tested with Student's T-test; 608 of these transcripts exhibited

significant differences, 306 with a fold change > 1.5 (152 up-regulated, 154 down-regulated in irradiated PBMCs). Four hours after irradiation, 17,428 transcripts were tested with Student's T-test; 4,746 of these transcripts exhibited significant differences, 2,626 with a fold change >1.5 (869 up-regulated, 1,757 down-regulated in irradiated PBMCs). Twenty hours after irradiation, 22,586 transcripts were processed after the filtering step; 5,286 of these transcripts exhibited significant differences, 4,674 with a fold change >1.5 (2,770 up-regulated, 1,904 down-regulated in irradiated PBMCs; Additional file 2). The Venn diagram in Figure 5A shows significantly up- or down-regulated transcripts at each time point and the intersection of the expression of these genes. Separate diagrams for up- and down-regulated genes are shown in Additional file 3. A set of 31 genes was significantly altered at every time point in any sample pair from each donor (Figure 5A). Five genes were up-regulated at 2 hours after irradiation, one gene was down-regulated at 2 hours and up-regulated at 4 and 20 hours, and the remaining 25 transcripts were down-regulated at all time points after irradiation (Additional file 4). Hierarchical clustering of
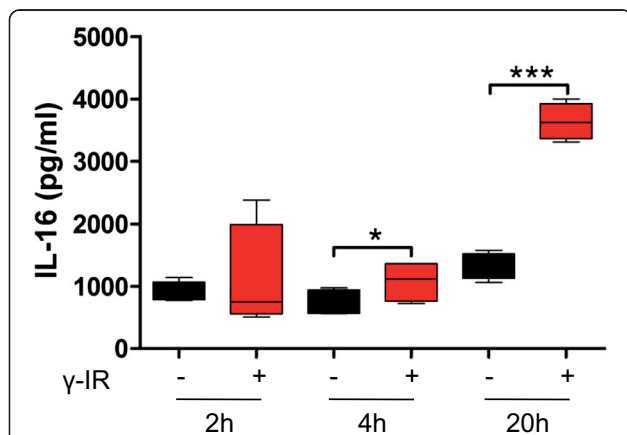
Figure 3 Caspase-3 activation follows a time-dependent up-regulation after exposure to ionizing radiation. IL-16 concentrations measured in the supernatant of non-irradiated (black box-plot) and irradiated (red box-plot) PBMCs are shown as a surrogate marker of caspase-3 activation. Supernatants were collected 2, 4, and 20 hours after exposure to IR and IL-16 concentrations measured with ELISA. A time-dependent increment in IL-16 was observed in the supernatant from irradiated PBMCs, with significantly higher levels starting 4 hours after irradiation compared to non-irradiated cells. *p < 0.05, **p < 0.01, ***p < 0.001; n = 4.

this core set of genes enabled us to discriminate irradiated from non-irradiated samples and aided in further identification of the samples at each time point (Figure 5B and Additional file 5).

Functional annotation clustering

Functional enrichment analysis was performed to identify pathways and biological processes affected in response to IR. Genes with known biological functions were uploaded into the WebGestalt database and classified according to GO terms and (KEGG pathway categories. Default parameters were used for data analysis. Two hours after irradiation, up-regulated genes attributed to processes such as the p53 signaling pathway, apoptosis, and microtubule-based movement were significantly enriched (Additional file 6). The most enriched pathway 4 hours after irradiation was p53 signaling with 16 associated transcripts and an enrichment ratio of 15.5 (Additional file 7). Up-regulated genes 20 hours after exposure to IR were clustered in a variety of biological processes and pathways, with a predominant induction of metabolic, lysosome, phagosome, and cancer-associated pathways (Additional file 8). The protein-protein interactions of 16 up-regulated transcripts coding for proteins in the p53 signaling
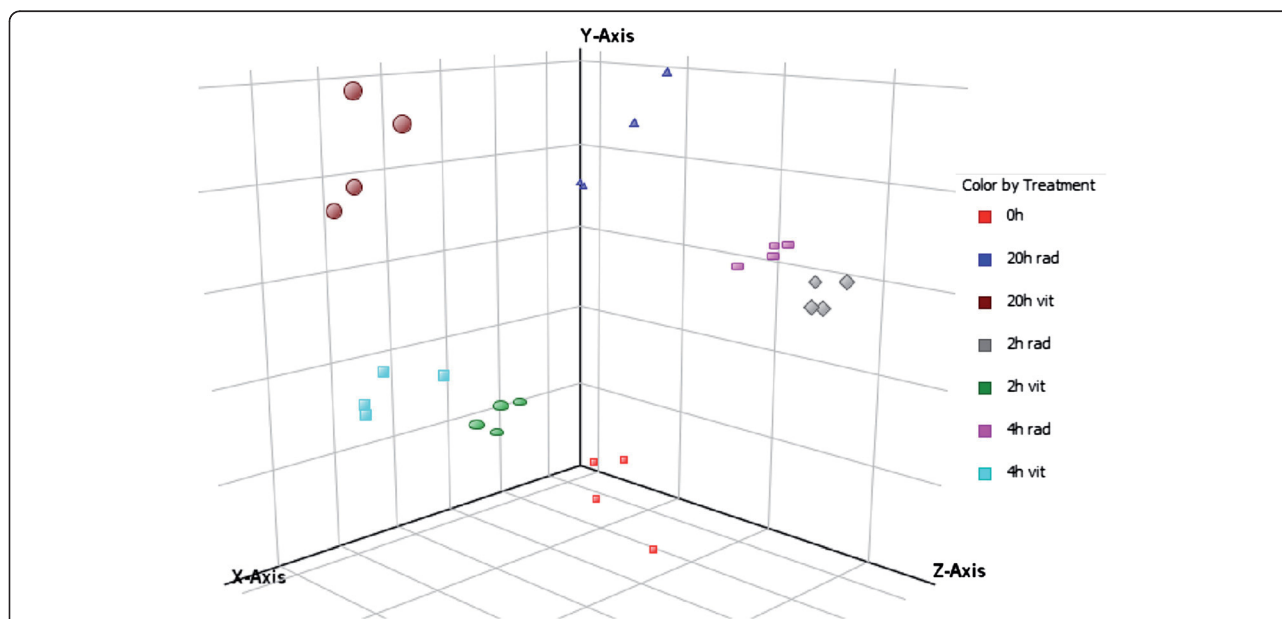
Figure 4 Principle component analysis (PCA) of mRNA expression data shows differences in response to irradiation and cultivation. Samples are displayed with respect to the first three components and are colored with respect to radiation and time point. A total of 28 unique experiments were performed and are displayed in the figure. Matched samples of irradiated and non-radiated PBMCs from four different donors at 2, 4, and 20 hours, as well as expression data from PBMCs isolated immediately after venipuncture without any cultivation period, were used for mRNA expression analysis. PCA allows visual identification of data patterns and highlights similarities and differences between samples. PCA was performed using GeneSpring and was based on conditions. All conditions can be clearly separated from each other. Irradiated PBMCs built three distinct clusters on the right side of the figure, displaying relative low X-axis values. In contrast, non-irradiated PBMCs formed three visible clusters, displaying completely distinct X-axis values compared to irradiated PBMCs, whereas the Y-axis and Z-axis values were comparable. The expression data for 0 h PBMCs formed a distinct cluster separate from 2 or 4 hours after cultivation, even without irradiation. 0 h = PBMCs without any cell culture period; rad = irradiated samples; vit = non-irradiated samples.
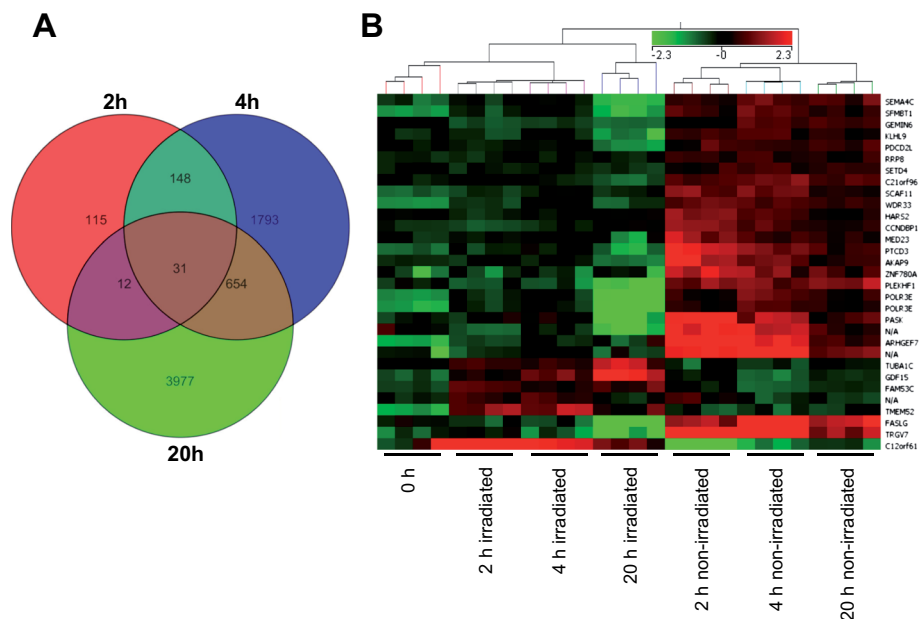
Figure 5 Ionizing radiation induces alterations in mRNA expression levels. (A) mRNA changes in irradiated human PBMCs incubated for 2, 4, and 20 hours using the Agilent Whole Human Genome Oligo Microarray (8 × 60 K) are shown. Venn diagram showing the overlap of up- and down-regulated genes with significant changes in expression 2, 4, and 20 hours after irradiation. A time-dependent increase in differentially expressed genes was observed. The greatest alterations in gene expression between irradiated and non-irradiated PBMCs were detected 20 hours after exposure. The inner triangle contains 31 transcripts that were differentially expressed in all samples at all time points. **(B)** Heat map showing the expression values of the 31 transcripts that were differentially expressed at all time points in all donors. The range of expression was from −2.3 (green, down-regulation) to 2.3 (red, up-regulation). Each time point can be clearly discriminated, and irradiated samples can be discriminated from non-irradiated samples. miRNA names are given on the right border of the heat map.

pathway 4 hours after irradiation were visualized with STRING (Additional file 9). The biological functions of down-regulated genes 2 and 4 hours after irradiation were associated with nucleic acid metabolic processes, RNA metabolic processes, and gene expression (Additional files 10 and 11). Twenty hours after IR, down-regulated genes were associated with lymphocyte activation, hemopoiesis, and somatic cell DNA recombination (Additional file 12). In order to reduce the number of false-positive transcripts, which were only up-regulated at one time point, we also ran analyses with genes that were significantly different at at least two of the three time points. Using this calculation strategy, we detected comparable results showing an induction of biological processes such as the intrinsic apoptotic signaling pathway, regulation of mitochondrial membrane permeability, and KEGG pathways p53 signaling, Wnt signaling, and ubiquitin-mediated proteolysis (Additional file 13).

Radio-responsive miRNAs

As miRNAs are involved in multiple cellular processes and exert regulatory functions, we investigated whether IR induces changes in the miRNA expression levels in irradiated PBMCs. Of the 1350 miRNAs present on the miRNA-array, 241 were considered for further analyses

after an initial filtering step. Though we did not identify any significant changes in miRNA expression 2 hours after irradiation, and only seven miRNAs were altered after 4 hours (Additional file 14 Sheet A), 80 miRNAs were up-regulated and 97 down-regulated 20 hours after irradiation (Additional file 14 Sheet B). These 177 miRNAs were clustered according to their expression, showing that miRNA changes were detectable 20 hours after cultivation with up- or down-regulation in irradiated cells compared to other time points (Figure 6).

miRNA target gene prediction based on mRNA expression with Sylamer analysis

Sylamer analysis is a bioinformatics program that identifies putative miRNA binding sites in the 3'UTR of mRNA based on the nucleotide sequences and calculates whether the predicted targeting miRNAs differ from random expectation in a rank-order list of mRNAs. In general, Sylamer analysis is used to detect alterations in gene expression after miRNA knock-down or in over-expression experiments. We used Sylamer analysis to evaluate whether differentially expressed mRNAs in irradiated PBMCs share an enrichment of specialized miRNA binding sites.

A total of 1,018 up-regulated mRNAs and 1,285 down-regulated mRNAs with a fold change >1.0 were used for

Figure 6 (See legend on next page.)

(See figure on previous page.)
Figure 6 Ionizing radiation induces alterations in microRNA expression levels. Differentially expressed miRNAs in irradiated versus non-irradiated PBMCs are shown. The heat map shows 177 miRNAs that were differentially expressed 20 hours after irradiation. Samples obtained 20 hours after irradiation formed a cluster visible on the right side of the figure, whereas prior time points did not cluster according to treatment or time. The range of expression was from −5 (green, down-regulation) to 5 (red, up-regulation). The names of the genes are given on the right border of the heat map. Sample labeling: "2" = 2 hours, "4" = 4 hours, "20" = 20 hours, "▬" = 0 h sample; "□" = non-irradiated sample; "■" = irradiated sample.

analysis. We did not detect enrichment of 3'UTR binding sites for a single miRNA. However, several miRNAs exhibited comparable enrichment of seed sequences in the set of regulated genes. In a further analysis, we evaluated whether we could detect binding sites of known regulated miRNAs in response to IR based on miRNA expression data. We focused on the 10 most differentially expressed genes in irradiated versus non-irradiated PBMCs. In addition, we evaluated the 10 miRNAs with the highest expression values because even small changes in expression could have a large impact on mRNA expression.

Thus, we were able to identify seven up-regulated miRNAs in irradiated PBMCs that exhibited a significant enrichment of seed sequences in the set of down-regulated mRNAs 20 h after irradiation (Table 1). Of these seven miRNAs, four were significantly more highly expressed in irradiated PBMCs and three miRNAs with high absolute ct-values were more highly expressed in irradiated PBMCs, although the difference was not significant. miR-1268 had the highest enrichment score of all detected miRNAs. The corresponding down-regulated target genes of these seven miRNA are given in Additional file 15.

We performed a similar analysis for up-regulated mRNAs in irradiated PBMCs 20 hours after irradiation. Six miRNAs exhibited significant enrichment of 3'UTR binding sites in the set of down-regulated mRNAs (Table 2). Their target genes are given in Additional file 16.

The same analysis was performed using bioinformatics algorithm cWords (http://servers.binf.ku.dk/cwords/) and revealed comparable results.

Integrated miRNA-mRNA correlation analysis based on Magia[2]

In order to correlate miRNA and mRNA data obtained by microarray analysis of the same biological samples, we performed negative correlation analysis using Magia[2]. Sylamer analysis was performed with mRNA expression exclusively, whereas the Magia[2] program combines paired miRNA and mRNA data to predict interaction networks. The miRNA and mRNA expression profiles of paired samples were analyzed only in the 20 hour miRNA data set, as the number of significant miRNAs in the 4 hour dataset was too low to obtain reliable results. Negatively correlated miRNA-mRNA pairs with a correlation coefficient < −0.7 were used for further analysis, and transcripts were uploaded into WebGestalt and classified according to GO terms and KEGG pathway enrichment. Down-regulated miRNA and corresponding up-regulated mRNA were found to be involved in endocytosis, regulation of cell communication, regulation of actin cytoskeleton polymerization, and apoptosis, among others (Additional file 17). Up-regulated mRNAs and corresponding miRNAs for apoptosis and endocytosis are given in Additional files 18 and 19.

Up-regulated miRNAs and their corresponding down-regulated target genes were associated with cell cycle, mRNA surveillance pathway, leukocyte proliferation, and regulation of gene expression (Additional file 20). Down-regulated mRNAs and corresponding miRNAs associated with the cell cycle are shown in Additional file 21.

Table 1 Identification of miRNA 3'UTR binding sites in the set of down-regulated mRNAs

miRNA	Non-irradiated 20 h	Irradiated 20 h	p-value	Target genes	Seed counts
miR-887	−0.06	7.83	5.46E-05	76	87
miR-1306	−0.06	7.31	4.13E-04	18	18
miR-1180	−0.06	6.71	4.25E-04	79	87
miR-1268	3.71	6.46	4.93E-03	199	272
miR-371-5p	7.07	8.55	ns.	79	87
miR-630	6.92	8.28	ns.	383	709

1018 down-regulated mRNAs 20 hours after irradiation with FC > 1.0 were used for Sylamer analysis. p-value: difference between non-irradiated and irradiated PBMCs based on microarray expression data; target genes: number of genes targeted by the miRNA; seed counts: number of unique seeding regions in the given miRNA.

Table 2 Identification of miRNA 3'UTR binding sites in the set of up-regulated mRNAs

miRNA	Non-irradiated 20 h	Irradiated 20 h	p-value	Target genes	Seed counts
miR-1237	−0.04	−4.84	1.83E-03	457	884
miR-30a	−0.14	−4.93	1.03E-03	398	796
miR-598	−0.51	−4.95	6.18E-04	69	74
miR-601	2.89	0.67	ns.	173	212
miR-205*	3.26	2.59	ns.	361	650
miR-328	2.24	0.08	ns.	371	633

1285 up-regulated mRNAs 20 hours after irradiation with FC > 1.0 were used for Sylamer analysis. p-value: difference between non-irradiated and irradiated PBMCs based on microarray expression data; target genes: number of genes targeted by the miRNA; seed counts: number of unique seeding regions in the given miRNA.

Identification of over-represented transcription factor binding sites in sets of differentially expressed genes in response to irradiation

To identify transcription factors involved in radio-responsive mRNA changes, oPOSSUM3 was used to identify over-represented transcription factor binding sites in the promoter sets of differentially expressed genes 2, 4, and 20 hours after exposure to IR. This analysis revealed that p53 binding sites were specifically enriched in the promoter regions of genes 2 hours after irradiation (Figure 7A and Additional file 22 Sheet A), suggesting an important role of p53, especially shortly after irradiation. In contrast, p53 could not be identified as a regulatory transcription factor 4 and 20 hours after exposure. At

these time points, Kruppel-like factor 4 (Klf4), zinc finger protein X-linked (Zfx), Sp1 transcription factor (SP1), and transcription factor CP2-like 1 (TFCP2L1) binding sites were significantly enriched within the promoter regions (Figure 7B, C). A total of 368 and 548 genes contained binding sites for Klf4 within their promoters 4 and 20 hours after irradiation, respectively (Additional file 22 Sheets B and C).

To further investigate the putative involvement of the predicted transcription factors in the modulation of IR-induced alterations in gene expression, we performed PCR analysis of these transcription factors. Firstly, we were able to show that Klf4, SP1, Zfx, and TFCP2L1 were detectable at the mRNA level (Figure 7D). Secondly, we analyzed
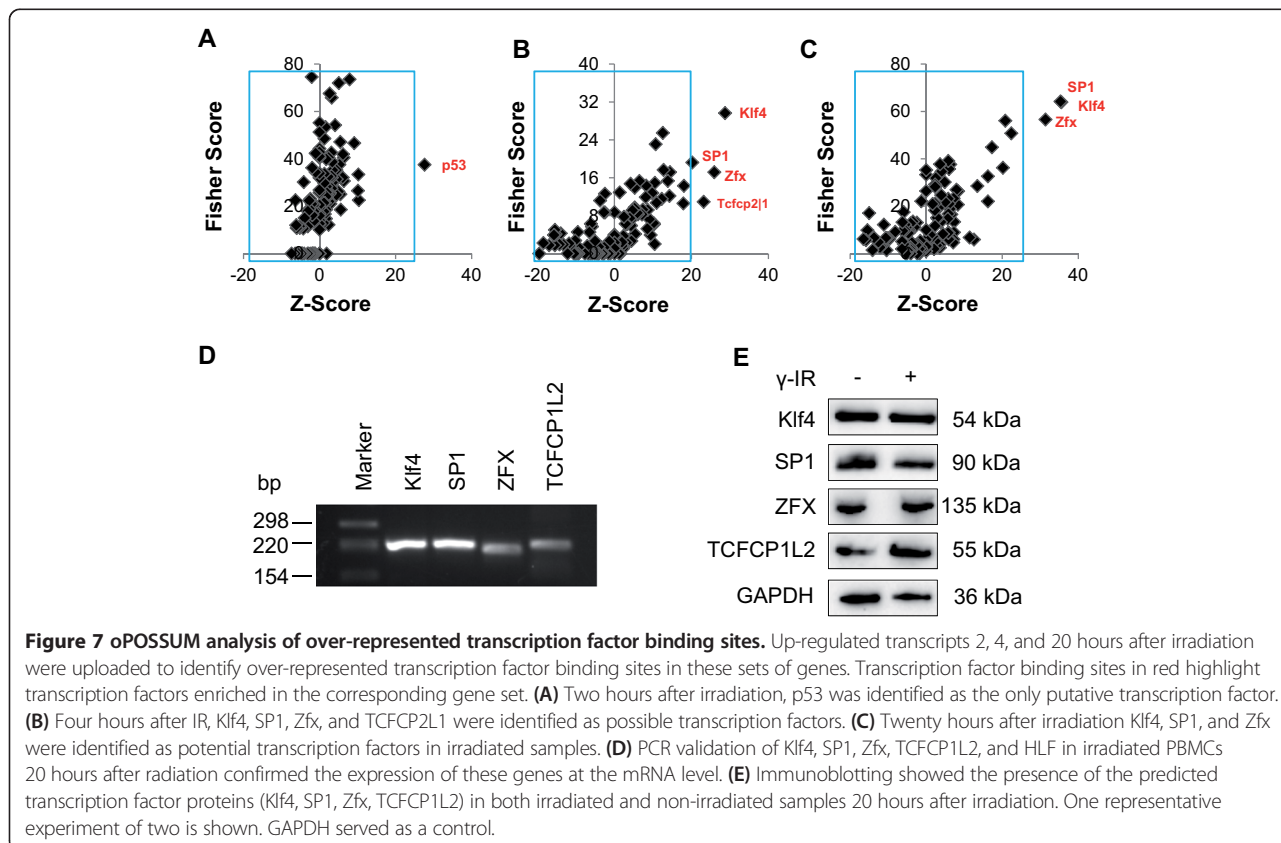
Figure 7 oPOSSUM analysis of over-represented transcription factor binding sites. Up-regulated transcripts 2, 4, and 20 hours after irradiation were uploaded to identify over-represented transcription factor binding sites in these sets of genes. Transcription factor binding sites in red highlight transcription factors enriched in the corresponding gene set. **(A)** Two hours after irradiation, p53 was identified as the only putative transcription factor. **(B)** Four hours after IR, Klf4, SP1, Zfx, and TFCP2L1 were identified as possible transcription factors. **(C)** Twenty hours after irradiation Klf4, SP1, and Zfx were identified as potential transcription factors in irradiated samples. **(D)** PCR validation of Klf4, SP1, Zfx, TCFCP1L2, and HLF in irradiated PBMCs 20 hours after radiation confirmed the expression of these genes at the mRNA level. **(E)** Immunoblotting showed the presence of the predicted transcription factor proteins (Klf4, SP1, Zfx, TCFCP1L2) in both irradiated and non-irradiated samples 20 hours after irradiation. One representative experiment of two is shown. GAPDH served as a control.

whether Klf4, SP1, Zfx, and TFCP2L1 are differentially expressed at the protein level. As shown in Figure 7E, all predicted transcription factors were present at the protein level in cell lysates from irradiated and non-irradiated PBMCs 20 hours after irradiation.

Integrated miRNA-mRNA analysis suggests hepatic leukemia factor involvement in IR-induced transcriptional regulation

Next, we sought to determine whether a transcription factor could be involved in regulatory events affecting both miRNA and mRNA using the Magia[2] database. Within the miRNA-mRNA correlation analysis, the transcription factor hepatic leukemia factor (HLF) occupies a central position. A representative interactive network with HLF is shown in Figure 8A. On one hand, HLF is the target of several up-regulated miRNAs in irradiated PBMCs, but on the other hand it is a transcription factor for many genes found to be down-regulated in irradiated

samples. Based on microarray data, HLF itself should be down-regulated in irradiated PBMCs. qPCR showed that HLF expression levels were significantly lower in irradiated PBMCs compared to non-irradiated PBMCs 20 hours after irradiation (Figure 8B). We performed immunoblot analysis in order to determine if HLF is also regulated at the protein level in response to IR. As shown in Figure 8C, HLF protein levels were lower in irradiated PBMCs compared to non-irradiated PBMCs, which is in line with the data obtained from the miRNA-mRNA expression profiles.

To determine the effect of reduced HLF levels we evaluated the biological function of genes containing a promoter sequence for HLF. These HLF targeted genes were significantly enriched in the regulation of endocytosis pathways (CBLB, IQSEC3), cytoskeleton organization processes, and actin cytoskeleton organization (SORBS3, MICAL, EPB41, OGT).

Figure 8 Regulatory network of hepatic leukemia factor (HLF) displaying the interplay among miRNAs, HLF, and mRNAs. (A) The network was constructed using MAGIA[2], which incorporates positive and negative correlations between expression profiles of possibly interacting miRNAs, transcription factors, and genes according to their predictions. These miRNAs were up-regulated in irradiated cells 20 hours after exposure, whereas their target mRNAs were down-regulated. mRNAs, transcription factors, and miRNAs are shown as light blue circles, green circles, and orange triangles, respectively, and positive and negative correlations are shown as red and blue arrows, respectively. **(B)** qPCR of HLF shows a significant reduction in HLF expression 20 hours after IR exposure, n = 3. **(C)** Cells were harvested 20 hours after irradiation and the HLF level assessed by immunoblotting. IR significantly reduced the HLF protein level compared to non-irradiated samples.

In conclusion, we identified HLF as a potential transcription factor involved in the regulation of both miRNA and mRNA transcription based on the over-representation of promoter binding sites.

qPCR validation study

To validate the results from the microarray experiments, 14 genes were chosen for qPCR. Among these genes, nine were up-regulated (Figure 9A-I) and five down-regulated in irradiated PBMCs (Figure 9J-N). We chose a panel of five irradiation-responsive genes (FDXR, CDKN1A, SESN1, BBC3, PHPT1) previously evaluated by Amundson et al., as well as nine genes based on our data analysis [7]. For all genes analyzed, the expression profiles agreed with the microarray data, though the sample size was too small to reach significance in all samples. These data suggest that the results of the microarray analysis were reliable indicators of overall alterations in gene expression. In addition, three miRNAs were chosen for qPCR validation and miRNA expression 4 and 20 hours after irradiation. All miRNAs were significantly up-regulated in irradiated PBMCs compared to non-irradiated PBMCs 20 hours after exposure, whereas no significant changes were observed 4 hours after exposure to IR, which was in line with the microarray data (Figure 10). The overall fold change in expression was comparable for miR-887 and miR-4299, but the fold change for miR-99b* was lower in qPCR than in the chip data.

Discussion

In this study we showed that high dose IR induces alterations in gene and miRNA expression in human PBMCs, with the greatest changes 20 hours after exposure. We identified p53 and its downstream target proteins as major key players in the modulation of IR-induced biological

Figure 9 Validation of the microarray data by qPCR. Irradiated and non-irradiated human PBMCs were cultured for 2, 4, or 20 hours prior to RNA isolation. Expression values were normalized relative to values in non-irradiated PBMCs. Relative gene expression levels were calculated based on the mean value from four samples using the comparative Ct method. Samples were normalized to the housekeeping gene B2M. Data are presented as mean + SD. Genes in panels **A-I** were up-regulated on the microarray, whereas genes in panels **J-N** were down-regulated in irradiated samples compared to non-irradiated samples. The qPCR data generally supported the microarray data. *p < 0.05, paired T-test; n = 4.

Figure 10 Validation of the miRNA data by qPCR. qPCR revealed a strong correlation between the microarray and PCR data. Expression values were normalized relative to values in non-irradiated PBMCs. The expression of miR-99b* (**A**), miR-887 (**B**), and miR-4299 (**C**), was significantly higher in irradiated PBMCs compared to non-irradiated PBMCs 20 hours after irradiation. Relative gene expression levels were calculated based on the mean value of four samples using the comparative Ct method. RNU44 served as internal reverence miRNA. Data are presented as the mean + SD. *$p < 0.05$, paired T-test; $n = 4$.

processes. In addition, miRNA target prediction analysis revealed their involvement in post-transcriptional regulation of gene expression in response to IR.

In the first part of this study we focused on morphological and post-translational changes induced by IR in human PBMCs. We showed that, even 2 hours after irradiation, apoptotic markers, such as phosphatidylcholine, were detectable on the outer side of the plasma membrane and that these markers increased in a time-dependent manner. In recent publications we have reported that, in response to IR, PBMCs are able to release paracrine factors that exert immune modulatory functions and have presented evidence that IR-induced apoptosis is responsible for the release of these paracrine mediators [32,36-40]. Here, we have identified several up-regulated proteins associated with irradiated apoptotic PBMCs. These proteins were either activated in response to radiation through phosphorylation or cleavage (e.g., phopho-rad17 or cleaved caspase-3) or synthesized de novo (e.g., BAD, XIAP, p21, BAX). Notably, not only proteins synthesized de novo, but also biological activation of stored pro-enzymes, contributed to IR-induced cell responses. Caspases are an example of such important pro-enzymes that are rapidly activated upon cell injury, ultimately leading to apoptosis [41]. As the biological activity of caspases is not reflected at the level of gene expression, we investigated the effects of IR on caspase-3 activation in our experimental setting by measuring IL-16 concentrations in the cell culture supernatant. Biologically inactive pro-IL-16 is stored in the cell nucleus. Caspase 3-mediated cleavage of pro-IL-16 releases mature IL-16 into the extracellular space [34]. Therefore, IL-16 has been proposed as a surrogate marker of caspase 3-mediated apoptosis in PBMCs [34].

In the second part of this study we investigated the extent to which IR induces changes in mRNA and miRNA expression, whether miRNAs are involved in IR-induced gene expression alterations, and whether these gene expression modifications are also reflected in corresponding protein concentrations. Several studies have highlighted that the time after irradiation is an important variable when measuring radiation-induced changes in gene expression [4,5]. We chose 2, 4, and 20 hours based on previous publications, which have shown a time-dependent increase in the variation in mRNA and miRNA expression, with a peak 20 to 24 hours after exposure [4]. Albrecht and colleges showed that in vitro cultivation of human cells itself alters gene expression over time [42]. To exclude artificial changes in expression due to different culture periods, we compared the mRNA and miRNA expression profiles of PBMCs in matched irradiated and non-irradiated samples incubated for the same time periods. Furthermore, we determined gene and miRNA expression in naïve PBMCs that were not cultured at all. In agreement with Albrecht et al., we observed that culturing human PBMCs induces transcriptome alterations as a function of time, independent of radiation treatment. Unspecific cell activation upon contact with foreign surfaces and unfavorable culture conditions for some sub-populations may be responsible for this observation [42].

IR-induced transcriptional changes 2 hours after exposure included pathways involved in apoptosis, signaling cascades, cell cycle regulation, and cancer formation. Surprisingly, early response genes were also significantly associated with protein polymerization, microtubule-based movement, de novo post-translational protein folding, and ribonucleotide binding. The tumor suppressor gene p53 was specifically up-regulated 2 hours after exposure. The p53 response to IR has been described extensively. More than 100 p53 target genes involved in regulation of the cell cycle, transcription, cell death, and DNA repair have been discovered [43]. The involvement of p53 has been described primarily for high dose radiation [44], whereas its role in the response to low doses remains controversial [45]. Our results are in line with those of others that have shown that IR induces rapid expression of p53, and that other genes associated with IR damage are not detectable at an early time point. In addition to p53, cytochrome c, a

second known IR responsive gene, was up-regulated 2 hours after exposure. Cytochrome c activates the caspase cascade and is a key player in initiating apoptosis. Therefore, these data indicate that, as early as 2 hours after IR injury, two key mediators of DNA repair and apoptosis were up-regulated, whereas other previously described radiation-induced genes were not detectable. These observations seem to be explicable by the fact that high dose radiation induces severe double strand breaks [46], as well as clustered DNA lesions [47], which are powerful inducers of p53 accumulation, activation, and expression. In addition to the described functions of p53 in response to high dose radiation, recent studies in a model of ex vivo irradiated human skin indicate that p53 also plays important roles during low dose irradiation. For example, in low dose radiation injury p53 seems to promote cell survival via activation of cell protective pathways, DNA repair, and cell cycle arrest, whereas in high radiation injury cell death executer functions are predominantly induced by p53 [42].

Functional clustering and analysis of genes significantly up-regulated compared to control samples 4 hours after irradiation revealed strong enhancement of apoptosis-related proteins. We were able to identify several novel pro-apoptotic transcripts up-regulated at this time point but not at 2 hours: SESN2, DDB2, TNFRSF10B, P21, CCND1, MDM2, PMAIP1, PTEN, GADD45B, CCND3, BAX, BBC3, ZMAT3, and SFN. These gene expression data are in line with our protein data; we observed higher concentrations of these proteins in irradiated PBMCs 20 hours after exposure. Apparently, between 2 and 4 hours after irradiation the transcriptional machinery of the IR-induced damage response is activated by p53, consequently up-regulating several transcripts. The importance of p53 was also confirmed by transcription factor binding site analysis. Two hours after exposure, p53 was the only enriched transcription factor. Interestingly, the transcription factor Klf4, a direct downstream target of p53, had binding sites in the promoter region of 368 and 548 up-regulated transcripts 4 and 20 hours after exposure, respectively. Transcription factor binding sites for p53 were not enriched in the gene set 4 and 20 hours after irradiation. The tumor suppressor Klf4 activates p21 transcription and inhibits cell proliferation [48]. These data suggest that rapid activation of p53 results in up-regulation of Klf4, which amplifies the p53-mediated response to IR.

We identified enrichment of transcription factor binding sites within p53 and Klf4 for SP1, Zfx, and TFCP2L1 in the set of up-regulated mRNAs 4 and 20 hours after irradiation. We validated these data using PCR to show that these transcription factors were expressed in irradiated PBMCs, and immunoblotting confirmed their presence at the protein level, though we could not detect an induction

of total protein content in response to IR. Translational modifications, such as phosphorylation or adenylylation, may also be involved in modulating the activity of Klf4, SP1, Zfx, and TFCP2L1; therefore, total protein content does not perfectly correspond to biological activity. Phosphorylation of p53 enhances Klf4 binding, increases Klf4 activity [49], and promotes cell cycle arrest via induction of p21 and p27 [50]. In addition, phosphorylation of SP1 and p53 promotes their regulatory activity and p21 activation [51]. Recently, SP1 was shown to be a central modulator of p53-induced apoptosis in humans [52]. Zfx and TFCP2L1 have multiple phosphorylation sites, though to the best of our knowledge no data exists as to whether post-translational modification is important in regulation of their biological function.

When comparing differentially expressed genes 20 hours after exposure to IR to those differentially expressed 2 and 4 hours after irradiation, we found 4,674 differentially expressed genes. Functional clustering revealed that the majority of these transcripts were involved in the regulation of signal transduction, vesicle-mediated transport, the cytoskeleton, and endocytosis. These data support our FACS analysis and EM photographs, which show that the majority of cells are in a late stage of apoptosis at these time points and that proteins associated with vesicle transport and endocytosis contribute to the formation of apoptotic bodies and cell membrane evaginations. Gene expression data revealed that the process of cellular fragmentation is actively controlled by proteins rather than being a spontaneous occurrence [53].

To further elucidate the IR-induced changes in gene expression, we evaluated whether the expression of miRNAs is affected in response to IR. IR altered the miRNA expression profile as a function of time, which was in accordance with data from human PBMCs [4] and normal human fibroblasts [16]. Significant differences became detectable after 4 hours. Twenty hours after exposure to IR, 177 miRNAs were differentially expressed. Only a minority of the radio-responsive miRNAs identified in this study have been reported in previous studies. One reason for this observation may be the high IR dosage used in our study. Furthermore, progress in the field of miRNA research over the last few years has led to a rapidly increasing number of detectable miRNAs. Eighty of the differentially regulated miRNAs were up-regulated and 97 down-regulated. The predominant down-regulation of miRNAs found in this study was in line with the findings of Joly-Tonetti et al., who showed that all modulated miRNAs of proliferating keratinocytes irradiated with 6 Gy were down-regulated [17]. Giardi and colleges observed a similar tendency, showing an excess of down-regulated miRNAs 24 hours after 2 Gy gamma irradiation of human PBMCs [4]. A possible explanation for this phenomenon is that miRNAs can affect cellular

radio-sensitivity by targeting radio-protective genes. Over-expression of miR-9, let-7 g [54], miR-100, miR-101, miR-181a, or miR-421 has been shown to enhance the vulnerability of cells to IR-induced injury [55] and direct cells towards an apoptotic pathway. We observed that several miRNAs with known cell survival activity were down-regulated in response to IR, whereas their pro-apoptotic target genes were up-regulated. For example, miR-21, a pro-oncogenic miRNA known to promote cell proliferation and the evasion of apoptosis, was down-regulated in our irradiated PBMCs, but its targets p53, BAX, PTEN, and BCL2 [56] were up-regulated at both the gene and protein levels. A further down-regulated miRNA in response to IR was miR-378. Caspase-3 is a target protein of miR-378, and over-expression of this miRNA has been shown to inhibit apoptosis, whereas inhibition of miR-378 aggravates hypoxia-induced apoptosis [35]. Moreover, members of the miR-30 family regulate apoptosis by controlling mitochondrial fission, suppressing p53 [57] and caspase 3 translation [58], as well as tumor necrosis factor-related apoptosis inducing ligand-mediated apoptosis [59]. In our data set, we detected a significant down-regulation of miR-30d, miR-30e*, and miR-30a 20 hours after irradiation (see Additional file 14). A down-regulation of these miRNAs in irradiated PBMCs can be interpreted as follows: basal expression of these miRNAs is needed to maintain balance in the translation and degradation of genes coding for proteins involved in cell proliferation and apoptosis. Upon cell injury, transcription of pro-apoptotic genes is enhanced and the expression of targeting miRNAs reduced simultaneously. This coupled mechanism may enable cells to rapidly amplify biological responses to stressful events and maintain cellular integrity.

In accordance with other studies [55], we have shown that miRNAs are involved in regulation of the MAPK pathway in response to IR and in the regulation of apoptosis [60]. Other pathways, such as the mRNA surveillance pathway or T-cell receptor signaling pathway, were repressed by miRNAs. Several studies have documented the involvement of the endocytosis and cytoskeleton pathways in response to radiation exposure [61-63], as well as their alteration through miRNAs [60]. We obtained similar results showing the up-regulation of genes (GATA2, SERPINE1, myosin VA, or ubiquitin specific peptidase 33) associated with endocytosis, vesicle-mediated transport, and signal transduction, whereas their corresponding miRNAs were down-regulated (e.g., mir-32, miR- 92a, miR-200c, miR, or miR-301b).

Using a combination of miRNA-mRNA correlation data, we identified HLF as a putative down-regulated transcription factor in response to IR. HLF is targeted by several up-regulated miRNAs, and its gene expression and protein levels were reduced in irradiated PBMCs compared to non-irradiated PBMCs. This reduction may be due to degradation or inhibition of miRNA-mediated mRNA translation. One previous study has shown that ectopic HLF expression attenuates IR-induced cell death by up-regulating anti-apoptotic genes and repressing the transcription of pro-apoptotic genes. These data are in line with our observation of reduced HLF levels in cells undergoing apoptosis. In addition to the involvement of HLF in the inhibition of cell death pathways, several target genes of HLF were down-regulated in irradiated PBMCs. These genes were involved in the regulation of cytoskeletal processes (SYNE2, EPB41, SORBS3), actin filament depolymerization (MICAL3), and endocytosis (CBLB, JQSEC3). We hypothesize that reduced HLF levels facilitate cell death and modulate morphological-cytoskeletal changes in irradiated samples.

This finding is of special interest because cells in the late phase of apoptosis form plasma membrane blebs containing organelles that are strangulated and released into the extracellular space [64]. The process of plasma membrane budding is actively enforced by cells and mediated by actin-myosin interactions [64]. We found 100 up-regulated mRNAs with known molecular functions in cytoskeletal protein binding, with actin and myosin being the most prominent genes. On the other hand, we detected distinct transcripts actively repressed by up-regulation of distinct miRNAs that were induced upon IR. These data support the notion that cellular dissolution is an active process in which cytoskeletal proteins are involved in the induction of apoptosis-mediated cell fragmentation. In addition, cells constantly release small membrane vesicles of endocytic origin termed exosomes, which are actively secreted upon late endosome fusion with the plasma membrane [65]. Exosomes are mediators of intercellular communication that can deliver information from cell to cell [66]. Sixty-seven genes were up-regulated 20 hours after irradiation, and these may be associated with endosomes or lysosomes with known function in exosomal signaling (e.g., CD68), indicating that IR affects the biological process of extracellular vesicle formation. Exosomes released from irradiated cells have been shown to exert bystander effects, as they induce genomic instability in non-irradiated cells [67]. Therefore, our data suggest that IR is not only a trigger for the induction of apoptotic body formation, but also for the production and release of small extracellular vesicles.

Conclusion

In this study, we comprehensively analyzed IR-induced changes in mRNA, miRNA, and protein levels and identified p53 as the major early response transcription factor regulated by IR. The miRNA target analysis identified the involvement of miRNAs in the regulation of IR-induced biological processes, and we discovered

previously unknown miRNAs involved in the response to IR. We described a complex interaction network of miRNAs and target mRNAs that will encourage future studies to examine the contribution of the specific newly identified miRNAs on the regulation of biological processes in response to IR in more detail.

Availability of supporting data

The data sets supporting the results of this article are included within the additional files and are available in the LabArchives (https://mynotebook.labarchives.com/) repository using DOI http://dx.doi.org/10.6070/H40V89S4. Gene expression data are available on the Gene Expression Omnibus (GEO) website (http://www.ncbi.nlm.nih.gov/geo/) under accession number GEO: GSE55955.

Additional files

Additional file 1: PCR primer sequences.

Additional file 2: mRNAs differentially expressed in irradiated vs. non-irradiated PBMCs. Differentially expressed mRNAs from irradiated vs. non-irradiated human PBMCs 2 (Datasheet A), 4 (Datasheet B), and 20 hours (Datasheet C) after irradiation are listed.

Additional file 3: Venn diagram of differentially expressed genes. Changes in the mRNA of irradiated human PBMCs incubated for 2, 4, and 20 hours are shown. (A) The overlap of up-regulated genes with significant expression changes after irradiation. Five genes were up-regulated at all time points. (B) The overlap of down-regulated genes with significant expression changes after irradiation. 25 genes were down-regulated at all time points.

Additional file 4: Differentially expressed core genes. Genes that were significantly up- or down-regulated (BH Corrected p-value <0.05, FC ≥1.5 in 2 of 4 samples) 2, 4, and 20 hours after irradiation are sorted by highest average FC. The values indicate the geometric mean of the FC value of irradiated samples compared to time-matched controls calculated for four different PBMC preparations. The Benjamini Hochberg FDR-corrected p-value is shown. FC = Fold Change.

Additional file 5: Principle component analysis (PCA) of selected genes. Thirty-one transcripts differentially expressed at all time points are shown with respect to the first three components and are colored with regard to radiation and time point. PCA allows visual identification of data patterns and highlights similarities and differences between samples. PCA was performed using GeneSpring and was based on conditions. All conditions can be clearly separated from each other. Irradiated cells located in three clusters significantly separated from non-irradiated cells. In contrast, 2 and 4 hours after irradiation, non-irradiated cells clustered next to naïve cells, and 20 hours after irradiated cells clustered above these three clusters.

Additional file 6: KEGG pathway and GO analysis of up-regulated genes 2 hours after irradiation. The KEGG pathway (Datasheet A) and enrichment of GO terms (Datasheet B) in up-regulated genes in irradiated PBMCs 2 hours after irradiation were analyzed using the WEBGESTALT analysis tool. All values are sorted by increasing p-values.

Additional file 7: KEGG pathway and GO analysis of up-regulated genes 4 hours after irradiation. The KEGG pathway (Datasheet A) and enrichment of GO terms (Datasheet B) in up-regulated genes in irradiated PBMCs 4 hours after irradiation were analyzed using the WEBGESTALT analysis tool. All values are sorted by increasing p-values.

Additional file 8: KEGG pathway and GO analysis of up-regulated genes 20 hours after irradiation. The KEGG pathway (Datasheet A) and enrichment of GO terms (Datasheet B) in up-regulated genes in irradiated PBMCs 20 hours after irradiation were analyzed using the WEBGESTALT analysis tool. All values are sorted by increasing p-values.

Additional file 9: p53 protein interaction network in irradiated cells. The predicted functional interaction of eight significantly up-regulated transcripts in irradiated PBMCs at two of three time points clustered in the canonical pathway "p53 signaling" were visualized using String v9.1 software. A direct interaction of 16 transcripts is evident. p53 and its downstream target MDM2 are in the center position, interacting with nine partner proteins. Linking line colors are based on their origin: yellow – text mining linkage; blue – database; pink – experiments; black – co-expression.

Additional file 10: KEGG pathway and GO analysis of down-regulated genes 2 hours after irradiation. The KEGG pathway (Datasheet A) and enrichment of GO terms (Datasheet B) in down-regulated genes in irradiated PBMCs 2 hours after irradiation were analyzed using the WEBGESTALT analysis tool. All values are sorted by increasing p-values.

Additional file 11: KEGG pathway and GO analysis of down-regulated genes 4 hours after irradiation. The KEGG pathway (Datasheet A) and enrichment of GO terms (Datasheet B) in down-regulated genes in irradiated PBMCs 4 hours after irradiation were analyzed using the WEBGESTALT analysis tool. All values are sorted by increasing p-values.

Additional file 12: KEGG pathway and GO analysis of down-regulated genes in irradiated PBMCs 20 hours after irradiation. The KEGG pathway (Datasheet A) and enrichment of GO terms (Datasheet B) in down-regulated genes in irradiated PBMCs 20 hours after irradiation were analyzed using the WEBGESTALT analysis tool. All values are sorted by increasing p-values.

Additional file 13: Up-regulated KEGG pathway and GO analysis and down-regulated KEGG pathway (Datasheet C) and GO analysis (Datasheet D) in irradiated PBMCs at two of three time points. The KEGG pathway (Datasheet A and C) and enrichment of GO terms (Datasheet B and D) in up-regulated (Datasheet A and B) and down-regulated genes (Datasheet C and D) in irradiated PBMCs at two of three time points after irradiation were analyzed using the WEBGESTALT analysis tool. All values are sorted by increasing p-values.

Additional file 14: miRNAs differentially expressed in irradiated vs. non-irradiated PBMCs. Differentially expressed miRNA in human PBMCs 4 (Datasheet A) and 20 hours (Datasheet B) after irradiation are shown.

Additional file 15: Seven up-regulated miRNAs 20 hours after IR and their negatively correlated target genes. Using Sylamer analysis, miR-887, miR-1306, miR-1180, miR-1268, miR-371-5p, miR-630, and miR-595 exhibited enrichment of seed regions in the set of mRNAs down-regulated 20 hours after IR. Each miRNA, its target genes, and the number of seed regions within each gene are shown.

Additional file 16: Six down-regulated miRNAs 20 hours after IR and their negatively correlated target genes. Using Sylamer analysis, miR-1237, miR-30a, miR-598, miR-601, miR-205*, and miR-328 exhibited enrichment of seed regions in the set of mRNAs up-regulated 20 hours after IR. Each miRNA, its target genes, and the number of seed regions within each gene are shown.

Additional file 17: KEGG pathways and GO analysis of up-regulated mRNAs controlled by miRNAs 20 hours after irradiation. 140 annotated genes up-regulated 20 hours after irradiation were classified into different canonical pathways according to KEGG pathway analysis (Datasheet A) or GO analysis (Datasheet B).

Additional file 18: Up-regulated genes targeted by down-regulated miRNAs involved in apoptosis. The given mRNAs were up-regulated 20 hours after irradiation but their targeting miRNAs were down-regulated. The genes were clustered according to their biological function: apoptosis. The statistic column lists the number of reference genes in the category (C), number of genes in the gene set and the category (O), expected number in the category (E), ratio of enrichment (R), p-value from the hypergeometric test (rawP), and the p-value adjusted by the multiple test adjustment (adjP). For mRNA, the gene symbol, Entrez gene ID, and value expressed as log2 (sample/control) are given. The corresponding miRNA, intensity value expressed as log2 (sample/control), and correlation coefficient are stated.

Additional file 19: Up-regulated genes targeted by down-regulated miRNAs involved in endocytosis. The given mRNAs were up-regulated 20 hours after irradiation but their targeting miRNAs were down-regulated. The genes were clustered according to their biological function: endocytosis. The statistic column lists the number of reference genes in the category (C), number of genes in the gene set and the category (O), expected number in the category (E), ratio of enrichment (R), p-value from the hypergeometric test (rawP), and the p-value adjusted by the multiple test adjustment (adjP). For mRNA, the gene symbol, Entrez gene ID, and the value expressed as log2 (sample/control) are given. The corresponding miRNA, intensity value expressed as log2 (sample/control), and correlation coefficient are stated.

Additional file 20: KEGG pathways and GO analysis of down-regulated mRNAs controlled by miRNAs 20 hours after irradiation. 208 annotated genes down-regulated 20 hours after irradiation were classified into different canonical pathways according to KEGG pathway analysis (Datasheet A) or GO analysis (Datasheet B).

Additional file 21: Down-regulated genes targeted by up-regulated miRNAs involved in the cell cycle. The given mRNAs were down-regulated 20 hours after irradiation but their targeting miRNAs up-regulated. The genes were clustered according to their biological function: cell cycle. The statistic column lists the number of reference genes in the category (C), number of genes in the gene set and the category (O), expected number in the category (E), ratio of enrichment (R), p-value from the hypergeometric test (rawP), and the p-value adjusted by the multiple test adjustment (adjP). For mRNA, the gene symbol, Entrez gene ID, and value expressed as log2 (sample/control) are given. The corresponding miRNA, intensity value expressed as log2 (sample/control), and correlation coefficient are stated.

Additional file 22: Bioinformatics analysis of putative transcription factor binding sites (oPOSSUM3 single site binding analysis method) in up-regulated genes 2, 4, and 20 hours after radiation. Significant results are shaded in red.

Abbreviations

PCA: Principle component analysis; GO: Gene ontology; GEO: Gene expression omnibus; IR: Ionizing radiation; mRNA: Messenger RNA; miRNA: Micro RNA; KEGG: Kyoto Encyclopedia of Genes and Genomes; PBMC: Peripheral blood mononuclear cells; qPCR: Quantitative real-time PCR; TF: Transcription factor; TFBS: Transcription factor binding site.

Competing interest

The authors declare that they have no competing interests.

Authors' contributions

LB, MK, AM, MZ, and MM performed the laboratory experiments; LB, RS, RR, and MG carried out the expression data analysis. LB performed the regulatory network reconstruction, transcription factor binding site analysis, and pathway enrichment analysis; AE performed EM; LB, MM, HJA, and MG designed the study and drafted the manuscript; and RS, RR, AE, CG, WK, and MG helped draft the manuscript. All authors have read and approved the final manuscript.

Author details

[1]Department of Thoracic Surgery, Medical University of Vienna, Währinger Gürtel 18-20, 1090 Vienna, Austria. [2]Christian Doppler Laboratory for Cardiac and Thoracic Diagnosis and Regeneration, Medical University of Vienna, Währinger Gürtel 18-20, 1090 Vienna, Austria. [3]University Hospital of Craniomaxillofacial and Oral Surgery, Medical University of Vienna, Vienna, Austria. [4]Center for Medical Statistics, Informatics, and Intelligent Systems, Section for Medical Statistics, Medical University of Vienna, Vienna, Austria. [5]Department of Cell Biology and Ultrastructure Research, Center for Anatomy and Cell Biology, Medical University of Vienna, Vienna, Austria. [6]Red Cross Blood Transfusion Service of Upper Austria, Linz, Austria. [7]Austrian Cluster for Tissue Regeneration, Linz, Austria. [8]Department of Cardiology, Medical University Vienna, Vienna, Austria. [9]Department of Dermatology, Research Division of Biology and Pathobiology of the Skin, Medical University Vienna, Lazarettgasse 14, 1090 Vienna, Austria.

References

1. Spitz DR, Azzam EI, Li JJ, Gius D: **Metabolic oxidation/reduction reactions and cellular responses to ionizing radiation: a unifying concept in stress response biology.** *Cancer Metastasis Rev* 2004, **23**(3–4):311–322.
2. Chaudhry MA: **Bystander effect: biological endpoints and microarray analysis.** *Mutat Res* 2006, **597**(1–2):98–112.
3. Wyrobek AJ, Manohar CF, Krishnan VV, Nelson DO, Furtado MR, Bhattacharya MS, Marchetti F, Coleman MA: **Low dose radiation response curves, networks and pathways in human lymphoblastoid cells exposed from 1 to 10 cGy of acute gamma radiation.** *Mutat Res* 2011, **722**(2):119–130.
4. Girardi C, De Pitta C, Casara S, Sales G, Lanfranchi G, Celotti L, Mognato M: **Analysis of miRNA and mRNA expression profiles highlights alterations in ionizing radiation response of human lymphocytes under modeled microgravity.** *PLoS One* 2012, **7**(2):e31293.
5. Knops K, Boldt S, Wolkenhauer O, Kriehuber R: **Gene expression in low- and high-dose-irradiated human peripheral blood lymphocytes: possible applications for biodosimetry.** *Radiat Res* 2012, **178**(4):304–312.
6. Mezentsev A, Amundson SA: **Global gene expression responses to low- or high-dose radiation in a human three-dimensional tissue model.** *Radiat Res* 2011, **175**(6):677–688.
7. Amundson SA, Lee RA, Koch-Paiz CA, Bittner ML, Meltzer P, Trent JM, Fornace AJ Jr: **Differential responses of stress genes to low dose-rate gamma irradiation.** *Mol Cancer Res* 2003, **1**(6):445–452.
8. Budworth H, Snijders AM, Marchetti F, Mannion B, Bhatnagar S, Kwoh E, Tan Y, Wang SX, Blakely WF, Coleman M, Peterson L, Wyrobek AJ: **DNA repair and cell cycle biomarkers of radiation exposure and inflammation stress in human blood.** *PLoS One* 2012, **7**(11):e48619.
9. Turtoi A, Brown I, Oskamp D, Schneeweiss FH: **Early gene expression in human lymphocytes after gamma-irradiation-a genetic pattern with potential for biodosimetry.** *Int J Radiat Biol* 2008, **84**(5):375–387.
10. Manning G, Kabacik S, Finnon P, Bouffler S, Badie C: **High and low dose responses of transcriptional biomarkers in ex vivo X-irradiated human blood.** *Int J Radiat Biol* 2013, **89**(7):512–522.
11. Turtoi A, Brown I, Schlager M, Schneeweiss FH: **Gene expression profile of human lymphocytes exposed to (211)At alpha particles.** *Radiat Res* 2010, **174**(2):125–136.
12. Bartel DP: **MicroRNAs: genomics, biogenesis, mechanism, and function.** *Cell* 2004, **116**(2):281–297.
13. Peterson SM, Thompson JA, Ufkin ML, Sathyanarayana P, Liaw L, Congdon CB: **Common features of microRNA target prediction tools.** *Front Genet* 2014, **5**:23.
14. Fabian MR, Sonenberg N: **The mechanics of miRNA-mediated gene silencing: a look under the hood of miRISC.** *Nat Struct Mol Biol* 2012, **19**(6):586–593.
15. Fujiwara T, Yada T: **miRNA-target prediction based on transcriptional regulation.** *BMC Genomics* 2013, **14**(Suppl 2):S3.
16. Crosby ME, Kulshreshtha R, Ivan M, Glazer PM: **MicroRNA regulation of DNA repair gene expression in hypoxic stress.** *Cancer Res* 2009, **69**(3):1221–1229.
17. Joly-Tonetti N, Vinuelas J, Gandrillon O, Lamartine J: **Differential miRNA expression profiles in proliferating or differentiated keratinocytes in response to gamma irradiation.** *BMC Genomics* 2013, **14**:184.
18. Templin T, Paul S, Amundson SA, Young EF, Barker CA, Wolden SL, Smilenov LB: **Radiation-induced micro-RNA expression changes in peripheral blood cells of radiotherapy patients.** *Int J Radiat Oncol Biol Phys* 2011, **80**(2):549–557.
19. Josson S, Sung SY, Lao K, Chung LW, Johnstone PA: **Radiation modulation of microRNA in prostate cancer cell lines.** *Prostate* 2008, **68**(15):1599–1606.
20. Brazma A, Hingamp P, Quackenbush J, Sherlock G, Spellman P, Stoeckert C, Aach J, Ansorge W, Ball CA, Causton HC, Gaasterland T, Glenisson P, Holstege FC, Kim IF, Markowitz V, Matese JC, Parkinson H, Robinson A, Sarkans U, Schulze-Kremer S, Stewart J, Taylor R, Vilo J, Vingron M: **Minimum information about a microarray experiment (MIAME)-toward standards for microarray data.** *Nat Genet* 2001, **29**(4):365–371.

21. Su AI, Cooke MP, Ching KA, Hakak Y, Walker JR, Wiltshire T, Orth AP, Vega RG, Sapinoso LM, Moqrich A, Patapoutian A, Hampton GM, Schultz PG, Hogenesch JB: **Large-scale analysis of the human and mouse transcriptomes.** *Proc Natl Acad Sci U S A* 2002, **99**(7):4465–4470.

22. Ramskold D, Wang ET, Burge CB, Sandberg R: **An abundance of ubiquitously expressed genes revealed by tissue transcriptome sequence data.** *PLoS Comput Biol* 2009, **5**(12):e1000598.

23. Hochberg YBY: **Controlling the false discovery rate: A practical and powerful approach to multiple testing.** *J R Stat Soc* 1995, **57**(1):289–300.

24. Wang J, Duncan D, Shi Z, Zhang B: **WEB-based GEne SeT AnaLysis Toolkit (WebGestalt): update 2013.** *Nucleic Acids Res* 2013, **41**(Web Server issue): W77–W83.

25. Franceschini A, Szklarczyk D, Frankild S, Kuhn M, Simonovic M, Roth A, Lin J, Minguez P, Bork P, von Mering C, Jensen LJ: **STRING v9.1: protein-protein interaction networks, with increased coverage and integration.** *Nucleic Acids Res* 2013, **41**(Database issue):D808–D815.

26. Bartonicek N, Enright AJ: **SylArray: a web server for automated detection of miRNA effects from expression data.** *Bioinformatics* 2010, **26**(22):2900–2901.

27. Bisognin A, Sales G, Coppe A, Bortoluzzi S, Romualdi C: **MAGIA(2): from miRNA and genes expression data integrative analysis to microRNA-transcription factor mixed regulatory circuits (2012 update).** *Nucleic Acids Res* 2012, **40**(Web Server issue):W13–W21.

28. Kwon AT, Arenillas DJ, Worsley Hunt R, Wasserman WW: **oPOSSUM-3: advanced analysis of regulatory motif over-representation across genes or ChIP-Seq datasets.** *G3 (Bethesda)* 2012, **2**(9):987–1002.

29. Jhas B, Sriskanthadevan S, Skrtic M, Sukhai MA, Voisin V, Jitkova Y, Gronda M, Hurren R, Laister RC, Bader GD, Minden MD, Schimmer AD: **Metabolic adaptation to chronic inhibition of mitochondrial protein synthesis in acute myeloid leukemia cells.** *PLoS One* 2013, **8**(3):e58367.

30. Kadl A, Huber J, Gruber F, Bochkov VN, Binder BR, Leitinger N: **Analysis of inflammatory gene induction by oxidized phospholipids in vivo by quantitative real-time RT-PCR in comparison with effects of LPS.** *Vascul Pharmacol* 2002, **38**(4):219–227.

31. Pfaffl MW: **A new mathematical model for relative quantification in real-time RT-PCR.** *Nucleic Acids Res* 2001, **29**(9):e45.

32. Ankersmit HJ, Hoetzenecker K, Dietl W, Soleiman A, Horvat R, Wolfsberger M, Gerner C, Hacker S, Mildner M, Moser B, Lichtenauer M, Podesser BK: **Irradiated cultured apoptotic peripheral blood mononuclear cells regenerate infarcted myocardium.** *Eur J Clin Invest* 2009, **39**(6):445–456.

33. Lakhani SA, Masud A, Kuida K, Porter GA Jr, Booth CJ, Mehal WZ, Inayat I, Flavell RA: **Caspases 3 and 7: key mediators of mitochondrial events of apoptosis.** *Science* 2006, **311**(5762):847–851.

34. Elssner A, Doseff AI, Duncan M, Kotur M, Wewers MD: **IL-16 is constitutively present in peripheral blood monocytes and spontaneously released during apoptosis.** *J Immunol* 2004, **172**(12):7721–7725.

35. Fang J, Song XW, Tian J, Chen HY, Li DF, Wang JF, Ren AJ, Yuan WJ, Lin L: **Overexpression of microRNA-378 attenuates ischemia-induced apoptosis by inhibiting caspase-3 expression in cardiac myocytes.** *Apoptosis* 2012, **17**(4):410–423.

36. Lichtenauer M, Mildner M, Baumgartner A, Hasun M, Werba G, Beer L, Altmann P, Roth G, Gyongyosi M, Podesser BK, Ankersmit HJ: **Intravenous and intramyocardial injection of apoptotic white blood cell suspensions prevents ventricular remodelling by increasing elastin expression in cardiac scar tissue after myocardial infarction.** *Basic Res Cardiol* 2011, **106**(4):645–655.

37. Lichtenauer M, Mildner M, Hoetzenecker K, Zimmermann M, Podesser BK, Sipos W, Berenyi E, Dworschak M, Tschachler E, Gyongyosi M, Ankersmit HJ: **Secretome of apoptotic peripheral blood cells (APOSEC) confers cytoprotection to cardiomyocytes and inhibits tissue remodelling after acute myocardial infarction: a preclinical study.** *Basic Res Cardiol* 2011, **106**(6):1283–1297.

38. Hoetzenecker K, Zimmermann M, Hoetzenecker W, Schweiger T, Kollmann D, Mildner M, Hegedus B, Mitterbauer A, Hacker S, Birner P, Gabriel C, Gyöngyösi M, Blyszczuk P, Eriksson U, Ankersmit HJ: **Mononuclear cell secretome protects from experimental autoimmune myocarditis.** *Eur Heart J* 2013. [Epub ahead of print].

39. Hoetzenecker K, Assinger A, Lichtenauer M, Mildner M, Schweiger T, Starlinger P, Jakab A, Berenyi E, Pavo N, Zimmermann M, Gabriel C, Plass C, Gyöngyösi M, Volf I, Ankersmit HJ: **Secretome of apoptotic peripheral blood cells (APOSEC) attenuates microvascular obstruction in a porcine closed chest reperfused acute myocardial infarction model: role of platelet aggregation and vasodilation.** *Basic Res Cardiol* 2012, **107**(5):292.

40. Pavo N, Zimmermann M, Pils D, Mildner M, Petrasi Z, Petnehazy O, Fuzik J, Jakab A, Gabriel C, Sipos W, Maurer G, Gyöngyösi M, Ankersmit HJ: **Long-acting beneficial effect of percutaneously intramyocardially delivered secretome of apoptotic peripheral blood cells on porcine chronic ischemic left ventricular dysfunction.** *Biomaterials* 2014, **35**(11):3541–3550.

41. Slee EA, Keogh SA, Martin SJ: **Cleavage of BID during cytotoxic drug and UV radiation-induced apoptosis occurs downstream of the point of Bcl-2 action and is catalysed by caspase-3: a potential feedback loop for amplification of apoptosis-associated mitochondrial cytochrome c release.** *Cell Death Differ* 2000, **7**(6):556–565.

42. Albrecht H, Durbin-Johnson B, Yunis R, Kalanetra KM, Wu S, Chen R, Stevenson TR, Rocke DM: **Transcriptional response of ex vivo human skin to ionizing radiation: comparison between low- and high-dose effects.** *Radiat Res* 2012, **177**(1):69–83.

43. Bisio A, De Sanctis V, Del Vescovo V, Denti MA, Jegga AG, Inga A, Ciribilli Y: **Identification of new p53 target microRNAs by bioinformatics and functional analysis.** *BMC Cancer* 2013, **13**:552.

44. El-Saghire H, Thierens H, Monsieurs P, Michaux A, Vandevoorde C, Baatout S: **Gene set enrichment analysis highlights different gene expression profiles in whole blood samples X-irradiated with low and high doses.** *Int J Radiat Biol* 2013, **89**(8):628–638.

45. Nosel I, Vaurijoux A, Barquinero JF, Gruel G: **Characterization of gene expression profiles at low and very low doses of ionizing radiation.** *DNA Repair (Amst)* 2013, **12**(7):508–517.

46. Rashi-Elkeles S, Elkon R, Shavit S, Lerenthal Y, Linhart C, Kupershtein A, Amariglio N, Rechavi G, Shamir R, Shiloh Y: **Transcriptional modulation induced by ionizing radiation: p53 remains a central player.** *Mol Oncol* 2011, **5**(4):336–348.

47. Hada M, Georgakilas AG: **Formation of clustered DNA damage after high-LET irradiation: a review.** *J Radiat Res* 2008, **49**(3):203–210.

48. McConnell BB, Yang VW: **Mammalian Kruppel-like factors in health and diseases.** *Physiol Rev* 2010, **90**(4):1337–1381.

49. Brandt T, Townsley FM, Teufel DP, Freund SM, Veprintsev DB: **Molecular basis for modulation of the p53 target selectivity by KLF4.** *PLoS One* 2012, **7**(10):e48252.

50. Wei D, Kanai M, Jia Z, Le X, Xie K: **Kruppel-like factor 4 induces p27Kip1 expression in and suppresses the growth and metastasis of human pancreatic cancer cells.** *Cancer Res* 2008, **68**(12):4631–4639.

51. Kim HS, Heo JI, Park SH, Shin JY, Kang HJ, Kim MJ, Kim SC, Kim J, Park JB, Lee JY: **Transcriptional activation of p21(WAF(1)/CIP(1)) is mediated by increased DNA binding activity and increased interaction between p53 and Sp1 via phosphorylation during replicative senescence of human embryonic fibroblasts.** *Mol Biol Rep* 2014, **41**(4):2397–2408.

52. Li H, Zhang Y, Strose A, Tedesco D, Gurova K, Selivanova G: **Integrated high-throughput analysis identifies Sp1 as a crucial determinant of p53-mediated apoptosis.** *Cell Death Differ* 2014, **21**:1493–1502.

53. Luttrell LM, Miller WE: **Arrestins as regulators of kinases and phosphatases.** *Prog Mol Biol Transl Sci* 2013, **118**:115–147.

54. Arora H, Qureshi R, Jin S, Park AK, Park WY: **miR-9 and let-7 g enhance the sensitivity to ionizing radiation by suppression of NFkappaB1.** *Exp Mol Med* 2011, **43**(5):298–304.

55. Metheetrairut C, Slack FJ: **MicroRNAs in the ionizing radiation response and in radiotherapy.** *Curr Opin Genet Dev* 2013, **23**(1):12–19.

56. Buscaglia LE, Li Y: **Apoptosis and the target genes of microRNA-21.** *Chin J Cancer* 2011, **30**(6):371–380.

57. Li J, Donath S, Li Y, Qin D, Prabhakar BS, Li P: **miR-30 regulates mitochondrial fission through targeting p53 and the dynamin-related protein-1 pathway.** *PLoS Genet* 2010, **6**(1):e1000795.

58. Shi S, Yu L, Zhang T, Qi H, Xavier S, Ju W, Bottinger E: **Smad2-dependent downregulation of miR-30 is required for TGF-beta-induced apoptosis in podocytes.** *PLoS One* 2013, **8**(9):e75572.

59. Quintavalle C, Donnarumma E, Iaboni M, Roscigno G, Garofalo M, Romano G, Fiore D, De Marinis P, Croce CM, Condorelli G: **Effect of miR-21 and miR-30b/c on TRAIL-induced apoptosis in glioma cells.** *Oncogene* 2013, **32**(34):4001–4008.

60. Lhakhang TW, Chaudhry MA: **Interactome of Radiation-Induced microRNA-Predicted Target Genes.** *Comp Funct Genomics* 2012, **2012**:569731.

61. Gewirtz DA, Hilliker ML, Wilson EN: **Promotion of autophagy as a mechanism for radiation sensitization of breast tumor cells.** *Radiother Oncol* 2009, **92**(3):323–328.

62. Berndt C, Kurz T, Selenius M, Fernandes AP, Edgren MR, Brunk UT: **Chelation of lysosomal iron protects against ionizing radiation.** *Biochem J* 2010, **432**(2):295–301.

63. Yue J, Wang Q, Lu H, Brenneman M, Fan F, Shen Z: **The cytoskeleton protein filamin-A is required for an efficient recombinational DNA double strand break repair.** *Cancer Res* 2009, **69**(20):7978–7985.

64. Akers JC, Gonda D, Kim R, Carter BS, Chen CC: **Biogenesis of extracellular vesicles (EV): exosomes, microvesicles, retrovirus-like vesicles, and apoptotic bodies.** *J Neurooncol* 2013, **113**(1):1–11.

65. Vlassov AV, Magdaleno S, Setterquist R, Conrad R: **Exosomes: current knowledge of their composition, biological functions, and diagnostic and therapeutic potentials.** *Biochim Biophys Acta* 2012, **1820**(7):940–948.

66. Simons M, Raposo G: **Exosomes–vesicular carriers for intercellular communication.** *Curr Opin Cell Biol* 2009, **21**(4):575–581.

67. Al-Mayah AH, Irons SL, Pink RC, Carter DR, Kadhim MA: **Possible role of exosomes containing RNA in mediating nontargeted effect of ionizing radiation.** *Radiat Res* 2012, **177**(5):539–545.

12.2 Analysis of the Secretome of Apoptotic Peripheral Blood Mononuclear Cells and its Impact on Tissue Regeneration

Degenerative diseases are a worldwide burden both individually for patients and economically for the health care system. Regenerative medicine aims to provide therapeutic strategies to enhance cell replacement and tissue regeneration [1]. Initially the application of cells to replace injured tissues was investigated in detail, but subsequently there has been a shift in focus towards paracrine factors, which are currently believed to be responsible for the beneficial effects seen. These paracrine factors can be released by various cells and promote endogenous regenerative capacities [21]. Stressed PBMCs have been shown to release paracrine factors that exert cytoprotective, pro-angiogenic and immune modulatory effects *in vitro* and *in vivo* [38-42, 139]. Although the biological effects of these paracrine factors have been described in detail little is known about their composition.

We have therefore examined paracrine factors present in the conditioned media of human PBMCs. We observed that irradiated cells secrete high amounts of cytokines and growth factors involved in angiogenesis and wound healing. In addition, ionizing irradiation induced the generation of oxidized phospholipids with known pro-angiogenic and immune modulatory capacities. *In vitro* assays revealed that exosomes and proteins augment cell migration and activation of fibroblasts and keratinocytes, whereas lipids and microparticles had no effect. In an *in vivo* porcine closed chest model of acute myocardial infarction we were able to show that these factors display high biological stability, since a pathogen reduced, manufactured PBMC secretome displayed similar potency to an unprocessed secretome.

The manuscript has been submitted to Scientific Reports.

Analysis of the Secretome of Apoptotic Peripheral Blood Mononuclear Cells: Impact of Released Proteins and Exosomes for Tissue Regeneration

Lucian Beer[1,2], Matthias Zimmermann[1,2], Andreas Mitterbauer[1,2], Adolf Ellinger[3], Florian Gruber[4,5], Marie-Sophie Narzt[4,5], Maria Zellner[6], Mariann Gyöngyösi[7], Sibylle Madlener[8], Elisabeth Simader[1,2]; Christian Gabriel[9], Michael Mildner[4*], Hendrik Jan Ankersmit[1,2*]

[1] Department of Thoracic Surgery, Medical University of Vienna, Austria
[2] Christian Doppler Laboratory for Cardiac and Thoracic Diagnosis and Regeneration, Medical University of Vienna, Austria
[3]Department of Cell Biology and Ultrastructure Research, Center for Anatomy and Cell Biology, Medical University of Vienna, Vienna, Austria.
[4]Department of Dermatology, Research Division of Biology and Pathobiology of the Skin, Medical University Vienna, Austria
[5] Christian Doppler Laboratory for Laboratory Biotechnology of Skin Aging, Medical, Austria
[6]Centre of Physiology and Pharmacology, Institute of Physiology, Medical University of Vienna, Austria
[7]Department of Cardiology, Medical University Vienna, Vienna, Austria
[8]Molecular Neuro-Oncology Research Unit, Department of Pediatrics and Adolescent Medicine and Institute of Neurology, Medical University of Vienna, Austria
[9]Red Cross Blood Transfusion Service of Upper Austria, Linz, Austria

*These authors share the last and corresponding authorship.

Corresponding authors:

Hendrik Jan Ankersmit, MD
Department of Thoracic Surgery, Medical University of Vienna
Christian Doppler Laboratory for Cardiac and Thoracic Diagnosis and Regeneration
Währinger Gürtel 18-20
1090 Vienna, Austria
Tel.: +43-1-40400-67770
Fax.: +43-1-40400-69770
e-mail: hendrik.ankersmit@meduniwien.ac.at

Michael Mildner, PhD
Medical University of Vienna
Department of Dermatology,
Research Division of Biology and Pathobiology of the Skin,
Lazarettgasse 14
1090 Vienna, Austria
Tel: +43-1-40400-73507
Fax: +43-1-40400-73590
e-mail: michael.mildner@meduniwien.ac.at

Short title: PBMC secretome in regenerative medicine

Abstract

We previously showed that, when peripheral blood mononuclear cells (PBMCs) were stressed with ionizing radiation, they released a plethora of paracrine factors that showed regenerative capacity *in vitro* and *in vivo*. This study aimed to characterize the secretome of irradiation-induced PBMCs and to investigate its biologically active components *in vitro* and *vivo*. Bioinformatics analysis revealed that irradiated PBMCs differentially expressed genes that encoded secreted proteins. These genes were primarily involved in (a) pro-angiogenic and regenerative pathways and (b) the generation of oxidized phospholipids with known pro-angiogenic and inflammation-modulating properties. Subsequently, *in vitro* assays showed that the exosome and protein fractions of the secretome were the major biological components that enhanced cell mobility; conversely, secreted lipids and microparticles had no effects. We tested a viral-cleared PBMC secretome, prepared according to good manufacturing practice (GMP), in a porcine model of closed chest, acute myocardial infarction. We found that the potency for preventing ventricular remodeling was similar with the GMP-compliant and experimentally-prepared PBMC secretomes. Our results indicate that irradiation modulates the release of proteins, lipid-mediators and extracellular vesicles from human PBMCs. In addition our findings implicate the use of secretome fractions as valuable material for the development of cell-free therapies in regenerative medicine.

Word count abstract: 202

Keywords: wound healing; paracrine signaling; regenerative medicine; exosome; lipidomics

Introduction

Regenerative medicine that aims to restore damaged or dysfunctional tissue has emerged as a new branch of research in the last century worldwide [1]. Despite major advances in drug therapies, surgical interventions, and organ transplantation, tremendous problems remain unresolved for the regeneration of injured organs, including the myocardium, kidney, the central nervous system, lung, and skin [2]. The use of stem cells as therapeutic agents has yielded promising results in preclinical and clinical studies in several experimental settings. However, the mode of action underlying stem cell transplantation continues to be debated. In recent years, it has become commonly accepted that transplanted stem cells release paracrine factors that enhance the capacity for endogenous regeneration, rather than directly replacing injured cells [3, 4]. Therefore, the use of paracrine factors instead of administering living, proliferating, potentially pluripotent stem cell populations would represent a great advantage with respect to meeting regulatory restrictions and safety issues.

Although the majority of cell therapy studies were performed with stem cells from different origins, we and others have shown that stressed peripheral blood mononuclear cells (PBMCs) could also promote tissue protection and repair through paracrine activities [5-11]. The secretome of stressed PBMCs has been shown to enhance angiogenesis and wound healing *in vitro* and *in vivo* [10]. These activities promoted regeneration of the myocardium [5-7] and brain [12] after acute ischemic injuries. In contrast to stem cells, which are available in limited cell numbers, large numbers of PBMCs can be readily obtained. Although several studies have demonstrated that the PBMC-derived secretome has biological effects on cardioprotection, angiogenesis, and wound healing, only a few studies have identified the paracrine factors involved [5, 6, 11].

To gain a better understanding of the *in vitro* and *in vivo* effects of the PBMC secretome, it is necessary to analyze in detail the biological components present in conditioned medium (CM). The secretome of cultured PBMCs comprises proteins, lipids, and extracellular vesicles; thus, a multidimensional methical approach must be implemented for this type of analysis. To date, several secreted proteins have been identified that exert cytoprotective

and regenerative capacities [13, 14]; thus, those proteins are thought to be important mediators in paracrine signaling. In addition, the lipids released in cell cultures have been shown to modulate immune function [15], induce angiogenesis, and enhance wound healing by upregulating pro-angiogenic proteins (reviewed in [16]). More recently, extracellular vesicles, including microparticles and exosomes, have come into focus in regenerative medicine, because extracellular vesicles isolated from donor cells could interact with recipient cells, and they displayed pleiotropic immunological functions [17]. Recent studies have revealed that, when exosomes released from mesenchymal stromal cells were administered in injured animals, they induced neurogenesis following a stroke [18], they induced cardioprotection after acute myocardial infarction, and they augmented angiogenesis and wound healing in a rodent skin burn model [19]. Extracellular vesicles mediate intercellular communication by delivering mRNAs, microRNAs (miRNAs), proteins, and lipids from one cell to another [20, 21]. Furthermore, several reports showed that cell stressors, like hypoxia, could enhance the release of pro-angiogenic exosomes and augment their biological efficacy [22, 23].

In the present study, we aimed to characterize in detail the secretome of non-irradiated and irradiated PBMCs with a combination of methods, including transcriptomics, lipidomics, and functional *in vitro* assays. Furthermore, we evaluated whether a viral-cleared, PBMC secretome, prepared in compliance with good manufacturing practice (GMP) guidelines, retained its preventative potency in a porcine, closed-chest-reperfusion, acute myocardial infarction (AMI) model.

We demonstrated that irradiation induced the expression of pro-angiogenic factors, the shedding of microparticles and exosomes, and the production and release of oxidized phospholipids, either in solution or incorporated into extracellular vesicles. We showed *in vitro* that exosomes and proteins were the two major biologically active components present in the secretome of irradiation-induced PBMCs. These components enhanced fibroblast and keratinocyte cell migration and the release of pro-angiogenic factors that are considered hallmarks of tissue regeneration. Finally, we demonstrated *in vivo* that "cell free" regenerative

medicine that met the requirements of regulatory authorities showed potency in preventing ventricular remodeling after an experimental AMI.

Materials and methods

Ethics statement

This study was performed in accordance with the Ethics Committee of the Medical University of Vienna (EK: 1236;2013). and according to the principles of the Helsinki Declaration and Good Clinical Practice. Written, informed consent was obtained from all participants. All experimental protocols were approved by the Ethics Committee of the Medical University of Vienna (EK: 1236;2013).

Cell separation and irradiation

Human peripheral blood mononuclear cells (PBMC) were isolated from four healthy male volunteers by venous blood draw and density gradient centrifugation with Ficoll-Paque (GE Healthcare Bio-Sciences AB, Sweden). PBMCs (25×10^6 cells/ml) were resuspended in serum-free medium (CellGro, CellGenix, Freiburg, Germany). An automated cell counter (Sysmex Inc., USA) was used to determine cell count. PBMCs were gamma-irradiated with 60 Gy to induce apoptosis. Both irradiated and non-irradiated PBMCs of the four donors were cultured for 24 h. CM was collected from cultures at 2, 4, and 20 h time points, and then, centrifuged ($500 \times g$ for 9 min) to remove cell debris. CM was stored at -80°C for subsequent protein and lipid analyses. Fresh CM was used for microparticle and exosome separations.

RNA isolation

PBMCs were collected immediately after isolation (0 h) and after culturing for the indicated times (2, 4, and 20 h) after treatment (radiation or no radiation). From these samples (25×10^6 cells/sample), total RNA was isolated with Trizol® Reagent (Invitrogen, Carlsbad, CA). RNA was quantified with a NanoDrop 1000 spectrophotometer (Peglab, Erlangen, Germany). RNA quality was verified with an Agilent 2100 Bioanalyzer (Agilent, Böblingen, Germany). All

RNA samples had an integrity score between 5.7 and 10. Overall, 28 samples were generated from the four individual donors.

Microarray analysis

Microarray expression profiling was performed with an Agilent, whole human genome oligo microarray, 8×60 Kb (G4851A; #028004; Agilent Technologies), which contained 27,958 target genes (Entrez IDs) and 7,419 lincRNAs. Staining and scanning were performed according the Agilent expression protocol (Agilent Technologies). Microarray gene analysis was performed by Miltenyi (Miltenyi Biotec, GmBH, Germany), according to the MIAME guidelines [24].

Background-corrected fluorescence intensity values of microarray data were statistically analyzed with Genespring v.11.5 software. Expression values were $\log_2$-transformed and normalized with the quantile-normalization method. Transcripts were further processed only when at all time points, the expression in at least one of the two conditions (irradiated or non-irradiated) was above the 40th percentile of the average expression measured over all samples. The threshold of 40% was chosen, because approximately 30-60% of all human genes are expressed [25]. A paired student´s t-test, in combination with a false discovery rate <5%, were used to calculate significant differences. Only genes that displayed a >2-fold change (FC) in expression were used for functional analyses. Array data was submitted to GEO (http://www.ncbi.nlm.nih.gov/geo/) under accession number GEO: GSE55955.

Secreted factor prediction

To identify transcripts that encoded secreted proteins, we used three web-based programs: SecretomeP 2.0, SignalP 4.1, and TMHMM 2.0. The workflow of data analysis is shown in Figure 1. The SignalP program predicts the presence and location of signal peptide cleavage sites in amino acid sequences [26]. Based on this information, a specific threshold (D-cutoff score ≥0.45) is generated, which predicts secretory proteins. Currently, the SignalP program shows the best performance and accuracy compared to similar available algorithms [27].

SecretomeP predicts whether a protein is secreted via a non-classical pathway, based on post-translational and localization information obtained from different protein-prediction servers. The information on protein characteristics is expressed with a neural network score (NN-score), and proteins with a NN-score ≥0.5 (cut-off value) are considered to be secreted via a non-classical pathway. TMHMM 2.0 predicts transmembrane helices in proteins, based on a hidden Markov model. This method discriminates between soluble and membrane proteins with a high degree of accuracy [28].

We used these three different programs to predict transcripts that encoded secretory proteins. We analyzed transcripts that were upregulated in at least 2 of 3 time points compared to control conditions (0 h), in irradiated or non-irradiated PBMCs.

Functional annotation clustering and pathway analysis

The identified transcripts that encoded secreted proteins were classified according to a web-based Gene Toolkit (WEBGESTAL) (http://bioinfo.vanderbilt.edu/webgestalt/analysis.php). The toolkit employed gene ontology term enrichment (Go-term) and the Kyoto Encyclopedia of Genes and Genomes (KEGG) to determine functional pathways [29]. PANTHER (Protein Analysis Through Evolutionary Relationships; http://www.pantherd.org) was used for phylogenetic inferences.

Visualization of protein-protein interactions

To visualize known and predicted protein-protein interactions, we used the web-based database, STRING v9.1 (Search Tool for the Retrieval of Interacting Genes/Proteins) [30].

Exosome enrichment

Exosomes were purified from the CM of irradiated and non-irradiated human PBMCs (~25 × 10^6 cells) after culturing for 20 h in serum-free cell culture media. We used either a total exosome isolation kit (Invitrogen), according to the manufacturer's instructions, or an ultracentrifuge centrifugation protocol. In both cases, CM was centrifuged at 500 ×*g* for 2 min

to remove cells, followed by centrifugation at 3500 ×*g* for 15 min to eliminate debris, and then, at 20,000 ×*g* for 15 min to eliminate microparticles. Next, the CM was filtered through 0.2-μm pore filters. For exosome isolation with the Invitrogen isolation kit, we transferred 1 ml CM into a new tube and added 0.5 ml total exosome reagent. After rigorous vortexing, the solution was incubated at 4°C overnight, followed by centrifugation at 10,000 ×*g* for 1 h at 4°C. For exosome isolation with the ultracentrifuge protocol, 10 ml of microparticle-depleted CM was centrifuged for 120 min at 110,000 ×*g* in a SW 41 swinging bucket ultracentrifuge (Beckman Coulter, Brea, California, USA). The pelleted exosomes were eluted in 500 μl PBS. The absolute number of exosomes was assessed with a NanoSight, NS500 instrument. All centrifugation procedures were performed at 4°C.

Exosome flow cytometry

Exosomes freshly isolated from cell culture media were labeled with a commercially available, human CD63 isolation/detection kit (Invitrogen), according to the manufacturer's instructions. Briefly, 50 μl of pre-enriched exosomes were mixed with dynabeads coated with anti-CD63 antibody. The mixture was incubated overnight under gentle agitation at 4°C. After several washing steps, exosomes bound to anti-CD63 beads were resuspended in 300 μl PBS with 0.1% BSA. Then, 100 μl of bead-bound exosomes were incubated with 4 μl anti-CD63-FITC and anti-CD9-PE or matching isotype controls (BioLegends). After 45 min, the labeled exosomes were washed twice and resuspended in 500 μl PBS with 0.1% BSA. Then, exosomes were detected on a FACSAria flow cytometer (Becton Dickinson). Data were analyzed with FlowJo Software (Tree Star, Inc, Ashland, OR, USA).

Microparticle preparation

Microparticles were isolated from 1 ml CM from irradiated and non-irradiated human PBMCs (~25 × 10^6 cells). The CM was initially centrifuged at 500 ×*g* for 2 min to separate the pellet from the supernatant. The supernatant was spun at 3500 ×*g* for 15 min to eliminate debris. The resulting cell-free CM was stored at -20°C.

Microparticle flow cytometry

Microparticles in CM samples were analyzed with a FACSAria flow cytometer. Briefly, 250 µl cell-free CM was centrifuged at 20,000 ×*g* for 15 min at 4°C to pellet the microparticles. Then, 225 µl supernatant was removed, and the microparticle pellet was resuspended in 200 µl of filtered annexin binding buffer. The annexin binding buffer had been previously filtered through 0.2-µm pore filters to remove background noise.

Microparticles are lipid vesicles shed from the cell membrane. We employed fluorescently-labeled annexin V to label microparticles, because annexin V spontaneously binds to cell membranes in the presence of calcium. Annexin V conjugated to FITC (4 µl, eBioscience) was resuspended in 100 µl annexin binding buffer and centrifuged at 20,000 ×*g* for 15 min. Then, 80 µl were added to 100 µl resuspended microparticles, and incubated for 20 min at room temperature. Then, the annexin-bound were pelleted at 20,000 ×*g* for 15 min, Next, the supernatant (180 µl) was discarded, and the microparticle pellet was resuspended in 480 µl annexin binding buffer. In summary, the microparticles present in 100 µl CM were diluted in 500 µl buffer for FACS analysis.

We used Megamix-Plus SSC beads (BioCytex, Marseille, France) to determine the gating for microparticles. The forward scatter (FSC), side scatter (SSC), and FITC FL-1 were set to log mode. Briefly, beads with 0.16 µm, 0.2 µm, 0.24 µm, and 0.5 µm diameters were detected on an SSC/FL1 plot. We next selected bead regions, and back-gated them onto the FSC/SSC plot. Then, the microparticle gate was set based on the FSC/SSC plot. A small microparticle gate was applied by using a particle size of 0.2 µm – 0.3 µm (small microparticles) and a large microparticle gate was set at a particle size of 0.3 µm - 0.5 µm (large microparticles). Particles that were 0.16 µm or smaller were not counted to remove false-positive events based on inaccurate measurements.

Nonspecific annexin V labeling was evaluated by preparing microparticles in PBS without calcium, which yielded no annexin V-positive events. As a negative control, CM was filtered

through a 0.2 μm filter, which removed >99.9% of the particles that might pass through the small microparticle gate.

During the entire analysis, the lowest available flow rate was chosen. TrueCount tubes (BD Biosciences) were used for detection at SSC/FL1 to measure the absolute counts of microparticles.

Absolute numbers of microparticles were calculated as recommended in the manufacturs instructionsWe acquired 100,000 events, and the data were analyzed with FlowJo Software (Tree Star, Inc, Ashland, OR, USA).

Silver staining

Exosomes were isolated with an exosome isolation kit. Briefly, exosomes were isolated from 0.5 ml CM by binding to anti-CD63 attached to magnetic beads. Exosomes were suspended in an SDS-PAGE loading buffer, lysed by sonication, and centrifuged. The anti-CD63 beads were removed with a magnet. Lysates with 20 μg protein content were separated by PAGE and visualized with silver stain.

Lipid extraction and thin layer chromatography

Total lipid extracts were subjected to thin-layer chromatography (TLC) analyses on Silica gel 60 TLC plates (Merck, Vienna, Austria). Briefly, 25×10^6 cells were cultured for 20 h after irradiation. CM was isolated, lipids were extracted, and 1/10 of the total extract from one ml CM was spotted onto the TCL plate.

For TLC separation of total lipids, we used the method described by Pappinen. . As the lipids migrated through the matrix, the following solvent systems were used sequentially: chloroform/methanol/water 40:10:1 (v/v/v) to 10 cm; chloroform/methanol/acetic acid 190:9:1 (v/v/v) to 16 cm; and hexane/diethylether/acetic acid 70:30:1 (v/v/v) to 20 cm.

In all experiments, the plates were dried under air stream before they were developed with a new mobile phase. Lipids were visualized by exposing the plates to 10% copper sulfate in an 8.5% aqueous solution of ortho-phosphoric acid, and subsequently, drying and heating at

150°C. Lipid classes were identified by comparing the bands of skin-equivalent lipids with standards for triglycerides, free fatty acids, ceramides, sodium cholesterylsulphate, sphingomyelin (all Sigma), and phosphatidylcholines (PCs; Avanti Lipids, Alabaster, AL). ImageJ 1.45 software (National Institutes of Health, Bethesda, MD, USA) was used for semi-quantitative analyses of lipids. The mean pixel intensities of lipids from the CM of irradiated PBMCs was plotted against those from the CM of non-irradiated PBMCs.

For mass spectrometry analyses, lipids were extracted with a liquid-liquid extraction procedure, as described recently [31]. Briefly, lipid extracts from complete cell culture supernatants were spiked with 1,2-dinonanoyl-sn-glycero-3-phosphocholine (DNPC; Avanti Lipids, Alabaster, Alabama) for standardization. Then, neutral lipids and fatty acids were removed with three rounds of hexane extraction. Reverse-phase chromatography, and subsequently, an online electronspray ionization-tandem mass spectrometry procedure were used to analyze non-oxidized and oxidized phosphocholines (oxPCs), with *m/z* 184 as a diagnostic fragment morker for PC [31]. Sample peak areas were normalized to the peak areas of the internal standard, DNPC.

Protein analysis

Irradiated and non-irradiated PBMCs (25×10^6/ml each) were cultured for 20 h. The CM was collected and analyzed with commercially available, enzyme-linked immunosorbent assay (ELISA) kits. We quantified the following proteins: angiogenin, CXCL13, PDGF-AA, PDGF-BB (Duoset, R&D Systems, Minneapolis, USA), complement C3, thrombospondin-1, neuropilin, and adrenomedullin (BG Bluegene Biotech). We used various biological components of the CM to stimulate fibroblasts (FBs) and keratinocytes (KCs), and then quantified the secretion of cytokines, CXCL1 and CXCL8 (Duoset, R&D Systems).

Transmission electron microscopy

Irradiated and non-irradiated PBMCs were cultured for 20 h. Then, PBMCs were examined with transmission electron microscopy (TEM), performed as described previously [32].

Isolation of biological components present in conditioned media

For *in vitro* assays, the CM samples from PBMCs of four donors were pooled before isolating biological components. In total, two independent experiments were performed by drawing blood samples from eight donors donor, and producing two independent CM pools. Microparticles and exosomes were purified as described. Lipids and proteins were isolated from the CM after removing the exosomes; the exosomes also contained lipid and protein fractions that were not analyzed here. Thus, the lipid and proteins analyzed were either soluble or attached to vesicles other than exosomes. Lipids were isolated as described above and in a previous study [33]. Proteins were precipitated with 30% v/v polyethylene glycol. The precipitated proteins were centrifuged for 15 min at 20,000 ×*g*. Aliquots were stored at -80°C before experiments were performed.

Generation of pathogen-reduced cell culture supernatant

Pathogens were reduced in CM, as described previously [12].

Large animal *in vivo* experiments

Large animal studies were performed as described previously [6]. Animal investigations were carried out in accordance with the "Position of the American Heart Association on Research Animal Use", as adopted by the AHA on November 11, 1984. The study was approved by the Ethics Committee on Animal Experimentation at the University of Kaposvar, Hungary.

Cell culture and *in vitro* stimulation assay

Human dermal FBs (Lonza) were cultured in DMEM (Gibco, BRL, Gaithersburg USA), supplemented with 10% fetal bovine serum, 25 mM L-glutamine (Gibco), and 1% penicillin/streptomycin (Gibco). Human primary KCs were cultured in KC-growth medium (KGM, Lonza). For stimulation assays, 3×10^5 FBs or KCs were seeded in 12-well plates. After reaching 80% confluence, cells were washed once with PBS. Unprocessed CM,

microparticles, exosomes, proteins, or lipids were resolved from (1) control medium cultivated without cells, (2) CM from non-irradiated PBMCs, or (3) CM from irradiated PBMCs. These components were resuspended in either DMEM or KGM. Each biological component was then added to FB and KC cultures. After 6 h, cells were washed once with PBS, and RNA was isolated with the RNAeasy kit (Qiagen, Hilden, Germany) according to the manufacturer´s instructions. Cell stimulation assays were performed twice, with two different preparations of stimulating components.

In vitro scratch assay

FBs and KCs (3×10^5 each) were seeded in 6-well plates. After reaching 100% confluence, cells were scratched horizontally and vertically with a pipette-tip. Then, cells were washed once with PBS. The scratches were investigated under the microscope, and four areas were marked for photographs. The first photographs of those 4 areas were acquired immediately (initial wound size), and the clear areas were marked. Unprocessed CM, microparticles, exosomes, proteins, or lipids were resolved from (1) control medium cultivated without cells, (2) CM from non-irradiated PBMCs, and (3) CM from irradiated PBMCs, and resuspended in either DMEM or KGM. Each biological component was then added to the scratch-wounds. Each component was diluted to achieve the content equivalent to that derived from 2.5×10^6 PBMCs/ml. The same areas of the scratch wounds were photographed again after 24 h (for FBs and KCs) and after 48 h (only for FBs). The wound closures were measured with ImageJ 1.45 software (National Institutes of Health, Bethesda, MD, USA). These wound repair assays were performed twice, with two different preparations of stimulating components.

Quantitative reverse-transcriptase PCR (qPCR) analysis of mRNA

Total RNA was reverse-transcribed with the IScript cDNA synthesis kit (BioRad, Hercules, CA, USA), as indicated in the instruction manual. Then, qPCR was performed with the Light Cycler Master SYBR Green I kit (Roche Applied Science, Penzberg, Germany) on a Light

Cycler 480 thermocycler (Roche Applied Science). The primer pairs were synthesized by

Microsynth AG (Vienna, Austria; sequences in supplementary Table 1). The reference gene

was beta-2-microglobulin (B2M).

Statistical analysis

Data distributions were tested with the Kolmogorow-Smirnow-Test. An ANOVA with

Bonferroni post hoc test or a Kruskal-Wallis test with Dunns post hoc test to analyze results.

A P-value <0.05 was taken to indicate a significant difference.

Results

Bioinformatics analysis of the secretome

Transcriptomic profiling and bioinformatics tools were used to identify proteins secreted from non-irradiated and irradiated PBMCs from four donors (Fig. 1). PBMCs were cultured for 2, 4, and 20 h; then, gene expression was profiled at each time point on DNA microarrays that covered 47,000 transcripts. Actively secreted factors were identified with the bioinformatics programs, SecretomeP, SignalP, and TMHMM.

We first identified transcripts that were upregulated during the cultivation period in either non-irradiated (Fig. 2A) or irradiated PBMCs (Fig. 2C). We only analyzed transcripts with a FC ≥ 2 compared to baseline values. The heatmaps displayed 525 and 1099 genes that were upregulated in at least two of the three time points in non-irradiated (Fig. 2B) and irradiated PBMCs (Fig. 2D), respectively. The bioinformatics analysis identified 167 transcripts that encoded actively secreted proteins in non-irradiated PBMCs and 213 that encoded secreted proteins in irradiated PBMCs (supplementary Table 1).

We then investigated the possible biological functions of these proteins with GO-term and KEGG pathway analyses. The 213 genes from the irradiated cells showed significant enrichment in genes involved in the biological processes of angiogenesis, wound healing, and leucocyte trafficking regulation ($p < 0.05$, supplementary Table 2). The 167 genes from the non-irradiated cells showed enrichment in genes involved in amino acid transport and endocrine regulation. These data suggested that gene expression shifted from metabolic processes in the non-irradiated state, towards tissue regeneration after irradiation.

Confirmation of microarray data by qPCR and ELISA

A selected set of genes that encoded pro-angiogenic proteins that were upregulated in non-irradiated or irradiated PBMCs were validated with qPCR (supplementary Fig. 1A-S). We observed a time-dependent increase in gene expression; the highest expression was observed at 20 h after irradiation. We used ELISA to quantify protein content in the

supernatant (supplementary Fig. 2A-H). Compared to non-irradiated PBMCs, the
supernatants of irradiated PBMCs contained significantly higher concentrations of neuropilin,
thrombospondin, CXCL13, and angiogenin, but similar concentrations of PDGF-AB, PDGF-
BB, C3, and adrenomedullin.

Lipid analysis

We investigated whether irradiation modulated the concentrations and composition of
different CM lipid classes with TLC assays. Irradiated and non-irradiated PBMCs were
cultured for 20 h, and CMs were analyzed. The TLC protocol [34] was designed to quantify a
broad range of different lipid classes. A representative TLC image is shown in supplementary
Fig. 3A. Cell culture medium alone (no cells) showed no detectable lipids (line 3, marked
"M"). Quantification of the TLC results showed that the CM of irradiated PBMCs contained
significantly higher concentrations of phospholipids, cholesterol sulfate, cholesterol, free fatty
acids, cholesterol esters, and triglycerides compared to CM from non-irradiated PBMCs
(supplementary Fig. 3B).

Ionizing radiation induces phospholipid oxidation

Previous studies have shown that UV radiation induced significant oxidation of PCs [35].
Here, we quantified oxPCs in the CM of irradiated and non-irradiated PBMCs at 20 h after
irradiation. High pressure lipid chromatography-tandem mass spectrometry was used to
detect selected oxidized phospholipid products that originated from selected, abundant PCs
with polyunsaturated fatty acids in the sn-2 position and palmitic or stearic acid in the *sn*-1
position. Peak intensities were normalized to the level of DNPC, which served as an internal
standard. The abundance of non-oxidized precursors, 1-palmitoyl-2-linoleoyl-sn-glycero-3-
PC (PLPC), 1-palmitoyl-2-arachidonyl-PC (PAPC), and 1-stearoyl-2-arachidonoyl-sn-glycero-
PC (SAPC), were not significantly different between the irradiated and non-irradiated
samples (Fig. 3A,D,G, respectively). However, products with intact, but oxidized sn-2 chains,
like PLPC-OH (Fig. 3B) and PLPC-OOH (Fig. 3C), were significantly more abundant after

irradiation. We also observed a comparable significant increase in the oxidation of PAPC with irradiation (Fig. 3D-F). In addition, in the CM of irradiated PBMCs, we observed higher concentrations of oxidized lipids with fragmented chains, like 1-stearoyl-2-glutaroyl- sn - glycero-3-PC (SGPC), and 1-palmitoyl-2-glutaroyl- sn-glycero-3-PC (PGPC) compared to the CM of non-irradiated PBMCs (Fig. 3G-I).

Ionizing radiation induces microparticle release

To extend our analysis, we investigated the content of extracellular vesicles present in the CM of non-irradiated and irradiated PBMCs. We first performed TEM imaging of non-irradiated and irradiated PBMCs after 20 h of culture. Non-irradiated PBMCs showed large nuclei with scant cytoplasm (Fig. 4A). Irradiated PMBCs showed dissolution of the cell membrane and more debris between cells (Fig. 4B); these findings suggested that irradiation caused cell fragmentation.

Apoptosis is known to induce shedding of plasma membrane microparticles [36-38]. Therefore, we investigated whether irradiation stimulated microparticle release. We isolated microparticles from CM at 20 h after irradiation with differentiated centrifugation procedures. Microparticles were stained with annexin V and detected with FACS analysis, based on SSC/FL1 characteristics. The vesicle diameters ranged from 0.2 to 1 µm, which was typical of microparticles. Filtration of CM through 0.2-µm pore filters removed >99.9% of microparticles, but exosomes were not removed (data not shown). We used counting beads to quantify absolute numbers of microparticles. Representative FACS images of microparticles obtained from non-irradiated and irradiated PBMCs are shown in Fig.4C and Fig.4D, respectively. Irradiation induced the release of both small and large microparticles. Small particle diameters were between 0.2 and 0.3 µm (non-irradiated: 566 ± 101 microparticles/µl vs. irradiated 1721±424 microparticles/µl; p=0.039; Fig. 4E); large microparticle diameters were between 0.3 and 0.5 µm (non-irradiated 1462 ± 444 microparticles/µl vs. irradiated 4282 ± 1735 microparticles/µl; p= 0.045; Fig. 4F).

Ionizing radiation induces release of exosomes

The presence of exosomes in the CM was verified by TEM, FACS, and NanoSight technology. For TEM visualization, exosomes were isolated from CM of irradiated and non-irradiated PBMCs at 20 h of culture with an ultracentrifugation protocol. In negative-stained TEM images, purified vesicles had an approximate diameter of 100 nm, and they were cup-shaped, characteristic of exosomes (Fig. 5A). NanoSight was used to quantify the absolute number of vesicles in the CM. CM samples derived from irradiated and non-irradiated PBMCs of 4 donors were pooled to improve statistical analysis. The number of exosomes was 3-fold higher in the CM from irradiated PBMCs than in the CM from non-irradiated PBMCs (Fig. 5B). For FACS analysis, exosomes were further purified with an anti-CD63 dynabead isolation procedure. Vesicles were separated based on positive detection of the exosome markers, CD63 and CD9 (Fig. 5C). In addition, the protein content in the exosome fraction was 1.5-fold greater in irradiated cells than in non-irradiated cells (Fig. 5D).

To determine whether irradiation induced changes in exosome protein content, we analyzed anti-CD63-isolated exosomes, pooled from four independent PBMC preparations, on SDS-PAGE gels. The separated proteins were visualized with silver stain. Fig. 5F shows that several bands were differentially expressed in exosomes isolated from irradiated and non-irradiated PBMCs. We used 2D-difference gel electrophoresis to analyze the differentially expressed proteins in more detail. Supplementary Fig. 4 shows that several protein spots (circled in white) were only detected in the lysates of exosomes purified from irradiated PBMCs; this result suggested that irradiation induced changes in exosome protein content.

Proteins and exosomes in conditioned media are biologically active

Previous studies have shown that the CM of stressed PBMCs promoted angiogenesis and wound healing *in vivo* and stimulated the migration and activation of FBs and KCs [10]. Here, we performed *in vitro* assays to investigate the biological effects of distinct components of the CM. First, primary human FBs were stimulated either with total CM (supernatant) or with different CM fractions, derived from irradiated and non-irradiated PBMCs. As expected,

CXCL1 and CXCL8 expression were induced in response to stimulation with total CM (Fig. 6A, B). In addition, the expression of both cytokines increased when stimulated with exosomes or the protein fraction of CM. Next, we isolated CXCL1 and CXCL 8 proteins from the CM of FBs and measured them with ELISA. We found that FB secretion of these cytokines was significantly induced by PBMC exosomes (Fig. 6C). When the same experiments were performed with primary human KCs, we again found that the total CM, the exosomes, and the protein fraction could stimulate CXCL1 and CXLC8 expression (supplementary Fig. 5A, B).

We performed scratch assays in FB cultures to examine simulated wound healing. We found that closure of the scratch wounds was significantly enhanced after 18(Fig. 7A, B), and 48 h (Fig. 7C), when cells were cultured in the presence of total CM, exosomes, or the protein fraction of CM isolated from PBMCs. Scratch assays were also performed with KCs with similar results (supplementary Fig. 6A-C). These results supported the notion that exosomes and proteins were the main biologically active components of CM. In these experiments, the lipid fraction was the water-soluble fraction derived from extracellular vesicles; it should be noted that exosomes contain lipids that are also biologically active.

Stability of CM components and a large animal model of myocardial infarction

Strict legal requirements must be met for therapeutic use of biological materials in humans. The experimental settings used in basic science and pre-clinical studies for testing *in vitro* and *in vivo* effects of substances typically must be altered for clinical studies, due to legal requirements. With these restrictions in mind, we produced and handled the CM according to good manufacturing practice (GMP) guidelines. Therefore, GMP-compliant CM could be used for cell-free therapy in humans. We compared the biological efficiency of these GMP-compliant and the experimentally-prepared supernatants. First, the quantity and quality of biological components derived from GMP-compliant CM samples were comparable to those of experimental CM samples (supplementary Fig. 7A-E). The lipid analysis revealed that the GMP-compliant CM was enriched in oxidized phospholipids, similar to those detected in the

experimental CM. However, the GMP-compliant CM did not contain microparticles, because it had to be filtered through 0.2-µm filters to eliminate all particles with diameters greater than 0.2 µm. However, the quantity and quality of CM exosomes were comparable between the experimental and GMP-compliant samples; this similarity suggested that the exosomes were relatively resistant to GMP procedures. Selected proteins were analyzed with ELISA, and we found comparable protein concentrations.

Furthermore, we compared the experimental CM and GMP-compliant CM for their *in vivo* effects in an experimental model of AMI in domestic pigs. In previous studies, we showed that, after coronary artery ligation, myocardial damage was attenuated when the CM of irradiated PBMCs was injected 45 min after the onset of ischemia [6]. As shown in Table 1, the experimental CM and GMP-compliant CM samples were comparable in their capacity to attenuate ischemic damage following coronary artery occlusion. Both treatment groups showed improved cardiac output and reduced infarct areas compared to controls at 30 days after infarction.

Discussion

In the present study, we investigated the paracrine factors released from non-irradiated and irradiated human PBMCs and explored the biologically active components. We demonstrated that irradiation quantitatively and qualitatively changed the release of proteins, lipids, and extracellular vesicles in human PBMCs. Subsequently, we showed that two biological components in CM, the protein and exosome fractions, exerted the majority of proliferative and stimulatory effects observed in selected *in vitro* experiments. Moreover, our analysis revealed that the biological activity of CM in experimental AMI was not influenced by GMP procedures.

Cell-based therapies have shown promise for treating multiple diseases related to hypoxia-induced inflammation (e.g., AMI, stroke) [39]. In the last decade, results from randomized controlled trials have shown that the infusion of cells derived from different sources improved clinical endpoints [40]. In the initial stages of stem cell therapy research, it was thought that the observed effects were due to the direct interactions between donor and host cells. However, a growing body of evidence has given rise to the current notion that the beneficial effects are mediated by paracrine signaling, rather than direct interactions [4, 41]. A growing number of studies have shown that paracrine factors can modulate the host immune system, improve survival after myocardial infarction and ischemic stroke, and attenuate neurological disorders [14, 17, 42, 43]. Most studies have focused on evaluating proteins as mediators of this paracrine capacity. However, conditioned medium (CM) contains proteins, lipids, and extracellular vesicles [15]. To our knowledge, no previous study has investigated these biological components in the field of regenerative medicine.

In this study, we quantitatively compared proteins, lipids, and extracellular vesicles present in the CM of non-irradiated and irradiated PBMCs. We used stressed PBMCs, because accumulating evidence has indicated that paracrine activity could be stimulated by hypoxia [22, 23], cell starvation [44], and apoptosis [5-9, 12, 45].

First, we implemented a bioinformatics-based analysis of the secretome designed to identify secreted proteins [46, 47]. We identified 213 genes that encoded secreted proteins, which

were upregulated in response to irradiation. In contrast, non-irradiated PBMCs showed upregulation of only 176 transcripts; this difference suggested that irradiation triggered additional secretion. The 213 genes upregulated in irradiated PBMCs showed an enrichment of proteins involved in biological processes related to angiogenesis, cell proliferation, and cytokine signaling. Interestingly, a previous study that analyzed proteins in a stem cell secretome revealed a similar enrichment in proteins involved in biological processes and pathways [48]. In another study, a proteomic analysis of a mesenchymal stem cell secretome showed an enrichment in genes annotated with biological processes involved in angiogenesis, blood vessel morphogenesis, chemotaxis, wound response, and stress response, among others [49]. Those results were partly comparable to the results of our study. In addition to the 213 proteins that we identified with stringent bioinformatics analysis, other proteins that were undetected with our methods might have been present in the CM, due to passive release from dying cells. Moreover, our method did not identify VEGF or PAI-1, two proteins involved in the regulation of angiogenesis, which are known to be present at high concentrations in the CM of irradiated PBMCs [6]. However, we identified several other factors in the CM of stressed PBMCs that have known effects in the field of regenerative medicine [48]. For example, adrenomedullin was released in response to irradiation. According to Okumara et al., adrenomedullin has pro-angiogenic properties, inhibits cardiac fibrosis, and exerts cardio-protective effects [50]. Also, administration of growth differentiation factor 15 was shown to attenuate ischemia reperfusion damage [51]. Insulin like growth factor exerted anti-apoptotic, pro-angiogenic, and cell proliferative activities [52]. In addition to these factors with known reparative potential, we identified several other factors in this study. For example, we showed that stressed PBMCs expressed MMP9, VEGFA, TIMP-1, TSP-1, PDGF, FGF, and several chemokines. In accordance with our bioinformatics data, we found that purified CM proteins could induce cell migration and CXCL1 and CXCL8 expression in FBs and KCs, which are both involved in wound healing and angiogenesis [53]. We also studied the presence and activity of other biological components in PBMC-derived CM, including lipids and extracellular vesicles. Extracellular vesicles (comprising exosomes

and microparticles) are currently gaining interest, because they have emerged as a new mechanism for intercellular communication. Extracellular vesicles contain mRNAs, miRNAs, and proteins [20, 21]. By direct horizontal transfer of mRNA, miRNAs, and proteins, extracellular vesicles have been shown to stimulate the regenerative capacity of injured tissues [54]. Although the exact mechanism by which extracellular vesicles exert their regenerative capacity is currently debated, accumulating evidence has indicated that extracellular vesicles increase endothelial cell proliferation, induce angiogenesis, modulate extracellular matrix interactions, and modulate immune activities (reviewed in [17]).

In the present study, PBMC-derived exosomes induced CXCL1 and CXCL8 expression and enhanced cell migration in primary human skin cells, but microparticles did not show any activities *in vitro*. We showed that irradiated cells released higher numbers of extracellular vesicles than non-irradiated cells. Our difference-gel electrophoresis analysis of lysed exosomes derived from irradiated and non-irradiated PBMCs showed that several proteins were differentially expressed. These findings indicated that irradiation induced exosome secretion and altered exosome protein content. However, a more focused investigation of the function of these proteins will require more sophisticated experiments; therefore, it was beyond the scope of the present study. We speculate that irradiation may increase CM exosome secretion through p53 signaling, based on the facts that irradiation activates the p53 pathway [32], and this pathway was shown to be involved in regulating exosome release [55, 56]. However, it remains to be determined how irradiation regulates the changes in exosome protein content.

Sirois and colleagues showed that exosomes released from apoptotic endothelial cells exerted anti-apoptotic activity in vascular smooth muscle cells by activating ERK 1/2 receptors [44]. In a previous study, Lichtenauer et al. showed that the secretome of apoptotic PBMCs displayed similar biochemical effects on human cardiomyocytes; they promoted resistance to apoptosis and activated ERK1/2 receptors [6]. It is tempting to speculate that these effects might be mediated by exosomes. Further studies are planned to investigate these interesting questions in a large animal model of AMI.

Our analyses of GMP-compliant CM prepared from irradiated PBMCs showed convincing evidence that the CM retained potency under restricted conditions. This was the first proof-of-principle to test whether the pathogen reduction process would abolish the biological efficiency of the CM in a standardized experimental setup. First, we tested the total CM (not fractionated) from irradiated PBMCs. We compared CM prepared with the experimental methods to that prepared with GMP-compliant methods. Both of these CM preparations had comparable biological effects in a model of AMI, compared to CM from non-irradiated PBMCs. These effects were most likely provoked by an interplay among several factors (e.g., proteins and exosomes), rather than by a single component, and these factors were retained in the GMP methods.

This was the first study to evaluate the effect of irradiation on the oxidized lipid content of the secretome, which includes microparticles, exosomes, and soluble lipids. We investigated irradiation-induced changes by performing lipidomics on CM samples from irradiated and non-irradiated PBMCs. We focused on oxPCs. High pressure lipid chromatography-tandem MS analysis of PCs showed that irradiation promoted the formation of oxidized lipid species with pro-angiogenic and immunomodulatory properties (reviewed in [16]). Our lipidomics protocol enabled detection of a large number of oxidation products derived from the most abundant cell membrane phospholipids [31]. We found that CM obtained from irradiated PBMCs contained significantly higher concentrations of specific oxPCs than CM from non-irradiated PBMCs. Microparticles represent the largest class of extracellular vesicles, and they are abundantly present in the CM from irradiated PBMCs. PCs are the most abundant lipid class in microparticles [57]; in contrast, exosomes have less phospholipid and more ceramide contents than microparticles. Therefore, we speculated that irradiation-induced changes in oxidation products might be predominantly mediated by the oxidation of PCs incorporated in microparticles. However, although oxPCs were previously shown to exert biological activity [31, 33, 58], induce expression of CXCL8, and modulate angiogenesis [59], we could not detect any *in vitro* effects of soluble CM lipids in our selected experiments. Also CM samples were depleted of exosomes, the extracted lipids lacked biological activity; that

result indicated that only lipids contained within microparticles or exosomes, not lipids freely soluble in CM my, contribute to CM effects. These findings should stimulate further research with different functional assays to clarify the role of PBMC-derived lipids as paracrine mediators.

In summary, we demonstrated that irradiation induced quantitative and qualitative changes in the secretome of human PBMCs. Irradiated cells expressed higher amounts of pro-angiogenic proteins, extracellular vesicles, and oxidized phospholipids than non-irradiated cells. In selected *in vitro* assays with primary human FBs and KCs, we showed that the two main biologically active components of CM were in the fractions that contained either proteins or exosomes. Validated, viral-cleared GMP-compliant, PBMC secretomes displayed cardioprotective effects comparable to those displayed with experimental-grade CM in an *in vivo* model of AMI. This study provided a basis for the development of cell-free therapies in the field of regenerative medicine.

Additional Information

Conflict of interest

H.J.A. is a shareholder of APOSIENCE AG, which owns the right to commercialize PBMC secretomes for therapeutic use.

Author contributions

LB, MM, HJA designed the study; LB, MZ, AM, AE, FG, MSN, MZ, SM, ES, CG and MM performed the *in vitro* experiments; LB, MZ, and MG performed large animal experiments. LB, MM an HJA drafted the manuscript.

References

[1] Ptaszek LM, Mansour M, Ruskin JN, Chien KR. Towards regenerative therapy for cardiac disease. Lancet. 2012;379:933-42.
[2] Gurtner GC, Werner S, Barrandon Y, Longaker MT. Wound repair and regeneration. Nature. 2008;453:314-21.
[3] Sahoo S, Losordo DW. Exosomes and cardiac repair after myocardial infarction. Circ Res. 2014;114:333-44.
[4] Gnecchi M, He H, Liang OD, Melo LG, Morello F, Mu H, et al. Paracrine action accounts for marked protection of ischemic heart by Akt-modified mesenchymal stem cells. Nat Med. 2005;11:367-8.
[5] Lichtenauer M, Mildner M, Baumgartner A, Hasun M, Werba G, Beer L, et al. Intravenous and intramyocardial injection of apoptotic white blood cell suspensions prevents ventricular remodelling by increasing elastin expression in cardiac scar tissue after myocardial infarction. Basic Res Cardiol. 2011;106:645-55.
[6] Lichtenauer M, Mildner M, Hoetzenecker K, Zimmermann M, Podesser BK, Sipos W, et al. Secretome of apoptotic peripheral blood cells (APOSEC) confers cytoprotection to cardiomyocytes and inhibits tissue remodelling after acute myocardial infarction: a preclinical study. Basic Res Cardiol. 2011;106:1283-97.
[7] Hoetzenecker K, Assinger A, Lichtenauer M, Mildner M, Schweiger T, Starlinger P, et al. Secretome of apoptotic peripheral blood cells (APOSEC) attenuates microvascular obstruction in a porcine closed chest reperfused acute myocardial infarction model: role of platelet aggregation and vasodilation. Basic Res Cardiol. 2012;107:292.
[8] Hoetzenecker K, Zimmermann M, Hoetzenecker W, Schweiger T, Kollmann D, Mildner M, et al. Mononuclear cell secretome protects from experimental autoimmune myocarditis. Eur Heart J. 2013.
[9] Pavo N, Zimmermann M, Pils D, Mildner M, Petrasi Z, Petnehazy O, et al. Long-acting beneficial effect of percutaneously intramyocardially delivered secretome of apoptotic peripheral blood cells on porcine chronic ischemic left ventricular dysfunction. Biomaterials. 2014;35:3541-50.
[10] Mildner M, Hacker S, Haider T, Gschwandtner M, Werba G, Barresi C, et al. Secretome of peripheral blood mononuclear cells enhances wound healing. PLoS One. 2013;8:e60103.
[11] Cervio M, Scudeller L, Viarengo G, Monti M, Del Fante C, Arici V, et al. gamma-Irradiated cord blood MNCs: Different paracrine effects on mature and progenitor endothelial cells. Microvasc Res. 2014;94:9-16.
[12] Altmann P, Mildner M, Haider T, Traxler D, Beer L, Ristl R, et al. Secretomes of apoptotic mononuclear cells ameliorate neurological damage in rats with focal ischemia. F1000Res. 2014;3:131.
[13] Korf-Klingebiel M, Kempf T, Sauer T, Brinkmann E, Fischer P, Meyer GP, et al. Bone marrow cells are a rich source of growth factors and cytokines: implications for cell therapy trials after myocardial infarction. Eur Heart J. 2008;29:2851-8.
[14] Korf-Klingebiel M, Reboll MR, Klede S, Brod T, Pich A, Polten F, et al. Myeloid-derived growth factor (C19orf10) mediates cardiac repair following myocardial infarction. Nat Med. 2015.
[15] Lauber K, Bohn E, Krober SM, Xiao YJ, Blumenthal SG, Lindemann RK, et al. Apoptotic cells induce migration of phagocytes via caspase-3-mediated release of a lipid attraction signal. Cell. 2003;113:717-30.
[16] Bochkov VN, Oskolkova OV, Birukov KG, Levonen AL, Binder CJ, Stockl J. Generation and biological activities of oxidized phospholipids. Antioxid Redox Signal. 2010;12:1009-59.
[17] De Jong OG, Van Balkom BW, Schiffelers RM, Bouten CV, Verhaar MC. Extracellular vesicles: potential roles in regenerative medicine. Front Immunol. 2014;5:608.
[18] Xin H, Li Y, Cui Y, Yang JJ, Zhang ZG, Chopp M. Systemic administration of exosomes released from mesenchymal stromal cells promote functional recovery and neurovascular plasticity after stroke in rats. J Cereb Blood Flow Metab. 2013;33:1711-5.
[19] Zhang B, Wang M, Gong A, Zhang X, Wu X, Zhu Y, et al. HucMSC-exosome mediated -Wnt4 signaling is required for cutaneous wound healing. Stem Cells. 2014.

[20] Valadi H, Ekstrom K, Bossios A, Sjostrand M, Lee JJ, Lotvall JO. Exosome-mediated transfer of mRNAs and microRNAs is a novel mechanism of genetic exchange between cells. Nat Cell Biol. 2007;9:654-9.

[21] Vlassov AV, Magdaleno S, Setterquist R, Conrad R. Exosomes: current knowledge of their composition, biological functions, and diagnostic and therapeutic potentials. Biochim Biophys Acta. 2012;1820:940-8.

[22] Salomon C, Ryan J, Sobrevia L, Kobayashi M, Ashman K, Mitchell M, et al. Exosomal signaling during hypoxia mediates microvascular endothelial cell migration and vasculogenesis. PLoS One. 2013;8:e68451.

[23] Zhang HC, Liu XB, Huang S, Bi XY, Wang HX, Xie LX, et al. Microvesicles derived from human umbilical cord mesenchymal stem cells stimulated by hypoxia promote angiogenesis both in vitro and in vivo. Stem cells and development. 2012;21:3289-97.

[24] Brazma A, Hingamp P, Quackenbush J, Sherlock G, Spellman P, Stoeckert C, et al. Minimum information about a microarray experiment (MIAME)-toward standards for microarray data. Nat Genet. 2001;29:365-71.

[25] Ramskold D, Wang ET, Burge CB, Sandberg R. An abundance of ubiquitously expressed genes revealed by tissue transcriptome sequence data. PLoS Comput Biol. 2009;5:e1000598.

[26] Petersen TN, Brunak S, von Heijne G, Nielsen H. SignalP 4.0: discriminating signal peptides from transmembrane regions. Nat Methods. 2011;8:785-6.

[27] Choo KH, Tan TW, Ranganathan S. A comprehensive assessment of N-terminal signal peptides prediction methods. BMC Bioinformatics. 2009;10 Suppl 15:S2.

[28] Krogh A, Larsson B, von Heijne G, Sonnhammer EL. Predicting transmembrane protein topology with a hidden Markov model: application to complete genomes. Journal of molecular biology. 2001;305:567-80.

[29] Wang J, Duncan D, Shi Z, Zhang B. WEB-based GEne SeT AnaLysis Toolkit (WebGestalt): update 2013. Nucleic Acids Res. 2013;41:W77-83.

[30] Franceschini A, Szklarczyk D, Frankild S, Kuhn M, Simonovic M, Roth A, et al. STRING v9.1: protein-protein interaction networks, with increased coverage and integration. Nucleic Acids Res. 2013;41:D808-15.

[31] Gruber F, Bicker W, Oskolkova OV, Tschachler E, Bochkov VN. A simplified procedure for semi-targeted lipidomic analysis of oxidized phosphatidylcholines induced by UVA irradiation. J Lipid Res. 2012;53:1232-42.

[32] Beer L, Seemann R, Ristl R, Ellinger A, Kasiri MM, Mitterbauer A, et al. High dose ionizing radiation regulates micro RNA and gene expression changes in human peripheral blood mononuclear cells. BMC genomics. 2014;15:814.

[33] Gruber F, Mayer H, Lengauer B, Mlitz V, Sanders JM, Kadl A, et al. NF-E2-related factor 2 regulates the stress response to UVA-1-oxidized phospholipids in skin cells. FASEB J. 2010;24:39-48.

[34] Pappinen S, Hermansson M, Kuntsche J, Somerharju P, Wertz P, Urtti A, et al. Comparison of rat epidermal keratinocyte organotypic culture (ROC) with intact human skin: lipid composition and thermal phase behavior of the stratum corneum. Biochim Biophys Acta. 2008;1778:824-34.

[35] Gruber F, Oskolkova O, Leitner A, Mildner M, Mlitz V, Lengauer B, et al. Photooxidation generates biologically active phospholipids that induce heme oxygenase-1 in skin cells. J Biol Chem. 2007;282:16934-41.

[36] Vion AC, Ramkhelawon B, Loyer X, Chironi G, Devue C, Loirand G, et al. Shear stress regulates endothelial microparticle release. Circ Res. 2013;112:1323-33.

[37] Reich CF, 3rd, Pisetsky DS. The content of DNA and RNA in microparticles released by Jurkat and HL-60 cells undergoing in vitro apoptosis. Exp Cell Res. 2009;315:760-8.

[38] Distler JH, Huber LC, Hueber AJ, Reich CF, 3rd, Gay S, Distler O, et al. The release of microparticles by apoptotic cells and their effects on macrophages. Apoptosis. 2005;10:731-41.

[39] Passier R, van Laake LW, Mummery CL. Stem-cell-based therapy and lessons from the heart. Nature. 2008;453:322-9.

[40] Otto WR, Wright NA. Mesenchymal stem cells: from experiment to clinic. Fibrogenesis Tissue Repair. 2011;4:20.

[41] Hsiao ST, Asgari A, Lokmic Z, Sinclair R, Dusting GJ, Lim SY, et al. Comparative analysis of paracrine factor expression in human adult mesenchymal stem cells derived from bone marrow, adipose, and dermal tissue. Stem cells and development. 2012;21:2189-203.

[42] Kumar AH, Caplice NM. Clinical potential of adult vascular progenitor cells. Arterioscler Thromb Vasc Biol. 2010;30:1080-7.

[43] Sahoo S, Klychko E, Thorne T, Misener S, Schultz KM, Millay M, et al. Exosomes from human CD34(+) stem cells mediate their proangiogenic paracrine activity. Circ Res. 2011;109:724-8.

[44] Sirois I, Raymond MA, Brassard N, Cailhier JF, Fedjaev M, Hamelin K, et al. Caspase-3-dependent export of TCTP: a novel pathway for antiapoptotic intercellular communication. Cell Death Differ. 2011;18:549-62.

[45] Ankersmit HJ, Hoetzenecker K, Dietl W, Soleiman A, Horvat R, Wolfsberger M, et al. Irradiated cultured apoptotic peripheral blood mononuclear cells regenerate infarcted myocardium. Eur J Clin Invest. 2009;39:445-56.

[46] Mukherjee P, Mani S. Methodologies to decipher the cell secretome. Biochim Biophys Acta. 2013.

[47] Caccia D, Dugo M, Callari M, Bongarzone I. Bioinformatics tools for secretome analysis. Biochim Biophys Acta. 2013.

[48] Ranganath SH, Levy O, Inamdar MS, Karp JM. Harnessing the mesenchymal stem cell secretome for the treatment of cardiovascular disease. Cell stem cell. 2012;10:244-58.

[49] Sze SK, de Kleijn DP, Lai RC, Khia Way Tan E, Zhao H, Yeo KS, et al. Elucidating the secretion proteome of human embryonic stem cell-derived mesenchymal stem cells. Mol Cell Proteomics. 2007;6:1680-9.

[50] Okumura H, Nagaya N, Itoh T, Okano I, Hino J, Mori K, et al. Adrenomedullin infusion attenuates myocardial ischemia/reperfusion injury through the phosphatidylinositol 3-kinase/Akt-dependent pathway. Circulation. 2004;109:242-8.

[51] Wollert KC. Growth-differentiation factor-15 in cardiovascular disease: from bench to bedside, and back. Basic Res Cardiol. 2007;102:412-5.

[52] Haider H, Jiang S, Idris NM, Ashraf M. IGF-1-overexpressing mesenchymal stem cells accelerate bone marrow stem cell mobilization via paracrine activation of SDF-1alpha/CXCR4 signaling to promote myocardial repair. Circ Res. 2008;103:1300-8.

[53] Spiekstra SW, Breetveld M, Rustemeyer T, Scheper RJ, Gibbs S. Wound-healing factors secreted by epidermal keratinocytes and dermal fibroblasts in skin substitutes. Wound Repair Regen. 2007;15:708-17.

[54] Yu B, Kim HW, Gong M, Wang J, Millard RW, Wang Y, et al. Exosomes secreted from GATA-4 overexpressing mesenchymal stem cells serve as a reservoir of anti-apoptotic microRNAs for cardioprotection. Int J Cardiol. 2014;182C:349-60.

[55] Yu X, Harris SL, Levine AJ. The regulation of exosome secretion: a novel function of the p53 protein. Cancer Res. 2006;66:4795-801.

[56] Lespagnol A, Duflaut D, Beekman C, Blanc L, Fiucci G, Marine JC, et al. Exosome secretion, including the DNA damage-induced p53-dependent secretory pathway, is severely compromised in TSAP6/Steap3-null mice. Cell Death Differ. 2008;15:1723-33.

[57] Bicalho B, Holovati JL, Acker JP. Phospholipidomics reveals differences in glycerophosphoserine profiles of hypothermically stored red blood cells and microvesicles. Biochim Biophys Acta. 2013;1828:317-26.

[58] Zhao Y, Zhang CF, Rossiter H, Eckhart L, Konig U, Karner S, et al. Autophagy is induced by UVA and promotes removal of oxidized phospholipids and protein aggregates in epidermal keratinocytes. J Invest Dermatol. 2013;133:1629-37.

[59] Bochkov VN, Philippova M, Oskolkova O, Kadl A, Furnkranz A, Karabeg E, et al. Oxidized phospholipids stimulate angiogenesis via autocrine mechanisms, implicating a novel role for lipid oxidation in the evolution of atherosclerotic lesions. Circ Res. 2006;99:900-8.

Table 1: Cardic MRI evaluation 3 and 30 days after AMI

	Parameters	Medium Control (n = 7)	CM (1,5 × 10^9; n = 4)	CM + PR (1,5 × 10^9; n = 6)	
After 3 days	Weight (kg)	31.9 ± 0.9	32.0 ± 1.2	34.2 ± 0.5	n.s.
	Age (days)	90 ± 0	90 ± 0	90 ± 0	n.s.
	LVEDV (ml)	67.6 ± 2.8	75.6 ± 2.2	83.0 ± 4.0 *	*
	LVESV(ml)	38.4 ± 2.5	47.4 ± 1.7 *	48.7 ± 4.3	n.s.
	LVSV (ml)	29.2 ± 1.3	28.3 ± 2.2	34.3 ± 2.0 *	n.s.
	LVEF (%)	43.4 ± 1.9	37.3 ± 2.2	41.7 ± 2.9	n.s.
	HR/min	111 ± 6	87 ± 9 *	77 ± 3 **	**
	CO (l/min)	3.2 ± 0.1	2.4 ± 0.1 *	2.6 ± 0.2 *	**
	CI (l/min/m2)	3.6 ± 0.1	3.1 ± 0.3	3.3 ± 0.2	n.s.
	Infarct %	18.2 ± 1.7	13.1 ± 2.8	12.3 ± 1.9 *	n.s.
After 30 days	Weight (kg)	39.4 ± 0.5	50.0 ± 1.8 ***	55.7 ± 0.7 ***	***
	Age (days)	120 ± 0	120 ± 0	120 ± 0	n.s.
	LVEDV (ml)	54.8 ± 4.1	107.5 ± 6.7 ***	102.5 ± 6.0 ***	***
	LVESV(ml)	32.9 ± 4.0	65.5 ± 3.4 ***	53.9 ± 4.3 **	***
	LVSV (ml)	21.8 ± 1.8	42.0 ± 4.4 **	48.6 ± 2.9 ***	***
	LVEF (%)	40.5 ± 3.6	38.9 ± 2.3	47.6 ± 2.1	n.s.
	HR/min	114 ± 7	123 ± 5	109 ± 3	n.s.
	CO (l/min)	2.4 ± 0.1	5.1 ± 0.4 ***	5.3 ± 0.3 ***	***
	CI (l/min/m2)	2.5 ± 0.1	5.0 ± 0.3 ***	4.7 ± 0.3 ***	***
	Infarct %	12.6 ± 1.4	9.8 ± 0.6	8.2 ± 1.7	n.s.

Three and 30 days after ischaemia/reperfusion injury, MRI was conducted and parameters of cardiac function were obtained from pigs treated with unprocessed CM (CM) and pathogen reducec CM (PR+CM) and from control animals

LVEDD left ventricular end-diastolic diameter, LVESD left ventricular end-systolic diameter, LVSV left ventricular stroke volume, LVEF left ventricular ejection fraction, HR heart rate, CI cardiac index, CO cardiac output, ns no significance versus control

ns   no significance vs control
* p < 0.05 vs control
** p < 0.01 vs control
*** p < 0.001 vs control

Figure Legends
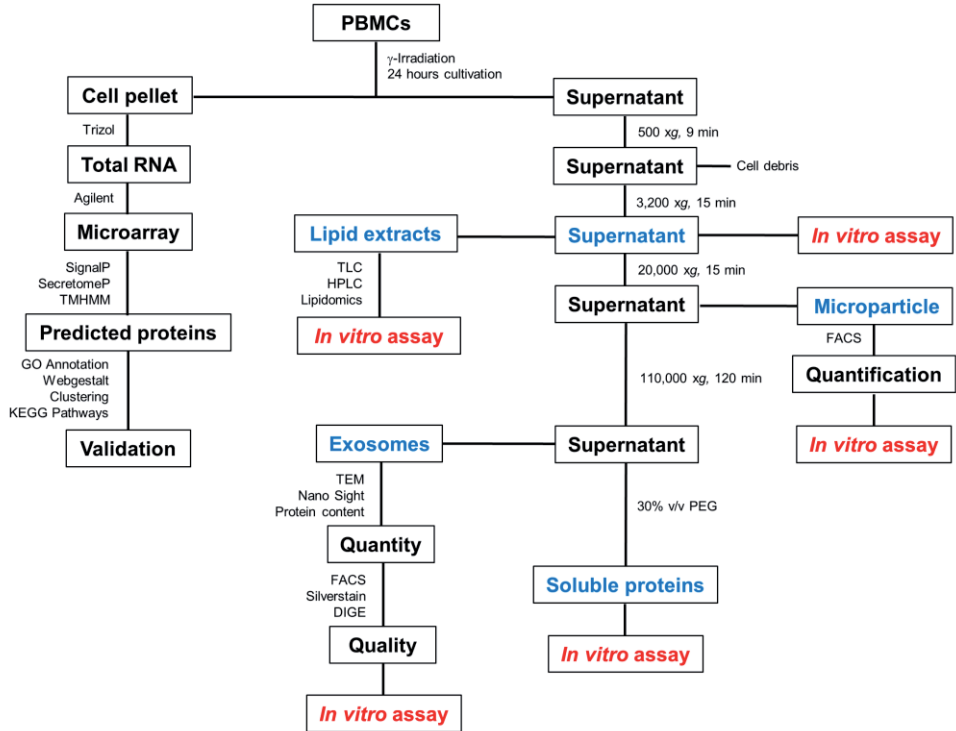
Figure 1. Schematic overview of experimental workflow

PBMCs were either gamma-irradiated with 60 Gy or not irradiated. After culturing for the indicated times, cells were centrifuged to separate the cell pellet and CM supernatant. The pellet was used to extract cellular RNA, which was used for microarray analysis. The CM supernatant was processed to separate and isolate different molecular components. The steps highlighted in blue indicate samples used for *in vitro* assays. The different methods and bioinformatics tools used for sample analyses are indicated at the appropriate links.
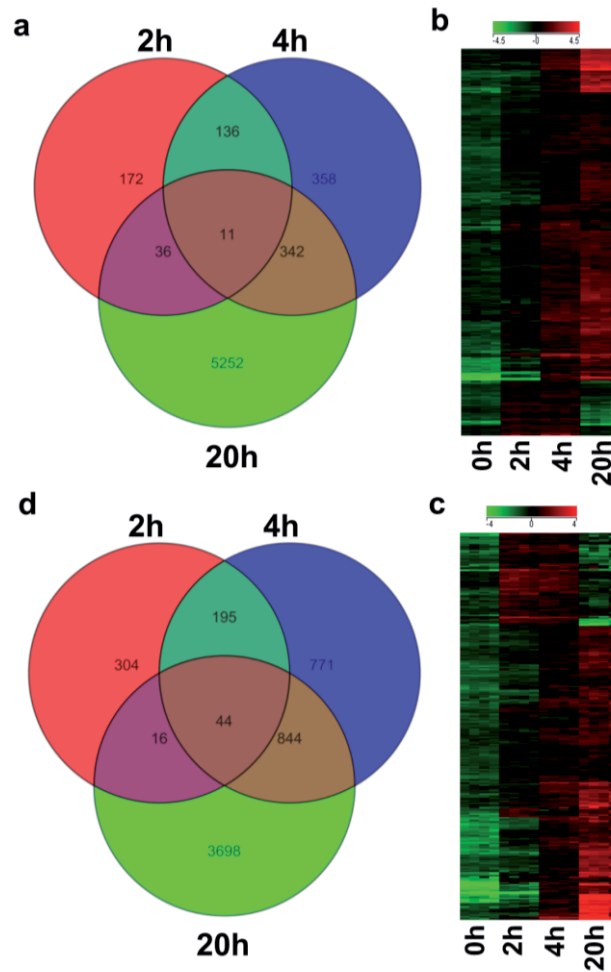
Figure 2. Analysis of changes in PBMC transcriptome

PBMCs were either irradiated or not irradiated *ex vivo*, before culturing for 2, 4, or 20 h. At the indicated time points, total RNA was isolated, and microarray analyses were performed to evaluate gene expression. (*Left*) Venn diagrams show the numbers of upregulated transcripts with expression changes >2-fold above expression after cell separation for (a) non-irradiated and (c) irradiated PBMCs. Each circle depicts the genes detected at the indicated time point; overlapping sections indicate the number of genes that were upregulated at multiple time points. (*Right*) The heatmaps show that a significant number of genes were upregulated in (b) non-irradiated and (d) irradiated PBMCs with a strong time dependence, and expression was most prominent at 20 h after cultivation; green = downregulated; red = upregulated in cultured samples; n=4 for each time point.
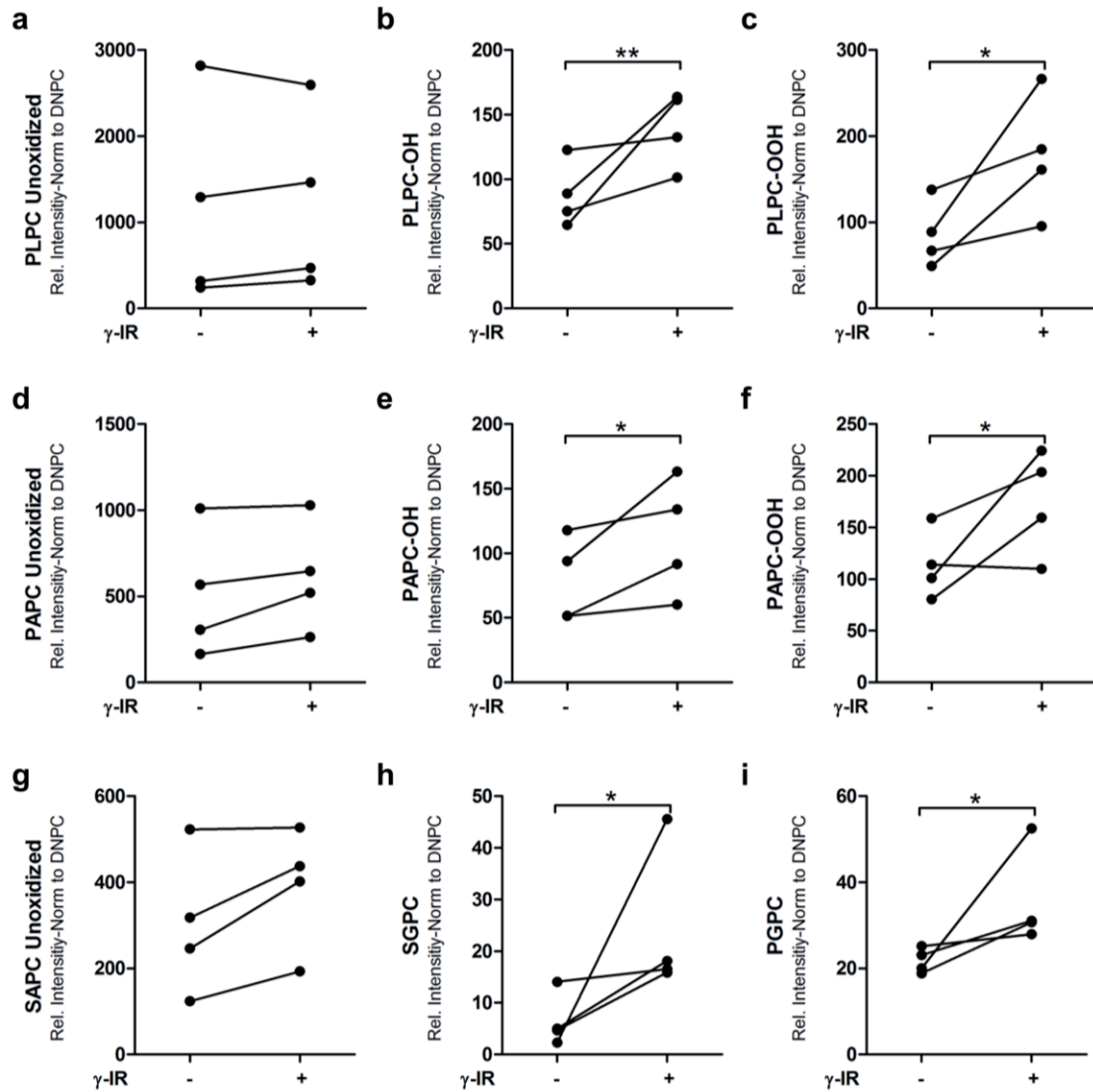
Figure 3. Ionizing radiation induces the release of oxidized phosphatidylcholines in human PBMCs.

Irradiated (+) and non-irradiated (-) PBMCs were cultured for 24 h. Then, cells and cell debris were removed with serial centrifugations, and the lipids were separated with a chloroform/methanol extraction protocol. Lipids were analyzed with high pressure lipid chromatography to determine the presence of oxidation products. (*Left column*, A, D, G) The non-oxidized precursor phospholipids were comparable between irradiated and non-irradiated samples. (*Middle and right columns*, B-I) Oxidized lipid products were detectable in significantly higher concentrations in the CM of irradiated samples compared to non-irradiated samples. Data are expressed as the mean ± SD intensity, relative to that of the DNPC standard; Dots on each line display values of a single donor; n=4. *p<0.05; **p<0.01
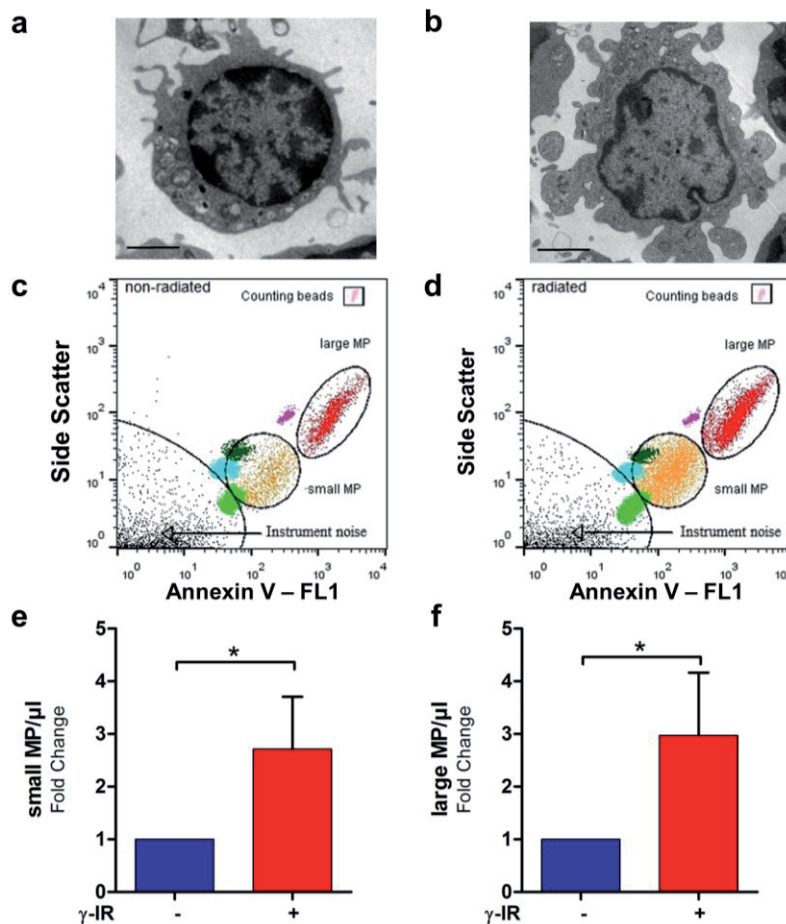
Figure 4. Ionizing radiation induces the release of microparticles.

(*Left*) Non-irradiated and (*right*) irradiated PBMCs were cultured for 20 h, then subjected to electron microscopy and FACS analysis. (a) Image of non-irradiated PBMC shows a largely intact plasma membrane and cell nucleus with minor plasma membrane shedding. Scale bar = 2.5 µm (b) Image of irradiated PBMC shows cellular shrinking, plasma membrane fragmentation, and chromatin condensation. (C,D) FACS quantification of the absolute number of microparticles released from PBMCs. Microparticles were purified from CM with a serial centrifugation protocol, and the absolute number of vesicles was calculated with control counting beads. Representative FACS analysis results are shown for (c) non-irradiated and (d) irradiated PBMCs; the counting beads are indicated on the upper right sides. The scaling beads are highlighted in light green, light blue, dark green, and pink; diameters range from 0.16 µm to 0.5 µm. Two distinct sizes of microparticles are highlighted in orange (small microparticles) and red (large microparticles). (E,F) Quantitative analyses of

non-irradiated (-) and irradiated (+) samples show that irradiation induced release of both (e) small and (f) large microparticles. n=3. *p<0.05
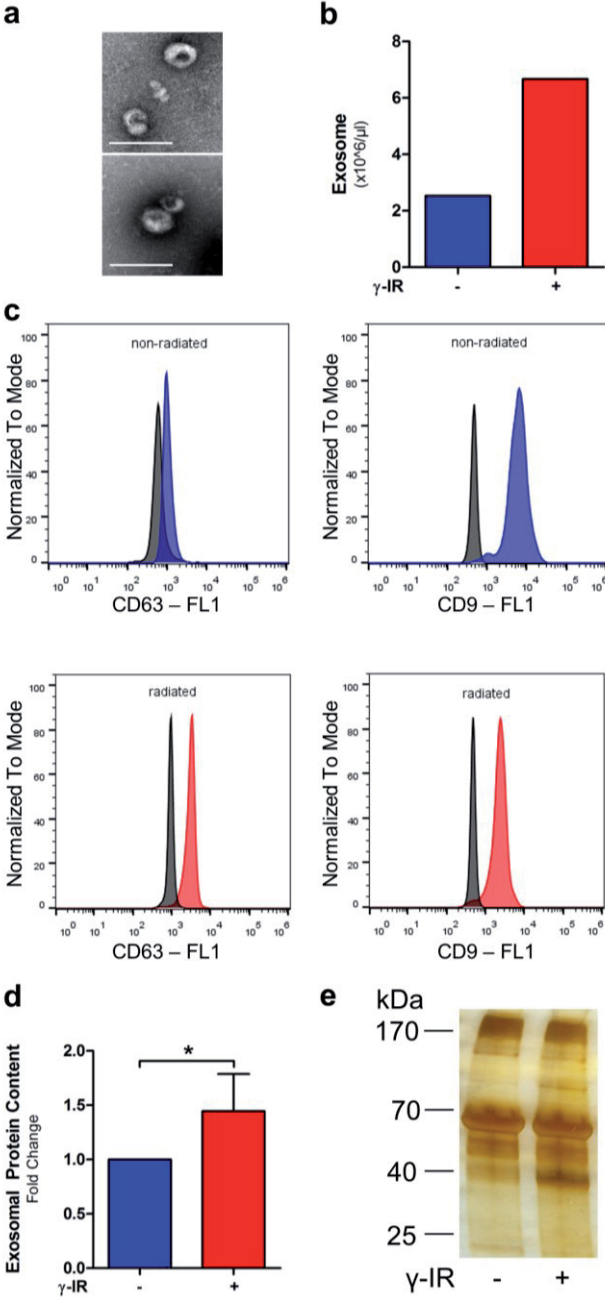
Figure 5. Ionizing radiation induces exosome release and modulates protein content.
Exosomes isolated from CM of non-irradiated (-) or irradiated (+) PBMCs were qualitatively analyzed with transmission electron microscopy (TEM). (a) TEM images confirm typical size and shape of exosomes derived from non-irradiated (*top*) and irradiated (*bottom*) PBMCs. Scale bar = 100 nm (b) NanoSight analysis shows absolute number of exosomes was higher

in CM of irradiated compared to the CM from non-irradiated PBMCs. (c) FACS analysis of CD63 and CD9 exosome markers. Exosomes were coupled to CD63 marker beads and labeled with either CD63 or CD9 antibodies. Isotope antibodies served as a negative control. Exosomes from non-irradiated (*top*) and irradiated (*bottom*) PBMCs were positive for both CD63 (*left*) and CD9 (*right*); thus, the purification procedure was sufficient to isolate exosomes. (d) Exosomes were lysed in SDS buffer and total protein content was quantified with the Bradford assay. The total protein content was significantly higher in exosomes from irradiated (+) PBMCs than in exosomes from non-irradiated (-) PBMCs. Data are given as mean ± SD of four samples; *p<0.05. (e) Proteins were separated on SDS gels and stained with silver stain. The large band at 66 kDa depicts the albumin fraction. Other proteins were differentially expressed in exosomes from irradiated and non-irradiated PBMCs (e.g., band at 37 kDa).
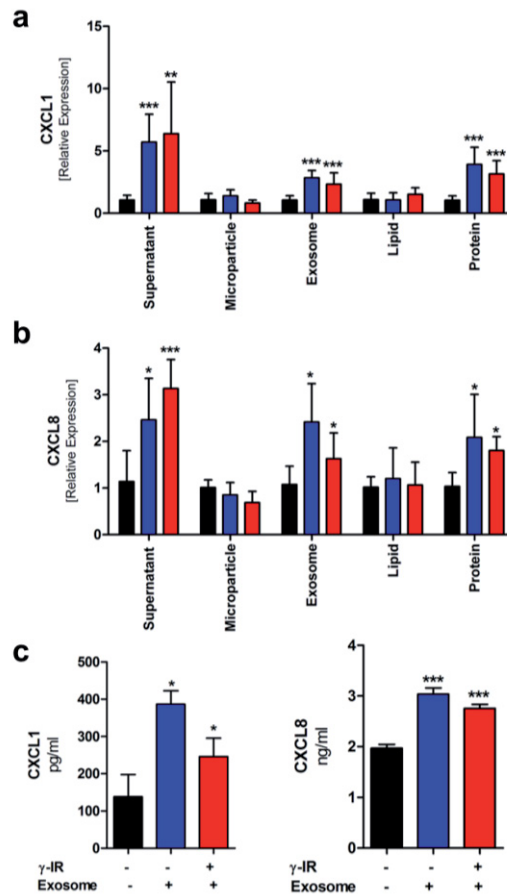
Figure 6. Exosomes and proteins stimulate CXCL1 and CLXCL8 expression.

Fibroblast gene expression of (a) CXCL1 and (b) CXCL8 was measured relative to B2M expression (control). Fibroblasts were stimulated with control cell culture media (black bars) or stimulated with total CM (supernatant) or the indicated CM fractions. CM was collected from irradiated (red bars) or non-irradiated (blue bars) PBMCs. RNA was isolated 6 h after cell stimulation. (c) ELISA results show CXCL1 and CXLC8 protein contents in the supernatant of fibroblasts after stimulation with exosomes. Protein content was measured at 6 h after stimulation. Bars represent the means ± SD of two experiments, each performed in triplicate; *p<0.05; **p<0.01; ***p<0.001.
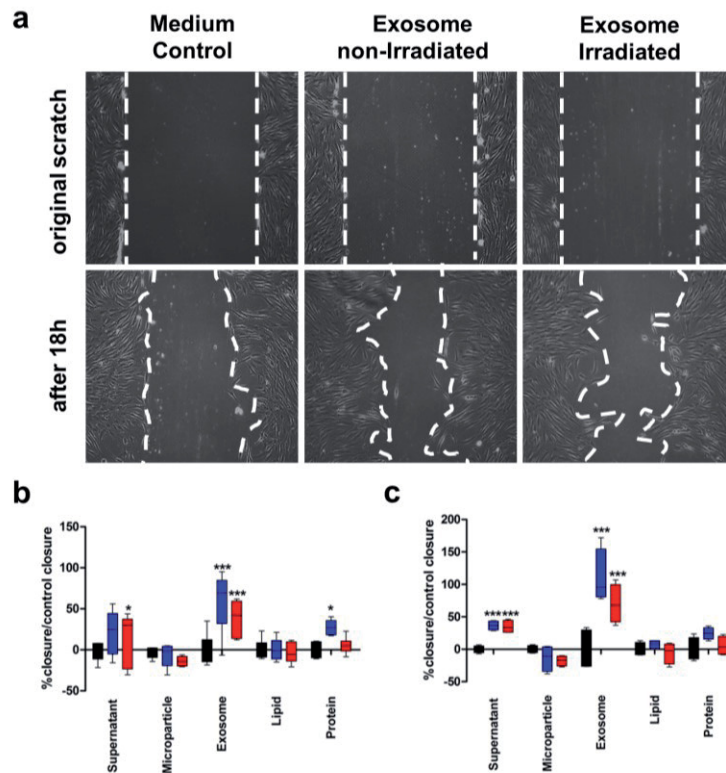
Figure 7. Exosomes and CM proteins enhance cell migration

(A, *top*) Fibroblast monolayers were scratched (cleared areas outlined in white dashed lines) to simulate a wound. Cultures were untreated or treated with exosome preparations from non-irradiated or irradiated PBMCs. (*Bottom*) After 18 h, fibroblast proliferation began to close the wound in (*left*) untreated and (*middle*, *right*) treated cultures. Treatment with PBMC-derived exosomes accelerated wound closure. 10 fold magnification (B,C) Wound areas were measured in 8 scratches after (b) 24 h and (c) 48 h. The percentage of closure compared to closure in control (untreated) was calculated. Data are expressed as the mean ± SD of two independent experiments. *p<0.05; ***p<0.001.

Supplementary information for:

Analysis of the Secretome of Apoptotic Peripheral Blood Mononuclear Cells: Impact of Released Proteins and Exosomes for Tissue Regeneration

Lucian Beer[1,2], Matthias Zimmermann[1,2], Andreas Mitterbauer[1,2], Adolf Ellinger[3], Florian Gruber[4,5], Marie-Sophie Narzt[4,5], Maria Zellner[6], Mariann Gyöngyösi[7], Sibylle Madlener[8], Elisabeth Simader[1,2]; Christian Gabriel[9], Michael Mildner[4*], Hendrik Jan Ankersmit[1,2*]

[1] Department of Thoracic Surgery, Medical University of Vienna, Austria
[2] Christian Doppler Laboratory for Cardiac and Thoracic Diagnosis and Regeneration, Medical University of Vienna, Austria
[3]Department of Cell Biology and Ultrastructure Research, Center for Anatomy and Cell Biology, Medical University of Vienna, Vienna, Austria.
[4]Department of Dermatology, Research Division of Biology and Pathobiology of the Skin, Medical University Vienna, Austria
[5] Christian Doppler Laboratory for Laboratory Biotechnology of Skin Aging, Medical, Austria
[6]Centre of Physiology and Pharmacology, Institute of Physiology, Medical University of Vienna, Austria
[7]Department of Cardiology, Medical University Vienna, Vienna, Austria
[8]Molecular Neuro-Oncology Research Unit, Department of Pediatrics and Adolescent Medicine and Institute of Neurology, Medical University of Vienna, Austria
[9]Red Cross Blood Transfusion Service of Upper Austria, Linz, Austria

*These authors share the last and corresponding authorship.

Corresponding authors:

Hendrik Jan Ankersmit, MD
Department of Thoracic Surgery, Medical University of Vienna
Christian Doppler Laboratory for Cardiac and Thoracic Diagnosis and Regeneration
Währinger Gürtel 18-20
1090 Vienna, Austria
Tel.: +43-1-40400-67770
Fax.: +43-1-40400-69770
e-mail: hendrik.ankersmit@meduniwien.ac.at

Michael Mildner, PhD
Medical University of Vienna
Department of Dermatology,
Research Division of Biology and Pathobiology of the Skin,
Lazarettgasse14
1090 Vienna, Austria
Tel: +43-1-40400-73507
Fax: +43-1-40400-73590
e-mail: michael.mildner@meduniwien.ac.at

Supplementary Figure 1
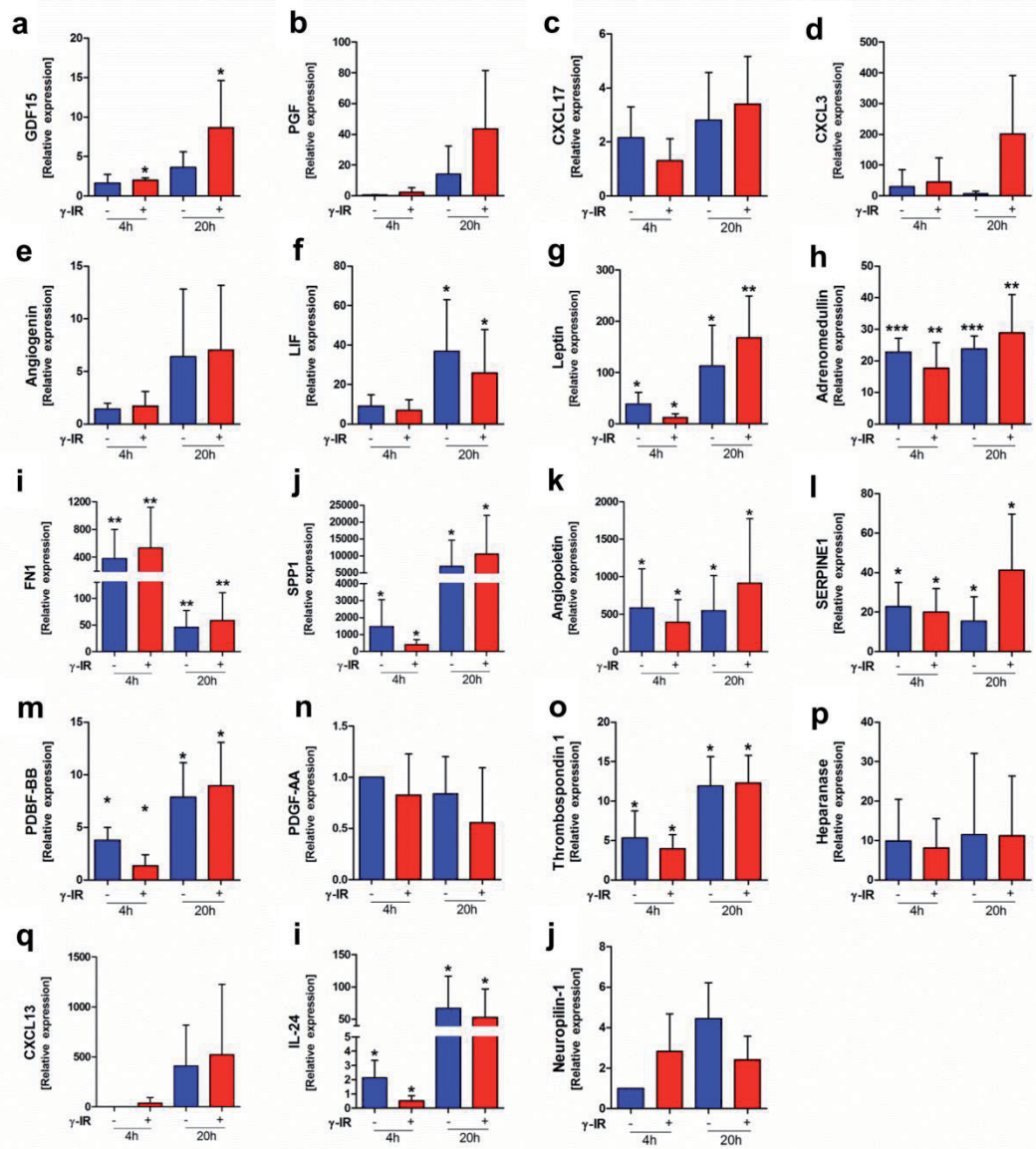
Supplementary Figure 1

Quantitative PCR results show expression of genes involved in angiogenesis, wound healing, or chemotaxis. (a-s) In comparing levels at 4 h and 20 h, most genes showed a time dependent increase, except FN1 (i) and PDGF-AA (n). A few genes tended to show higher expression in irradiated (+, red) compared to non-irradiated (-, blue) PBMCs. Expression values were normalized to the gene expression values at 0 h. B2M served as an internal control gene. Data represent the mean ± SD of four samples; *p<0.05; **p<0.01; ***p<0.001

Supplementary Figure 2
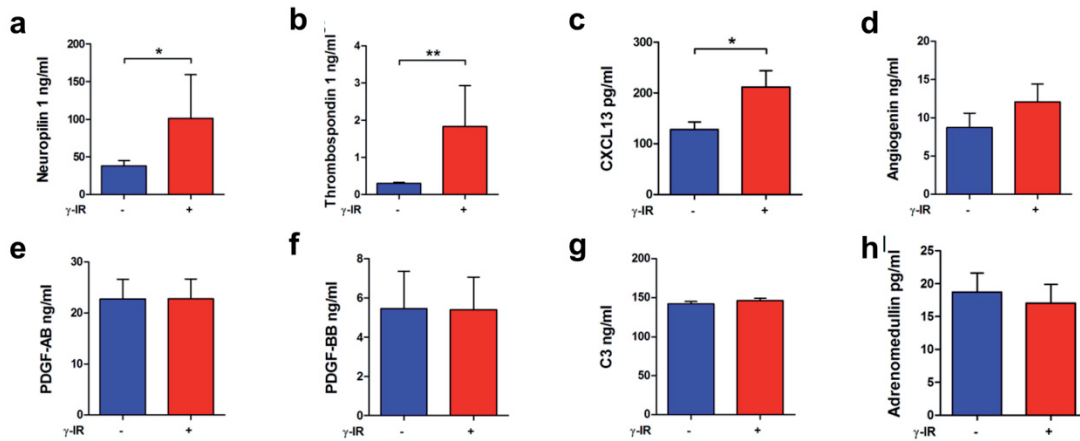
Supplementary Figure 2

ELISA detection identified proteins isolated from the CM of non-irradiated and irradiated PBMCs measured after 20 h of culture. Cell culture medium alone (without cells) did not contain detectable amounts of any measured mediators. Protein concentrations of (a) neuropilin, (b) thrombospondin, and (c) CXCL13 were significantly higher in CM from irradiated (+, red) than in non-irradiated (-, blue) PBMCs; however, levels of (d) angiogenin, (e) PDGF-AB, (f) PDGF-BB, (g) C3, and (h) adrenomedullin were comparable in both groups. Data are given as mean ± SD of five samples; *p<0.05; **p<0.01.

Supplementary Figure 3
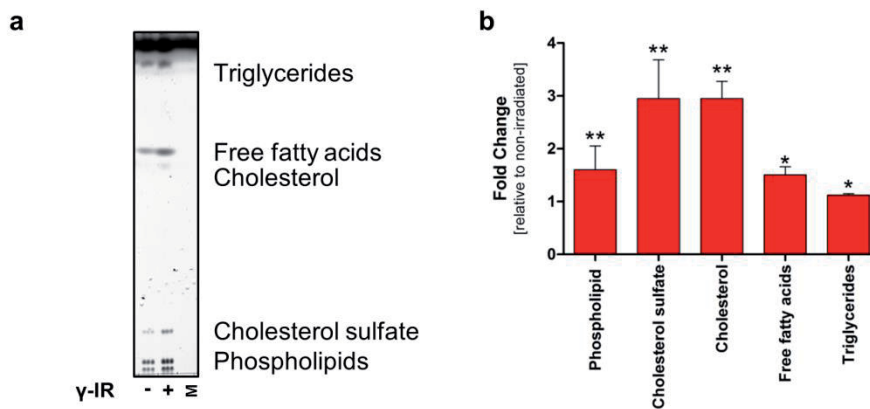
Supplementary Figure 3

Ionizing radiation induced the release of soluble and membrane-bound lipids from human PBMCs. PBMCs were either irradiated (+) or non-irradiated (-), and cultured for 24 h. Then, the cells and cell debris were removed by serial centrifugation, and the lipids were isolated with a chloroform/methanol extraction protocol. (a) Dissolved lipids were resolved with thin layer chromatography (TLC; Pappinen et al.). Cell medium (M) cultured without cells did not contain any lipids. The CM of PBMCs contained triglycerides, free fatty acids, cholesterol, cholesterol sulfate, and phospholipids. (b) Quantitative analysis of TLC data showed that the CM samples from irradiated PBMCs had significant increases in absolute concentrations of all lipid classes compared to non-irradiated samples. Data are expressed as the mean ± SD of four samples; *$p<0.05$; **$p<0.01$.

Supplementary Figure 4
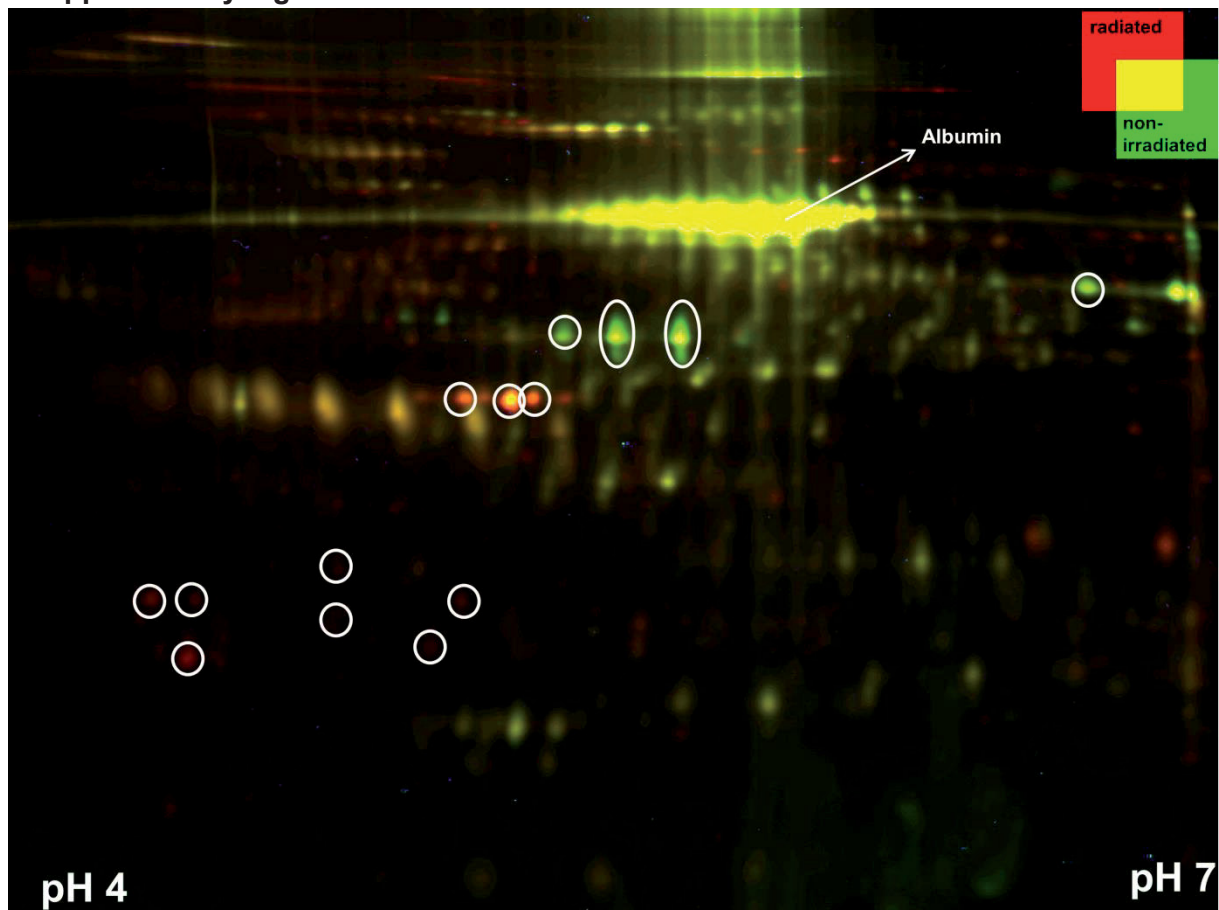
Supplementary Figure 4

2D-Difference gel electrophoresis results show different exosome protein contents of non-irradiated and irradiated PBMCs. The total CyDye-labeled, exosome protein extract sample (45 µg) comprised a combination of four samples (15 µg each pooled from 4 donors): The proteins were separated in the pH range of 4-7. The red and green spots are proteins that showed increased and decreased expression, respectively, in exosomes from irradiated PBMCs, compared to exosomes from non-irradiated PBMCs. Yellow spots are proteins that show comparable concentrations in exosomes from irradiated and non-irradiated PBMCs. The white circles indicate proteins that were detected in irradiated or non-irradiated samples exclusively. The large protein spot at 66 kDa represents the albumin fraction (arrow). Exosomes from 4 donors were used for this experiment.

Supplementary Figure 5
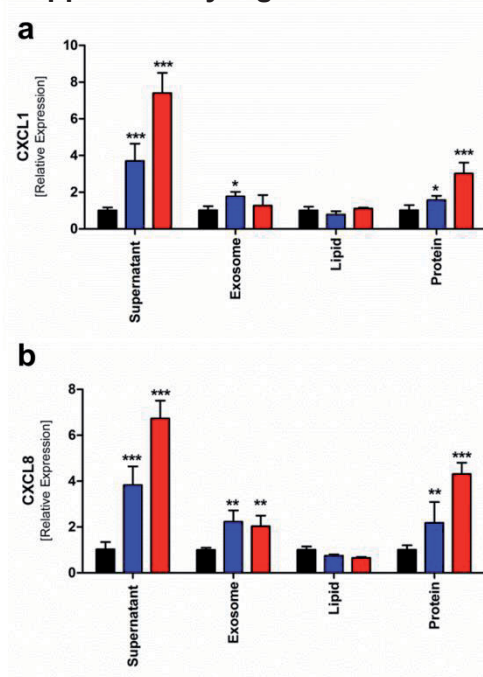
Supplementary Figure 5

Exosomes and proteins stimulate CXCL1 and CLXCL8 expression in keratinocytes.

Keratinocyte gene expression of (a) CXCL1 and (b) CXCL8 was measured relative to B2M

expression (control). Keratinocytes were unstimulated (black bars) or stimulated with total

CM (supernatant) or the indicated CM fractions, collected from irradiated (red bars) or non-

irradiated (blue bars) PBMCs. RNA was isolated 6 h after cell stimulation. Bars represent the

mean ± SD of n=2 experiments performed in triplicate.*p<0.05; **p<0.01; ***p<0.001.

Supplementary Figure 6
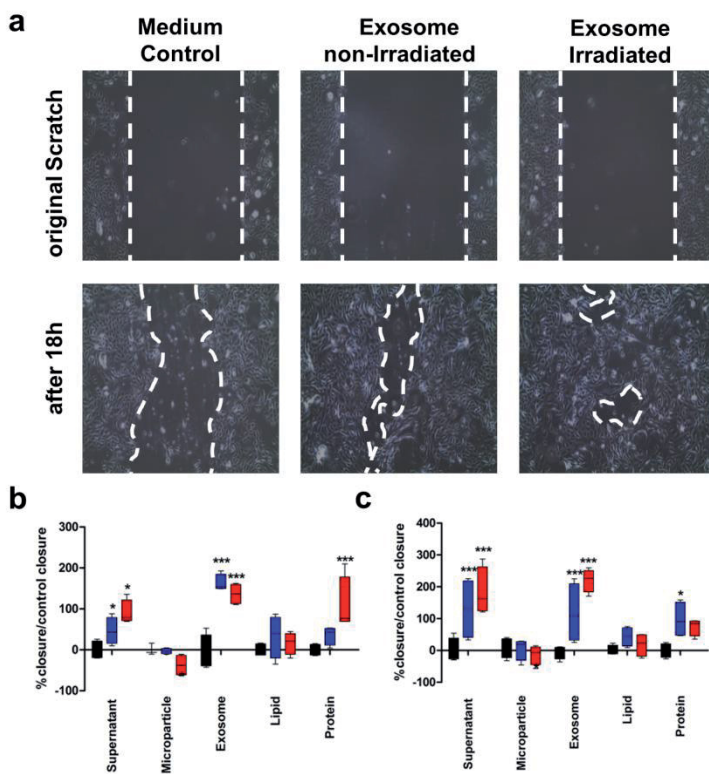
Supplementary Figure 6

Exosomes and CM proteins enhance keratinocyte migration. (A, *top*) Keratinocyte monolayers were scratched (clear areas outlined in white dashed lines) to simulate a wound. Wounds were untreated or treated with exosome preparations from non-irradiated or irradiated PBMCs. (*Bottom*) After 18 h, fibroblast proliferation began to close the wound in (*left*) untreated and (*middle*, *right*) treated cultures. Treatment with PBMC-derived exosomes accelerated wound closure. 10 fold magnification (b) Wound areas were measured in 8 scratches after 24 h. The percentage of closure compared to closure in control (untreated) was calculated. (c) The same experiment was performed with keratinocytes, but without using 10% CellGro medium as basal medium. In this experimental setup, the proliferative effects of primary CM, exosomes, and CM proteins were more pronounced than the effects observed in the initial experimental setting. Data are expressed as the mean ± SD of two independent experiments. *p<0.05; ***p<0.001.

Supplementary Figure 7
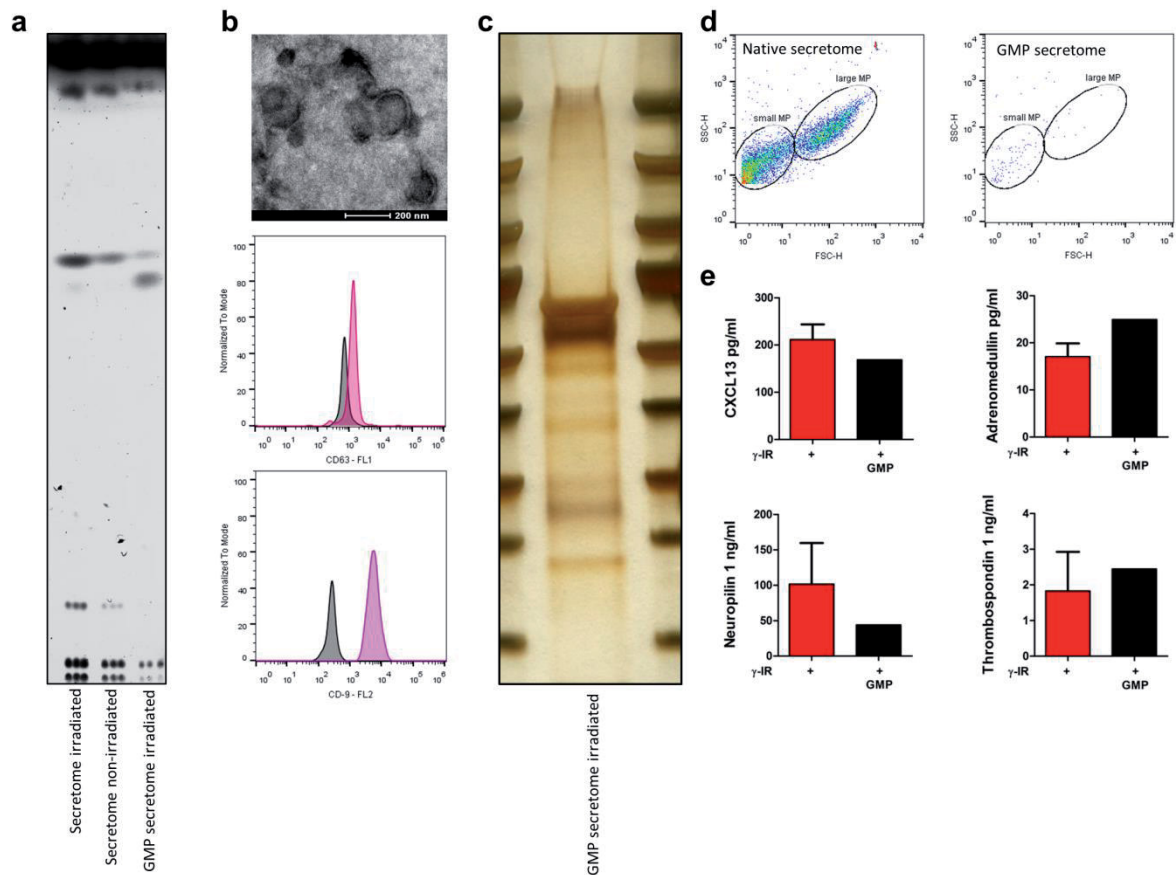
Supplementary Figure 7

Comparability of biological components of the PBMC secretome, isolated with experimental methods or under GMP conditions. (a) TLC shows secretomes from CM isolated from irradiated (*line 1*) and non-irradiated (*line 2*) PBMCs, and CM from irradiated PBMCs, but processed under GMP-compliant conditions (*line 3*). The absolute concentration of lipids was lower in the GMP-compliant CM; however, except for cholesterol, the lipid compositions were comparable in the two different preparations. (b) *Top:* TEM image of exosomes derived from GMP-compliant CM showed vesicles with a diameter of ~100 nm. Scale bar = 200 nm. (*Middle, bottom*) FACS analysis showed that these vesicles were positive for CD63 and CD9, as indicated. (c) After exosomes were lysed, the proteins were separated with 1-D gel electrophoresis and stained with silver stain. Several different protein bands were detected with quality comparable to that observed in exosomes derived from CM with the experimental protocols. (d) GMP-compliant CM did not contain considerable numbers of microparticles. In the GMP protocol, microparticles were removed by filtration through 0.2-µm filters. (e)

Selected CM proteins were compared between experimental (+, red) and GMP-compliant

(black) preparations. Similar concentrations were detectable for CXCL13, andrenomedullin,

and thrombospondin. Neuropilin concentrations tended to be lower in GMP-compliant CM.

Supplementary Table 1: Enrichment of GO-terms in up-regulated genes coding for secretory proteins in **irradiated** PBMCs.

GO-Term	Enriched terms	p-value	Enrichment Score	Number of Genes
GO:0001568	blood vessel development	1.53e-07	5.32	22
GO:0045766	positive regulation of angiogenesis	3.00e-05	6.34	10
GO:0042060	wound healing	0.0012	2.74	21
GO:0032502	developmental processes	0.0007	1.65	83
GO:0007599	hemostasis	0.0007	3.08	19
GO:0050819	negative regulation of coagulation	0.0007	11.68	6
GO:0050900	leukocyte migration	0.0007	4.28	13

Biological Function of the 213 gene products. The 213 genes were classified into different biological processes. Biological processes that were over-represented in the data set relative to the frequency of genes in a reference database with a corrected p value <0.05 are given.

Enrichment of GO-terms in up-regulated genes coding for secretory proteins in **non-irradiated** PBMCs.

GO-Term	Enriched terms	p-value	Enrichment Score	Number of Genes
GO:0051955	regulation of amino acid transport	0.0403	15.39	3
GO:0050855	regulation of B cell receptor signaling pathway	0.0490	33.71	2
GO:0044060	regulation of endocrine process	0.0116	20.52	4

Biological Function of the 179 gene products. The 179 genes were classified into different biological processes. Biological processes that were over-represented in the data set relative to the frequency of genes in a reference database with a corrected p value <0.05 are given.

Supplementary Table 2: 213 Up-regulated transcripts in **irradiated** PBMC coding for secretory proteins

Gene Symbol	EntrezGene	Gene Name
C16orf74	404550	chromosome 16 open reading frame 74
CYP17A1	1586	cytochrome P450, family 17, subfamily A, polypeptide 1
HIST1H2AD	3013	histone cluster 1, H2ad
TESK2	10420	testis-specific kinase 2
GSTT2	2953	glutathione S-transferase theta 2
P4HA1	5033	prolyl 4-hydroxylase, alpha polypeptide I
SPINK1	6690	serine peptidase inhibitor, Kazal type 1
RRAD	6236	Ras-related associated with diabetes
TIPARP	25976	TCDD-inducible poly(ADP-ribose) polymerase
HIST1H2AK	8330	histone cluster 1, H2ak
SERPINE1	5054	serpin peptidase inhibitor, clade E (nexin, plasminogen activator inhibitor type 1), member 1
CHMP1B	57132	charged multivesicular body protein 1B
VCAN	1462	versican
AHRR	57491	aryl-hydrocarbon receptor repressor
UBE2A	7319	ubiquitin-conjugating enzyme E2A
IBA57	200205	IBA57, iron-sulfur cluster assembly homolog (S. cerevisiae)
MDGA1	266727	MAM domain containing glycosylphosphatidylinositol anchor 1
MANF	7873	mesencephalic astrocyte-derived neurotrophic factor
IVNS1ABP	10625	influenza virus NS1A binding protein
CXCL3	2921	chemokine (C-X-C motif) ligand 3
EYA3	2140	eyes absent homolog 3 (Drosophila)
SH2D6	284948	SH2 domain containing 6
EDARADD	128178	EDAR-associated death domain
TGIF1	7050	TGFB-induced factor homeobox 1
LRRC6	23639	leucine rich repeat containing 6
ALCAM	214	activated leukocyte cell adhesion molecule
MSL1	339287	male-specific lethal 1 homolog (Drosophila)
IL24	11009	interleukin 24
ASPHD1	253982	aspartate beta-hydroxylase domain containing 1
GDF15	9518	growth differentiation factor 15
GRB10	2887	growth factor receptor-bound protein 10
LPO	4025	lactoperoxidase
STX5	6811	syntaxin 5
PLEKHH3	79990	pleckstrin homology domain containing, family H (with MyTH4 domain) member 3
RAB42	115273	RAB42, member RAS oncogene family
FANCL	55120	Fanconi anemia, complementation group L
P4HA2	8974	prolyl 4-hydroxylase, alpha polypeptide II
S100A5	6276	S100 calcium binding protein A5
MFAP4	4239	microfibrillar-associated protein 4
GATSL3	652968	GATS protein-like 3
PATE2	399967	prostate and testis expressed 2
FLT1	2321	fms-related tyrosine kinase 1 (vascular endothelial growth factor/vascular permeability factor receptor)
DENND5A	23258	DENN/MADD domain containing 5A
DLG4	1742	discs, large homolog 4 (Drosophila)
DRGX	644168	dorsal root ganglia homeobox
LAD1	3898	ladinin 1
CST6	1474	cystatin E/M
GNA12	2768	guanine nucleotide binding protein (G protein) alpha 12
IL23A	51561	interleukin 23, alpha subunit p19

Gene	ID	Description
SEC24A	10802	SEC24 family, member A (S. cerevisiae)
TSHB	7252	thyroid stimulating hormone, beta
PPIF	10105	peptidylprolyl isomerase F
TBX6	6911	T-box 6
KCNE1	3753	potassium voltage-gated channel, Isk-related family, member 1
IL1A	3552	interleukin 1, alpha
GADD45G	10912	growth arrest and DNA-damage-inducible, gamma
FHL3	2275	four and a half LIM domains 3
NAGS	162417	N-acetylglutamate synthase
ACOX2	8309	acyl-CoA oxidase 2, branched chain
EFEMP2	30008	EGF containing fibulin-like extracellular matrix protein 2
AK2	204	adenylate kinase 2
PDE2A	5138	phosphodiesterase 2A, cGMP-stimulated
TUBB2A	7280	tubulin, beta 2A class IIa
VWCE	220001	von Willebrand factor C and EGF domains
TFPI2	7980	tissue factor pathway inhibitor 2
TOB2	10766	transducer of ERBB2, 2
THBS1	7057	thrombospondin 1
MFI2	4241	antigen p97 (melanoma associated) identified by monoclonal antibodies 133.2 and 96.5
SMOX	54498	spermine oxidase
IFNA7	3444	interferon, alpha 7
CDKN1A	1026	cyclin-dependent kinase inhibitor 1A (p21, Cip1)
BBC3	27113	BCL2 binding component 3
PCOLCE2	26577	procollagen C-endopeptidase enhancer 2
PPFIA1	8500	protein tyrosine phosphatase, receptor type, f polypeptide (PTPRF), interacting protein (liprin), alpha 1
NOTCH3	4854	notch 3
PLD2	5338	phospholipase D2
PPP1R3B	79660	protein phosphatase 1, regulatory subunit 3B
H2AFX	3014	H2A histone family, member X
ALOX15B	247	arachidonate 15-lipoxygenase, type B
HIST1H2AG	8969	histone cluster 1, H2ag
CXCL13	10563	chemokine (C-X-C motif) ligand 13
PDGFB	5155	platelet-derived growth factor beta polypeptide
RNASET2	8635	ribonuclease T2
NRP1	8829	neuropilin 1
LIF	3976	leukemia inhibitory factor
LACC1	144811	laccase (multicopper oxidoreductase) domain containing 1
TIMP1	7076	TIMP metallopeptidase inhibitor 1
PRSS53	339105	protease, serine, 53
PINLYP	390940	phospholipase A2 inhibitor and LY6/PLAUR domain containing
ANGPTL4	51129	angiopoietin-like 4
LEP	3952	leptin
ERO1L	30001	ERO1-like (S. cerevisiae)
RGL3	57139	ral guanine nucleotide dissociation stimulator-like 3
PPP1R3G	648791	protein phosphatase 1, regulatory subunit 3G
CXCL5	6374	chemokine (C-X-C motif) ligand 5
COL27A1	85301	collagen, type XXVII, alpha 1
PLOD2	5352	procollagen-lysine, 2-oxoglutarate 5-dioxygenase 2
C4orf47	441054	chromosome 4 open reading frame 47
NMNAT1	64802	nicotinamide nucleotide adenylyltransferase 1
DCAF4L2	138009	DDB1 and CUL4 associated factor 4-like 2
IGLON5	402665	IgLON family member 5
FUT11	170384	fucosyltransferase 11 (alpha (1,3) fucosyltransferase)

C16orf72	29035	chromosome 16 open reading frame 72
PELI3	246330	pellino E3 ubiquitin protein ligase family member 3
EPPIN-WFDC6	100526773	EPPIN-WFDC6 readthrough
RGS13	6003	regulator of G-protein signaling 13
RSPH9	221421	radial spoke head 9 homolog (Chlamydomonas)
GPNMB	10457	glycoprotein (transmembrane) nmb
PCNA	5111	proliferating cell nuclear antigen
RND1	27289	Rho family GTPase 1
TMEM189	387521	transmembrane protein 189
C20orf96	140680	chromosome 20 open reading frame 96
AVPI1	60370	arginine vasopressin-induced 1
THAP8	199745	THAP domain containing 8
LACTB	114294	lactamase, beta
FGF11	2256	fibroblast growth factor 11
ATP7A	538	ATPase, Cu++ transporting, alpha polypeptide
NIM1	167359	serine/threonine-protein kinase NIM1
INHBA	3624	inhibin, beta A
HIST1H2AI	8329	histone cluster 1, H2ai
RBP4	5950	retinol binding protein 4, plasma
C6orf170	221322	chromosome 6 open reading frame 170
HIST1H2AC	8334	histone cluster 1, H2ac
TGM2	7052	transglutaminase 2 (C polypeptide, protein-glutamine-gamma-glutamyltransferase)
QSOX1	5768	quiescin Q6 sulfhydryl oxidase 1
TKTL1	8277	transketolase-like 1
SERTAD1	29950	SERTA domain containing 1
PDLIM7	9260	PDZ and LIM domain 7 (enigma)
NPTX1	4884	neuronal pentraxin I
AGRN	375790	agrin
COL7A1	1294	collagen, type VII, alpha 1
WBP5	51186	WW domain binding protein 5
CIRBP	1153	cold inducible RNA binding protein
SLC5A6	8884	solute carrier family 5 (sodium-dependent vitamin transporter), member 6
HIST1H2AL	8332	histone cluster 1, H2al
ADM	133	adrenomedullin
IGF2	3481	insulin-like growth factor 2 (somatomedin A)
PGF	5228	placental growth factor
PDK4	5166	pyruvate dehydrogenase kinase, isozyme 4
PLA2G7	7941	phospholipase A2, group VII (platelet-activating factor acetylhydrolase, plasma)
SPP1	6696	secreted phosphoprotein 1
ZNF697	90874	zinc finger protein 697
HIST1H2AM	8336	histone cluster 1, H2am
TP53INP2	58476	tumor protein p53 inducible nuclear protein 2
S100A11	6282	S100 calcium binding protein A11
HTRA1	5654	HtrA serine peptidase 1
DFNA5	1687	deafness, autosomal dominant 5
EFNA3	1944	ephrin-A3
FOXR1	283150	forkhead box R1
INPP1	3628	inositol polyphosphate-1-phosphatase
SLC25A19	60386	solute carrier family 25 (mitochondrial thiamine pyrophosphate carrier), member 19
ADAMDEC1	27299	ADAM-like, decysin 1
EGLN3	112399	egl nine homolog 3 (C. elegans)

ENO2	2026	enolase 2 (gamma, neuronal)
RAB17	64284	RAB17, member RAS oncogene family
ARL8B	55207	ADP-ribosylation factor-like 8B
GPX3	2878	glutathione peroxidase 3 (plasma)
MATN1	4146	matrilin 1, cartilage matrix protein
ADAMTSL4	54507	ADAMTS-like 4
WDR54	84058	WD repeat domain 54
ANXA5	308	annexin A5
FGF5	2250	fibroblast growth factor 5
PLAT	5327	plasminogen activator, tissue
LYPD3	27076	LY6/PLAUR domain containing 3
METTL12	751071	methyltransferase like 12
VMO1	284013	vitelline membrane outer layer 1 homolog (chicken)
ITGBL1	9358	integrin, beta-like 1 (with EGF-like repeat domains)
GATA4	2626	GATA binding protein 4
SERAC1	84947	serine active site containing 1
GNA15	2769	guanine nucleotide binding protein (G protein), alpha 15 (Gq class)
COL16A1	1307	collagen, type XVI, alpha 1
SIX3	6496	SIX homeobox 3
IER5L	389792	immediate early response 5-like
MICALL2	79778	MICAL-like 2
ZNF808	388558	zinc finger protein 808
CD109	135228	CD109 molecule
SFTPA1	653509	surfactant protein A1
IL18BP	10068	interleukin 18 binding protein
GSTT2B	653689	glutathione S-transferase theta 2B (gene/pseudogene)
FCAR	2204	Fc fragment of IgA, receptor for
RAB13	5872	RAB13, member RAS oncogene family
FN1	2335	fibronectin 1
CLLU1OS	574016	chronic lymphocytic leukemia up-regulated 1 opposite strand
DHRS9	10170	dehydrogenase/reductase (SDR family) member 9
GADD45B	4616	growth arrest and DNA-damage-inducible, beta
PLIN5	440503	perilipin 5
SLC26A6	65010	solute carrier family 26, member 6
EIF4A3	9775	eukaryotic translation initiation factor 4A3
DPCD	25911	deleted in primary ciliary dyskinesia homolog (mouse)
RFX2	5990	regulatory factor X, 2 (influences HLA class II expression)
PRSS37	136242	protease, serine, 37
SLAMF9	89886	SLAM family member 9
HPSE	10855	heparanase
UBE2V1	7335	ubiquitin-conjugating enzyme E2 variant 1
EPPIN	57119	epididymal peptidase inhibitor
TPI1	7167	triosephosphate isomerase 1
PROC	5624	protein C (inactivator of coagulation factors Va and VIIIa)
EGFL7	51162	EGF-like-domain, multiple 7
DEFB128	245939	defensin, beta 128
PLXNB3	5365	plexin B3
ATF5	22809	activating transcription factor 5
ANGPT4	51378	angiopoietin 4
TGM5	9333	transglutaminase 5
ANG1	7556	Angiogenin
MOB3B	79817	MOB kinase activator 3B
MMP9	4318	matrix metallopeptidase 9 (gelatinase B, 92kDa gelatinase, 92kDa type IV collagenase)
WDR74	54663	WD repeat domain 74

TFPI	7035	tissue factor pathway inhibitor (lipoprotein-associated coagulation inhibitor)
ST8SIA4	7903	ST8 alpha-N-acetyl-neuraminide alpha-2,8-sialyltransferase 4
SCUBE1	80274	signal peptide, CUB domain, EGF-like 1
C3	718	complement component 3
NOL3	8996	nucleolar protein 3 (apoptosis repressor with CARD domain)
PLXNA3	55558	plexin A3

The list was generated by positive selection of up-regulated genes in irradiated PBMC with SignalP and SecretomeP analysis followed by negative selection with TMHMM analyisis excluding proteins with transmembrane helices.

Supplementary Table 3: 179 Up-regulated transcripts in **non-irradiated** PBMC coding for secretory proteins

Gene Symbol	EntrezGene	Gene Name
HIST1H2AD	3013	histone cluster 1, H2ad
C1orf151-NBL1	100532736	C1orf151-NBL1 readthrough
IDS	3423	iduronate 2-sulfatase
UFSP2	55325	UFM1-specific peptidase 2
ZNF143	7702	zinc finger protein 143
TUBE1	51175	tubulin, epsilon 1
NXPH4	11247	neurexophilin 4
AGXT2L2	85007	alanine-glyoxylate aminotransferase 2-like 2
P4HA1	5033	prolyl 4-hydroxylase, alpha polypeptide I
TTC9C	283237	tetratricopeptide repeat domain 9C
SUPV3L1	6832	suppressor of var1, 3-like 1 (S. cerevisiae)
SDS	10993	serine dehydratase
VPS37A	137492	vacuolar protein sorting 37 homolog A (S. cerevisiae)
HIST1H2AK	8330	histone cluster 1, H2ak
VASH2	79805	vasohibin 2
PPM1K	152926	protein phosphatase, Mg2+/Mn2+ dependent, 1K
RSPRY1	89970	ring finger and SPRY domain containing 1
PHRF1	57661	PHD and ring finger domains 1
AHRR	57491	aryl-hydrocarbon receptor repressor
EPAS1	2034	endothelial PAS domain protein 1
XPA	7507	xeroderma pigmentosum, complementation group A
IVNS1ABP	10625	influenza virus NS1A binding protein
SPOCK2	9806	sparc/osteonectin, cwcv and kazal-like domains proteoglycan (testican) 2
IL4R	3566	interleukin 4 receptor
ZNF250	58500	zinc finger protein 250
ALCAM	214	activated leukocyte cell adhesion molecule
N4BP2L1	90634	NEDD4 binding protein 2-like 1
IL24	11009	interleukin 24
ZNF563	147837	zinc finger protein 563
WDFY2	115825	WD repeat and FYVE domain containing 2
KRTAP4-8	728224	keratin associated protein 4-8
MAP1LC3A	84557	microtubule-associated protein 1 light chain 3 alpha
B3GALNT2	148789	beta-1,3-N-acetylgalactosaminyltransferase 2
LPO	4025	lactoperoxidase
RPL28	6158	ribosomal protein L28
SRSF1	6426	serine/arginine-rich splicing factor 1
C15orf53	400359	chromosome 15 open reading frame 53
P4HA2	8974	prolyl 4-hydroxylase, alpha polypeptide II
NUP43	348995	nucleoporin 43kDa
CHORDC1	26973	cysteine and histidine-rich domain (CHORD) containing 1
SNED1	25992	sushi, nidogen and EGF-like domains 1
SP140	11262	SP140 nuclear body protein
VENTX	27287	VENT homeobox
FEZ1	9638	fasciculation and elongation protein zeta 1 (zygin I)
EBLN2	55096	endogenous Bornavirus-like nucleoprotein 2
FAM115C	285966	family with sequence similarity 115, member C
PDK1	5163	pyruvate dehydrogenase kinase, isozyme 1
ACAN	176	aggrecan
APOL4	80832	apolipoprotein L, 4
RELB	5971	v-rel reticuloendotheliosis viral oncogene homolog B
RCOR1	23186	REST corepressor 1

ETV6	2120	ets variant 6
ACTRT3	84517	actin-related protein T3
PPP1R16B	26051	protein phosphatase 1, regulatory subunit 16B
KIF3A	11127	kinesin family member 3A
SEC24A	10802	SEC24 family, member A (S. cerevisiae)
DOCK9	23348	dedicator of cytokinesis 9
ZBTB25	7597	zinc finger and BTB domain containing 25
TBX6	6911	T-box 6
TCP1	6950	t-complex 1
NBL1	4681	neuroblastoma, suppression of tumorigenicity 1
AK2	204	adenylate kinase 2
THAP6	152815	THAP domain containing 6
FST	10468	follistatin
YPEL4	219539	yippee-like 4 (Drosophila)
YPEL5	51646	yippee-like 5 (Drosophila)
SERPINH1	871	serpin peptidase inhibitor, clade H (heat shock protein 47), member 1, (collagen binding protein 1)
ARPP19	10776	cAMP-regulated phosphoprotein, 19kDa
ZNF230	7773	zinc finger protein 230
PHF20L1	51105	PHD finger protein 20-like 1
SMAD7	4092	SMAD family member 7
RNF145	153830	ring finger protein 145
GK	2710	glycerol kinase
HIST1H2AG	8969	histone cluster 1, H2ag
CMSS1	84319	cms1 ribosomal small subunit homolog (yeast)
MTMR1	8776	myotubularin related protein 1
RNASET2	8635	ribonuclease T2
CHD1	1105	chromodomain helicase DNA binding protein 1
HSPB11	51668	heat shock protein family B (small), member 11
CACYBP	27101	calcyclin binding protein
ERO1L	30001	ERO1-like (S. cerevisiae)
LEP	3952	leptin
RAB8B	51762	RAB8B, member RAS oncogene family
KLHL28	54813	kelch-like 28 (Drosophila)
SDCBP2	27111	syndecan binding protein (syntenin) 2
ZFP42	132625	zinc finger protein 42 homolog (mouse)
C4orf47	441054	chromosome 4 open reading frame 47
FUT11	170384	fucosyltransferase 11 (alpha (1,3) fucosyltransferase)
CHM	1121	choroideremia (Rab escort protein 1)
CHKA	1119	choline kinase alpha
DNAJB4	11080	DnaJ (Hsp40) homolog, subfamily B, member 4
GPNMB	10457	glycoprotein (transmembrane) nmb
C1orf74	148304	chromosome 1 open reading frame 74
NDRG4	65009	NDRG family member 4
LRP5L	91355	low density lipoprotein receptor-related protein 5-like
BAGE	574	B melanoma antigen
KRAS	3845	v-Ki-ras2 Kirsten rat sarcoma viral oncogene homolog
JHDM1D	80853	jumonji C domain containing histone demethylase 1 homolog D (S. cerevisiae)
ATP7A	538	ATPase, Cu++ transporting, alpha polypeptide
HIST1H2AI	8329	histone cluster 1, H2ai
INHBA	3624	inhibin, beta A
CSH1	1442	chorionic somatomammotropin hormone 1 (placental lactogen)
HIST1H2AC	8334	histone cluster 1, H2ac
KIAA1147	57189	KIAA1147
TKTL1	8277	transketolase-like 1

COL7A1	1294	collagen, type VII, alpha 1
PHLDB3	653583	pleckstrin homology-like domain, family B, member 3
RAB33A	9363	RAB33A, member RAS oncogene family
WBP5	51186	WW domain binding protein 5
JAG1	182	jagged 1
HIST1H2AL	8332	histone cluster 1, H2al
ADAMTS17	170691	ADAM metallopeptidase with thrombospondin type 1 motif, 17
ZNF616	90317	zinc finger protein 616
TRH	7200	thyrotropin-releasing hormone
SPP1	6696	secreted phosphoprotein 1
PASK	23178	PAS domain containing serine/threonine kinase
TSC1	7248	tuberous sclerosis 1
SENP2	59343	SUMO1/sentrin/SMT3 specific peptidase 2
ZNF562	54811	zinc finger protein 562
LPXN	9404	leupaxin
CBFA2T2	9139	core-binding factor, runt domain, alpha subunit 2; translocated to, 2
HIST1H2AM	8336	histone cluster 1, H2am
SERPINA1	5265	serpin peptidase inhibitor, clade A (alpha-1 antiproteinase, antitrypsin), member 1
GMNN	51053	geminin, DNA replication inhibitor
CTSL1	1514	cathepsin L1
CNOT2	4848	CCR4-NOT transcription complex, subunit 2
POLR2M	81488	polymerase (RNA) II (DNA directed) polypeptide M
ENO2	2026	enolase 2 (gamma, neuronal)
RAB17	64284	RAB17, member RAS oncogene family
SAR1B	51128	SAR1 homolog B (S. cerevisiae)
OXSM	54995	3-oxoacyl-ACP synthase, mitochondrial
CSH2	1443	chorionic somatomammotropin hormone 2
AK4	205	adenylate kinase 4
GFPT2	9945	glutamine-fructose-6-phosphate transaminase 2
FAM131A	131408	family with sequence similarity 131, member A
CWC25	54883	CWC25 spliceosome-associated protein homolog (S. cerevisiae)
LOH12CR1	118426	loss of heterozygosity, 12, chromosomal region 1
C1orf21	81563	chromosome 1 open reading frame 21
CAMK2N2	94032	calcium/calmodulin-dependent protein kinase II inhibitor 2
CD109	135228	CD109 molecule
NDRG1	10397	N-myc downstream regulated 1
RGCC	28984	regulator of cell cycle
GFI1	2672	growth factor independent 1 transcription repressor
ZCCHC18	644353	zinc finger, CCHC domain containing 18
KDM2B	84678	lysine (K)-specific demethylase 2B
CCDC47	57003	coiled-coil domain containing 47
UBR2	23304	ubiquitin protein ligase E3 component n-recognin 2
PLIN5	440503	perilipin 5
RAPH1	65059	Ras association (RalGDS/AF-6) and pleckstrin homology domains 1
CCNH	902	cyclin H
NSUN4	387338	NOP2/Sun domain family, member 4
HSP90AA1	3320	heat shock protein 90kDa alpha (cytosolic), class A member 1
AP3M2	10947	adaptor-related protein complex 3, mu 2 subunit
LOC100507855	100507855	adenylate kinase isoenzyme 4, mitochondrial-like
NAA30	122830	N(alpha)-acetyltransferase 30, NatC catalytic subunit
CYSTM1	84418	cysteine-rich transmembrane module containing 1
DNAJA4	55466	DnaJ (Hsp40) homolog, subfamily A, member 4
RSC1A1	6248	regulatory solute carrier protein, family 1, member 1
ST6GAL1	6480	ST6 beta-galactosamide alpha-2,6-sialyltranferase 1
CHTOP	26097	chromatin target of PRMT1

NR3C1	2908	nuclear receptor subfamily 3, group C, member 1 (glucocorticoid receptor)
PTPRC	5788	protein tyrosine phosphatase, receptor type, C
PLXNA3	55558	plexin A3
ANKRD37	353322	ankyrin repeat domain 37
CCNDBP1	23582	cyclin D-type binding-protein 1

The list was generated by positive selection of up-regulated genes in non-irradiated PBMC with SignalP and SecretomeP analysis followed by negative selection with TMHMM analyisis excluding proteins with transmembrane helices.

13 Materials and Methods

Ethics statement

This PhD thesis was in accordance with the requirements of the Ethics Committee of the Medical University of Vienna (Ethics Committee vote number: 1236; 2013) and conducted according to the principles of the Helsinki Declaration and Good Clinical Practice. Written informed consent was obtained from all volunteers.

Separation of human PBMCs for in vitro experiments

Human PBMCs were obtained from healthy male volunteers by venous blood withdrawal using heparin coated blood tubes. Immediately thereafter specimens were diluted 1:2 in Hanks balanced salt solution (HBBS, Lonza, Basel, Switzerland) and PBMCs were separated by Ficoll-Paque solution (GE Healthcare Bio-Sciences AB, Sweden) density gradient centrifugation: The specimens were centrifuged at 800g for 15 minutes at room temperature without braking. The uppermost plasma containing layer was discarded and the interphase, consisting of PBMCs, was transferred to a new tube. Thereafter, the cells were washed twice with HBSS, resuspended in CellGro serum-free medium (CellGenix, Freiburg, Germany) at a concentration of 25×10^6 cells/ml, and incubated in a humidified atmosphere (5% CO2 and 37°C). A Sysmex automated cell counter (Sysmex Inc., USA) was used to quantify cell numbers.

Induction of apoptosis

Apoptosis of PBMCs was induced by Caesium-137 gamma irradiation with 60 Grey (Gy). The non-irradiated and irradiated PBMCs from the same volunteer were then cultured for 2h, 4h, and 20 hours, after which time the PBMC suspensions were centrifuged for 9 minutes with 500g to remove cell debris, and cells or supernatant were used for further experiments.

Generation of viral cleared secretome

Supernatants were produced as described above. After obtaining the supernatant, methylene blue (MB) plus light treatment was performed using the Theraflex MB-Plasma bag system (REF SDV 0001XQ) and an LED-based illumination device (MacoTronic B2, MacoPharma). Light energy was supervised and was set at 120 J/cm2. Each bag system contained 85mg MB (0.8 – 1.2 nM per unit) that was released after injection of the supernatant. Blueflex filtration was used to remove photoproducts and MB. After lyophilisation, the cell culture supernatant was gamma irradiated with a Mediscan (Gammatron 1500, Mediscan, Seibersdorf, Austria). Cobalt 60 was used to generate gamma rays. To achieve a homogeneously distributed irradiation dose the PBMC secretomes were seeded in metal sterilization boxes that move in a meandering path through the irradiation vault around the

irradiation source in five layers. Polymethly methacrylate (PMMA) dosimeters were used to validate the irradiation dose (25,000 Gy after 23 hours of irradiation).

RNA isolation

Total RNA was separated from 25×10^6 cultured cells/ml immediately after PBMC separation, at 2 hours, 4 hours and 20 hours after irradiation.

In total 28 samples were obtained from four different donors. RNA was isolated using Trizol® Reagent (Invitrogen, Carlsbad, CA) according to the manufacturer´s instructions. A NanoDrop-1000 spectrophotometer (Peglab, Erlangen, Germany) was used for RNA quantification and an Agilent 2100 Bioanalyzer (Agilent, Böblingen, Germany) was used to evaluate RNA quality. The RNA integrity score ranking of all samples was between 5.7 to 10.

Microarray hybridization

Agilent Whole Human Genome Oligo Microarray (8x60K; G4851A; #028004; Agilent Technologies) and Agilent Human miRNA Microarray Kit (8x60K; G4872A; #031181) were used from mRNA and miRNA expression profiling according to the manufacturers' instructions.

Gene expression data are available on the Gene Expression Omnibus (GEO) website (http://www.ncbi.nlm.nih.gov/geo/) under accession number GEO: GSE55955.

Bioinformatics analysis GeneSpring v.11 was used for analyzing gene expression data. Background-corrected fluorescence intensity values were log2-transformed and normalized by quantile normalization. To reduce the number of false positive results a filtering step was applied and only genes above the 40th percentile of the percentile of the average expression of all samples in one condition (non-irradiated vs. irradiated) were used for further analysis. "Filter on Flags" was used for miRNA data processing using default parameters in GeneSpring. In total 241 miRNAs were used for miRNA analysis based on these filtering methods.

A paired t-test in GeneSpring was used to identify differentially expressed RNAs. The Benjamini-Hochberg adjustment procedure was used to correct the p-values for multiplicity testing. Genes with an adjusted p-value <0.05 and an false discovery rate (FDR) <5% were considered significant.

Functional analysis of differentially expressed genes

In order to identify the biological function of differentially expressed genes we categorized their function using the WEB-based Gene Stet Analysis Toolkit (WebGestalt) database. WebGestalt tests whether gene-ontology (GO) terms or canonical pathway annotations in a

given gene list are overrepresented compared to all expected distributions. The Kyoto Encyclopedia of Genes and Genomes (KEGG) annotation database was used for the identification of canonical pathways.

The remaining p-values were corrected using the Benjamini-Hochberg method for multiple testing with a significance level of p≤0.05 and FDR < 5%.

Secretory protein identification

The bioinformatics tools SecretomeP 2.0, SignalP 4.1 and TMHMM 2.0 were used to identify genes that encode secreted proteins. SecretomeP 2.0 and SignalP 4.1 predict the presence and location of signal peptide cleavage sites in amino acid sequences and whether genes are secreted by a classical or non-classical secretory pathway. On the other hand TMHMM 2.0 identifies transmembrane helices in proteins based on a hidden Markov model. Proteins containing transmembrane helices are less likely to be secreted and were therefore excluded for further analysis. The TMHMM tool thereby discriminates between secreted and membrane anchored proteins with a high precision. In this PhD thesis we used a combination of these three bioinformatics programs to identify genes that encode secretory proteins.

Clustering

A Euclidean distance metric and complete average-linkage clustering was used for hierarchic clustering of differentially expressed genes.

Visualization of protein-protein interactions

Interactions between different proteins were visualized using the web based tool STRING v9.1 1 (Search Tool for the Retrieval of Interacting Genes/Proteins) using default parameters.

Predicting miRNA binding sides

The Sylamer tool was used to identify miRNA binding site differences in the 3'UTRs of differentially expressed mRNAs. This program enables the identification of miRNA that might be involved in the regulation of gene expression alterations in large sets of mRNAs.

mRNA – miRNA – transcription factor interaction analysis

In order to identify differentially expressed mRNAs and miRNAs, we calculated mRNA-miRNA-TF networks using the Magia2 tool. This tool detects negatively correlated mRNA-miRNA pairs (e.g. down regulated miRNA and up regulated mRNA target). The TargetScan miRNA target prediction algorithm was used with default parameters. Due to the small sample size the non-parametric Spearman correlation coefficient was applied.

Secreted factor prediction

To identify transcripts that encode secreted proteins, we used three web-based programs: SecretomeP 2.0, SignalP 4.1, and TMHMM 2.0. The SignalP program predicts the presence and location of signal peptide cleavage sites in amino acid sequences. Based on this information, a specific threshold (D-cutoff score ≥0.45) is generated which identifies secretory proteins. SecretomeP predicts whether a protein is secreted via a non-classical pathway, based on post-translational information obtained from different protein prediction servers. TMHMM 2.0 predicts transmembrane helices in proteins, based on a hidden Markov model. This method discriminates between soluble and membrane bound proteins

Transcription factor binding site analysis

Transcription factor binding site (TFBS) analysis was performed using the freely available oPOSSUM3.0 tool (http://opossum.cisreg.ca/oPOSSUM3). oPOSSUM3 tests whether TFBS are enriched in a given gene list. We used the single site analysis mode and restricted analysis for upstream TFBS up to 2000 bp.

Quantitative reverse transcriptase PCR (qPCR) analysis of mRNA

cDNA synthesis of RNA samples was performed using the IScriptc DNA synthesis kit (BioRad, Hercules, USA) according to the manufacturer´s protocol. The single-stranded cDNA was finally diluted 1:3 with distilled water for qPCR analysis. The expression of mRNA was quantified by qPCR using Light Cycler Fast Start DNA Master SYBR Green I (Roche Applied Science, Penzberg, Germany) according to the manufacturer's protocol.

The PCR cycle conditions were set as follows: 10 minutes pre-incubation with 95°C, followed by 55 cycles, with each cycle including 10 seconds at 95°C. I have never come across a PCR protocol like this. Did you not have annealing and extension temperatures as well? Relative quantification was performed with Light Cycler Software 1.5.0 (Roche Applied Science) based on crossing point (Cp) values. The Cp values denote the cycle number at which the fluorescence signal of the sample exceeds a background florescence value.

The primer pairs were designed as described previously by Pfaffl et al. and synthesized by Microsynth AG (Vienna, Austria). The specificity of the PCR products was confirmed by sequencing. The relative expression of target genes was compared to the housekeeping gene beta-2-microglobulin using a formula described by Pfaffl et al.

qPCR analysis of miRNA

A TaqMan® MicroRNA Assay Kit was used for miRNA expression validation analysis. The experiments were performed according to the manufacturer's instructions. The miRNA miR-RNU44 served as an internal control. The relative expression values were calculated using the formula described by Pfaff et al. Please check the spelling of this person's name.

ELISA and membrane array

An apoptosis antibody membrane-array (Proteom Profiler Arrays, R&D Systems, Minneapolis USA) was used to quantify the amount of 35 apoptosis related proteins in the cell lysates of irradiated and non-irradiated PBMCs at 20 hours after irradiation. The experiments were performed according to the manufacturer's instructions. BioRad Image Lab software was used for semi-quantitative analysis of the protein concentrations.

Cell culture supernatants of irradiated and non-irradiated PBMCs, or keratinocytes and fibroblasts were analyzed using the following commercially available enzyme-linked immunosorbent assays (ELISA): IL-16, angiogenin, CXCL1, CXCL8, CXCL13, PDGF-AA, PDGF-BB (Duoset, R&D Systems, Minneapolis, USA), complement C3, thrombospondin-1, neuropilin, and adrenomedullin (BG Bluegene Biotech). All reactions were carried out in ninety-six-well plates (Nunc Maxisorp plates, Nunc GmbH & Co. KG, Germany) at room temperature. The wells for both samples and standards were coated with capture antibodies and incubated over-night in the dark. They were subsequently blocked with 1% bovine serum albumin for 2 hours, washed twice with PBS, and incubated with a biotin-labelled antibody for two hours. The wells were then washed, and a streptavidin-horseradish peroxidase enzyme complex was added for 15 minutes. Tetramethylbenzidine substrate solution (TMB; Sigma Aldrich, USA) was used to produce a color reaction, which was stopped by adding 1N sulphuric acid (Merck, Germany). Optical density values were quantified at 450 nm on a Victor3 Multilabel plate reader, PerkinElmer, USA.

Western blot analysis

For Western blot analysis, 10^6 PBMCs were lysed in SDS–PAGE loading buffer, sonicated, centrifuged, and denatured before loading. SDS–PAGE was performed on 8–18% gradient gels (GE Amersham Pharmacia Biotech, Uppsala, Sweden). The proteins were then electro-transferred onto nitrocellulose membranes (Bio-Rad, Hercules, CA, USA) and immunodetected using primary antibodies against p21(1 µg/ml; Abcam), p53 (1 µg/ml; Abcam, Cambridge, UK),), CRTR1 (also known as TFCP2L1; 2 µg/ml; Abcam), HLF (2 µg/ml; Abcam), SP1 (2 µg/ml; New England Biolabs, Beverly, MA, USA), ZFX (1 µg/ml; New England Biolabs and KLF4 (1 µg/ml; Abcam). Glyceraldehyde-3-phosphate dehydrogenase (GAPDH) served as the control protein (0.2 µg/ml; Biogenesis, Poole, UK). Chemi Glow reagent (Biozyme Laboratories Limited, South Wales, UK) was used for the chemiluminescence detection.

Microparticle isolation

PBMC suspensions were centrifuged at 500g for 9 min to separate the cells from the medium. The supernatant then was centrifuged at 3,500g for 15 min to remove cell debris.

The remaining cell culture supernatant was centrifuged at 20,000g for 20 min at 4°C to pellet microparticles. These were diluted in PBS and were either used directly or stored at -20°C.

Exosome purification

Irradiated and non-irradiated PBMCs were centrifuged for 2 minutes at 500g to separate cells and cell culture supernatant. The resulting 'conditioned medium' (CM) was centrifuged at 3,500g for 15 min to remove debris and again at 20,000g for 15 minutes to isolate microparticles. The remaining CM was filtered through 0.2 µm pore filters.

Two different exosome isolation methods were used: a total exosome isolation kit (Invitrogen, Carlsbad, CA) and an ultracentrifugation protocol to isolate exosomes. When using the total exosome isolation kit the 1ml CM was transferred into 2ml tubes and 0.5 ml of exosome isolation reagent was added to the CM. This solution was vortexted for 1 minute and then incubated at 4°C for 12 hours. Thereafter the tubes were centrifuged at 10,000g for 60 min at 4°C to pellet the exosomes.

For the ultracentrifuge protocol, 10 ml of microparticle-depleted cell culture supernatant was centrifuged at 4°C at 110,000g for 120 min in a SW41 swinging bucked ultracentrifuge (Beckman Coulter, Brea, California, USA). PBS was used to elute the exosome pellet and a **NanoSight, NS500 instrument was used to quantify the absolute number of exosomes.**

Silver staining

Exosomes isolated with the total exosome isolation kit were used for protein analysis in combination with anti-CD63 magnetic bead purification (Invitrogen, Carlsbad, CA) in order to obtain a highly enriched exosome population. Exosomes were lysed using SDS-PAGE lysis buffer, sonicated, and the remaining magnetic beads were removed with a magnet. 20 µg protein thus obtained were separated by PAGE and visualized with by silver staining. Three individual experiments with pooled exosomes from at least two individual donors were performed.

Lipid extraction and thin layer chromatography

Lipids were isolated from CM of non-irradiated and irradiated PBMCs using the chloroform/methanol (2:1) extraction method. The isolated lipids were either separated and visualized using thin layer chromatography or further purified for mass spectrometry.

Separation of biological components present in cell culture supernatant

For *in vitro* assays, the pooled cell culture supernatant from 4 donors was used to isolate lipids, proteins and extracellular vesicles. Proteins were precipitated with 30% v/v polyethylene glycol and thereafter centrifuged for 15 min at 20,000 *g* at 4°C. Aliquots of the

different biological components were stored at -80°C before being used for *in vitro* experiments.

In vitro stimulation assays

Human dermal fibroblasts (FBs) (Lonza) were grown in DMEM (Gibco, BRL, Gaithersburg USA), supplemented with 25 mM L-glutamine (Gibco), 10% fetal bovine serum and 1% penicillin/streptomycin (Gibco), while human primary keratinocytes (KCs) were cultured in KC-growth medium (KGM, Lonza). $3x10^6$ of both cell types were seeded in 12 well plates. After reaching 80% confluence, cells were washed once with PBS, then stimulated with unprocessed CM, proteins, lipids, microparticles or exosomes derived from (a) control medium cultivated without PBMCs, (b) CM from non-irradiated PBMCs, or (c) CM from irradiated PBMCs. The biological ingredients were diluted in either basal FB media or basal KC media. Each biological ingredient was then added to the FB and KC cell cultures. 6 hours thereafter the cells were washed once with PBS and RNA was obtained using RNAeasy kit (Qiagen, Hilden, Germany) according to the manufacturer´s instructions.

In vitro scratch assay

$3x10^5$ FBs or KCs were seeded in 6 well plates. After reaching 100% confluence, cells were scratched vertically and horizontally with a blue pipette-tip. Thereafter, cells were washed once with PBS. Photographs were taken from the scratched areas immediately after wounding (initial wound area) and at 18 hours and 48 hours thereafter.

Cells were stimulated with unprocessed CM, proteins, lipids, microparticles or exosomes derived from (a) control medium cultivated without PBMCs, (b) CM from non-irradiated PBMCs, or (c) CM from irradiated PBMCs. The biological ingredients were diluted in either basal FB media or basal KC media. Each biological ingredient was diluted to obtain the content equivalent to that derived from 2.5×10^6 PBMCs/ml. Wound closure was quantified with ImageJ 1.45 software (National Institutes of Health, Bethesda, MD, USA).

Transmission electron microscopy (TEM)

PBMCs were dehydrated in a graded ethanol series (50%, 70%, 90%, 96%, and twice in 100%) and embedded in Epon (Serva, Heidelberg, Germany). Ultrathin sections (80–100 nm) were cut using an UltraCut-UCT ultramicrotome (Leica Inc., Vienna, Austria), transferred to copper grids, and viewed either unstained or stained with 1% uranyl acetate and 5% lead citrate (Merck, Darmstadt, Germany) using an EM-900 TEM (Carl Zeiss, Oberkochen, Germany) at an acceleration voltage of 50 kV. Digital images were recorded using a wide-angle dual speed CCD camera (Albert Tröndle, Dünzelbach, Moorenweis, Germany).

Large animal AMI model

To test the biological activity of viral cleared secretomes of irradiated PBMCs a porcine closed chest reperfused AMI infarction model was chosen. This model simulates the clinical setting of human AMI with primary percutaneous coronary intervention by generating ischemia and reperfusion injury.

The experiments were performed at the Institute of Diagnostics and Oncoradiology, University of Kaposvar, Hungary and were approved by the University of Kaposvar (ethics vote: 246/002/SOM2006, MAB-28-2005).

In total, 17 adolescent pigs (female Large Whites; ~ 32kg) were anaesthetized with 1 mg/kg xylazine, 12 mg/kg ketamine hydrochloride and 0.04 mg/kg atropine. Pigs were thereafter intubated via the tracheal. Aneasthesia was maintained with a combination of isoflurane, O2 and N2O. Vascular access to the right femoral artery and the right femoral vein was performed and 6 Fr (French scale) and 7 Fr introduction sheaths were then inserted into artery and vein, respectively. 200 IU/kg heparin was administered and coronary angiography (using Ultravist contrast medium, Bayer Healthcare, Germany) was performed using a 6 Fr guiding catheter (Medtronic Inc., USA)

AMI was induced by inflation of a balloon catheter (diameter: 3 mm, length: 15 mm; Boston Scientific, USA) inside the LAD immediately after the descendent of the second major diagonal branch. The LAD occlusion was performed by inflating the balloon at 4-6 standard atmospheres (atm) and was validated by angiography. 40 minutes after occlusion, the lyophilized control medium CellGro Medium, Cell Genix, Germany), the viral cleared and non-viral cleared supernatants of $1*10^9$ irradiated human PBMCs reconstituted in 250 ml of 0,9% physiological sodium chloride solution was administered intravenously over 25 minutes. In addition, all animals received 100mg acetylsalicylic acid and 75 mg clopidogrel. 90 minutes after onset of ischemia the balloon was deflated and blood flow was reestablished. Control angiography was performed to rule out arterial injury

Functional imaging

A 1.5 T MR scanner (Avanto, Siemens, Germany) was used for ECG-triggered cardiac MRI imaging at 30 days after onset of ischemia. Gadolinium (0.05 mmol/kg) recoded 15 minutes after injection was used as contrast agent to determine necrotic myocardium. Mass 6.1.6 software (Medis, The Netherlands) was used for image analysis. End-diastolic and end-systolic volumes and left ventricular ejection fractions were calculated and the amount of myocardial infarction was expressed relative to the ventricular mass of the left ventricle. Data were analyzed by a blinded observer.

Statistical analysis

Statistical analysis was performed using GraphPad Prism4 software (GraphPad Software, La Jolla, CA, USA). Data distributions were tested with a Kolmogorow-Smirnow-Test. Comparisons between the two groups at a given time point were tested by a paired t-test or the non-parametric Wilcoxon signed-rank test. Data are expressed as mean ± standard deviation (SD) or displayed as box plots. A two-sided corrected p-value <0.05 was considered significant.

14 Discussion

14.1 General discussion

In this thesis, transcriptomic characteristics and paracrine factors released from non-irradiated and irradiated human PBMCs were examined. We were able to show that ionizing radiation induced time dependent changes in mRNA and miRNA expression. The construction of mRNA-miRNA-transcription factor interaction networks enabled us to identify regulatory networks in IR induced biological processes. Irradiated PBMCs released pro-angiogenic proteins, oxidized lipids and extracellular vesicles. Proteins and exosomes were identified as the two biologically active components that induce fibroblast and keratinocyte cell migration and activation. A viral cleared PBMC secretome displayed comparable biological potency to a non-processed supernatant, indicating that the biologically active components are resistant to external forces. Our findings add considerable information to the understanding of IR induced transcriptomic alterations in human PBMCs and the contribution of their paracrine factors to regenerative medicine.

Despite major advances in technical and pharmaceutical treatment approaches and changes in lifestyle, cardiovascular and neurodegenerative diseases result in considerable morbidity and mortality [205]. During the last two decades regenerative medicine has become an important topic in basic research as well as clinical practice, in order to develop alternative therapy strategies. Currently a broad spectrum of disease entities ranging from ischemic heart disease, blood disorders, immune disease, cancers, neoplasms, nervous system diseases and wounds has been described to be suitable for regenerative therapy. Ischemic heart disease especially has become a flagship model disease in the field of regenerative medicine. As previous treatment strategies have mainly focused on the restoration of early reperfusion of blood flow to hypoxic myocardium, little attention was paid to the central problem of injured myocardium that undergoes a remodeling process with subsequent loss of vital contractile cardiomyocytes. Patients displaying these non-contractile tissues are prone to develop heart failure, a major cause of mortality.

In order to attenuate the process of cardiomyocyte apoptosis and loss of functional tissue, cell based therapies were developed in cardiovascular medicine, including the application of stem cells from different sources. Whereas preclinical experiments showed promising results in the regeneration of injured tissue, clinical trials yielded mixed results, but indicated that stem cell therapy improves myocardial function and long-term survival [10, 206, 207]. Initially it was thought that direct cell-cell interaction and transformation of stem cells into local tissue cells was responsible for the effects seen. However, it is now commonly accepted that paracrine factors released by the transferred cells are responsible for large parts of the

effects observed [21, 22, 36]. For instance, Lichtenauer *et al* were able to show that paracrine factors from PBMCs attenuated myocardial infarction and improved cardiac function in a rodent model of AMI, as well as in a large animal model [41, 42].

Instead of stem cells, we used the more easily obtainable PBMCs to produce paracrine factors . The secretome of these cells was comparable to that of bone marrow derived cells [208], but to enhance paracrine activity we established a protocol to induce IR mediated apoptosis. Subsequent work further established that these paracrine factors secreted from apoptotic PBMCs inhibit platelet aggregation, thereby attenuating microvascular obstruction [38]. Hence CM of stressed PBMCs not only exerts direct cytoprotective effects on resident cells but also exerts systemic effects on circulating blood cells, indicating that pleiotropic factors might be involved in cell signaling. Similar to the effects seen in a model of acute and chronic myocardial infarction, the application of CM derived from apoptotic PBMCs ameliorated neurological function and attenuated tissue injury after ischemic stroke [139] and spinal cord injury (Haider et al. in preparation). Beside these effects in cardiovascular disease, Hötzenecker and colleagues showed that CM of stressed PBMCs is able to reduce myocardial inflammation in a murine model of autoimmune myocarditis, predominantly via the inhibition of CD4* T-cells. In a murine and porcine model of wound healing we showed that factors from stressed and non-stressed PBMCs enhance angiogenesis *in vitro* and *in vivo* and significantly improve wound healing [40].

While we had investigated the biological effects of these paracrine factors *in vitro* and *in vivo* in detail, several questions still remained unanswered. The effects of high dose IR on PBMC morphology and physiology were not known, the majority of biological components present in the CM of irradiated cells had not yet been discovered, and there was no study available that investigated the lipid and extracellular vesicles content in the supernatant of these cells. Furthermore, it remained unknown which biological components of the cell supernatant were responsible for the effects seen *in vitro* and *in vivo*.

We thus first focused on morphological changes occurring in PBMCs in response to high dose IR. IR induced several morphological changes that were typical for cells undergoing apoptosis [141, 147]: a shrunken nucleolus, chromatin condensation in the nucleus and dissolution of cell membranes with subsequent membrane bleb formation. Specialized markers for apoptosis and secondary necrosis were detectable on irradiated cells. In addition, the p53 signaling pathway was activated in irradiated PBMCs, an opbservation which is in line with previous data showing that p53 is a central regulatory hub, mediating IR induced biological processes [209, 210]. Using a membrane array, several other proteins besides p53 and p21, were found to be up regulated in irradiated samples. In particular, RAD17 was highly expressed in irradiated cells. RAD17 is a known cell cycle arrest and DNA

damage response protein that regulates DNA damage induced cell cycle arrest [211]. We also observed an activation of the caspase cascade, with an induction of cleaved caspase-3 and high concentrations of cleaved IL-16 in the supernatant of irradiated PBMCs. Pre-IL-16 is stored in the nucleus of monocytes and released upon cleavage of active caspase-3, thereby serving as a surrogate parameter for caspase-3 mediated apoptosis [212]. Based on these findings it must be assumed that caspase mediated apoptosis takes place in PBMCs after high dose IR. This is of special interest as a growing body of evidence suggests that caspase-3 signaling mediates the release of paracrine factors that exert pro-angiogenic and proliferative activity [62, 91, 213].

To further extend our knowledge on IR induced biological changes we performed transcriptomic analysis. Transcriptomics is a rapidly growing sector in modern research, based on sophisticated bioinformatics analysis to extract reliable information from large sets of genomic data. We designed an experimental setup that enabled us to generate a time dependent network containing mRNA, miRNA, and TF interactions in the same biological samples. In line with published data, irradiated PBMCs displayed a time dependent increase of differentially expressed mRNAs and miRNAs. As we suspected that cell cultivation itself would change transcriptomic expression, we compared gene expression of matched non-irradiated and irradiated samples from the same donor. Indeed, the PCA on the normalized data revealed that cell cultivation itself significantly altered gene expression, since all different experimental conditions were clearly separated from each other. Analysis of biological function of differentially expressed genes (DEGs) revealed an enrichment of up-regulated proteins associated with apoptosis and p53 signaling pathway at 2 hours after IR. While p53 was identified to be of central importance at this short time period after IR, several of its downstream targets were found up-regulated at 4 hours after IR. In addition, we showed that several targets of the caspase cascade, which are known to be key molecules in the induction of apoptosis, such as cytocrome c, were activated immediately after IR. Taken together, these data indicate that as early as 2 hours after IR two main executors of cell cycle arrest and apoptosis, namely p53 and cytochrome c, are activated, guiding the cells towards programmed cell death. This observation is explained by the fact that high dose IR is a strong inducer of clustered DNA lesions [214] and double strand breaks [215], both of which are activators of p53.

To further identify upstream modulatory elements that might be involved in IR induced cell signaling, we performed bioinformatics based transcription factor analysis. Putative TFs were identified based on their transcription factor binding sites in the set of up regulated genes. While at 2 hours after IR, only p53 was identified as an active TF, at 4 and 20 hours the TFs Klf4, SP1, Zfx and TFCP2L1 were predicted to be activated. These data are in line with the

current literature, since p53 is a known rapid response TF that itself activates further downstream TFs, such das SP1 or Klf4, which orchestrate the p53 induced signaling. p53 mediated Klf4 activation [216] enhances cell cycle arrest via phosphorylation of p21 and p27 [217]. In addition SP1 has recently been identified as a co-regulating binding factor of p53 that is needed for the pro-apoptotic gene repression of p53 [218].

Beside protein coding mRNA, we analyzed expression of small regulatory non-protein coding miRNAs in the same set of samples. During the last decade, miRNAs have gained a growing body of interest, because it has been shown that they are tinvolved in the regulation of nearly all biological processes. Whereas at 2 hours after IR no miRNA was differentially expressed, at 4 hours 7 miRNAs, and at 20 hours 177 miRNAs were found to be regulated by IR. As miRNAs are regulatory elements that mainly inhibit mRNA translation or even degrade mRNAs, an integrative analysis using mRNA-miRNA interaction data provides valuable data sets that could reveal the involvement of miRNA in the regulation of distinct biological processes. Here, we focused on mRNA and miRNA transcripts that were differentially expressed at 20 hours after irradiation. We identified several miRNAs that were involved in the regulation of the biological processes of the MAPK pathway [219] and regulation of apoptosis [220]. Further pathways such as the T-receptor signaling pathway and mRNA surveillance pathway were repressed by up regulated miRNAs. Interestingly we also observed an involvement of miRNAs in the regulation of cytoskeleton pathways, endocytosis, vesicle-mediated transport and signal transduction, which is in line with previous data [219]. Whereas the miRNAs were down regulated (e.g. miR-32, miR-92a, miR-200c or miR-301b) their target genes (myosin, actin, GATA2, SERPINE1) were up regulated. In the light of our subsequent extracellular vesicle analysis, in which we found that IR induces the release of small and large EVs, it might be speculated that miRNAs are involved in the regulation of EV formation due to the de-repression of endocytotic proteins.

Beside newly identified biological processes that might be regulated by miRNAs, we detected several miRNAs with known molecular functions involved in apoptotic processes. On the one hand, miRNAs can enhance apoptotic vulnerability, as has been shown for miR-9, let-7g [221], miR-100, miR-101, miR-181a, or miR-421 [219] which drive cells into programmed cell death. On the other hand, IR repressed expression of distinct miRNAs that exert proliferative and anti-apoptotic capacities, probably the most prominent being miR-21. In contrast, its targets p53, BAX, BCL2 and PTEN were up regulated [222]. As already mentioned, caspase-3 and p53 exert significant biological functions in the execution of IR mediated signaling. Our analysis revealed that miRNAs are involved in the regulation of both p53 and caspase-3. miR-378, a known repressor of caspase-3, was down regulated in irradiated PBMCs. In vitro studies have shown that overexpression of miR-378 in cardiomyocytes can inhibit hypoxia

mediated apoptosis, whereas inhibition of this miRNA induces apoptosis via caspse-3 dependent signaling [223]. In addition, apoptosis is controlled by members of the miR-30 cluster that repress caspase-3 [224] and p53 translation [225], modulate mitochondrial fusion and suppress TRAIL-mediated programmed cell death [226].

The mRNA-miRNA-TF network performed with computational modeling tools using differentially expressed mRNAs and miRNAs at 20 hours after irradiation was used to incorporate gene expression values with miRNA and TF target prediction models. This type of analysis is a novel method designed to detect more delicate interaction constructs than classic miRNA target prediction tools. Rather than focusing on relative expression values of single miRNAs or mRNAs this program combines absolute expression values with target prediction values derived from bioinformatics programs and large manually curated databases. We identified the TF hepatic leukemia factor (HLF) as a centrally repressed hub node that is targeted by several up-regulated miRNAs in response to IR. To our knowledge there is currently only one study describing an involvement of HLF as an anti-apoptotic factor. Over-expression of HLF attenuated programmed cell death of human keratinocytes via the transcriptional up-regulation of anti-apoptotic genes and inhibition of pro-apoptotic genes [227]. Bioinformatics analyses were validated using immunoblot analysis, which revealed a significant suppression of HLF at the protein level. In summary, we applied a new strategy to uncover central regulatory motives by constructing transcriptomic interaction networks.

Whereas in the first part of this study we focused exclusively on biological processes occurring in non-irradiated or irradiated PBMCs, in the second part of the study we evaluated paracrine factors released by PBMCs and their ability to induce cell migration and activation. A multi-methodical approach using bioinformatics based secretome analysis, high pressure liquid chromatography and extracellular vesicle analysis were used.

Previous studies have indicated that the secretome of mesenchymal stem cells is comparable to those of PBMCs [208]. Ankersmit et al [32] and Lichtenauer and colleagues [41] as well as other groups [44] confirmed that PBMCs are capable of secreting pleiotropic proteins, and that IR serves as an additional stimulus that activates protein release. In addition, several growth factors secreted by PBMCs (e.g. VEGF, CXCL1, CXCL8) have been described to exert beneficial effects in the field of regenerative medicine [21]. By using a bioinformatics based approach we selected highly expressed genes coding for secretory proteins that were either up-regulated in response IR or in response to *in vivo* cell cultivation. First we confirmed previous data showing that irradiated PBMCs express more genes coding for secretory proteins (213 proteins) than non-irradiated (167 proteins) PBMCs. Second, the secreted proteins of irradiated PBMCs were associated with biological processes of wound

healing, angiogenesis and regulation of leukocyte trafficking, which are all valuable targets in the field of regenerative medicine. Among these proteins, some are known pro-angiogenic factors, such as angiogenin, C3, GDF-15, ADM and neuropilin. Interestingly, no enrichment of comparable biological processes was seen in the non-irradiated PBMCs. These observations are in line with previous studies showing that initial stimulation of cells via irradiation [41], hypoxia [45] or small molecules [228] enhance the release of paracrine factors, and increases their biological efficacy.

We furthermore investigated the quantity and quality of lipids present in the CM. Lipids in the CM belong to a wide variety of different molecular classes displaying significant differences in their molecular structure and biological function. Using thin layer chromatography and high pressure liquid chromatography, we were able to show that especially cholesterol and cholesterol sulfate, but also phospholipids, cholesterol, free fatty acids and triglycerides were enriched in the CM of irradiated PBMCs compared to non-irradiated PBMCs. This phenomenon might be due to the presence of EVs (e.g. microparticles and exosomes) which contain higher amounts of cholesterol, sphingomyelin and phoshpolipids [120] than their donor cells. If we assume that irradiation induces apoptosis [204] that triggers the release of microparticles and exosomes, we should detect an enrichment of lipid classes that are typical for EVs in the CM of irradiated PBMCs. Therefore, the selective enrichment of cholesterol and cholesterol sulfate might be due to the higher amount of EVs in the CM of irradiated cells.

To further extend our analysis we performed high pressure lipid analysis, focusing on oxidized phospholipids. Oxidized phospholipids exert pleiotropic biological effects ranging from the induction of endothelial cell proliferation and angiogenesis [229], to the inhibition of inflammation via blocking of TLR signaling [230] and the oxidative burst in neutrophil granulocytes [231]. We observed that the CM of irradiated PBMCs contained higher concentrations of oxidized phosphatidylcholines in comparison to control CM. These data are in line with published data highlighting that IR generates oxidized molecular species of cardiolipin and phosphatidylserine [232, 233]. To further extend our knowledge on the biological effectiveness of these lipids, we performed *in vitro* assays assessing their ability to induce cell migration and activation of fibroblasts and keratinocytes. Contrary to our expectations, we did not observe any *in vitro* effects of purified lipids on fibroblasts and keratinocytes. Neither cell migration nor expression of CXLC1 and CXLCL8 was influenced by lipids in these *in vitro* assays. We propose two explanations for this observation. Firstly, in the *in vitro* assays only soluble lipids were used, whereas EV associated lipids were removed prior to lipid extraction. Therefore, we cannot exclude that lipids present in EVs might exert biological activity while the soluble lipids themselves do not. Secondly, the efficacy of some

lipids is closely related to their ability to interact with proteins [113]. Given that the method of lipid extraction destroys the interaction between lipids and proteins, one would assume that the biological effect is attenuated or even abolished. Furthermore, we currently cannot exclude that lipids of stressed PBMCs exert pro-angiogenic and proliferative effects on endothelial cells. Our results indicate that soluble lipids in the CM of PBMCs are not capable of inducing either fibroblast or keratinocyte migration, nor CXLC1 and CXLC8 expression. However, further *in vitro* assays or the isolation of lipids selectively from EVs will be necessary to elucidate the significance of lipids in the paracrine signaling of PBMCs.

As mentioned above, the CM not only contains soluble proteins and lipids but also EVs. EVs have gained growing interest in the research community as they have been shown to transfer biologically intact mRNAs, miRNAs proteins and lipids [117, 234] between cells, and are important effectors in the field of regenerative medicine [45]. EVs can be separated based on their sedimentation characteristic during centrifugation. In our study we focused on exosomes and MPs, whereas apoptotic bodies were not evaluated. By using FACS analysis, we were able to show that irradiated PBMCs released higher number of MPs in comparison to non-irradiated PBMCs. This is in line with previous studies showing that apoptosis triggers formation and release of MPs [235]. In addition, we were able to show that IR promotes the generation and release of exosomes in human PBMCs. NanoSight analysis as well as protein quantification revealed that the CM of irradiated PBMCs contained ~2 times higher numbers of exosomes in comparison to non-irradiated PBMCs CM. We speculate that the IR induced activation of p53 and caspase-3 [204] stimulates the release of exosomes. Gamma irradiation has been shown to increase the abundance of exosomes released by primary cells and a tumor cell line [66]. These exosomes display significantly enhanced chemotactic potential compared to exosomes derived from non-irradiated cells [66]. In addition, Lehmann et al. showed that irradiated human prostate cancer cells release eosomes in a p53 dependent manner [126]. Apoptotic endothelial cells release vesicles that exert anti-apoptotic activity in smooth muscle cells in a caspase-3 dependent manner, highlighting the connection between programmed cell death and EV release [125]. Beside an enhanced release of exosomes, we also observed an altered protein composition of exosomes derived from irradiated PMBCs. These observations are in line with those of Arscott *et al.* who described an altered protein expression in exosomes derived from irradiated cells. Proteomic analysis of these exosomal proteins revealed an involvement in biological processes of cell migration and proliferation [66]. We speculate that IR triggers the release of exosomes that have an improved capacity to induce regenerative processes. This hypothesis in indirectly supported by other groups who have been shown that exosomes derived from hypoxic cells induce endothelial cell migration, vasculogenesis [236] and HUVEC tube formation [237].

In 2013 Mildner *et al* demonstrated that CM of PBMCs induces fibroblast and keratinocyte cell migration, endothelial cell proliferation and enhances wound closure in human primary cells and in a murine full thickness wound model. We decided to use comparable *in vitro* assays in order to test the different fractions of the CM in terms of their biological efficiency. FB and KC migration assays revealed that the complete CM as well as the protein fraction and exosomes induce cell migration. In addition, the same components enhanced expression of CXCL1 and CXLC8, key mediators of angiogenesis and wound healing, [238]. in FB and KC. On the other hand, MPs and lipids did not induce cell migration or cytokine release in the two cell types investigated. Based on these observations, we deduced that exosomes and proteins are the most promising components for further research in the field of regenerative medicine, and in fact, they are already the most commonly investigated components of CM. Their effects have been studied in preclinical [63] as well as in clinical studies [239].

The application of biological material in clinical research has several legal requirements and restrictions. It must be proved that the material is handled without any non-sterile contact in a clean room. Furthermore, potency assays are required, which should ensure that the final material is effective, and no errors occurred during the generation process. While autologous biological material (e.g. cells, cell culture supernatant) can be used without strict requirements, there are stringent criteria that must be fulfilled for the testing of allogenic material. Probably the most crucial step is to introduce pathogen reducing production-steps in the experimental workflow. Pathogen reduction requires two independent methods (namely ionizing radiation and methylene-blue incorporation), that are proven to reduce pathogens. These steps aim to guarantee that transmission of pathogens (e.g. virus, bacteria) between study subjects is prevented.

In this study we implemented a workflow that is in line with the above mentioned criteria (according to GMP guidelines) and enabled us to generate CM that could be used for clinical trials. In order to ensure the comparability of components present in the unprocessed CM that is routinely used for preclinical research, and the CM which can be used in clinical studies, all experiments were performed with both preparations. Protein and lipid analyses revealed that the unprocessed and processed CM of irradiated PBMCs is comparable in terms of protein and lipid quantity and quality. However, processed CM contains fewer MPs compared to unprocessed CM. During the process of pathogen reduction CM is passed through 0.22 µm pore filters that exclude all particles with a diameter >0.22 µm. In contrast, smaller EVs such as exosomes pass through these filters and can be found in the processed CM, although their absolute numbers tend to be reduced.

To further investigate whether the process of pathogen reduction attenuates the biological efficacy we performed *in vivo* experiments. This question is of major importance as the application of CM in clinical trials is restricted to products undergoing viral clearance steps. Given that the biologically active component is relatively unstable it might be that the process of viral clearance inactivates it and any further clinical evaluation will fail.

To rule out the possibility that viral clearance attenuates the biological activity of CM from irradiated PBMCs, we decided to use an experimental porcine model of closed chest AMI. Lichtenauer *et al.* had shown that the application of CM from stressed PBMCs attenuates ventricular remodeling and improves functional parameters at 3 weeks after injury [42]. In the current study the same experimental design as published in 2011 was applied. Following AMI, pigs either received unprocessed or viral cleared, GMP CM. Both groups showed comparable improvements in cardiac function and prevented ventricular remodeling at three weeks after ischemia compared to controls. There were no differences in any of the outcome parameters measured, indicating that pathogen reduction does not affect the biological efficacy. To our knowledge this is the first study showing that viral cleared conditioned media attenuates myocardial damage and ventricular remodeling following AMI. We conclude that the viral cleared PBMC secretome can be considered as a feasible option in clinical trials which must meet the requirements of regulatory authorities.

14.2 Conclusion and outlook

In conclusion, this thesis provides additional data on the transcriptional changes of human peripheral blood mononuclear cells after high dose ionizing radiation, as well as on their paracrine factors. We were able to show that exosomes and proteins released by PBMCs display pro-angiogenic capacities. Further studies are warranted to investigate the molecular mechanisms by which these factors exert their biological effects.

15 References

1.   Fisher MB, Mauck RL: **Tissue engineering and regenerative medicine: recent innovations and the transition to translation**. *Tissue Eng Part B Rev* 2013, **19**(1):1-13.

2.   WHO: **The top 10 causes of death**. *http://wwwwhoint/mediacentre/factsheets/fs310/en/* 2012.

3.   Beltrami AP, Urbanek K, Kajstura J, Yan SM, Finato N, Bussani R, Nadal-Ginard B, Silvestri F, Leri A, Beltrami CA *et al*: **Evidence that human cardiac myocytes divide after myocardial infarction**. *N Engl J Med* 2001, **344**(23):1750-1757.

4.   Laflamme MA, Myerson D, Saffitz JE, Murry CE: **Evidence for cardiomyocyte repopulation by extracardiac progenitors in transplanted human hearts**. *Circ Res* 2002, **90**(6):634-640.

5.   Laflamme MA, Murry CE: **Regenerating the heart**. *Nat Biotechnol* 2005, **23**(7):845-856.

6.   Assmus B, Schachinger V, Teupe C, Britten M, Lehmann R, Dobert N, Grunwald F, Aicher A, Urbich C, Martin H *et al*: **Transplantation of Progenitor Cells and Regeneration Enhancement in Acute Myocardial Infarction (TOPCARE-AMI)**. *Circulation* 2002, **106**(24):3009-3017.

7.   Strauer BE, Brehm M, Zeus T, Kostering M, Hernandez A, Sorg RV, Kogler G, Wernet P: **Repair of infarcted myocardium by autologous intracoronary mononuclear bone marrow cell transplantation in humans**. *Circulation* 2002, **106**(15):1913-1918.

8.   Wollert KC, Meyer GP, Lotz J, Ringes-Lichtenberg S, Lippolt P, Breidenbach C, Fichtner S, Korte T, Hornig B, Messinger D *et al*: **Intracoronary autologous bone-marrow cell transfer after myocardial infarction: the BOOST randomised controlled clinical trial**. *Lancet* 2004, **364**(9429):141-148.

9.   Abdel-Latif A, Bolli R, Tleyjeh IM, Montori VM, Perin EC, Hornung CA, Zuba-Surma EK, Al-Mallah M, Dawn B: **Adult bone marrow-derived cells for cardiac repair: a systematic review and meta-analysis**. *Arch Intern Med* 2007, **167**(10):989-997.

10.   Jeevanantham V, Butler M, Saad A, Abdel-Latif A, Zuba-Surma EK, Dawn B: **Adult bone marrow cell therapy improves survival and induces long-term improvement in cardiac parameters: a systematic review and meta-analysis**. *Circulation* 2012, **126**(5):551-568.

11.   de Jong R, Houtgraaf JH, Samiei S, Boersma E, Duckers HJ: **Intracoronary stem cell infusion after acute myocardial infarction: a meta-analysis and update on clinical trials**. *Circ Cardiovasc Interv* 2014, **7**(2):156-167.

12.   Francis DP, Mielewczik M, Zargaran D, Cole GD: **Autologous bone marrow-derived stem cell therapy in heart disease: discrepancies and contradictions**. *Int J Cardiol* 2013, **168**(4):3381-3403.

13.   Broeze KA, Opmeer BC, van der Veen F, Bossuyt PM, Bhattacharya S, Mol BW: **Individual patient data meta-analysis: a promising approach for evidence synthesis in reproductive medicine**. *Hum Reprod Update* 2010, **16**(6):561-567.

14.   Gyongyosi M, Wojakowski W, Lemarchand P, Lunde K, Tendera M, Bartunek J, Marban E, Assmus B, Henry TD, Traverse JH *et al*: **Meta-Analysis of Cell-based CaRdiac stUdiEs (ACCRUE) in Patients with Acute Myocardial Infarction Based on Individual Patient Data**. *Circ Res* 2015.

15.   Kandala J, Upadhyay GA, Pokushalov E, Wu S, Drachman DE, Singh JP: **Meta-analysis of stem cell therapy in chronic ischemic cardiomyopathy**. *Am J Cardiol* 2013, **112**(2):217-225.

16.   De Feo D, Merlini A, Laterza C, Martino G: **Neural stem cell transplantation in central nervous system disorders: from cell replacement to neuroprotection**. *Curr Opin Neurol* 2012, **25**(3):322-333.

17.   Chen YT, Sun CK, Lin YC, Chang LT, Chen YL, Tsai TH, Chung SY, Chua S, Kao YH, Yen CH *et al*: **Adipose-derived mesenchymal stem cell protects kidneys against ischemia-reperfusion injury through suppressing oxidative stress and inflammatory reaction**. *J Transl Med* 2011, **9**:51.

18.   Pittenger MF, Martin BJ: **Mesenchymal stem cells and their potential as cardiac therapeutics**. *Circ Res* 2004, **95**(1):9-20.

19.   Leiker M, Suzuki G, Iyer VS, Canty JM, Jr., Lee T: **Assessment of a nuclear affinity labeling method for tracking implanted mesenchymal stem cells**. *Cell Transplant* 2008, **17**(8):911-922.

20.   Gyongyosi M, Hemetsberger R, Wolbank S, Pichler V, Kaun C, Posa A, Petrasi Z, Petnehazy O, Hofer-Warbinek R, de Martin R *et al*: **Delayed recovery of myocardial blood flow after intracoronary stem cell administration**. *Stem Cell Rev* 2011, **7**(3):616-623.

21.   Gnecchi M, Zhang Z, Ni A, Dzau VJ: **Paracrine mechanisms in adult stem cell signaling and therapy**. *Circ Res* 2008, **103**(11):1204-1219.

22.   Lamichhane TN, Sokic S, Schardt JS, Raiker RS, Lin JW, Jay SM: **Emerging Roles for Extracellular Vesicles in Tissue Engineering and Regenerative Medicine**. *Tissue Eng Part B Rev* 2014.

23.   Kinnaird T, Stabile E, Burnett MS, Shou M, Lee CW, Barr S, Fuchs S, Epstein SE: **Local delivery of marrow-derived stromal cells augments collateral perfusion through paracrine mechanisms**. *Circulation* 2004, **109**(12):1543-1549.

24.   Uemura R, Xu M, Ahmad N, Ashraf M: **Bone marrow stem cells prevent left ventricular remodeling of ischemic heart through paracrine signaling**. *Circ Res* 2006, **98**(11):1414-1421.

25.   Chen L, Tredget EE, Wu PY, Wu Y: **Paracrine factors of mesenchymal stem cells recruit macrophages and endothelial lineage cells and enhance wound healing**. *PLoS One* 2008, **3**(4):e1886.

26.   Gatti S, Bruno S, Deregibus MC, Sordi A, Cantaluppi V, Tetta C, Camussi G: **Microvesicles derived from human adult mesenchymal stem cells protect against ischaemia-reperfusion-induced acute and chronic kidney injury**. *Nephrol Dial Transplant* 2011, **26**(5):1474-1483.

27.   Thum T, Bauersachs J, Poole-Wilson PA, Volk HD, Anker SD: **The dying stem cell hypothesis: immune modulation as a novel mechanism for progenitor cell therapy in cardiac muscle**. *J Am Coll Cardiol* 2005, **46**(10):1799-1802.

28.   Schachinger V, Assmus B, Britten MB, Honold J, Lehmann R, Teupe C, Abolmaali ND, Vogl TJ, Hofmann WK, Martin H *et al*: **Transplantation of progenitor cells and regeneration enhancement in acute myocardial infarction: final one-year results of the TOPCARE-AMI Trial**. *J Am Coll Cardiol* 2004, **44**(8):1690-1699.

29.   Stamm C, Westphal B, Kleine HD, Petzsch M, Kittner C, Klinge H, Schumichen C, Nienaber CA, Freund M, Steinhoff G: **Autologous bone-marrow stem-cell transplantation for myocardial regeneration**. *Lancet* 2003, **361**(9351):45-46.

30.   Fadok VA, Bratton DL, Konowal A, Freed PW, Westcott JY, Henson PM: **Macrophages that have ingested apoptotic cells in vitro inhibit proinflammatory cytokine production through autocrine/paracrine mechanisms involving TGF-beta, PGE2, and PAF**. *J Clin Invest* 1998, **101**(4):890-898.

31.   Wang D, Wang H, Brown J, Daikoku T, Ning W, Shi Q, Richmond A, Strieter R, Dey SK, DuBois RN: **CXCL1 induced by prostaglandin E2 promotes angiogenesis in colorectal cancer**. *J Exp Med* 2006, **203**(4):941-951.

32.   Ankersmit HJ, Hoetzenecker K, Dietl W, Soleiman A, Horvat R, Wolfsberger M, Gerner C, Hacker S, Mildner M, Moser B *et al*: **Irradiated cultured apoptotic peripheral blood mononuclear cells regenerate infarcted myocardium**. *Eur J Clin Invest* 2009, **39**(6):445-456.

33.   Matuszczak S, Czapla J, Jarosz-Biej M, Wisniewska E, Cichon T, Smolarczyk R, Kobusinska M, Gajda K, Wilczek P, Sliwka J *et al*: **Characteristic of c-Kit+ progenitor cells in explanted human hearts**. *Clin Res Cardiol* 2014, **103**(9):711-718.

34.   Nigro P, Perrucci GL, Gowran A, Zanobini M, Capogrossi MC, Pompilio G: **c-kit cells: the tell-tale heart of cardiac regeneration** *Cell Mol Life Sci* 2015.

35. Camussi G, Deregibus MC, Cantaluppi V: **Role of stem-cell-derived microvesicles in the paracrine action of stem cells**. *Biochem Soc Trans* 2013, **41**(1):283-287.

36. Gnecchi M, He H, Liang OD, Melo LG, Morello F, Mu H, Noiseux N, Zhang L, Pratt RE, Ingwall JS *et al*: **Paracrine action accounts for marked protection of ischemic heart by Akt-modified mesenchymal stem cells**. *Nat Med* 2005, **11**(4):367-368.

37. Pavo N, Charwat S, Nyolczas N, Jakab A, Murlasits Z, Bergler-Klein J, Nikfardjam M, Benedek I, Benedek T, Pavo IJ *et al*: **Cell therapy for human ischemic heart diseases: Critical review and summary of the clinical experiences**. *Journal of molecular and cellular cardiology* 2014, **75C**:12-24.

38. Hoetzenecker K, Assinger A, Lichtenauer M, Mildner M, Schweiger T, Starlinger P, Jakab A, Berenyi E, Pavo N, Zimmermann M *et al*: **Secretome of apoptotic peripheral blood cells (APOSEC) attenuates microvascular obstruction in a porcine closed chest reperfused acute myocardial infarction model: role of platelet aggregation and vasodilation**. *Basic Res Cardiol* 2012, **107**(5):292.

39. Hoetzenecker K, Zimmermann M, Hoetzenecker W, Schweiger T, Kollmann D, Mildner M, Hegedus B, Mitterbauer A, Hacker S, Birner P *et al*: **Mononuclear cell secretome protects from experimental autoimmune myocarditis**. *Eur Heart J* 2013.

40. Mildner M, Hacker S, Haider T, Gschwandtner M, Werba G, Barresi C, Zimmermann M, Golabi B, Tschachler E, Ankersmit HJ: **Secretome of peripheral blood mononuclear cells enhances wound healing**. *PLoS One* 2013, **8**(3):e60103.

41. Lichtenauer M, Mildner M, Baumgartner A, Hasun M, Werba G, Beer L, Altmann P, Roth G, Gyongyosi M, Podesser BK *et al*: **Intravenous and intramyocardial injection of apoptotic white blood cell suspensions prevents ventricular remodelling by increasing elastin expression in cardiac scar tissue after myocardial infarction**. *Basic Res Cardiol* 2011, **106**(4):645-655.

42. Lichtenauer M, Mildner M, Hoetzenecker K, Zimmermann M, Podesser BK, Sipos W, Berenyi E, Dworschak M, Tschachler E, Gyongyosi M *et al*: **Secretome of apoptotic peripheral blood cells (APOSEC) confers cytoprotection to cardiomyocytes and inhibits tissue remodelling after acute myocardial infarction: a preclinical study**. *Basic Res Cardiol* 2011, **106**(6):1283-1297.

43. Pavo N, Zimmermann M, Pils D, Mildner M, Petrasi Z, Petnehazy O, Fuzik J, Jakab A, Gabriel C, Sipos W *et al*: **Long-acting beneficial effect of percutaneously intramyocardially delivered secretome of apoptotic peripheral blood cells on porcine chronic ischemic left ventricular dysfunction**. *Biomaterials* 2014, **35**(11):3541-3550.

44. Cervio M, Scudeller L, Viarengo G, Monti M, Del Fante C, Arici V, Perotti C: **gamma-Irradiated cord blood MNCs: Different paracrine effects on mature and progenitor endothelial cells**. *Microvasc Res* 2014, **94**:9-16.

45. Sahoo S, Klychko E, Thorne T, Misener S, Schultz KM, Millay M, Ito A, Liu T, Kamide C, Agrawal H *et al*: **Exosomes from human CD34(+) stem cells mediate their proangiogenic paracrine activity**. *Circ Res* 2011, **109**(7):724-728.

46. Chimenti I, Smith RR, Li TS, Gerstenblith G, Messina E, Giacomello A, Marban E: **Relative roles of direct regeneration versus paracrine effects of human cardiosphere-derived cells transplanted into infarcted mice**. *Circ Res* 2010, **106**(5):971-980.

47. Ranganath SH, Levy O, Inamdar MS, Karp JM: **Harnessing the mesenchymal stem cell secretome for the treatment of cardiovascular disease**. *Cell stem cell* 2012, **10**(3):244-258.

48. Li Z, Wei H, Deng L, Cong X, Chen X: **Expression and secretion of interleukin-1beta, tumour necrosis factor-alpha and interleukin-10 by hypoxia- and serum-deprivation-stimulated mesenchymal stem cells**. *FEBS J* 2010, **277**(18):3688-3698.

49. Oskowitz A, McFerrin H, Gutschow M, Carter ML, Pochampally R: **Serum-deprived human multipotent mesenchymal stromal cells (MSCs) are highly angiogenic**. *Stem Cell Res* 2011, **6**(3):215-225.

50. Przybyt E, Krenning G, Brinker MG, Harmsen MC: **Adipose stromal cells primed with hypoxia and inflammation enhance cardiomyocyte proliferation rate in vitro through STAT3 and Erk1/2**. *J Transl Med* 2013, **11**:39.

51. Kinnaird T, Stabile E, Burnett MS, Lee CW, Barr S, Fuchs S, Epstein SE: **Marrow-derived stromal cells express genes encoding a broad spectrum of arteriogenic cytokines and promote in vitro and in vivo arteriogenesis through paracrine mechanisms**. *Circ Res* 2004, **94**(5):678-685.

52. Mirotsou M, Jayawardena TM, Schmeckpeper J, Gnecchi M, Dzau VJ: **Paracrine mechanisms of stem cell reparative and regenerative actions in the heart**. *Journal of molecular and cellular cardiology* 2011, **50**(2):280-289.

53. Gnecchi M, He H, Noiseux N, Liang OD, Zhang L, Morello F, Mu H, Melo LG, Pratt RE, Ingwall JS *et al*: **Evidence supporting paracrine hypothesis for Akt-modified mesenchymal stem cell-mediated cardiac protection and functional improvement**. *FASEB J* 2006, **20**(6):661-669.

54. Mirotsou M, Zhang Z, Deb A, Zhang L, Gnecchi M, Noiseux N, Mu H, Pachori A, Dzau V: **Secreted frizzled related protein 2 (Sfrp2) is the key Akt-mesenchymal**

stem cell-released paracrine factor mediating myocardial survival and repair. *Proc Natl Acad Sci U S A* 2007, **104**(5):1643-1648.

55.   Haider H, Jiang S, Idris NM, Ashraf M: **IGF-1-overexpressing mesenchymal stem cells accelerate bone marrow stem cell mobilization via paracrine activation of SDF-1alpha/CXCR4 signaling to promote myocardial repair**. *Circ Res* 2008, **103**(11):1300-1308.

56.   Yang F, Cho SW, Son SM, Bogatyrev SR, Singh D, Green JJ, Mei Y, Park S, Bhang SH, Kim BS *et al*: **Genetic engineering of human stem cells for enhanced angiogenesis using biodegradable polymeric nanoparticles**. *Proc Natl Acad Sci U S A* 2010, **107**(8):3317-3322.

57.   Tang J, Wang J, Guo L, Kong X, Yang J, Zheng F, Zhang L, Huang Y: **Mesenchymal stem cells modified with stromal cell-derived factor 1 alpha improve cardiac remodeling via paracrine activation of hepatocyte growth factor in a rat model of myocardial infarction**. *Mol Cells* 2010, **29**(1):9-19.

58.   Lee MJ, Kim J, Kim MY, Bae YS, Ryu SH, Lee TG, Kim JH: **Proteomic analysis of tumor necrosis factor-alpha-induced secretome of human adipose tissue-derived mesenchymal stem cells**. *J Proteome Res* 2010, **9**(4):1754-1762.

59.   Yao Y, Zhang F, Wang L, Zhang G, Wang Z, Chen J, Gao X: **Lipopolysaccharide preconditioning enhances the efficacy of mesenchymal stem cells transplantation in a rat model of acute myocardial infarction**. *J Biomed Sci* 2009, **16**:74.

60.   Bergmann A, Steller H: **Apoptosis, stem cells, and tissue regeneration**. *Sci Signal* 2010, **3**(145):re8.

61.   Li F, Huang Q, Chen J, Peng Y, Roop DR, Bedford JS, Li CY: **Apoptotic cells activate the "phoenix rising" pathway to promote wound healing and tissue regeneration**. *Sci Signal* 2010, **3**(110):ra13.

62.   Huang Q, Li F, Liu X, Li W, Shi W, Liu FF, O'Sullivan B, He Z, Peng Y, Tan AC *et al*: **Caspase 3-mediated stimulation of tumor cell repopulation during cancer radiotherapy**. *Nat Med* 2011, **17**(7):860-866.

63.   Korf-Klingebiel M, Reboll MR, Klede S, Brod T, Pich A, Polten F, Napp LC, Bauersachs J, Ganser A, Brinkmann E *et al*: **Myeloid-derived growth factor (C19orf10) mediates cardiac repair following myocardial infarction**. *Nat Med* 2015.

64.   Hsiao ST, Lokmic Z, Peshavariya H, Abberton KM, Dusting GJ, Lim SY, Dilley RJ: **Hypoxic conditioning enhances the angiogenic paracrine activity of human adipose-derived stem cells**. *Stem cells and development* 2013, **22**(10):1614-1623.

65.   Di Santo S, Yang Z, Wyler von Ballmoos M, Voelzmann J, Diehm N, Baumgartner I, Kalka C: **Novel cell-free strategy for therapeutic angiogenesis: in vitro generated conditioned medium can replace progenitor cell transplantation**. *PLoS One* 2009, **4**(5):e5643.

66.   Arscott WT, Tandle AT, Zhao S, Shabason JE, Gordon IK, Schlaff CD, Zhang G, Tofilon PJ, Camphausen KA: **Ionizing radiation and glioblastoma exosomes: implications in tumor biology and cell migration**. *Transl Oncol* 2013, **6**(6):638-648.

67.   Khatri P, Sirota M, Butte AJ: **Ten years of pathway analysis: current approaches and outstanding challenges**. *PLoS Comput Biol* 2012, **8**(2):e1002375.

68.   Pavlou MP, Diamandis EP: **The cancer cell secretome: a good source for discovering biomarkers?** *J Proteomics* 2010, **73**(10):1896-1906.

69.   Mukherjee P, Mani S: **Methodologies to decipher the cell secretome**. *Biochim Biophys Acta* 2013.

70.   Kupcova Skalnikova H: **Proteomic techniques for characterisation of mesenchymal stem cell secretome**. *Biochimie* 2013, **95**(12):2196-2211.

71.   Polaskova V, Kapur A, Khan A, Molloy MP, Baker MS: **High-abundance protein depletion: comparison of methods for human plasma biomarker discovery**. *Electrophoresis* 2010, **31**(3):471-482.

72.   Steel LF, Trotter MG, Nakajima PB, Mattu TS, Gonye G, Block T: **Efficient and specific removal of albumin from human serum samples**. *Mol Cell Proteomics* 2003, **2**(4):262-270.

73.   Tucholska M, Bowden P, Jacks K, Zhu P, Furesz S, Dumbrovsky M, Marshall J: **Human serum proteins fractionated by preparative partition chromatography prior to LC-ESI-MS/MS**. *J Proteome Res* 2009, **8**(3):1143-1155.

74.   Stastna M, Van Eyk JE: **Investigating the secretome: lessons about the cells that comprise the heart**. *Circ Cardiovasc Genet* 2012, **5**(1):o8-o18.

75.   Pirkmajer S, Chibalin AV: **Serum starvation: caveat emptor**. *Am J Physiol Cell Physiol* 2011, **301**(2):C272-279.

76.   Francis GL: **Albumin and mammalian cell culture: implications for biotechnology applications**. *Cytotechnology* 2010, **62**(1):1-16.

77.   Ellmerer M, Schaupp L, Brunner GA, Sendlhofer G, Wutte A, Wach P, Pieber TR: **Measurement of interstitial albumin in human skeletal muscle and adipose tissue by open-flow microperfusion**. *Am J Physiol Endocrinol Metab* 2000, **278**(2):E352-356.

78. Oettl K, Stauber RE: **Physiological and pathological changes in the redox state of human serum albumin critically influence its binding properties**. *Br J Pharmacol* 2007, **151**(5):580-590.

79. Garcia-Gonzalo FR, Izpisua Belmonte JC: **Albumin-associated lipids regulate human embryonic stem cell self-renewal**. *PLoS One* 2008, **3**(1):e1384.

80. Bolitho C, Bayl P, Hou JY, Lynch G, Hassel AJ, Wall AJ, Zoellner H: **The anti-apoptotic activity of albumin for endothelium is mediated by a partially cryptic protein domain and reduced by inhibitors of G-coupled protein and PI-3 kinase, but is independent of radical scavenging or bound lipid**. *J Vasc Res* 2007, **44**(4):313-324.

81. Yang J, Klassen H, Pries M, Wang W, Nissen MH: **Vitreous humor and albumin augment the proliferation of cultured retinal precursor cells**. *J Neurosci Res* 2009, **87**(2):495-502.

82. Caccia D, Dugo M, Callari M, Bongarzone I: **Bioinformatics tools for secretome analysis**. *Biochim Biophys Acta* 2013.

83. Blumenberg M: **SKINOMICS: Transcriptional Profiling in Dermatology and Skin Biology**. *Curr Genomics* 2012, **13**(5):363-368.

84. Petersen TN, Brunak S, von Heijne G, Nielsen H: **SignalP 4.0: discriminating signal peptides from transmembrane regions**. *Nat Methods* 2011, **8**(10):785-786.

85. Emanuelsson O, Brunak S, von Heijne G, Nielsen H: **Locating proteins in the cell using TargetP, SignalP and related tools**. *Nat Protoc* 2007, **2**(4):953-971.

86. Bendtsen JD, Jensen LJ, Blom N, Von Heijne G, Brunak S: **Feature-based prediction of non-classical and leaderless protein secretion**. *Protein Eng Des Sel* 2004, **17**(4):349-356.

87. Krogh A, Larsson B, von Heijne G, Sonnhammer EL: **Predicting transmembrane protein topology with a hidden Markov model: application to complete genomes**. *Journal of molecular biology* 2001, **305**(3):567-580.

88. Szalowska E, Dijkstra M, Elferink MG, Weening D, de Vries M, Bruinenberg M, Hoek A, Roelofsen H, Groothuis GM, Vonk RJ: **Comparative analysis of the human hepatic and adipose tissue transcriptomes during LPS-induced inflammation leads to the identification of differential biological pathways and candidate biomarkers**. *BMC Med Genomics* 2011, **4**:71.

89. Mutch DM, Rouault C, Keophiphath M, Lacasa D, Clement K: **Using gene expression to predict the secretome of differentiating human preadipocytes**. *Int J Obes (Lond)* 2009, **33**(3):354-363.

90. McIlwain DR, Berger T, Mak TW: **Caspase functions in cell death and disease**. *Cold Spring Harb Perspect Biol* 2013, **5**(4):a008656.

91. Boland K, Flanagan L, Prehn JH: **Paracrine control of tissue regeneration and cell proliferation by Caspase-3**. *Cell Death Dis* 2013, **4**:e725.

92. Lauber K, Bohn E, Krober SM, Xiao YJ, Blumenthal SG, Lindemann RK, Marini P, Wiedig C, Zobywalski A, Baksh S *et al*: **Apoptotic cells induce migration of phagocytes via caspase-3-mediated release of a lipid attraction signal**. *Cell* 2003, **113**(6):717-730.

93. Chang MK, Binder CJ, Miller YI, Subbanagounder G, Silverman GJ, Berliner JA, Witztum JL: **Apoptotic cells with oxidation-specific epitopes are immunogenic and proinflammatory**. *J Exp Med* 2004, **200**(11):1359-1370.

94. Elliott MR, Ravichandran KS: **Clearance of apoptotic cells: implications in health and disease**. *J Cell Biol* 2010, **189**(7):1059-1070.

95. Tyurin VA, Balasubramanian K, Winnica D, Tyurina YY, Vikulina AS, He RR, Kapralov AA, Macphee CH, Kagan VE: **Oxidatively modified phosphatidylserines on the surface of apoptotic cells are essential phagocytic 'eat-me' signals: cleavage and inhibition of phagocytosis by Lp-PLA2**. *Cell Death Differ* 2014, **21**(5):825-835.

96. Greenberg ME, Sun M, Zhang R, Febbraio M, Silverstein R, Hazen SL: **Oxidized phosphatidylserine-CD36 interactions play an essential role in macrophage-dependent phagocytosis of apoptotic cells**. *J Exp Med* 2006, **203**(12):2613-2625.

97. Dillon SR, Mancini M, Rosen A, Schlissel MS: **Annexin V binds to viable B cells and colocalizes with a marker of lipid rafts upon B cell receptor activation**. *J Immunol* 2000, **164**(3):1322-1332.

98. Borisenko GG, Matsura T, Liu SX, Tyurin VA, Jianfei J, Serinkan FB, Kagan VE: **Macrophage recognition of externalized phosphatidylserine and phagocytosis of apoptotic Jurkat cells--existence of a threshold**. *Arch Biochem Biophys* 2003, **413**(1):41-52.

99. Castellone MD, Teramoto H, Williams BO, Druey KM, Gutkind JS: **Prostaglandin E2 promotes colon cancer cell growth through a Gs-axin-beta-catenin signaling axis**. *Science* 2005, **310**(5753):1504-1510.

100. Liu C, Li CY, Yuan F: **Mathematical modeling of the phoenix rising pathway**. *PLoS Comput Biol* 2014, **10**(2):e1003461.

101. Bonner C, Bacon S, Concannon CG, Rizvi SR, Baquie M, Farrelly AM, Kilbride SM, Dussmann H, Ward MW, Boulanger CM *et al*: **INS-1 cells undergoing caspase-dependent apoptosis enhance the regenerative capacity of neighboring cells**. *Diabetes* 2010, **59**(11):2799-2808.

102. Jager R, Fearnhead HO: **"Dead Cells Talking": The Silent Form of Cell Death Is Not so Quiet**. *Biochem Res Int* 2012, **2012**:453838.

103. Sebbagh M, Renvoize C, Hamelin J, Riche N, Bertoglio J, Breard J: **Caspase-3-mediated cleavage of ROCK I induces MLC phosphorylation and apoptotic membrane blebbing**. *Nat Cell Biol* 2001, **3**(4):346-352.

104. Crawford N: **The presence of contractile proteins in platelet microparticles isolated from human and animal platelet-free plasma**. *Br J Haematol* 1971, **21**(1):53-69.

105. Kowal J, Tkach M, Thery C: **Biogenesis and secretion of exosomes**. *Curr Opin Cell Biol* 2014, **29C**:116-125.

106. Witwer KW, Buzas EI, Bemis LT, Bora A, Lasser C, Lotvall J, Nolte-'t Hoen EN, Piper MG, Sivaraman S, Skog J *et al*: **Standardization of sample collection, isolation and analysis methods in extracellular vesicle research**. *J Extracell Vesicles* 2013, **2**.

107. Ling ZL, Combes V, Grau GE, King NJ: **Microparticles as immune regulators in infectious disease - an opinion**. *Front Immunol* 2011, **2**:67.

108. Thery C, Ostrowski M, Segura E: **Membrane vesicles as conveyors of immune responses**. *Nat Rev Immunol* 2009, **9**(8):581-593.

109. Wickman G, Julian L, Olson MF: **How apoptotic cells aid in the removal of their own cold dead bodies**. *Cell Death Differ* 2012, **19**(5):735-742.

110. Akers JC, Gonda D, Kim R, Carter BS, Chen CC: **Biogenesis of extracellular vesicles (EV): exosomes, microvesicles, retrovirus-like vesicles, and apoptotic bodies**. *J Neurooncol* 2013, **113**(1):1-11.

111. Wickman GR, Julian L, Mardilovich K, Schumacher S, Munro J, Rath N, Zander SA, Mleczak A, Sumpton D, Morrice N *et al*: **Blebs produced by actin-myosin contraction during apoptosis release damage-associated molecular pattern proteins before secondary necrosis occurs**. *Cell Death Differ* 2013, **20**(10):1293-1305.

112. Coleman ML, Sahai EA, Yeo M, Bosch M, Dewar A, Olson MF: **Membrane blebbing during apoptosis results from caspase-mediated activation of ROCK I**. *Nat Cell Biol* 2001, **3**(4):339-345.

113. Bochkov VN, Oskolkova OV, Birukov KG, Levonen AL, Binder CJ, Stockl J: **Generation and biological activities of oxidized phospholipids**. *Antioxid Redox Signal* 2010, **12**(8):1009-1059.

114. Mause SF, von Hundelshausen P, Zernecke A, Koenen RR, Weber C: **Platelet microparticles: a transcellular delivery system for RANTES promoting monocyte recruitment on endothelium**. *Arterioscler Thromb Vasc Biol* 2005, **25**(7):1512-1518.

115. Del Conde I, Shrimpton CN, Thiagarajan P, Lopez JA: **Tissue-factor-bearing microvesicles arise from lipid rafts and fuse with activated platelets to initiate coagulation**. *Blood* 2005, **106**(5):1604-1611.

116. Stratton D, Lange S, Inal JM: **Pulsed extremely low-frequency magnetic fields stimulate microvesicle release from human monocytic leukaemia cells**. *Biochem Biophys Res Commun* 2013, **430**(2):470-475.

117. Valadi H, Ekstrom K, Bossios A, Sjostrand M, Lee JJ, Lotvall JO: **Exosome-mediated transfer of mRNAs and microRNAs is a novel mechanism of genetic exchange between cells**. *Nat Cell Biol* 2007, **9**(6):654-659.

118. Nolte-'t Hoen EN, Buermans HP, Waasdorp M, Stoorvogel W, Wauben MH, t Hoen PA: **Deep sequencing of RNA from immune cell-derived vesicles uncovers the selective incorporation of small non-coding RNA biotypes with potential regulatory functions**. *Nucleic Acids Res* 2012, **40**(18):9272-9285.

119. Villarroya-Beltri C, Baixauli F, Gutierrez-Vazquez C, Sanchez-Madrid F, Mittelbrunn M: **Sorting it out: Regulation of exosome loading**. *Semin Cancer Biol* 2014.

120. Record M, Carayon K, Poirot M, Silvente-Poirot S: **Exosomes as new vesicular lipid transporters involved in cell-cell communication and various pathophysiologies**. *Biochim Biophys Acta* 2014, **1841**(1):108-120.

121. Rappa G, Mercapide J, Anzanello F, Pope RM, Lorico A: **Biochemical and biological characterization of exosomes containing prominin-1/CD133**. *Mol Cancer* 2013, **12**:62.

122. Kalra H, Simpson RJ, Ji H, Aikawa E, Altevogt P, Askenase P, Bond VC, Borras FE, Breakefield X, Budnik V *et al*: **Vesiclepedia: a compendium for extracellular vesicles with continuous community annotation**. *PLoS Biol* 2012, **10**(12):e1001450.

123. Kim DK, Kang B, Kim OY, Choi DS, Lee J, Kim SR, Go G, Yoon YJ, Kim JH, Jang SC *et al*: **EVpedia: an integrated database of high-throughput data for systemic analyses of extracellular vesicles**. *J Extracell Vesicles* 2013, **2**.

124. Yu X, Harris SL, Levine AJ: **The regulation of exosome secretion: a novel function of the p53 protein**. *Cancer Res* 2006, **66**(9):4795-4801.

125. Sirois I, Raymond MA, Brassard N, Cailhier JF, Fedjaev M, Hamelin K, Londono I, Bendayan M, Pshezhetsky AV, Hebert MJ: **Caspase-3-dependent export of TCTP: a novel pathway for antiapoptotic intercellular communication**. *Cell Death Differ* 2011, **18**(3):549-562.

126. Lehmann BD, Paine MS, Brooks AM, McCubrey JA, Renegar RH, Wang R, Terrian DM: **Senescence-associated exosome release from human prostate cancer cells**. *Cancer Res* 2008, **68**(19):7864-7871.

127. Momen-Heravi F, Balaj L, Alian S, Mantel PY, Halleck AE, Trachtenberg AJ, Soria CE, Oquin S, Bonebreak CM, Saracoglu E *et al*: **Current methods for the isolation of extracellular vesicles**. *Biol Chem* 2013, **394**(10):1253-1262.

128. Taylor DD, Zacharias W, Gercel-Taylor C: **Exosome isolation for proteomic analyses and RNA profiling**. *Methods Mol Biol* 2011, **728**:235-246.

129. Yeo RW, Lai RC, Zhang B, Tan SS, Yin Y, Teh BJ, Lim SK: **Mesenchymal stem cell: an efficient mass producer of exosomes for drug delivery**. *Adv Drug Deliv Rev* 2013, **65**(3):336-341.

130. Chen TS, Arslan F, Yin Y, Tan SS, Lai RC, Choo AB, Padmanabhan J, Lee CN, de Kleijn DP, Lim SK: **Enabling a robust scalable manufacturing process for therapeutic exosomes through oncogenic immortalization of human ESC-derived MSCs**. *J Transl Med* 2011, **9**:47.

131. Alvarez-Erviti L, Seow Y, Yin H, Betts C, Lakhal S, Wood MJ: **Delivery of siRNA to the mouse brain by systemic injection of targeted exosomes**. *Nat Biotechnol* 2011, **29**(4):341-345.

132. Tian Y, Li S, Song J, Ji T, Zhu M, Anderson GJ, Wei J, Nie G: **A doxorubicin delivery platform using engineered natural membrane vesicle exosomes for targeted tumor therapy**. *Biomaterials* 2014, **35**(7):2383-2390.

133. Wang Q, Zhuang X, Mu J, Deng ZB, Jiang H, Zhang L, Xiang X, Wang B, Yan J, Miller D *et al*: **Delivery of therapeutic agents by nanoparticles made of grapefruit-derived lipids**. *Nat Commun* 2013, **4**:1867.

134. Ju S, Mu J, Dokland T, Zhuang X, Wang Q, Jiang H, Xiang X, Deng ZB, Wang B, Zhang L *et al*: **Grape exosome-like nanoparticles induce intestinal stem cells and protect mice from DSS-induced colitis**. *Mol Ther* 2013, **21**(7):1345-1357.

135. Basu J, Ludlow JW: **Cell-based therapeutic products: potency assay development and application**. *Regen Med* 2014, **9**(4):497-512.

136. Organization WH: **Guidelines on viral inactivation and removal**. *WHO Technical Report* 2004, **924**.

137. Gauvin G, Nims R: **Gamma-irradiation of serum for the inactivation of adventitious contaminants**. *PDA J Pharm Sci Technol* 2010, **64**(5):432-435.

138. Nims RW, Gauvin G, Plavsic M: **Gamma irradiation of animal sera for inactivation of viruses and mollicutes--a review**. *Biologicals* 2011, **39**(6):370-377.

139. Altmann P, Mildner M, Haider T, Traxler D, Beer L, Ristl R, Golabi B, Gabriel C, Leutmezer F, Ankersmit HJ: **Secretomes of apoptotic mononuclear cells ameliorate neurological damage in rats with focal ischemia**. *F1000Res* 2014, **3**:131.

140. Haider T, Hoftberger R, Ruger B, Mildner M, Blumer R, Mitterbauer A, Buchacher T, Sherif C, Altmann P, Redl H *et al*: **The secretome of apoptotic human peripheral blood mononuclear cells attenuates secondary damage following spinal cord injury in rats**. *Exp Neurol* 2015, **267**:230-242.

141. Kerr JF, Wyllie AH, Currie AR: **Apoptosis: a basic biological phenomenon with wide-ranging implications in tissue kinetics**. *Br J Cancer* 1972, **26**(4):239-257.

142. Nikoletopoulou V, Markaki M, Palikaras K, Tavernarakis N: **Crosstalk between apoptosis, necrosis and autophagy**. *Biochim Biophys Acta* 2013, **1833**(12):3448-3459.

143. Stark MA, Huo Y, Burcin TL, Morris MA, Olson TS, Ley K: **Phagocytosis of apoptotic neutrophils regulates granulopoiesis via IL-23 and IL-17**. *Immunity* 2005, **22**(3):285-294.

144. Erwig LP, Henson PM: **Immunological consequences of apoptotic cell phagocytosis**. *Am J Pathol* 2007, **171**(1):2-8.

145. Palmer E: **Negative selection--clearing out the bad apples from the T-cell repertoire**. *Nat Rev Immunol* 2003, **3**(5):383-391.

146. de la Rosa EJ, de Pablo F: **Cell death in early neural development: beyond the neurotrophic theory**. *Trends Neurosci* 2000, **23**(10):454-458.

147. Elmore S: **Apoptosis: a review of programmed cell death**. *Toxicol Pathol* 2007, **35**(4):495-516.

148. Saraste A, Pulkki K: **Morphologic and biochemical hallmarks of apoptosis**. *Cardiovasc Res* 2000, **45**(3):528-537.

149. Xu G, Shi Y: **Apoptosis signaling pathways and lymphocyte homeostasis**. *Cell Res* 2007, **17**(9):759-771.

150. Fan TJ, Han LH, Cong RS, Liang J: **Caspase family proteases and apoptosis**. *Acta Biochim Biophys Sin (Shanghai)* 2005, **37**(11):719-727.

151. Wang L, Du F, Wang X: **TNF-alpha induces two distinct caspase-8 activation pathways**. *Cell* 2008, **133**(4):693-703.

152. Ren G, Su J, Zhao X, Zhang L, Zhang J, Roberts AI, Zhang H, Das G, Shi Y: **Apoptotic cells induce immunosuppression through dendritic cells: critical roles of IFN-gamma and nitric oxide**. *J Immunol* 2008, **181**(5):3277-3284.

153. Martin SJ, Henry CM, Cullen SP: **A perspective on mammalian caspases as positive and negative regulators of inflammation**. *Mol Cell* 2012, **46**(4):387-397.

154. Zhao X, Wang D, Zhao Z, Xiao Y, Sengupta S, Zhang R, Lauber K, Wesselborg S, Feng L, Rose TM *et al*: **Caspase-3-dependent activation of calcium-independent phospholipase A2 enhances cell migration in non-apoptotic ovarian cancer cells**. *J Biol Chem* 2006, **281**(39):29357-29368.

155. Kudriashov Y: **Radiation Biophysics (Ionizing Radiation)**: Mikhail F. Lomanov; Nova Science Pub Inc; 2008.

156. Story M, Ding LH, Brock WA, Ang KK, Alsbeih G, Minna J, Park S, Das A: **Defining molecular and cellular responses after low and high linear energy transfer radiations to develop biomarkers of carcinogenic risk or therapeutic outcome**. *Health Phys* 2012, **103**(5):596-606.

157. Unated Nations Scientific Committee: **Effects of Ionizing Radiation**. In.; 2006.

158. Azzam EI, Jay-Gerin JP, Pain D: **Ionizing radiation-induced metabolic oxidative stress and prolonged cell injury**. *Cancer Lett* 2012, **327**(1-2):48-60.

159. Mahaney BL, Meek K, Lees-Miller SP: **Repair of ionizing radiation-induced DNA double-strand breaks by non-homologous end-joining**. *Biochem J* 2009, **417**(3):639-650.

160. Jackson SP, Bartek J: **The DNA-damage response in human biology and disease**. *Nature* 2009, **461**(7267):1071-1078.

161. Zhou BB, Elledge SJ: **The DNA damage response: putting checkpoints in perspective**. *Nature* 2000, **408**(6811):433-439.

162. Filipowicz W, Bhattacharyya SN, Sonenberg N: **Mechanisms of post-transcriptional regulation by microRNAs: are the answers in sight?** *Nat Rev Genet* 2008, **9**(2):102-114.

163. Bartel DP: **MicroRNAs: genomics, biogenesis, mechanism, and function**. *Cell* 2004, **116**(2):281-297.

164. Da Sacco L, Masotti A: **Recent Insights and Novel Bioinformatics Tools to Understand the Role of MicroRNAs Binding to 5' Untranslated Region**. *Int J Mol Sci* 2012, **14**(1):480-495.

165. Peterson SM, Thompson JA, Ufkin ML, Sathyanarayana P, Liaw L, Congdon CB: **Common features of microRNA target prediction tools**. *Front Genet* 2014, **5**:23.

166. Du T, Zamore PD: **microPrimer: the biogenesis and function of microRNA**. *Development* 2005, **132**(21):4645-4652.

167. Bernardo BC, Charchar FJ, Lin RC, McMullen JR: **A microRNA guide for clinicians and basic scientists: background and experimental techniques**. *Heart Lung Circ* 2012, **21**(3):131-142.

168. Truesdell SS, Mortensen RD, Seo M, Schroeder JC, Lee JH, LeTonqueze O, Vasudevan S: **MicroRNA-mediated mRNA translation activation in quiescent cells and oocytes involves recruitment of a nuclear microRNP**. *Sci Rep* 2012, **2**:842.

169. Orom UA, Nielsen FC, Lund AH: **MicroRNA-10a binds the 5'UTR of ribosomal protein mRNAs and enhances their translation**. *Mol Cell* 2008, **30**(4):460-471.

170. Panda AC, Sahu I, Kulkarni SD, Martindale JL, Abdelmohsen K, Vindu A, Joseph J, Gorospe M, Seshadri V: **miR-196b-Mediated Translation Regulation of Mouse Insulin2 via the 5'UTR**. *PLoS One* 2014, **9**(7):e101084.

171. Girardi C, De Pitta C, Casara S, Sales G, Lanfranchi G, Celotti L, Mognato M: **Analysis of miRNA and mRNA expression profiles highlights alterations in ionizing radiation response of human lymphocytes under modeled microgravity**. *PLoS One* 2012, **7**(2):e31293.

172. Josson S, Sung SY, Lao K, Chung LW, Johnstone PA: **Radiation modulation of microRNA in prostate cancer cell lines**. *Prostate* 2008, **68**(15):1599-1606.

173. Joly-Tonetti N, Vinuelas J, Gandrillon O, Lamartine J: **Differential miRNA expression profiles in proliferating or differentiated keratinocytes in response to gamma irradiation**. *BMC genomics* 2013, **14**:184.

174. Templin T, Paul S, Amundson SA, Young EF, Barker CA, Wolden SL, Smilenov LB: **Radiation-induced micro-RNA expression changes in peripheral blood cells of radiotherapy patients**. *Int J Radiat Oncol Biol Phys* 2011, **80**(2):549-557.

175. Wang Y, Taniguchi T: **MicroRNAs and DNA damage response: implications for cancer therapy**. *Cell Cycle* 2013, **12**(1):32-42.

176. Pothof J, Verkaik NS, van IW, Wiemer EA, Ta VT, van der Horst GT, Jaspers NG, van Gent DC, Hoeijmakers JH, Persengiev SP: **MicroRNA-mediated gene silencing modulates the UV-induced DNA-damage response**. *EMBO J* 2009, **28**(14):2090-2099.

177. Simone NL, Soule BP, Ly D, Saleh AD, Savage JE, Degraff W, Cook J, Harris CC, Gius D, Mitchell JB: **Ionizing radiation-induced oxidative stress alters miRNA expression**. *PLoS One* 2009, **4**(7):e6377.

178. Hummel R, Wang T, Watson DI, Michael MZ, Van der Hoek M, Haier J, Hussey DJ: **Chemotherapy-induced modification of microRNA expression in esophageal cancer**. *Oncol Rep* 2011, **26**(4):1011-1017.

179. Zhang X, Wan G, Berger FG, He X, Lu X: **The ATM kinase induces microRNA biogenesis in the DNA damage response**. *Mol Cell* 2011, **41**(4):371-383.

180. He L, He X, Lim LP, de Stanchina E, Xuan Z, Liang Y, Xue W, Zender L, Magnus J, Ridzon D *et al*: **A microRNA component of the p53 tumour suppressor network**. *Nature* 2007, **447**(7148):1130-1134.

181. Bommer GT, Gerin I, Feng Y, Kaczorowski AJ, Kuick R, Love RE, Zhai Y, Giordano TJ, Qin ZS, Moore BB *et al*: **p53-mediated activation of miRNA34 candidate tumor-suppressor genes**. *Curr Biol* 2007, **17**(15):1298-1307.

182. Saleh AD, Savage JE, Cao L, Soule BP, Ly D, DeGraff W, Harris CC, Mitchell JB, Simone NL: **Cellular stress induced alterations in microRNA let-7a and let-7b expression are dependent on p53**. *PLoS One* 2011, **6**(10):e24429.

183. Raver-Shapira N, Marciano E, Meiri E, Spector Y, Rosenfeld N, Moskovits N, Bentwich Z, Oren M: **Transcriptional activation of miR-34a contributes to p53-mediated apoptosis**. *Mol Cell* 2007, **26**(5):731-743.

184. Zhang DG, Zheng JN, Pei DS: **P53/microRNA-34-induced metabolic regulation: new opportunities in anticancer therapy**. *Mol Cancer* 2014, **13**:115.

185. Wagner-Ecker M, Schwager C, Wirkner U, Abdollahi A, Huber PE: **MicroRNA expression after ionizing radiation in human endothelial cells**. *Radiat Oncol* 2010, **5**:25.

186. Hermeking H: **MicroRNAs in the p53 network: micromanagement of tumour suppression**. *Nat Rev Cancer* 2012, **12**(9):613-626.

187. Duggan DJ, Bittner M, Chen Y, Meltzer P, Trent JM: **Expression profiling using cDNA microarrays**. *Nat Genet* 1999, **21**(1 Suppl):10-14.

188. Pritchard CC, Cheng HH, Tewari M: **MicroRNA profiling: approaches and considerations**. *Nat Rev Genet* 2012, **13**(5):358-369.

189. Meyer SU, Pfaffl MW, Ulbrich SE: **Normalization strategies for microRNA profiling experiments: a 'normal' way to a hidden layer of complexity?** *Biotechnol Lett* 2010, **32**(12):1777-1788.

190. Priness I, Maimon O, Ben-Gal I: **Evaluation of gene-expression clustering via mutual information distance measure**. *BMC Bioinformatics* 2007, **8**:111.

191. Bisognin A, Sales G, Coppe A, Bortoluzzi S, Romualdi C: **MAGIA(2): from miRNA and genes expression data integrative analysis to microRNA-transcription factor mixed regulatory circuits (2012 update)**. *Nucleic Acids Res* 2012, **40**(Web Server issue):W13-21.

192. Huang GT, Athanassiou C, Benos PV: **mirConnX: condition-specific mRNA-microRNA network integrator**. *Nucleic Acids Res* 2011, **39**(Web Server issue):W416-423.

193. Harris MA, Clark J, Ireland A, Lomax J, Ashburner M, Foulger R, Eilbeck K, Lewis S, Marshall B, Mungall C *et al*: **The Gene Ontology (GO) database and informatics resource**. *Nucleic Acids Res* 2004, **32**(Database issue):D258-261.

194. Wang J, Duncan D, Shi Z, Zhang B: **WEB-based GEne SeT AnaLysis Toolkit (WebGestalt): update 2013**. *Nucleic Acids Res* 2013, **41**(Web Server issue):W77-83.

195. Huang da W, Sherman BT, Lempicki RA: **Systematic and integrative analysis of large gene lists using DAVID bioinformatics resources**. *Nat Protoc* 2009, **4**(1):44-57.

196. Franceschini A, Szklarczyk D, Frankild S, Kuhn M, Simonovic M, Roth A, Lin J, Minguez P, Bork P, von Mering C *et al*: **STRING v9.1: protein-protein interaction networks, with increased coverage and integration**. *Nucleic Acids Res* 2013, **41**(Database issue):D808-815.

197. Hu Z, Hung JH, Wang Y, Chang YC, Huang CL, Huyck M, DeLisi C: **VisANT 3.5: multi-scale network visualization, analysis and inference based on the gene ontology**. *Nucleic Acids Res* 2009, **37**(Web Server issue):W115-121.

198. Warde-Farley D, Donaldson SL, Comes O, Zuberi K, Badrawi R, Chao P, Franz M, Grouios C, Kazi F, Lopes CT *et al*: **The GeneMANIA prediction server: biological network integration for gene prioritization and predicting gene function**. *Nucleic Acids Res* 2010, **38**(Web Server issue):W214-220.

199. Niu Y, Otasek D, Jurisica I: **Evaluation of linguistic features useful in extraction of interactions from PubMed; application to annotating known, high-throughput and predicted interactions in I2D**. *Bioinformatics* 2010, **26**(1):111-119.

200. Wong AK, Park CY, Greene CS, Bongo LA, Guan Y, Troyanskaya OG: **IMP: a multi-species functional genomics portal for integration, visualization and prediction of protein functions and networks**. *Nucleic Acids Res* 2012, **40**(Web Server issue):W484-490.

201. von Mering C, Huynen M, Jaeggi D, Schmidt S, Bork P, Snel B: **STRING: a database of predicted functional associations between proteins**. *Nucleic Acids Res* 2003, **31**(1):258-261.

202. Spitz DR, Azzam EI, Li JJ, Gius D: **Metabolic oxidation/reduction reactions and cellular responses to ionizing radiation: a unifying concept in stress response biology**. *Cancer Metastasis Rev* 2004, **23**(3-4):311-322.

203. Chaudhry MA: **Bystander effect: biological endpoints and microarray analysis**. *Mutat Res* 2006, **597**(1-2):98-112.

204. Beer L, Seemann R, Ristl R, Ellinger A, Kasiri MM, Mitterbauer A, Zimmermann M, Gabriel C, Gyongyosi M, Klepetko W *et al*: **High dose ionizing radiation regulates micro RNA and gene expression changes in human peripheral blood mononuclear cells**. *BMC genomics* 2014, **15**:814.

205. Mozaffarian D, Benjamin EJ, Go AS, Arnett DK, Blaha MJ, Cushman M, de Ferranti S, Despres J, Fullerton HJ, Howard VJ *et al*: **Heart Disease and Stroke Statistics-2015 Update: A Report From the American Heart Association**. *Circulation* 2014.

206. Meyer GP, Wollert KC, Lotz J, Steffens J, Lippolt P, Fichtner S, Hecker H, Schaefer A, Arseniev L, Hertenstein B *et al*: **Intracoronary bone marrow cell transfer after myocardial infarction: eighteen months' follow-up data from the randomized,**

controlled BOOST (BOne marrOw transfer to enhance ST-elevation infarct regeneration) trial. *Circulation* 2006, **113**(10):1287-1294.

207. Meyer GP, Wollert KC, Lotz J, Pirr J, Rager U, Lippolt P, Hahn A, Fichtner S, Schaefer A, Arseniev L *et al*: **Intracoronary bone marrow cell transfer after myocardial infarction: 5-year follow-up from the randomized-controlled BOOST trial**. *Eur Heart J* 2009, **30**(24):2978-2984.

208. Korf-Klingebiel M, Kempf T, Sauer T, Brinkmann E, Fischer P, Meyer GP, Ganser A, Drexler H, Wollert KC: **Bone marrow cells are a rich source of growth factors and cytokines: implications for cell therapy trials after myocardial infarction**. *Eur Heart J* 2008, **29**(23):2851-2858.

209. El-Saghire H, Thierens H, Monsieurs P, Michaux A, Vandevoorde C, Baatout S: **Gene set enrichment analysis highlights different gene expression profiles in whole blood samples X-irradiated with low and high doses**. *Int J Radiat Biol* 2013, **89**(8):628-638.

210. Bisio A, De Sanctis V, Del Vescovo V, Denti MA, Jegga AG, Inga A, Ciribilli Y: **Identification of new p53 target microRNAs by bioinformatics and functional analysis**. *BMC Cancer* 2013, **13**:552.

211. Wang X, Zou L, Lu T, Bao S, Hurov KE, Hittelman WN, Elledge SJ, Li L: **Rad17 phosphorylation is required for claspin recruitment and Chk1 activation in response to replication stress**. *Mol Cell* 2006, **23**(3):331-341.

212. Elssner A, Doseff AI, Duncan M, Kotur M, Wewers MD: **IL-16 is constitutively present in peripheral blood monocytes and spontaneously released during apoptosis**. *J Immunol* 2004, **172**(12):7721-7725.

213. Galluzzi L, Kepp O, Kroemer G: **Caspase-3 and prostaglandins signal for tumor regrowth in cancer therapy**. *Oncogene* 2012, **31**(23):2805-2808.

214. Hada M, Georgakilas AG: **Formation of clustered DNA damage after high-LET irradiation: a review**. *Journal of Radiation Research* 2008, **49**(3):203-210.

215. Rashi-Elkeles S, Elkon R, Shavit S, Lerenthal Y, Linhart C, Kupershtein A, Amariglio N, Rechavi G, Shamir R, Shiloh Y: **Transcriptional modulation induced by ionizing radiation: p53 remains a central player**. *Molecular oncology* 2011, **5**(4):336-348.

216. Brandt T, Townsley FM, Teufel DP, Freund SM, Veprintsev DB: **Molecular basis for modulation of the p53 target selectivity by KLF4**. *PLoS One* 2012, **7**(10):e48252.

217. Wei D, Kanai M, Jia Z, Le X, Xie K: **Kruppel-like factor 4 induces p27Kip1 expression in and suppresses the growth and metastasis of human pancreatic cancer cells**. *Cancer Res* 2008, **68**(12):4631-4639.

218. Li H, Zhang Y, Strose A, Tedesco D, Gurova K, Selivanova G: **Integrated high-throughput analysis identifies Sp1 as a crucial determinant of p53-mediated apoptosis**. *Cell Death Differ* 2014.

219. Metheetrairut C, Slack FJ: **MicroRNAs in the ionizing radiation response and in radiotherapy**. *Curr Opin Genet Dev* 2013, **23**(1):12-19.

220. Lhakhang TW, Chaudhry MA: **Interactome of Radiation-Induced microRNA-Predicted Target Genes**. *Comp Funct Genomics* 2012, **2012**:569731.

221. Arora H, Qureshi R, Jin S, Park AK, Park WY: **miR-9 and let-7g enhance the sensitivity to ionizing radiation by suppression of NFkappaB1**. *Experimental & molecular medicine* 2011, **43**(5):298-304.

222. Buscaglia LE, Li Y: **Apoptosis and the target genes of microRNA-21**. *Chin J Cancer* 2011, **30**(6):371-380.

223. Fang J, Song XW, Tian J, Chen HY, Li DF, Wang JF, Ren AJ, Yuan WJ, Lin L: **Overexpression of microRNA-378 attenuates ischemia-induced apoptosis by inhibiting caspase-3 expression in cardiac myocytes**. *Apoptosis* 2012, **17**(4):410-423.

224. Shi S, Yu L, Zhang T, Qi H, Xavier S, Ju W, Bottinger E: **Smad2-dependent downregulation of miR-30 is required for TGF-beta-induced apoptosis in podocytes**. *PLoS One* 2013, **8**(9):e75572.

225. Li J, Donath S, Li Y, Qin D, Prabhakar BS, Li P: **miR-30 regulates mitochondrial fission through targeting p53 and the dynamin-related protein-1 pathway**. *PLoS Genet* 2010, **6**(1):e1000795.

226. Quintavalle C, Donnarumma E, Iaboni M, Roscigno G, Garofalo M, Romano G, Fiore D, De Marinis P, Croce CM, Condorelli G: **Effect of miR-21 and miR-30b/c on TRAIL-induced apoptosis in glioma cells**. *Oncogene* 2013, **32**(34):4001-4008.

227. Waters KM, Sontag RL, Weber TJ: **Hepatic leukemia factor promotes resistance to cell death: implications for therapeutics and chronotherapy**. *Toxicol Appl Pharmacol* 2013, **268**(2):141-148.

228. Crisostomo PR, Wang Y, Markel TA, Wang M, Lahm T, Meldrum DR: **Human mesenchymal stem cells stimulated by TNF-alpha, LPS, or hypoxia produce growth factors by an NF kappa B- but not JNK-dependent mechanism**. *Am J Physiol Cell Physiol* 2008, **294**(3):C675-682.

229. Bochkov VN, Philippova M, Oskolkova O, Kadl A, Furnkranz A, Karabeg E, Afonyushkin T, Gruber F, Breuss J, Minchenko A *et al*: **Oxidized phospholipids stimulate angiogenesis via autocrine mechanisms, implicating a novel role for lipid oxidation in the evolution of atherosclerotic lesions**. *Circ Res* 2006, **99**(8):900-908.

230. von Schlieffen E, Oskolkova OV, Schabbauer G, Gruber F, Bluml S, Genest M, Kadl A, Marsik C, Knapp S, Chow J *et al*: **Multi-hit inhibition of circulating and cell-associated components of the toll-like receptor 4 pathway by oxidized phospholipids**. *Arterioscler Thromb Vasc Biol* 2009, **29**(3):356-362.

231. Bluml S, Rosc B, Lorincz A, Seyerl M, Kirchberger S, Oskolkova O, Bochkov VN, Majdic O, Ligeti E, Stockl J: **The oxidation state of phospholipids controls the oxidative burst in neutrophil granulocytes**. *J Immunol* 2008, **181**(6):4347-4353.

232. Tyurina YY, Tyurin VA, Kapralova VI, Wasserloos K, Mosher M, Epperly MW, Greenberger JS, Pitt BR, Kagan VE: **Oxidative lipidomics of gamma-radiation-induced lung injury: mass spectrometric characterization of cardiolipin and phosphatidylserine peroxidation**. *Radiat Res* 2011, **175**(5):610-621.

233. Tyurina YY, Tyurin VA, Epperly MW, Greenberger JS, Kagan VE: **Oxidative lipidomics of gamma-irradiation-induced intestinal injury**. *Free Radic Biol Med* 2008, **44**(3):299-314.

234. Vlassov AV, Magdaleno S, Setterquist R, Conrad R: **Exosomes: current knowledge of their composition, biological functions, and diagnostic and therapeutic potentials**. *Biochim Biophys Acta* 2012, **1820**(7):940-948.

235. Distler JH, Huber LC, Hueber AJ, Reich CF, 3rd, Gay S, Distler O, Pisetsky DS: **The release of microparticles by apoptotic cells and their effects on macrophages**. *Apoptosis* 2005, **10**(4):731-741.

236. Salomon C, Ryan J, Sobrevia L, Kobayashi M, Ashman K, Mitchell M, Rice GE: **Exosomal signaling during hypoxia mediates microvascular endothelial cell migration and vasculogenesis**. *PLoS One* 2013, **8**(7):e68451.

237. Tadokoro H, Umezu T, Ohyashiki K, Hirano T, Ohyashiki JH: **Exosomes derived from hypoxic leukemia cells enhance tube formation in endothelial cells**. *J Biol Chem* 2013, **288**(48):34343-34351.

238. Spiekstra SW, Breetveld M, Rustemeyer T, Scheper RJ, Gibbs S: **Wound-healing factors secreted by epidermal keratinocytes and dermal fibroblasts in skin substitutes**. *Wound Repair Regen* 2007, **15**(5):708-717.

239. Dai S, Wei D, Wu Z, Zhou X, Wei X, Huang H, Li G: **Phase I clinical trial of autologous ascites-derived exosomes combined with GM-CSF for colorectal cancer**. *Mol Ther* 2008, **16**(4):782-790.

16 Curriculum Vitae

Dr. med. univ. Lucian Beer

PERSONAL BACKGROUND

Born: May 16th, 1989,Vienna, Austria
Citizen: Austrian
Home address: Weinberggasse 1
                 3702 Stranzendorf
email: lucian.beer@meduniwien.ac.at

EDUCATION

1995 – 1999	Primary School
1999 – 2007	Erzbischöfliches Real- und Aufbaugymnasium Hollabrunn, Austria (High School)
2007/06	Matura (high school graduation) with distinction
2007 – 2008	Zivildienst
2008/10 – 2014/08	Medical Student at the Medical University of Vienna, Austria
2009/11 – Present	Student Research Fellow at the Department of Cardio-Thoracic Surgery, General Hospital Vienna, Medical University of Vienna, Austria
2012/09 – 2015/06	MD-PhD Student at the Medical University of Vienna, Austria
2015/03 – Present	Heal Care Management (MBA) Medical University of Vienna, Austria

CLINICAL TRAINING

2010/09	Clinical Clerkship at the Department of Internal Medicine, LKH Hollabrunn, Austria (4 weeks)
2010/08	Clinical Clerkship at the Department of Surgery, LKH Hollabrunn, Austria (2 weeks)
2011/02	Clinical Clerkship at Surgery of Dr. Michael Putz; Göstling an der Ybbs, Austria (2 weeks)
2011/08	Clinical Clerkship at the Department of Gynaecology, LKH Tulln (2 weeks)
2011/09	Clinical Clerkship at the Department of Paediatrics, LKH Tulln (2 weeks)
2011/09	Clinical Clerkship at the Department of Ambulance Station; LKH Korneuburg (2 weeks)
2012/02	Clinical Clerkship at the Department of Cardiac Surgery; AKH Vienna (2 weeks)
2012/06	Clinical Clerkship at the Department of Radiology, LKH Tulln (2 weeks)
2012/08	Clinical Clerkship at the Department of Pathologie; LKH Horn (2 weeks)
2014/02	Clinical Clerkship at the Department of Radiology, AKH Vienna (2 weeks)
2014/11 – 2015/04	Resident at the LKH Hollabrunn

2015/04 – Present   Resident at the Department of Radiology and Nuclear Medicine, Medical University of Vienna

CONTINUING EDUCATION

2011/11	Methodenseminar "Statistik" – Methods Seminar "Statistics" MMag. Dr. Alexandra Graf
2012/02	Biometrie I: Beschreibung und Visualisierung medizinischer Daten – Biometry I: Description and Visualization of Medical Data, Vienna, Austria
2012/02	Biometrie II: Statistische Tests und Lebensdaueranalyse bei medizinischen Fragestellungen – Biometrie II: Statistical Tests and Analysis of Survival in Medical Research, Vienna, Austria
2012/05	Methodenseminar: "Fluoreszenzbasierte Methoden in der zellbiologischen Forschung"– Methods Seminar „Fluoreszenz Based Methods in cell-biologicalscience"
2013/09	ARGE Bildungsforschung – Fortbildungsseminar: "Multiple Regressionsanalyse"; "Einführung in R"
2013/11	Design, Analysis, Interpretation – Clinical Studies, Vienna, Austria

ORIGINAL PAPERS (13)   IF: 36,00 [06/2015]

All original articles:	**13**	
Cumulative Impact Factor :	36.0	
Average Impact Factor:	2.8	
First authorship:	**6**	
Cumulative Impact Factor :	15.2	
Average Impact Factor:	2.5	

Lichtenauer M, Mildner M, Baumgartner A, Hasun M, Werba G, <u>Beer L</u>, Altmann P, Roth G, Gyöngyösi M, Podesser BK, Ankersmit HJ.:
Intravenous and intramyocardial injection of apoptotic white blood cell suspensions prevents ventricular remodelling by increasing elastin expression in cardiac scar tissue after myocardial infarction.
*Basic Res Cardiol.*2011 Jun; 106 (4): 645-55   IF: 7,304 [2011]

<u>Beer L</u>*, Szerafin T*, Mitterbauer A, Debreceni T, Maros T, Dworschak M, Roth GA, Ankersmit HJ.:
Continued mechanical ventilation during coronary artery bypass graft operation attenuates the systemic immune response.
Eur J Cardiothorac Surg. 2013 Aug;44(2):282-7   IF: 2,814 [2013]
*both authors contributed equally – shared first authorship

Lichtenauer M, Mildner M, Werba G, <u>Beer L</u>, Hoetzenecker K, Baumgartner A, Hasun M, Nickl S, Mitterbauer A, Zimmermann M, Gyöngyösi M, Podesser BK, Klepetko W, Ankersmit HJ.:
Anti-thymocyte globulin induces neo angiogenesis and preserves cardiac function after experimental myocardial infarction.
PLoSOne. 2012;7(12):e52101   IF: 3,730 [2012]

Hoetzenecker K, Mitterbauer A, Guenova E, Schweiger T, Altmann P, Zimmermann M, Hofbauer H, <u>Beer L</u>, Klepetko W, Ankersmit HJ.:
High levels of lung resident CD4+CD28null cells in COPD: implications of autoimmunity.
Wien Klin Wochenschr. 2013 Mar;125(5-6):150-5.   IF: 0,791 [2013]

<u>Beer L</u>, Szerafin T, Debreceni T, Palatás L, Mitterbauer A, Dworschak M, Roth GA, Ankersmit HJ.:
Ventilation during cardiopulmonary bypass: impact on heat shock protein release;
J CardiovascSurg (Torino). 2014 Dec; 55 (6): 849-56   IF: 1,365 [2013]
*both authors contributed equally – shared first authorship

Zimmermann M, Mueller T, Dieplinger B, Bekos C, <u>Beer L</u>, Hofbauer H, Dome B, Ankersmit HJ.:
Circulating heat shock protein 27 as a biomarker for the differentiation of patients with lung cancer and healthy controls -- a clinical comparison of different enzyme linked immunosorbent.
Clin Lab. 2014;60(6):999-1006.   IF: 1,084 [2013]

Lichtenauer M, Schreiber C, Jung C, <u>Beer L</u>, Mangold A, Gyöngyösi M, Podesser BK, Ankersmit HJ.:
Myocardial infarct size measurement using geometric angle calculation;
European Journal of Clinical Investigation, Volume 44, Issue 2, pages 160–167, February 2014   IF: 2,834 [2013]

Altmann P, Mildner M, Haider T, Traxler D, <u>Beer L</u>, Ristl R, Golabi B, Gabriel C, Leutmezer F, Ankersmit HJ.:
Secretomes of Apoptotic Mononuclear Cells Ameliorate Neurological Damage in Rats with Focal Ischemia
F1000Research 2014, **3**:131   no IF available

<u>Beer L</u>*, Szerafin T*, Mitterbauer A, Debreceni T, Maros T, Dworschak M, Roth GA, Ankersmit HJ.:
Low Tidal Volume Ventilation during Cardiopulmonary Bypass Reduces Chemokine Postoperative Serum Concentrations. A randomised trial
*Thorac Cardiovasc Surg*2014 Dec; 62(8): 677-82   IF: 1,075 [2013]
*both authors contributed equally – shared first authorship

<u>Beer L</u>, Seemann R, Ristl R, Ellinger A, Kasiri MM, Mitterbauer A, Zimmermann M, Gabriel C, Gyöngyösi M, Klepetko W, Mildner M, Ankersmit HJ.: **High Dose Ionizing Radiation Regulates Micro RNA and Gene Expression Changes in Human Peripheral Blood Mononuclear Cells**
BMC Genomics, 2014 Sep 25;15(1):814.   IF: 4.04 [2014]

<u>Beer L</u>*, Warszawska JA*, Kasiri MM, Schenk P, Debreceni T, Maros T, Dworschak M, Roth GA, Szerafin T, and Ankersmit HJ:
Intraoperative ventilation strategy during cardiopulmonary bypass
*both authors contributed equally – shared first authorship
J Surg Res. 2015 May 1;195(1):294-302.   *IF: 2.12 [2014]*

<u>Beer L,</u> Mlitz V, Gschwandtner M, Berger T, Narzt MS, Gruber F, Brunner P, Tschachler E, Mildner M.:
Bioinformatics approach for choosing the correct reference genes when studying gene expression in human keratinocytes

Schuster C, Mildner M, Bottaiorfila A, Nemec L, Rogojanu R, <u>Beer L</u>, Fiala C, Bauer W, Petzelbauer P, Elbe-Buerger A.:
Development of Blood and Lymphatic Endothelial Cells in Embryonic and Fetal Human Skin

---

MANUSCRIPTS SUBMITTET (4)

<u>Beer L</u>, Mitterbauer A, Nickl S, Zimmermann M, Ankersmit HJ and Lichtenauer M,:
Effects of Blood Sample Handling Procedures on Measured Chemokine Concentrations in Human Serum and Plasma

<u>Beer L</u>, Zimmermann M, Mitterbauer A, Ellinger A, Gruber F, Narzt MS, Zellner M, Gyöngyösi M, Madlener S, Simader E; Gabriel C, Mildner M, Ankersmit HJ.:
Analysis of the Secretome of Apoptotic Peripheral Blood Mononuclear Cells: Impact of Released Proteins and Exosomes for Tissue Regeneration

<u>Beer L</u>, Simader E, Ankersmit HJ, Mildner M.:
Ionizing radiation induced regulation of long noncoding RNAs in human peripheral blood mononuclear cells

Hacker S, Mittermayr R, Nickl S, Haider T, Lebherz-Eichinger D, <u>Beer L</u>, Mitterbauer A, Leiss H, Zimmermann M, Schweiger T, Keibl C, Hofbauer H, Gabriel C, Pavone-Gyöngyösi M, Redl H, Tschachler E, Mildner M, Ankersmit HJ.:
Paracrine Factors from Peripheral Blood Mononuclear Cells Improve Wound Healing, Scar Quality, and Angiogenesis in a Porcine Burn Model

---

BOOKS

<u>Beer L.</u> **Guidelines for Measurement of Cytokines in Human Serum and Plasma**; 2013, Saarbrücken, Germany, AV

ABSCTRACTS AND POSTERPRESENTATIONS (31)

<u>L. Beer,</u> K. Hoetzenecker, M. Hasun, A. Baumgartner, S. Hacker, M. Wolfsberger, A. Mangold, S. Nickl, M. Zimmerman, A. Mitterbauer, B. K. Podesser, H. J. Ankersmit, M. Lichtenauer.: **Serum-free Cell Culture Medium Reduces Myocardial Damage After Ischemia in an Experimental Model of Myocardial Infarction: Importance for Cell Therapeutic Methods.** Austrian Journal of Cardiology 2010; 17 (5-6), 165-233.

K. Hoetzenecker, S. Hacker, A. Mitterbauer, <u>L. Beer</u>, M. Rauch, W. Hotzenecker, E. Guenova, M. Lichtenauer, W. Kleptko, H. K. Ankersmit,: **Expansion of a unique, lung-specific auto reactive T helpe cell polpulation in COPD**. European Surgery, ActaChirurgicaAustriaca, Volume 42, Suppl 236, 2010.

K. Hotzenecker, M. Töpker, M. Rauch, <u>L. Beer</u>, S. Hacker, M. Zimmermann, W. Klepetko, H. J. Ankersmit.: **Seldom referral to the thoracic surgeon: spontanously ruptured left**

inferior thyroid artery. European Surgery, ActaChirurgicaAustriaca, Volume 42, Suppl 236, 2010.

L. Beer, G. Werba, S. Nickl, M. Zimmerman, A. Mitterbauer, H. J. Ankersmit, M. Lichtenauer: **Secretion of cytokines and chemokines by peripheral blood mononuclear cells is triggered by coagulation products**. ÖKG 2011, Salzburg – Congress, *Salzburg*

L. Beer, G. Werba, S. Nickl, M. Zimmerman, A. Mitterbauer, H. J. Ankersmit, M. Lichtenauer: **Secretion of cytokines and chemokines by peripheral blood mononuclear cells is triggered by coagulation products**. ÖGIM 2011, Wien Klin Wochenschr (October 2011) 123/17-18;

G. Werba, M. Mildner, A. Baumgartner, L. Beer, M. Gyöngyösi, B. K. Podesser, H. J. Ankersmit, M. Lichtenauer.: **Anti-thymocyte globulin (ATG) reduces damage caused by ischemia and preserves cardiac function after experimental myocardial infarction**. European Surgery, ActaChirurgicaAustriaca; Volume 43, Suppl 242/11, 2011.

L. Beer, G. Werba, S. Nickl, M. Zimmerman, A. Mitterbauer, H. J. Ankersmit, M. Lichtenauer: **Secretion of cytokines and chemokines by peripheral blood mononuclear cells is triggered by coagulation products**. European Surgery, ActaChirurgicaAustriaca; Volume 43, Suppl 242/11, October 2011.

Michael Lichtenauer, Lucian Beer[1], Michael Mildner, Matthias Zimmermann, Bruno Karl Podesser, Wolfgang Sipos, Erwin Tschachler, Mariann Gyöngyösi, Hendrik Jan Ankersmit: **Secretome of apoptotic peripheral blood cells (APOSEC) confers cytoprotection to cardiomyocytes and inhibits tissue remodelling after acute myocardial infarction.** European Surgery, ActaChirurgicaAustriaca; Volume 43, Suppl 243/11, 2011
[1]presenting author

L. Beer, T. Szerafin, A. Mitterbauer, P. Altmann T. Haider, B. Steinlechner, M. Dworschak, G. Lang, W. Klepetko, H. J. Ankersmit.: **Continued Ventilation During Open Heart Surgery Attenutes Inflammatory Response,** Journal für Kardiologie – Austrian Journal of Cardiologie May 2012; 19 (5-6) 131;

L. Beer, T. Szerafin, A. Mitterbauer, P. Altmann T. Haider, B. Steinlechner, M. Dworschak, G. Lang, W. Klepetko, H. J. Ankersmit.: **Continued Ventilation During Open Heart Surgery attenuates Systemic Heat-Shock Proetin 70 Release.** Journal für Kardiologie – Austrian Journal of Cardiologie May 2012; 19 (5-6) 136;

M. Lichtenauer, G. Werba, M. Mildner, A. Baumgartner, K. Hoetzenecker, S. Nickl, L. Beer, B. K. Podesser, H. J. Ankersmit.: **Erhalt der linksventrikulären Funktion durch Anti-Thymozyten-Globulin (ATG) im Modell des experimentellen Myokardinfarkts an der Ratte durch Induktion von pro-angiogenetischen und antiapoptotischen Mechanismen;** Journal für Kardiologie – Austrian Journal of Cardiology 2012; 19 (5-6) 134;

L. Beer, T. Szerafin, A. Mitterbauer, T. Haider, G.A. Roth, M. Dworschak, H. J. Ankersmit.: **Continued lung ventilation during open heart surgery attenuates systemic heat-shock protein 70 release.** European Surgery, ActaChirurgicaAustriaca. Volume 44, Suppl 245/ 126 June 2012,

L. Beer, T. Szerafin, A. Mitterbauer, T. Haider, G.A. Roth, M. Dworschak, H. J. Ankersmit.: **Continued ventilation during open heart surgery reduces systemic secretion of soluble ST2.** European Surgery, ActaChirurgicaAustriaca. Volume 44, Suppl 245/ 68, 2012

A. Mitterbauer, T. Szerafin, L. Beer, T. Haider, G.A. Roth, M. Dworschak, H. J. Ankersmit.: **Can continued ventilation during open heart surgery inhibit polymorphonuclear cell activation?** European Surgery, ActaChirurgicaAustriaca. Volume 44, Suppl 245/ 126, 2012

L. Beer, G. Werba, S. Nickl, M. Zimmerman, A. Mitterbauer, H. J. Ankersmit, M. Lichtenauer: **Stability of cytokines and chemokines in serum and plasma samples**. European Surgery, ActaChirurgicaAustriaca. Volume 44, Suppl 245/ 144, 2012

L. Beer, T. Szerafin, A. Mitterbauer, T. Haider, M. Mildner, H. J. Ankersmit.: **Continued mechanical ventilation during CABG operation attenuates systemic immune modulation;** Wien KlinWochenschr (2012) 124: 578

L. Beer, T. Szerafin, A. Mitterbauer, T. Haider, M. Mildner, H. J. Ankersmit.: **Continued lung ventilation during open heart surgery attenuates systemic heat-shock protein 70 release and polymorph nuclear cell activation** Wien KlinWochenschr (2012) 124: 578

L. Beer, T. Szerafin, A. Mitterbauer, M. Zimmermann, G. Roth, H. J. Ankersmit: **Einfluss von kontinuierlicher mechanischer Beatmung während Operationen am offenen Herzen auf die Systemische Sekretion von Inflammationsmarkern**. EurSurg Vol. 44 · Supplement Nr. 246 /18 2012

A. Mitterbauer, T. Szerafin, L. Beer, M. Zimmermann, G. Roth, H. J. Ankersmit.: **Kontinuierliche mechanische Beatmung reduziert die Freisetzung von Hitze-Schock-Proteinen und Chemokinen**. EurSurg Vol. 44 · Supplement Nr. 246 /18 2012

L. Beer, T. Szerafin, A. Mitterbauer, T. Haider, M. Dworschak, B. Steinlechner, G. Roth, H.J. Ankersmit.:**Continued ventilation during open heart surgery reduces systemic secretion of soluble ST2 and inhibits polymorph nuclear cell activation**. Intensive Care Medicine Supplement 1 (October 2012).1075

L. Beer, T. Szerafin, A. Mitterbauer, T. Haider, M. Dworschak, B. Steinlechner, G. Roth, H.J. Ankersmit.: **Continued lung ventilation during open heart surgery attenuates systemic HSP-70 release**. Intensive Care Medicine Supplement 1 (October 2012). 1077

P. Altmann, M. Mildner, C. Sherif, L. Beer, T. Haider,H.-J. Ankersmit.:**Der Überstand apoptotischer Leukozyten reduziert zerebrale Läsionsvolumina und verbessert das klinische Outcome in Ratten mit ischämischem Schlaganfall**

Lucian Beer, Tamás Szerafin, Andreas Mitterbauer, Thomas Haider, Martin Dworschak, Georg A. Roth and Hendrik Jan Ankersmit: **Continued mechanical ventilation during coronary artery bypass graft operation attenuates systemic immune response**, 1st vascular biology meeting, Vienna, 2013. 30

L. Beer, M. Mildner, M. Zimmermann, B. K. Podesser, M.Gyöngyösi, H. J. Ankersmit, M. Lichtenauer.: **Isoflurane and ketamine anaesthesia reduce cardiac injury after myocardial infarction in the rat** Journal für Kardiologie – Austrian Journal of Cardiology May 2013.

L. Beer. T. Haider, M. Mildner, A. Mitterbauer, HJ. Ankersmit.: **Ionizing Radiation induced**

Gene Expression Alterations in Human Peripheral Blood Mononuclear Cells. 37. Seminar der Österreichischen Gesellschaft für Chirurgische Forschung. Gosau, Österreich, 2014

L. Beer, Tamás Szerafin, Andreas Mitterbauer, Thomas Haider, Martin Dworschak, Georg A. Roth, HJ. Ankersmit.: **Continued Mechanical Ventilation during Cardiopulmonary Bypass Dampens Matrix Metalloproteinase – Tissue Inhibitor of Metalloproteinase– Lipocalin 2 Axis- A prospective randomized controlled trial**. 37. Seminar der Österreichischen Gesellschaft für Chirurgische Forschung. Gosau, Österreich , 2014

L. Beer, Tamás Szerafin, Andreas Mitterbauer, Thomas Haider, Martin Dworschak, Georg A. Roth, HJ. Ankersmit.: **Immunological effects of continued mechanical ventilation during coronary artery bypass graft operation- a randomized controlled trail**. 37. Seminar der Österreichischen Gesellschaft für Chirurgische Forschung. Gosau, Österreich

L. Beer. E. Simader, A. Mitterbauer, HJ. Ankersmit.: 7. **Ionizing Radiation Induced Gene Expression Changes in Human Peripheral Blood Mononuclear Cells**, 2nd Vascular Biology Meeting, Wien, Österreich, 2014

L. Beer, T Szerafin, A Mitterbauer, T Haider, M Dworschak, GA Roth, HJ. Ankersmit.: **Immunological effects of continued mechanical ventilation during coronary artery bypass graft operation- a randomized controlled trail**. 2nd Vascular Biology Meeting, Wien, Österreich, 2014

L. Beer, T Szerafin, A Mitterbauer, T Haider, M Dworschak, GA Roth, HJ. Ankersmit.: **Continued Mechanical Ventilation during Cardiopulmonary Bypass Reduces Matrix Mstalloproteinase-TIMP1 and Lipocalin 2 Secretion**. 55. Österreichischer Chirurgenkongress. Graz, Österreich, 2014

L. Beer; E. Simader, A. Mitterbauer, HJ. Ankersmit.: **Ionizing Radiation Induced Gene Expression Changes in Human Peripheral Blood Mononuclear Cells**, 55. Österreichischer Chirurgenkongress; Graz, Österreich, 2014

ETHICS COMITTEE APPROVAL

„Proliferative Capacity of CD4+ cells is modulated by PBMC secretoma derived from SLE and haemodialysis patients"**EK: 2010/034**

"Therapeutische Applikation von PBMC-Sekretomen im Modell der Collagen induzierten Arthritis in der Maus."**BMWF66.009/0202II/3b/2011**

„Einfluss von ex vivo hochdosis Bestrahlung auf die Geneexpression von mononukleären Zellen des peripheren Blutes" **EK: 1326/2013**

CONGRESSES AND MEETINGS

2010/12	2nd EACTS Meeting on Cardiac and Pulmonary Regeneration, *Vienna*
2011/05	Jahrestagung der Österreichischen Kardiologischen Gesellschaft; *Salzburg*
2011/10	Jahrestagung der Österreichischen Gesellschaft für Innere Medizin; *Innsbruck*

2011/10	Jahrestagung der Österreichischen Gesellschaft für Transplantation, Transfusion und Genetik; *Graz*
2011/10	35. Seminar der Österreichischen Gesellschaft für Chirurgische Forschung, *Wagrain*; Salzburg
2012/05	Jahrestagung der Österreichischen Kardiologischen Gesellschaft; *Salzburg*
2012/06	53. Kongress Österreichische Gesellschaft für Chirurgie, *Salzburg*
2012/09	Jahrestagung der Österreichischen Gesellschaft für Innere Medizin; *Graz*
2012/10	25. Congress of the European Society of Intensive Care Medicine; *Lissabon - Portugal*
2012/10	Jahrestagung der Österreichischen Gesellschaft für Transplantation, Transfusion und Genetik; *Rust*
2012/1	1stVascular Biology Meeting; Vienna
2012/12	3rd EACTS Meeting on Cardiac and Pulmonary Regeneration, *Berlin*
2013/05	54. Kongress Österreichische Gesellschaft für Chirurgie, *Wien*
2013/06	Jahrestagung der Österreichischen Kardiologischen Gesellschaft; *Salzburg*
2014/1	EACTS Meeting; Bern
2014/1	2nd Vascular Biology Meeting; Vienna
2014/05	55. Kongress Österreichische Gesellschaft für Chirurgie, *Wien*
2014/06	Jahrestagung der Österreichischen Kardiologischen Gesellschaft; *Salzburg*
2015/1	4th EACTS Meeting on Cardiac and Pulmonary Regeneration; Bern

AWARDS AND GRANTS

2007/06	Matura (High School Graduation) with Distinction
2009/12	Leistungsstipendium – Medical University Vienna
2010/12	Leistungsstipendium – Medical University Vienna
2011/12	Leistungsstipendium – Medical University Vienna
2012/12	Leistungsstipendium – Medical University Vienna
2012/08	MD.PhD Student - Medical University Vienna
2013/05	*Wolfgang Denk Preis* der Österreichischgen Gesellschaft für Chirurgie im Bereich Herzchirurgie
2013/12	Förderstipendium – Medical University Vienna
2013/12	Leistungsstipendium – Medical University Vienna
2013/12	Leistungsstipendium – Medical University Vienna
2014/12	Förderstipendium der Medizinischen Universität Wien
2014/12	Leistungsstipendium – Medical University Vienna
2014/12	Würdigungspreis des Bundesministeriums für Wissenschaft, Forschung und Wirtschaft für hervorragende Studienleistungen

TEACHING ACTIVITY

2011/12 – 2013/12	Teaching Assistant at the Department of Physiology, General Hospital Vienna, Medical University of Vienna, Univ. Prof. Ivo Volf
2012/05 – 2014/5	Teaching Assistant at the Department of Physiology, General Hospital Vienna, Medical University of Vienna, Univ. Prof. Ahnelt and Prof. Pflug
2014/03	Teaching Assistant at the Department of Public Health, General Hospital Vienna, Medical University of Vienna
2014/03 - Present	Teaching Assistant at the Karl Landsteiner University of Health Sciences

MEMBERSHIPS

2011/12	Austrian Society of Transplantation, Transfusion and Genetics

EXCURSIONS

2011/4/28-29	Kaposvar; APOSEC study
2012/8/23	Kaposvar; APOSEC study
2014/09	Schladming; Statistic Training

Projects

Diploma thesis on triggers of chemokine release of peripheral blood mononuclear cells

Collagen induces Arthritis – Mice model

Mechanical lung ventilation during cardiopulmonary bypass – immunological effects

Identification of Radiation Specific Responses from Global Gene Expression Profiles in Human Blood Mononuclear Cells

Lipid, Proteomic and Extracellular Vesicle Analysis of Conditioned Media

Transcriptomic Analysis of Differentiating Keratinocytes

Identification of Suitable Reference Genes in Dermatological Research

METHODS

Cultivation of human cell lines

Knock-out in vitro experiments

ELISA; RT-PCR; FACS

Experience in working with different animal models (mice, rat, domestic pig)

Microarray Analysis

Transcription Factor Analysis

Exosome Isolation and Detection

Microparticle Isolation and Detection